University of Passau

Faculty of Computer Science and Mathematics
Chair of Computer Networks and Computer Communications

PhD Thesis

E-Mobility Management: Towards a Grid-friendly Smart Charging Solution

Ammar Alyousef

1. Reviewer Prof. Dr.-Ing. Hermann de Meer
Chair of Computer Networks and Computer Communications
University of Passau

2. Reviewer Prof. Dr.-Ing. Reinhard German
Computer Networks and Communication Systems
Friedrich-Alexander University, Erlangen-Nürenberg

August 03, 2021

Ammar Alyousef
E-Mobility Management: Towards a Grid-friendly Smart Charging Solution
PhD Thesis, August 03, 2021
Reviewers: Prof. Dr.-Ing. Hermann de Meer and Prof. Dr.-Ing. Reinhard German

University of Passau

Chair of Computer Networks and Computer Communications
Faculty of Computer Science and Mathematics
Innstrasse 43
94032 Passau

Abstract

Replacing fossil-fueled vehicles with Electric Vehicles (EVs) poses new challenges for power distribution networks. Specifically speaking, the electrification of the mobility sector relies on the ability to process and analyze information on when, where, for how long, or how fast charging processes will take place. Nevertheless, such kind of information is typically difficult to acquire or insufficiently predictable due to the dynamic nature of the system. Also, the increasing adoption rate of the renewable energy sources, specifically the domestic Photovoltaic (PV) systems, and the potentially associated grid defection scenarios will significantly impact the cost and efforts required to operate the grid in terms of power quality and demand-supply aspects. However, such emerging requirements have arguably not been taken into account when the distribution grid was built originally. Besides, expanding the distribution and transmission capacity is a very costly and lengthy process. Therefore, any proposed solution should be cost-effective as well as environment-, grid- and user-friendly. To this end, the advancements in Information and Communications Technology (ICT) are increasingly adopted and applied. This thesis addresses the rapidly growing EV sector and deals with the problems to overcome potential power quality degradation caused by the challenges mentioned above.

Since time switch and radio ripple control as existing solutions in Germany are costly and neither very effective nor scalable as it requires hardware retrofitting of existing public Charging Stations (CSs), the primary focus of this work is the development of an appropriate, standards-based, scalable, and smart charging solution of EVs. Such a solution can, in turn, boost the usage of renewable energy by ensuring that the existing grid infrastructure can operate within its permissible limits while maintaining acceptable levels of power quality.

This work introduces a new definition of the concept, “grid-friendly EV charging”, where the power demand of a CS is adjusted depending on the real-time status of a power grid. In this regard, the conflicting concerns of stakeholders in an EV ecosystem are considered. For example, a Distribution System Operator (DSO) does not want to reveal a lot of technical details about the power grid or its status. Similarly, a Charging Service Provider (CSP) wants to keep its clients happy without sharing the details of its business model with others, namely, DSOs. For that sake, a distributed smart charging architecture is proposed in this thesis. It is event-driven and responds in nearly real-time to unforeseen and critical grid situations such as high/low voltage, congestion, phase unbalance, and harmonics. In that regard, the publish/subscribe messaging pattern, used as a part of the architecture, enables

an efficient and well-performing communication scheme among the different components. Moreover, an indication mechanism about the different issues in a power grid is developed; it adopts the traffic light model. It works as a black box to separate smart controllers for each CS and configured only by the CSP. Smart chargers enable a smooth adjustment of the charging power to avoid drastic changes in the grid state. To that end, two types of intelligent controllers are developed and tested. While the first controller is inspired by the fuzzy logic, the second one is inspired by the slow-start mechanism used in TCP to control congestion in computer networks.

A simulative approach is applied to evaluate the solution, thereby, a topology of a real low voltage grid with realistic load and generation profiles is used. Furthermore, a set of metrics is defined regarding the main concerns of stakeholders: voltage, overloading, fairness, the satisfaction of EV users and grid operator, as well as the grid-friendly behavior of a CS/ EV user. The evaluation shows that the solution is able to guarantee a safe operation of the grid. The proposed system can ensure a grid-friendly charging by sacrificing of a small portion of user satisfaction, that sacrifice of a user is awarded via a points-based reward system. Last but not least, the proposed distributed controllers are compared to two other controllers: (1) a decentralized controller based only on sensing the local voltage and (2) a very strict centralized controller focusing on grid-friendliness. The latter ensures proportional fairness among users regarding the objective function of the optimization problem solved in each simulation step. The distributed controllers are superior to the decentralized controller in terms of grid friendly and fairness and converge in general to the centralized one.

Acknowledgment

This work was enabled and supported by many people to whom I want to express my honest gratitude. First of all, I am thankful for the support and guidance of my supervisor Prof. Dr.-Ing Hermann de Meer. He had believed in me and my capabilities before six years when he gave me the chance to do my research in his Lab and under his supervision. Further, I also would like to cordially thank Prof. Dr.-Ing. Reinhard German for kindly agreeing to serve as a second reviewer.

Many thanks to the consortium of the EU project "ELECTRIFIC" for all fruitful discussion and the knowledge sharing which helped not only to build the required experience for conducting the research related to this thesis but also to run a test of the proposed system in the field.

Throughout the time of my thesis, I want to thank all my former and current colleagues at the Chair of Computer Networks and Computer Communications. On this occasion, I would like to thank Dominik Danner for enabling and supporting me to pursue this work. I am very grateful that I could discuss, receive advice, and support work with Philipp Danner and Wolfgang Duschl. Moreover, I highly value the support I received from Michael Niedermeier through the writing process. Apart from the colleagues in my group, I would like to give special credit to all my students, who provided invaluable programming work in the development of the simulation framework.

I would like to say a special thank you to my friends, Ali ALshawish and Waseem Mandarawi, and their families. They have supported me and not only enriched my work but also my personal life, turning parts of this very intense period into moments I will always appreciate.

I must express my gratitude to ♡ Lama ♡, my wife, for her unconditional support, encouragement, and love; and without her I would not have come this far. I was continually amazed by her patience through the ups and downs of my research. Definitely, I can not forget my angels, ♡ Gazal & Maya ♡, who add more love and fondness to the family all the time.

Last but definitely not least, I would like to thank my big family, my parents, my brothers, and sisters for their continued loving support and encouragement.

Table of Contents

List of Acronyms

AC	Alternating Current	11
ACN	Adaptive Charging Network	92
AIMD	Additive Increase Multiplicative Decrease	106
AMI	Advanced Metering Infrastructure	15
ASC	Average Service Coverage	94
BEBM	Binary Exponential Backoff Mechanism	84
BDEW	“Bundesverband der Energie- und Wasserwirtschaft e.V”	38
BMS	Battery Management System	129
BSS	Battery Swapping Station	24
CA	Congestion Avoidance	9
CAPEX	CAPital EXpenditure	50
CC	Constant Current	129
CP	Control Pilot	131
CPU	Central Processing Unit	123
CS	Charging Station	iii
CSO	Charging Station Operator	18
CSP	Charging Service Provider	iii
CV	Constant Voltage	129
Cwnd	Congestion Window	9
DB	Database	28
DC	Direct Current	11
DCS	Distributed Control System	55
DG	Distributed Generation	5
DR	Demand Response	57
DSL	Digital Subscriber Line	128
DSM	Demand Side Management	114
DSO	Distribution System Operator	iii
EDV	Electric Drive Vehicle	15
eMSP	e-Mobility Service Provider	17
EPBD	Energy Performance of Buildings Directive	2
ES	Energy Supplier	18
EU	European Union	14

EV	Electric Vehicle	iii
EVSE	Electric Vehicle Supply Equipment	19
FDM	Frequency-Division Multiplexing	83
FIFO	First-In-First-Out	70
FRR	Fast Re-transmit and Recovery	9
FSM	Finite State Machine	9
G2V	Grid-to-Vehicle	21
GF	Grid Friendliness	97
GOOSE	Generic Object Oriented Substation Event	60
GSI	Grid State Indicator	57
ICS	Industrial Control System	55
ICT	Information and Communications Technology	iii
QoS	Quality of Service	94
QoE	Quality of Experience	94
QoG	Quality of Grid	95
MaOP	Many-objective Optimization Problem	46
MOP	Multi-Objective Problems	47
MoP	German Mobility Panel	91
MP	Measurement Point	6
MQTT	Message Queuing Telemetry Transport	89
OCPP	Open Charge Point Protocol	6
OLTC	On Load Tap Changer	50
OPF	Optimal Power Flow	50
OSCP	Open Smart Charging Protocol	18
PF	Power Factor	15
PFC	Power Factor Correction	35
PHIL	Power Hardware In the Loop	9
PP	Proximity Pilot	131
PQ	Power Quality	1
PMU	Phasor Measurement Unit	15
PV	Photovoltaic	iii
PWM	Pulse Width Modulation	131
LCV	Light Commercial Vehicle	2
LTE	Long-Term Evolution	61
RAID	Redundant Array of Independent Disks	123
RAM	Random Access Memory	123
RES	Renewable Energy Source	15
RMS	Root Mean Square	13
RTT	Round Trip Time	75
RTO	Re-Transmission Timeout	75
SC	Smart Charger	9
SCADA	Supervisory Control And Data Acquisition	55

SoC	State of Charge	9
SM	Smart Meter	60
SMGW	Smart Meter Gateway	127
SS	Slow Start	9
SSD	Solid-State-Drive	123
SSM	Supply Side Management	114
TCP	Transmission Control Protocol	9
TDM	Time-Division Multiplexing	83
THD	Total Harmonic Distortion	14
TMM	Time Management Mechanism	82
TSO	Transmission System Operator	30
UC	Uncontrolled Charging	20
UUID	Universally Unique IDentifier	61
V2B	Vehicle-to-Building	22
V2G	Vehicle-to-Grid	1
V2H	Vehicle-to-Home	22
V2V	Vehicle-to-Vehicle	22
V2X	Vehicle-to-X	22
VPP	Virtual Power Plant	1

List of Figures

List of Tables

1 Introduction

EVs are becoming a more and more popular choice to fight climate change when it comes to CO_2-Emission. Although EVs are certainly promising means of tackling this problematic issue, they also impose their concerns and challenges such as the lack of information on when, where, for how long, or how fast the charging process of EVs will take place. With all the innovations and developments - like an increasing number of EVs and a growing amount of renewable energy sources - getting integrated into the grids infrastructure, electrical grids nowadays are facing challenges they have been just not built for. Notably, new requirements on low voltage distribution grids have to be fulfilled since the increase in EV penetration brings another set of problems in terms of Power Quality (PQ) and congestion in the different parts of distribution grids [1, 2, 3]. In this thesis, a grid-friendly solution using EVs is presented. In Section 1.1, a definition of the concept "grid-friendliness" is introduced. Thereafter, in Section 1.2, the motivations, challenges, and the thesis' objective are stated. Section 1.3 delineates the contributions of this thesis to the research area. Finally, Section 1.4 gives a structural overview of the remaining parts of this thesis.

1.1 Definition of Grid-Friendliness

Shen et al. [4] define three types of controllable loads in any power grid: (1) Passive loads that can not inject power to the grid and can be interrupted or shifted, e. g., residential loads such as fridges. (2) Active loads that can inject energy to the grid in comparison to the passive loads, e. g., battery storage, and Vehicle-to-Grid (V2G). (3) Large controllable loads that are in the connected-grid mode and include micro-grid, renewable energy, and Virtual Power Plant (VPP). However, those loads are used by grid operators for local grid stability measures[1] in some cases as an alternative solution to costly grid enhancement. The behavior of them would be adjusted to be more grid-friendly, so they operate in a manner that supports electrical power grid reliability through demand response. Nowadays, it is only a simple ripple control. Due to countless varieties of electronic devices, individual consumption behaviors, and grid topologies, the determination of a grid-friendly situation can be very different from a sub-grid to a sub-grid or even from a busbar to a busbar inside the same grid. Generally, the quantifying of a grid-friendly behavior is missing, and the price signal is the main factor in incentivizing end users.

[1] The operation of any power grid is subjected to very strict limits of PQ parameters (e. g., voltage and harmonics) defined by norms and standards such as EN 50160 and ISO 6100. More details in Section 2.1.2

Throughout this work, the grid-friendliness is defined as the sum of measurable reactions of a controllable load on critical levels of PQ parameters. Those reactions can be seen as positive, negative, and neutral in terms of stabilizing the grid. That requires a specific mechanism to evaluate the situation in the grid and quantify the size of the required response by controllable loads. However, those load reactions can be locally or remotely controlled with three possibilities: (1) shifting the load only in time without changing the size, (2) adjusting the load size without changing the time , and (3) switching off the load entirely for a specified period. Regardless of the type of load control, it can be done either proactively based on proper planning and prediction by the DSO or re-actively based on collecting real-time data about PQ parameters in the grid. Further, three terms can be included in a possible definition of the grid-friendliness regarding the authors of [5]. Those terms are derived from the use case of distributed battery storage [6]:

1. Grid compatibility: The technology must meet the requirements of the grid operators for quality, reliability, and safety to be considered compatible, namely, ISO 6100 series. However, meeting these requirements is the responsibility of the manufacturer.

2. Usefulness for the grid: It includes the behavior of a load when it contributes actively to the grid stabilization.

3. Usefulness for the system: A load is considered as useful for the system if it enables an increase in the total flexibility of the whole energy system. For example, charging EVs during the peak times of renewable sources not only increases the greenness of EVs but also minimize the fluctuation in the residual load with high penetration of PVs.

In this thesis, the author focuses on the reactive grid-friendly behavior of a CS and excludes the proactive one or the combination of both concepts discussed in other work [7, 8]*[2]. Thereby, an intelligent charging algorithm can react to individual grid situations during a charging process by controlling the charging power.

1.2 Motivation, Challenges and Objective

The EV Outlook 2019 [9] predicts that EVs will make up more than 80% of sales for new buses by 2040, and just about 60% for Light Commercial Vehicles (LCVs). The growth of EVs will have significant flow-on effects on other energy markets. Shifting transport from fuel to electric technologies will result in a predicted increase in global electrical consumption by 6.8% by 2040.

However, as several European countries are expected to exceed the deployment targets, the ratio of one publicly accessible charger per ten cars is likely to be achieved in 2020 [10]. Furthermore, the European Energy Performance of Buildings Directive (EPBD) makes mandatory at least one-fifth of the parking places of new or renovated non-residential

[2] (⋆) means that the author contributed to aforementioned work.

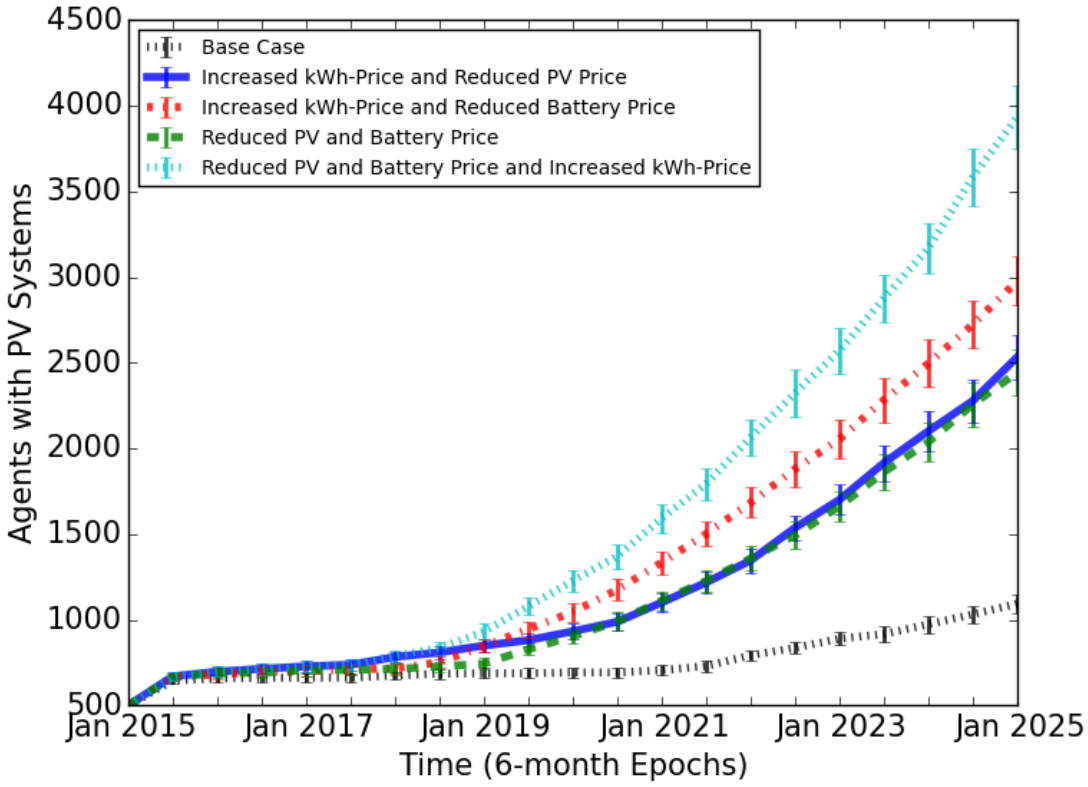

Figure 1.1.: Prediction of PV Adoption in Germany until 2025; Agents are homeowners and the total number of agents in the model is ≈ 14k [12].

buildings to be equipped with conduits allowing the installation of chargers. On top of that, any parking place with more than ten places should contain an installed charging point. Regarding the new or renovated residential with more than ten parking places, the EPBD mandates that all parking places need to be prepared with conduits for future chargers. Hence, the number of installations of CS increases not only in Europe but also globally, either public ones with a minimum charging capacity of 22kW or private(semi) fast charging wall-boxes.

Beyond the EV adoption, many research studies depict that the adoption of small PV systems will increase in the next ten years by the increasing price of kWh and the reduction of battery and PV prices. Currently, those price changes are actually facts more than predictions. For example, Alyousef et al. show in [11, 12]* via using an agent-based model that the adoption rate could reach 28% and 15% in Germany and Ontario at the end of 2025, respectively, which in turn will cause more stress on the distribution grid. In Figure 1.1, the impact of the policy change on the total number of PV-adopting agents in Germany until 2025 can be seen. Agents are homeowners that have a social network and exist in an environment that can affect their decision and desires. The highest rate of adoption can be achieved by combining an extreme increase of electricity prices [13] with reduced PV and battery prices [14, 15].

However, EVs are going to be more relevant for power systems than they have been in the past. Except that we already have enough generation capacity[3] so long as people avoid charging on the on-peak times, which means, EVs could drive incremental needs for peak power generation and transmission capacity with uncontrolled charging. That looks easy to be achieved with peak demand or time of use tariffs or similar, but the reality is something else. However, understanding the extent to which power systems could be impacted depends on the total annual electricity demand of EVs, the impact of daily charging patterns on load profiles and the location of power levels used for charging.

Heretofore, infrastructure dimensioning [16, 17] has been adopted by DSOs as a guaranteed solution for those emerging requirements. Thereby, a compromise between the investment/operating costs and the cost of supply interruption is considered where the regularity presses towards better operational conditions, as depicted in Figure1.2. That dimensioning has been based on worst-case conditions in all cases. Nevertheless, such a procedure is no longer attractive from an economic and technical point of view because of the variability and unpredictability of EV loads. In particularly, State-of-the-art 22 kW charging power [18] by far exceeds the 4 kW estimate for a residential grid connection in central Europe. Consequently, more on-line monitoring and even active interventions during grid operation will be necessary to maintain critical boundary conditions such as line voltages and assets loading within safe limits. A recent study from E.ON in 2019 [4] shows the need of €400 per EV in average as an enhancement of E.ON's distribution grids if we want to achieve 100% EV share within the next 25 years, namely, 6.5 million EVs [19] . That includes the required cost for upgrading the different grid elements, specifically, transformers and cables. The study above also shows that optimizing the charging load using ICT can save up to 50% of the cost.

As a result, smart approaches that make use of available excess capacities of the grid elements can help to reduce grid connection costs, mainly, for the expected large number of private (semi) fast charging wall-boxes. Therefore, smart techniques of charging management are a necessity to help for a smooth transition of a high EV penetration in the coming years. To meet the emerging requirements and consider the complexity of the EV ecosystem, as will be discussed in Section 2.2.1, the following design requirements(challenges) have to be taken into account to guarantee a wide-deployed, efficient, and stakeholder-satisfying solution:

R_1) Realizing grid-friendliness: The primary concern of CSPs is the satisfaction of their customer, the sacrificing of that satisfaction even partially because of being grid-friendly has to be awarded by DSOs. Therefore, any smart solution has to realize a reward system reflecting the definition of grid-friendliness stated in Section 1.1.

[3] Particularly with the increasing rate of PV adoption in this context.

[4] E.ON is a German electric utility. It runs one of the world's largest investor-owned electric utility service providers.

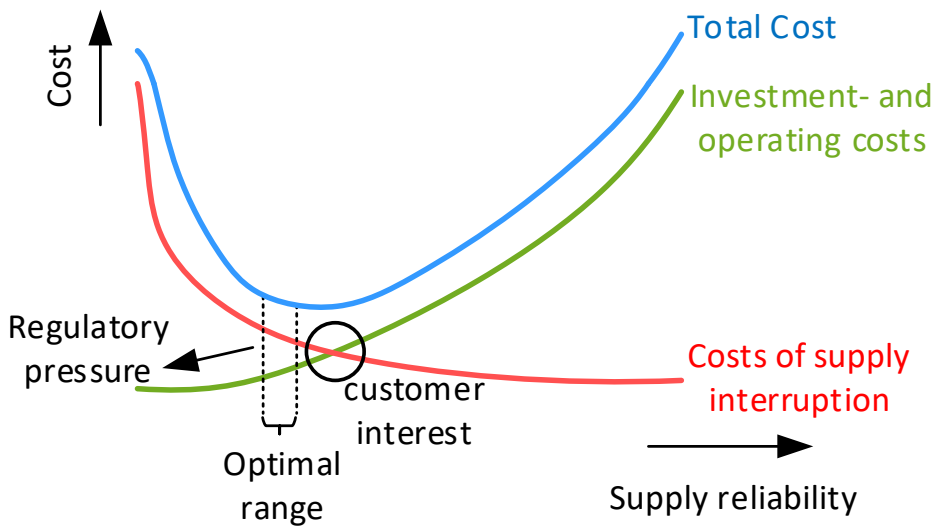

Figure 1.2.: Fundamental Relationships Between Quality and Costs [20]

R_2) Enhancing power quality: Voltage maintenance is an essential factor in any power grid since a stable operation of the power grid units can be ensured by only guaranteeing a sufficient supply voltage according to EN 50160 [21]. Demand controlling could counteract possible voltage fluctuations in some cases. It is often suggested to be used as an economical alternative for grid enhancement. Thus, a crucial goal in the design of a control mechanism for charging EVs is to maintain the voltage level in the allowed boundaries locally at the CS or other critical points in the grid.

R_3) Maintaining grid reliability: The authors of [22] show the impact of the new technologies such as Distributed Generation (DG) and EVs on the life of assets of the distribution systems. Since those emerging technologies have not been considered in the design of the traditional power system, they cause overloading of the assets. Without protective relays, that are designed to mitigate the overloading of feeder lines and transformers, many outages are introduced due to uncontrolled loads such as EV charging. In this regard, the proposed system has to control the charging operation to maintain the same level of system reliability.

R_4) High utilization: The fees on the number of kWh transferred through DSO grids represents a significant part of the DSO revenue. Consequently, a DSO would like to maximize the utilization of the distribution system as it implies better expenditure management. Without EV smart charging solutions, this maximization will be hard or even impossible. Hence, the DSO sets some thresholds to be satisfied and not be passed during the charging times. Those thresholds allow the DSO to achieve the maximum gain in terms of operating conditions.

R_5) Separation of concerns: Due to the different interests of the involved actors in the EV charging ecosystem, the indication of the power quality issues and the controlling of the CSs have to be separated. From the perspective of CSPs, the indication process of the grid status is a black box, which is configured by DSOs depending on the individual characteristics of each low voltage grid. However, the DSO does not want to share information about the network, neither its topology nor operating conditions, with any external actor. In contrast, the CSP configures smart actuators according to its business model. Additionally, such separation enables engagement of different controllable loads in the system via responding to the indication signal regarding their technical capabilities, e. g., reactive power control through PVs.

R_6) Fairness and quality of service: From the point of view of an operator, the quality of service is an essential aspect in keeping the customer satisfied and thus diminishing churn. Hence, numerous mechanisms are introduced for quality of experience driven networks resource management with the purpose of maintaining quality above a certain threshold for every user; a challenge arises in terms of a fair allocation of available resources among users.

R_7) Scalability: With an expected increasing number of EVs, more CSs will be integrated into low voltage grids. It includes not only public ones but also private (semi-) fast charging wall-boxes. The proposed system has to deal with a large number of active CSs. Hence, a distributed solution could be necessary for any widely adopted solution.

R_8) Low communication overhead: CS does not have an impact on all PQ parameters measured at different Measurement Points (MPs) through the grid. Therefore, the transferred data over the communication channel should be kept as small as possible. The messaging pattern among the different components in the system adopts a "publish/subscribe" paradigm to support the scalability and loose coupling.

R_9) Robustness: The overall system is expected to be robust against the failure of the signaling network.

R_{10}) Interoperability: The advantages of open standards-based smart charging solution are flexibility and wide deployment. Open standards allow easy integration of many different hardware and network provider into the system. For example, when you install Open Charge Point Protocol (OCPP)-compliant charging stations, you are free to select the smart solution that meets your needs.

R_{11}) Concurrency/Synchronization: A smart solution has to support a kind of timing management among the active smart controllers in order to avoid unnecessary simultaneous reactions.

To the best of the author's knowledge, an appropriate solution deals with all the challenges mentioned above is missing, as will be discussed in Chapter 2. Such a smart charging architecture is the primary goal of this thesis. Hence, the author introduces in this work a

novel, standard-based, and distributed smart charging architecture that helps in maintaining the power quality of the grid. The proposed architecture complies with five design criteria. First, it is scalable in terms of the number of involved CSs. Second, it considers not only local power quality issues but also global ones. Third, it guarantees a smooth charging process. Fourth, it adopts modular design to guarantees a separation of concerns of the main stakeholders. Finally, it is applicable in reality. Three main assumptions are made in the context of this work: (1) an EV battery can be charged at any rate less than the maximum amperage rating of its charger. (2) Overload or voltage issues can be detected within a few cycles of its occurrence before the invocation of protection mechanisms. Hence, it gives the controlling mechanism the chance to reduce/increase the transient EV loads. (3) Neither CSs nor EV users are malicious in terms of exposing the power system to risk.

1.3 Contributions

In the following, the contributions of this thesis are briefly listed:

C_1) **A new definition of the grid-friendliness**: The concept of the grid-friendliness is defined in a new way as the sum of the measurable reactions of a controllable load on critical situations in the power grid. Those reactions are systematized as: positive, negative, and neutral. Consequently, a point-based award system is proposed for the sake of awarding or penalizing the individual reaction of a CS.

C_2) **A classification of the existing smart charging approaches**: This thesis classifies the different strategies of EV charging management, focusing on the algorithmic way of controlling and scheduling the active charging operations. The classification enables an in-depth analysis of each smart charging class, showing its pros and cons. Hence, a real-time charging control has an advantage over the charging scheduling in terms of responding to unforeseen issues in the grid. Moreover, the distributed solutions have the upper hand over the centralized and decentralized ones in terms of either communications efficiency or considering the different conflicting concerns of stakeholders in a composite EV ecosystem.

C_3) **Investigating and analyzing the main factors for developing a smart charging approach**: In this thesis, the main five design factors of an intelligent charging solution are extracted and discussed, namely, the direction of power flow, stakeholder precedence, mobility pattern, charging mode, and application domain. The different factors are used as an input for designing and testing the proposed solution in this thesis.

C_4) **Formulating the problem of grid-friendly smart charging as a linear and fair optimization problem**: a CS, like any other load in the grid, has its own impact on

different grid parameters, namely, voltage, overloading, and phase imbalance. Theoretically, the load of any CS can be adjusted by setting the active power and reactive power for the sake of keeping the grid operating within the allowed boundaries. In this thesis, the different means of controlling EV charging system are analyzed not only theoretically but also by using simulation. Four different means are identified: location, real power control, power factor correction, and phase balancing. The goal behind that is understanding the different abilities of a CS to support PQ in distribution grids. Subsequently, the problem of providing a fair and grid-friendly charging service is formulated as a linear optimization problem. Thereby, the optimization problem has six decision variables, representing active and reactive power on three phases, with an objective function of providing a fair charging service among the active CSs. For that sake, proportional fairness is adopted. Moreover, typical power flow constraints are used in addition to specific constraints about both the local voltage at the CS and the remote one at critical points in the grid. Finally, an extra constraint considering phase imbalance is included.

C_5) **A novel notification mechanism for events in the distribution grid**: The proposed notification mechanism provides information about not only the congestion but also about other grid issues, i.e., power quality. The notification signals have three colors: red, yellow, and green. Similar to a traffic light, those colors point out critical, warning, and stable situations, respectively. A normalized value within [-1,1] is tagged with each signal to determine the size of the required reaction to move the grid back to a stable situation. While (-1) corresponds to either a complete shutdown of the charging process or a reduction to the minimum required power in order to be able to control the EV later, the value (+1) represents the maximum power capacity of the CS. The notification mechanism introduced in this work uses a hierarchical logic, so it prioritizes the local conditions over the remote ones. Moreover, it considers the different importance among the grid elements; for example, the transformer is more critical than a fuse or a cable in the grid since it represents a single point of failure. Using such a mechanism enables hiding the details of the power grid, so the DSO shares no critical information about its grid with other stakeholders.

C_6) **A novel distributed grid-friendly smart charging architecture**: The main challenges of any intelligent charging architecture are: (1) dealing with a massive amount of high-resolution real-time data from MPs, (2) increasing number of CS either private or public, (3) conflicting concerns and business models of the different actors in the EV ecosystem, and (4) the different technical specification of EV. Hence, a distributed smart charging architecture is described and included in this work; it takes into consideration those challenges, and others described in detail in Section 1.2.

C_7) **Two smart-charging controllers**: Based on the proposed notification mechanism, two smart controllers for adjusting the used charging capacity are developed. Both controllers are evaluated using realistic EV data and compared with decentralized

and centralized controllers. Furthermore, Power Hardware In the Loop (PHIL) test is carried out by one controller to show the applicability of such a solution in the field. The two controllers are:

$C_{7.1}$) **A Finite State Machine (FSM)-Smart Charger (SC)**: The charging operation is described as a set of different states. Some of them represent the grid status as critical, not critical, and optimal. Other states reflect the user concern in terms of the State of Charge (SoC). The transition between these states is based on the notifications coming from the grid. The controller guarantees a smooth change of used power capacity, thereby, two kinds of transitions among states are implemented: slow linear ones among non-critical states and fast polynomial among the critical states; more details in Section 4.5.1

$C_{7.2}$) **A SC inspired by the congestion mechanism of Transmission Control Protocol (TCP)**: Based on the similarity of the congestion problem in TCP and the demand controlling in the distribution grid discussed in details in Section 4.5.2 and in literature [23, 24, 25], an EV smart charger inspired by the TCP-Reno Slow Start (SS) mechanism is developed. It uses a discrete charging rate similar to the Congestion Window (Cwnd) in TCP. Thanks to a notification mechanism proposed by the author, the smart controller mimics the different reactions of the TCP congestion mechanism on events occurring in the communication network, namely, time out, crossing the thresholds, and duplicated ACKs. Respectively, the TCP-like SC imitates the different approaches of the congestion mechanism: SS, Congestion Avoidance (CA), and Fast Re-transmit and Recovery (FRR).

1.4 Thesis Structure

The thesis is structured as follows (cf. Figure 1.3): Chapter 2 lays the foundations for a comprehensive understanding of the power system structure, power quality, electric vehicles, and the current and future developments with respect to the Smart Grid and power quality. It also addresses previous work from the context of EV charging management and its technical objective, design factors, and a classification.

Chapter 3 discusses the two existing EV charging systems, namely, on-board and off-board chargers. Additionally, the possible means that can be used for supporting power quality in the grid are analyzed. Hence, six control parameters are identified, including active and reactive power on all phases. A simulative approach is applied for understanding to what extent the impact of a CS propagates through the distribution grid. Furthermore, an optimization problem is formulated and discussed, describing a possible grid-friendly behavior of CS operation.

In Chapter 4, a distributed smart charging solution is introduced, the main components are described and discussed including a novel indication mechanism in the

low voltage grid, event-driven data collection of real-time data, and two smart controllers.

Chapter 5 performs the potential analysis with respect to the main concerns of grid operators and end-users using a set of defined metrics. Moreover, the practical applicability of the proposed architecture is discussed.

In Chapter 6, main outcomes and results of this thesis are summed up. Additionally, possible future work directions are given.

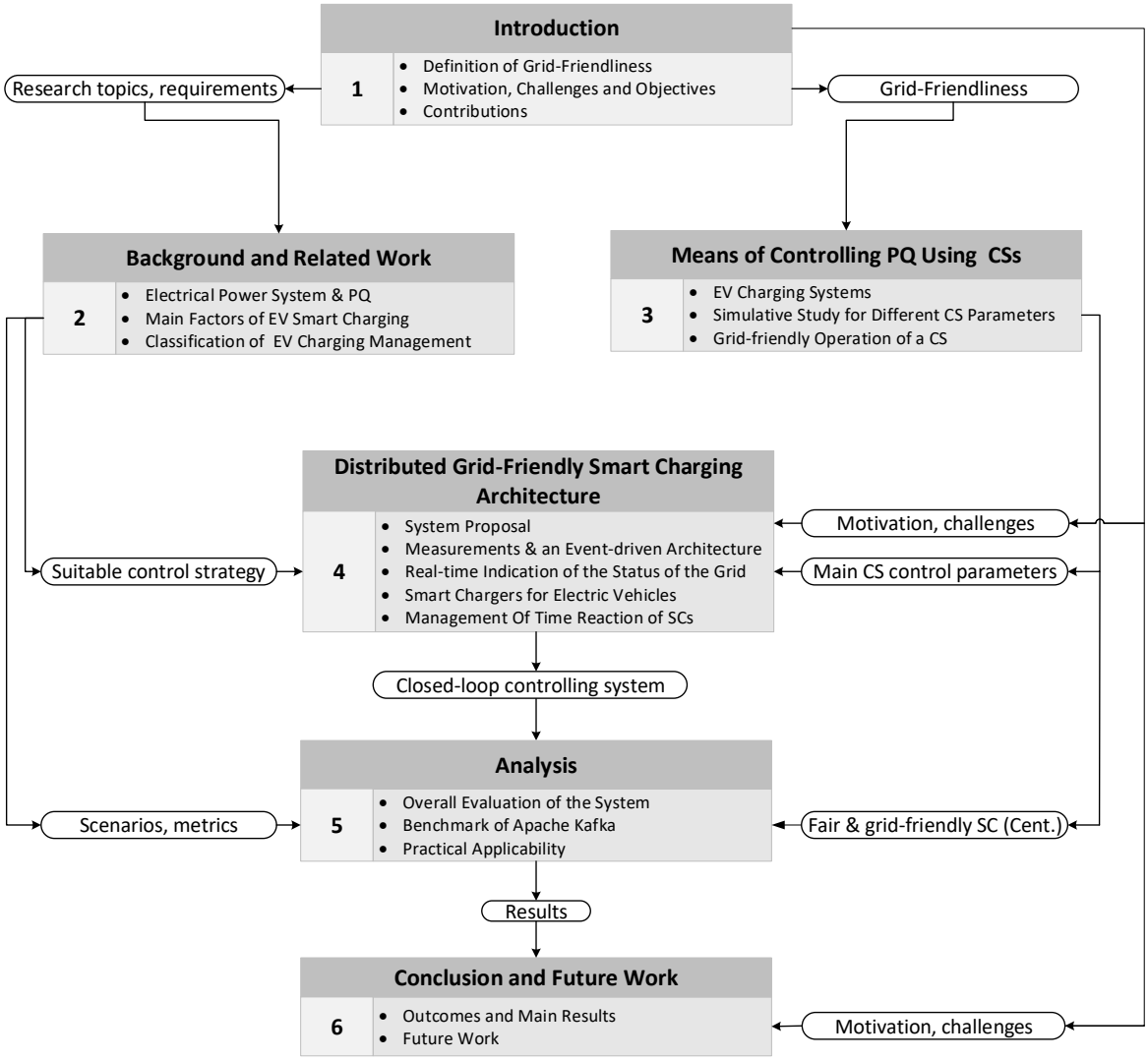

Figure 1.3.: Chapter Structure and Dependencies

2 Background and Related Work

This chapter is split into two main parts: the first discusses the history and development of power grids towards the currently emerging Smart Grid. In this section, a major focus is on the PQ; therefore, its technical meaning in power systems and how the Smart Grid can help to that end is analyzed. The second explains the concept of the EVs; thereby, the different types of electric drive vehicles are explored briefly. Furthermore, the EV charging process is clarified from the physical connection to the different kinds of coordination. Since the main subject of this thesis is the smart charging, the main factors of smart charging and the classification of existing charging management approaches are stated. The chapter ends with a discussion regarding the main PQ parameters that are going to be considered in this work besides the main reasons behind adopting a distributed smart charging solution.

2.1 Electrical Power System

2.1.1 Developments and Structure

The road to our existing Alternating Current (AC) power system has been very long. The English physician William Gilbert (1544-1603) was the first to use the term 'electric' which is a derivation from the Greek word for amber ($\eta\lambda\varepsilon\kappa\Gamma\rho o\nu$). After groundbreaking electrophysical discoveries in the beginning and the mid of the 18^{th} century (e.g. by Alessandro Volta, Michael Farraday, and James Clark Maxwell), the first commercial power system was a Direct Current (DC) lightning system (Pearl Street station) developed by Thomas Edison in 1882. Thereby, the concept of power sold as a metered commodity is introduced. Ironically, the success of Edisons original lighting system in some ways proved its undoing or, rather, its forced modification. The demand for electricity and the rapid distribution of industrial electric motors soon led to the need to build ever-larger power plants and transmit that power over greater distances. The DC-system was ill-suited to meet these new demands. That was mainly due to the fact that with increasing the distance from the generator, higher supply current is required. Thus, the line losses in a DC system increase, practically, a direct result of applying Ohms's law.

The emerging requirements of the power system at that time - particularly the different voltage levels and the long transmission distance - led to adopting an AC system significantly advanced by Nikola Tesla and promoted by George Westinghouse. The AC enables decoupling of the transmission and the distribution of electricity since its physical properties

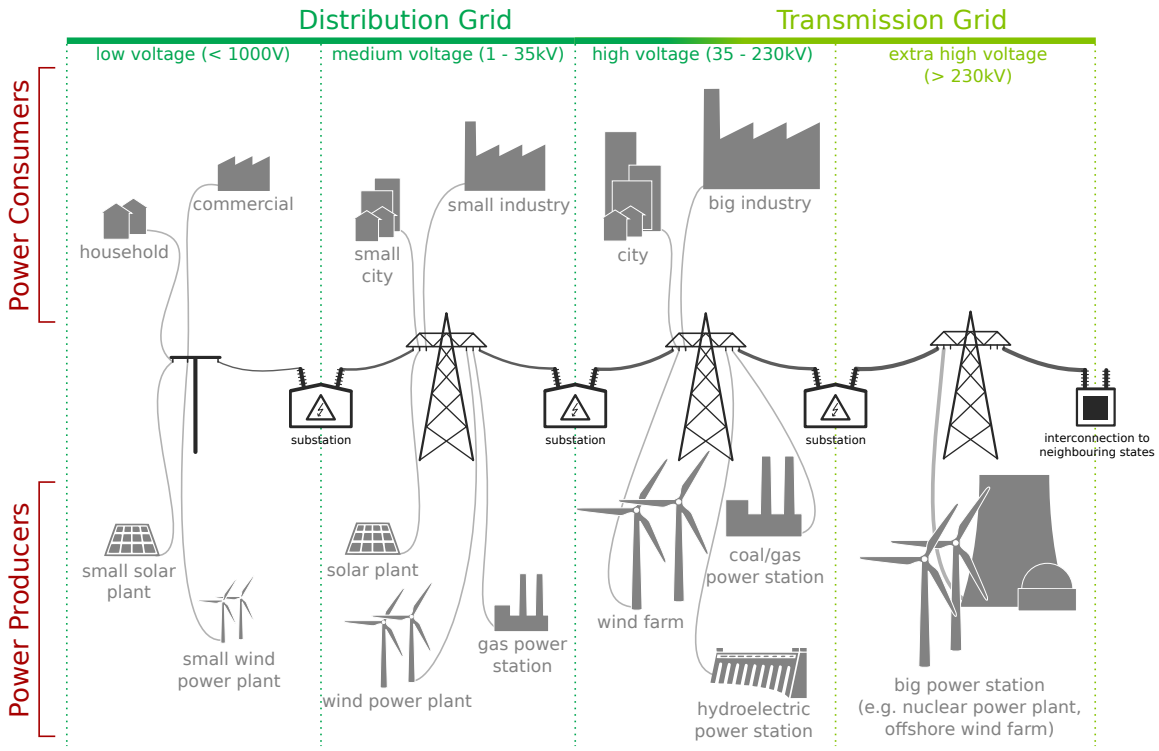

Figure 2.1.: Power Grid with Different Voltage Levels
(created by Philipp Danner / CC BY SA 4.0)

allow carrying out the transmission at a higher voltage but at lower currents, which in turn reduces the losses considerably. Apart from those advantages, AC was not without problems of its own, however. AC power flow is subject to both magnetic (inductive) and electrostatic (capacitive) effects, which cause power loss because of the proximity effect [26].

AC based systems finally became the world standard being implemented in different fashions but mainly with a frequency of either 50 or 60 Hz [27]. Thus, the current power grid became a very complex system that consists of many interconnected networks composed of generators, transformer substations, transformers, cables, and electrical loads.

In Principle, the power is generated by large power plants (600 -1700 MW) located far away from the consumption locations. It is transported via a network of ultra-high and high voltages to be distributed to individual grid areas and consumers through distribution networks. However, there are four different voltage levels according to IEC 60038 [28], as depicted in Figure 2.1: ultra-high voltage, high voltage, medium voltage, and low voltage. However, DG enables the production of electricity near the consumption place, the different distributed energy resources are generally interconnected directly to a distribution provider's electric system.

2.1.2 Power Quality

PQ can be defined in different ways depending on the context [29]. On one hand, the utility (supplier) sees it as the ability of a system to function as intended in terms of availability and performance. On the other hand, manufacturers see it as the characteristics enabling the proper working of the equipment. Both utilities and manufacturers define PQ taking customer's perception into account, thereby, failing of the system to deliver the designated service due to a problem with the aspects of the power is considered as an inferior or unstable PQ. Characteristics of the power supply in a distribution grid such as supply voltage[1], current, harmonics, and frequency should stay within acceptable ranges according to the EN 50160 and IEC 60038 standards; Table 2.1 depicts some of common ranges.

Parameters	Supply characteristics
Frequency (averaged over 10 s)	$\pm$1% for 99.5% of a week
Voltage magnitude (RMS)	$\pm$10% for 95% of a week
Rapid voltage changes (flicker)	$P_{lt} \leq 1$ for 95% of a week [2]
Supply voltage dips	duration $<$ 1s, depth $<$60%
Short voltage interruptions ($\leq$ 3 Min.)	Few hundreds/year, 70% of them $<$ 1 s
Supply voltage imbalance	Up to 2% for 95% of a week

Table 2.1.: Supply Characteristics of the Main PQ Parameters in a Low-Voltage Grid According to EN 50160

Figure 2.2 illustrates the main concepts of voltage in terms of PQ as follows:

- The Root Mean Square (RMS) of the voltage (U): It is the square root of the time average of the voltage squared; $U(RMS) = \sqrt{\frac{\sum_{t=1}^{T}(U_t)^2}{T}}$
- The nominal voltage of the system U_n: It is the generic operating parameters for a given electrical system by which a system is designated or identified.
- The amplitude of the supply voltage U_A: It is the peak value of the sine-wave of the voltage.
- The voltage dip: An unexpected decrease of the supply voltage followed by speedy recovery of the voltage, particularly, the recovery time has to be between 10ms and 1min. If the voltage changes do not reduce the supply voltage to less than 90% of U_n, they are not considered as dips.

[1] According to the standards IEC 60038, the supply voltage is the line-to-line or line-to-neutral at the point of common coupling.

[2] Long term severity (P_{lt}) calculated from a sequence of 12 short term severity (P_{st}) values over a two-hour interval [30].

- The supply interruption: It is the case when the voltage at the supply terminal is lower than 1% of U_n.

One further main PQ issue in the power grid is harmonic distortion. It is defined as a deviation of the current or voltage waveform from a perfect sinusoidal shape. Any equipment with non-linear characteristics (e. g., CSs or EVs see [31, 32]) can introduce current or voltage distortions into the system. Harmonic content or Total Harmonic Distortion (THD) is the relative contribution of higher-frequency harmonics compared to the base frequency. Vibration, buzzing, or other distortions in motors and electronic equipment, as well as losses and overheating in transformers, are direct results of harmonic in equipment that is sensitive to the waveform [33]. For harmonics regulation, the IEC 61000-3-2 standard [34] is established.

Heretofore, PQ issues are estimated to cost industry and commerce in the European Union (EU) around 10 billion€ a year, whereas expenses on preventive expenditure account for less than 5% of this [35]. Harmonic distortion, blackouts, dips, or sags represent the main power quality problems from the point of view of their business interruption potential.

It is worth mentioning that various European countries have additional rules beyond EN 50160, which provides only general limits for PQ. The national authorities believe in the insufficiency of EN 50160 to represent the typical conditions appropriately. Therefore, Germany has the national standard VDE 0100 for example, while Poland, Italy, and the United Kingdom have their own standards as well.

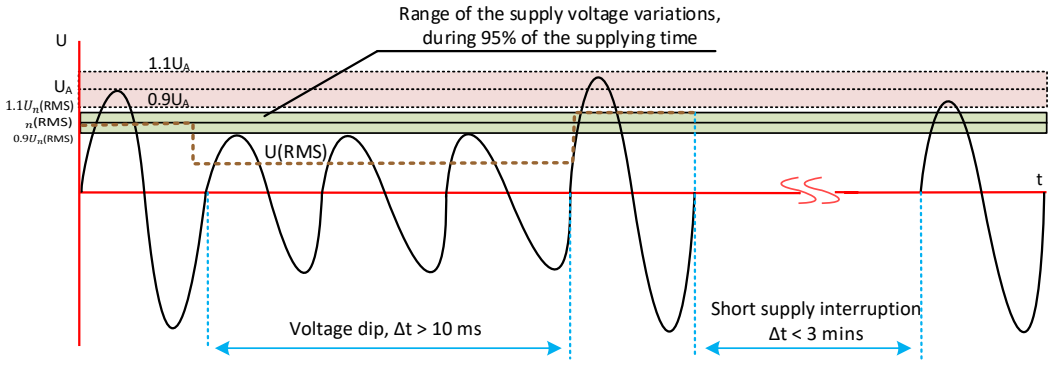

Figure 2.2.: Illustration of Voltage Dip and a short supply interruption according to EN50160 [30]

2.1.3 Smart Grids and Power Quality

The Smart Grid is defined as an electrical grid comprising a variety of operational and energy control, including smart meters, smart appliances, renewable energy resources, and energy efficiency resources [36]. So by analogy, just like the Internet is the networking of people, the Smart Grid is the networking of things that generate, distribute, and transmit energy. According to the European initiative envision [37], the Smart Grid must be flexible, accessible,

reliable, and economically efficient. These features can be enabled by installing automation and monitoring technologies at the distribution level, which facilitate system status to be captured in local and regional settings and allow the DSO to detect and fix imminent outages sooner than before and rapidly confine fault areas [38].

The ICT infrastructure allows a flow of information that has never existed before the Smart Grid. Thus, the power grid can also support self-healing with detection, isolation, and probable corrections of faults [39].

The Smart Grid comprises several elements that help utilities to deliver better quality power to miscellaneous consumers, e. g., Advanced Metering Infrastructure (AMI) and technology on the distribution grid that facilitates to control voltage and Power Factor (PF)[3]. AMI is one of the most critical components of the Smart Grid, which provides bidirectional communication between smart meters and utilities. However, smart meters are advanced electric meters that provide more information about the power delivered to consumers[4], e.g., what the actual voltage delivered to a household is. Before smart meters, the configurations of grid equipment are set by the DSOs based on voltage readings at an electric substation and engineering estimates of what that would imply for actual voltage at each consumption node. thereby, the voltages are often set "unnecessarily" higher to ensure that the last load node on a feeder line does not receive voltage below $U_n \pm 10\%$, according to EN 50160. Whereas, a more efficient and accurate supply of power is enabled through actual information on voltage, which allows in its turn an optimization of the voltage for every customer using Smart Grid technology.

2.2 Electric Vehicles

EVs are one of the emerging technologies that are counted on to minimize the carbon footprint of the transport sector hand in hand along with the usage of Renewable Energy Source (RES). Researchers expect impressive results in that direction endorsed by the fact that electric motors are very efficient energy converters (85%) in comparison to a combustion engine (30%) [40].

However, the term EV is very generic and hides many types behind it; therefore, it must be clarified within the context of this work. To that end, any vehicle using electrical energy partially or entirely for moving is called Electric Drive Vehicle (EDV). As depicted in Figure 2.3, they can be distinguished in supply line bound vehicles like trains, or trams, and grid-independent vehicles. The latter includes: (1) vehicles powered completely or significantly by direct solar energy via PV cells, (2) pure electric vehicles using chemical energy stored in rechargeable battery packs, (3) hybrid vehicles using an additional energy source besides

[3]Power factor measures how much of the electricity delivered is actually usable by customers.

[4]Typically, the installation and interconnection of more expensive and advanced measurement devices, Phasor Measurement Units (PMUs), is designed by electrical engineers at a substation or at a generation plant.

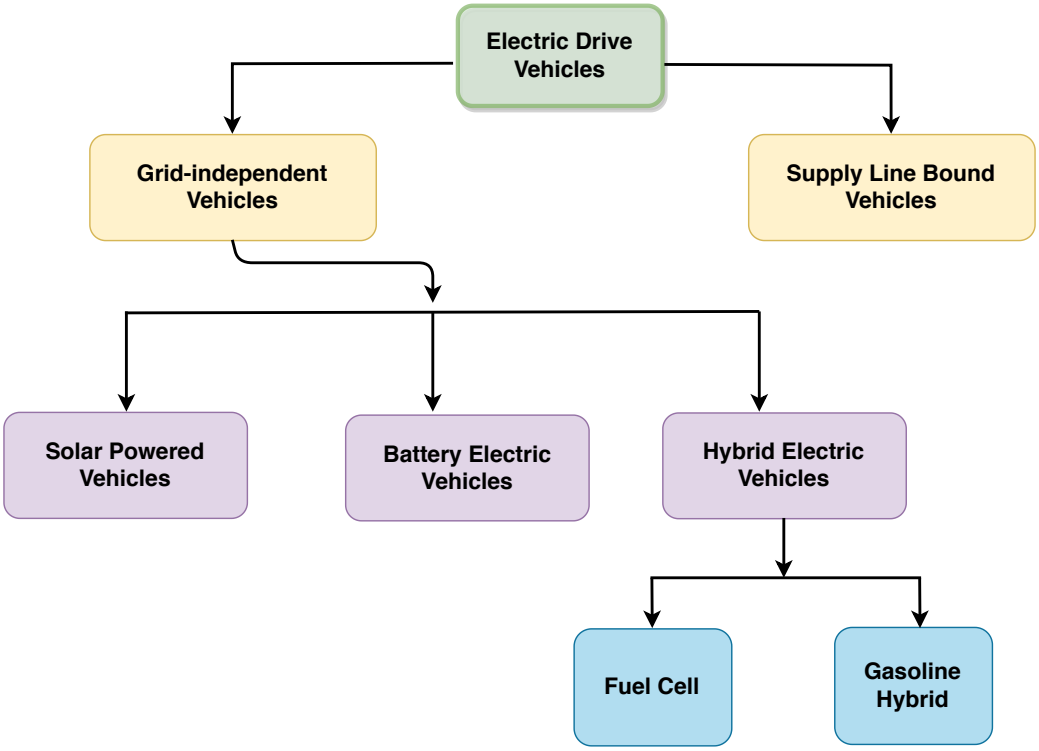

Figure 2.3.: Classification of Electrical Drive Vehicles, Adapted from [38, 41]

the electrical storage element. Though, this work focuses on the second type, "Battery Electric Vehicles", which needs installation of public or private CSs to provide them with the required energy from the grid.

EVs provide some exclusive benefits; for example, they are very responsive and have outstanding torque since their motors react quickly. Furthermore, they are often more digitally connected than conventional vehicles, and the maintenance cost of these cars has come down as well. Apart from those specific benefits, EVs have some general advantages according to [42]:

- No local emission, which is beneficial for urban areas.
- Less noise pollution with speeds under 30 km/h since they are quieter and drivers experience less stress.
- Representing potential storage and demand flexibility for the power grid, which leads to more integration of RES.

Although the evidence of the advantages has become very clear, there are also some drawbacks as well:

- Range anxiety.
- Very expensive because of battery technology. Batteries of almost all EVs have an 8-year warranty [43].

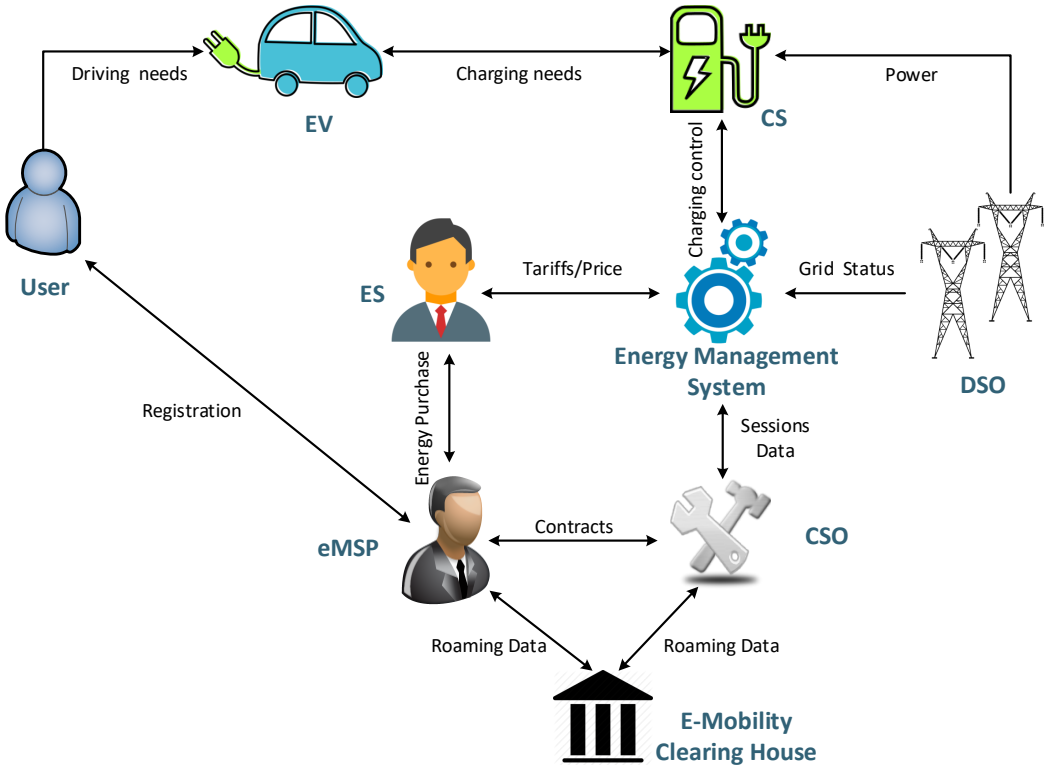

Figure 2.4.: Interaction Among Energy-related Actors in EV Ecosystem

- Recharging points are not available everywhere and still in the roll out stage.
- Charging times are usually too long in comparison to the refueling time of conventional vehicles.
- EVs represent additional and relatively big loads in the power system, notably, in the distribution grid, which in turn cause new challenges to the grid operators, e. g., voltage instability, increased peak demands, and overloading of transformers.

2.2.1 Ecosystem of Electric Vehicles

Many different actors (Stakeholders) do exist in the EV ecosystem as depicted in Figure 2.4, directly and indirectly increasing the complexity of such a system. Throughout this section, the concepts should be held as generic and clear as possible, without defining business models or realistic system integration or implementation. Next, the main actors are described:

1. EV (User): A private person who owns an EV with(out) adopting the sharing mobility model. (S)He needs to register by an e-Mobility Service Provider (eMSP) to be able to use its public CSs. The fundamental role of this actor is to drive from A to B and give information about the trip to the eMSP, e. g., driving distance, and time of availability.

2. eMSP: It grants access for EV users to the charging infrastructure by issuing a RFID-card. Thus, it handles all communication and billing of EV users.

3. Energy Management System: It is a logical function that optimizes energy consumption based on grid signals, market environment, contracts, and device minimum performance standards. It can be a part of the CS management system operated by the Charging Station Operator (CSO) or the home/building energy management system.

4. CSO: It might own and operates CSs. Its responsibilities probably extend to contain the operation of parking spots and granting physical access to them. The management of CSs is carried out by implementing communication protocols such as OCPP[5] and IEC 61850 [44], which enables, in its turn, to collect the required data for billing. However, these roles of eMSP and CSO are not separated in all markets; they are filled in by the same party so-called CSP in some countries.

5. DSO: It is operating in the medium and low voltage power grid and is responsible for distributing electricity to end-users in a reliable way. Furthermore, it is assumed to be able to provide information about the different sections of its grid, e. g., 24-hours forecast of available power capacity or real-time data. An example of such a communication is given in the Open Smart Charging Protocol (OSCP) standard[6]. Thereby, the CSO proposes a set of charging profiles[7] to an EV to select from. The CSO builds those profiles based on capacity forecasts provided by the DSO through OSCP messages, energy tariffs, and the business model of the CSO.

6. Energy Supplier (ES): The ES buys energy from the market or via direct contracts and sells it to the end consumers. As an exception from the EU unbundling legislation package, for small utilities, the ES may also be an energy producer, namely, an owner of a small renewable system. The ES provides the CSO with energy tariffs for a predefined time horizon.

7. e-Mobility Clearing House: It is responsible for enabling the roaming service through establishing an open and neutral service for making the charging activities accessible between different operators. For example, It provides eMSP by global charge point information via communication with CSOs.

In addition to this relatively big number of different stakeholders in this immature market, a variety of different technical integration and standards is observed as outlined in Figure 2.5. Smart charging is now adding another layer complexity to a highly complex ecosystem.

[5] https://www.openchargealliance.org/

[6] https://www.openchargealliance.org/protocols/oscp-10/

[7] Charging profile is defined regarding the specifications of OCPP 2.0 as time depending profile containing information about the maximum charging capacity and the used phase that can be used by the CS during a certain time slot

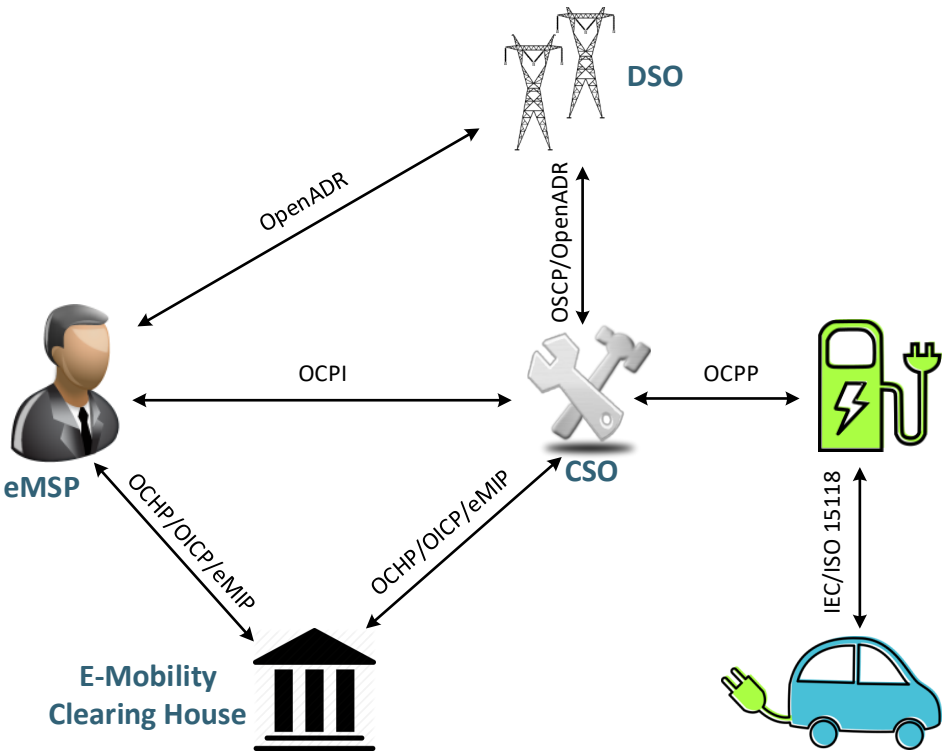

Figure 2.5.: Non-exhaustive Overview of Existing Standards in EV Charging

2.2.2 EV Charging

To recharge, EVs must be typically connected to the power grid. Such integration has two dimensions: first, the physical connection of the EV to the power grid, and second, the charging coordination in order to guarantee a smooth charging operation without any negative impact on the grid [45, 46]

The physical connection is carried out through Electric Vehicle Supply Equipment (EVSE) or shortly CS that provides a range of heavy-duty or special connectors that conform to the variety of standards. There have been a variety of different connector types and charging modes. Mostly they map the geographical area requirements of the vehicle being run or manufactured in. For example, those developments were influenced in particular by the unique voltage characteristics of the U.S. power grid and the European network. As a result, there are two dominating standards: SAE J1772 and IEC 62196.

"Charging can be performed in different modes and with different types of connectors. In addition, there are different power levels that are specified for the respective charging modes. Charging modes refer to the specifications and the infrastructure employed for charging. The modes also specify charging currents and, therefore, the power that can be used for a given system voltage . The charging power determines the impact the demand of the EV has on the grid." [38]. As depicted in Table 2.2, the available power ranges between 1.8 and 43.6 kW. The EU standard outlets and residential connections allow charging of the

EV at rates up to 11.1 kW. Higher powers are restricted to the public and dedicated private charging stations with powers from 11.1 to 43.6 AC, or 50kW DC.

Charging Mode	Charging Levels	Charging Plug	Voltage [V]	Phase [#]	Current [A]	Power [kW]
1, 3	EU Standard	CEE 7/Type 2	230	1	16	3.7
	EU Semi-Fast	Type 2	230	1	32	7.4
	EU Semi-Fast	Type 2	400	3	16	11.1
	EU Semi-Fast	Type 2	400	3	32	22.2
	EU Fast	Type 2	400	3	63	43.6
1, 2	US Level 1	Nema 5-20/Type 1	120	1	15	1.8
2, 3	US Level 1	Type 1	240	1	30	7.2
4	US Level 3 DC	CHAdeMO/Type 4	50-500	-	100	50
	EU Fast DC	Type 2 Combo	500	-	140-200	100

Table 2.2.: Overview of Charging Modes, Levels, Plugs and their Specifications, Values for $cos\phi = 1$ [38]

In general, EV charging can be performed in the following three ways:

1. **Uncontrolled Charging (UC):** refers to a scenario where charging of EVs is not controlled by any mechanism. That can also be referred to as a dumb charging strategy where EV is charged continuously from the time it is plugged in till the charge is complete, for example, as soon as the user arrives home [47]. The charging starts as soon as the car is connected to the socket, like any other electrical equipment. Concerns of the grid operator are not taken into account as electric cars typically charge with maximum power to achieve a high SoC by the end of the charging cycle[8]. This type of charging during peak hours leads to increased grid stress, particularly into distributions networks. Uncontrolled charging of EVs can lead to several problems in terms of grid stability and cannot be continued with the increasing EV penetration in the grid in the near future.

2. **Plain load shifting:** To avoid the problems of uncontrolled scenario, strategies like charging the EVs during designated off-peak hours of the day are usually applied. This method works to some extent in shifting the load to off-peak hours, but it might result in a new peak with an increasing number of EV adoptions [48]. Time switches and ripple control implemented commonly in Germany are examples of his straightforward approach. While time switches just switch off the charge point during envisaged peak times of the grid, the radio ripple control is sending a signal via the power line, which is then read by a specific device which switches off the power supply to the charge point. This type of charging can be considered as a preliminary smart charging strategy.

[8] Precisely, the battery management system determines by itself the required power as soon as the EV is connected.

3. **Advanced Smart Charging:** The simplest and straightforward definition of intelligent charging is applying any kind of control through the charging operation unlike unconditional charging. Thereby, the power availability of the grid and the distributions of resources with consideration of both grid stability and user satisfaction [49] are taken into account. There are two possibilities for its realization: (a) The open-loop where the charging is controlled using price signals, which can be considered or ignored by the customer. (b) The closed-loop where the charging is controlled using price and technical signals in relation to a combination of constraints such as overload risk. The solution proposed in this thesis adopts the second option.

However, different kinds of smart charging approaches (including a and b) enable EVs to provide flexibility to the power grid as depicted in Figure 2.6

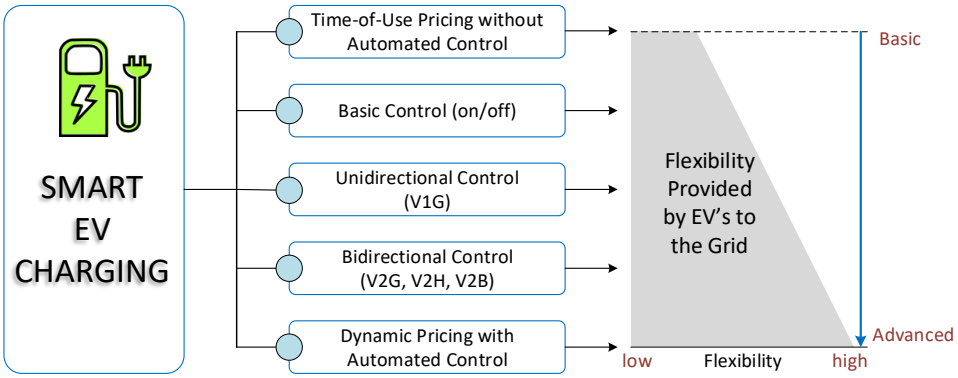

Figure 2.6.: Flexibility enabled by EV Smart Charging (Source IRENA [50])

2.2.3 Main Factors of EV Smart Charging

Intending to increase the EV penetration in order to reduce the carbon footprint of the transportation sector [51], researchers focus on EV smart charging as a solution for making EVs more attractive to customers. Every smart charging approach has to be clear on its objectives. Hence, it is crucial to distinguish among the different design factors through developing new intelligent charging strategies. In the following section, the main design factors depicted in Figure 2.7 are highlighted.

A. Direction of Power Flow

The direction of the power flow is an essential factor to be considered when designing a smart charging algorithm. The power flow can be either unidirectional or bidirectional. While a vehicle can only fill up its battery by charging through the former, the vehicle can also feed in a portion of the stored energy back to the grid for other purposes by the latter.

A.1 Unidirectional: It is the traditional method of charging, the so-called Grid-to-Vehicle (G2V) or (V1G), where the power flows from the power grid to the rechargeable batteries of EVs like any other electric load, thereby, the vehicle is charged enough to be

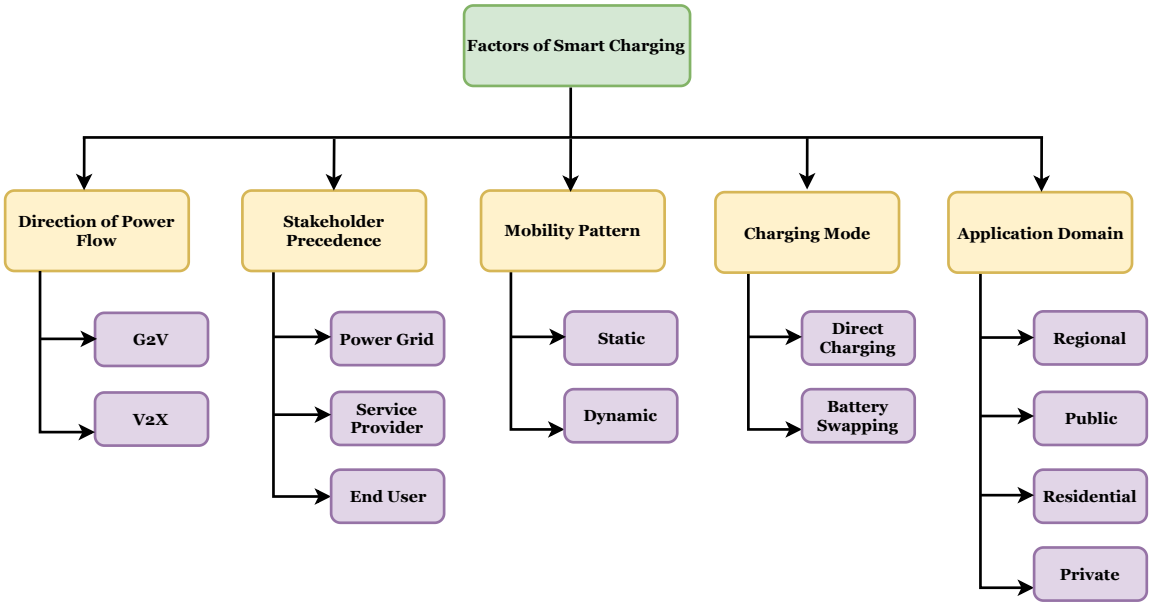

Figure 2.7.: Smart Charging Factors

used for the next trip. Since the charging demand is seen as a relatively big and extra load in the distribution grid in comparison with the other loads, smart charging algorithms are applied to facilitate the network operation without any concrete difficulties because of the limitation of grid resources.

A.2 Bidirectional: The algorithm incorporates control strategies for both charging and discharging of vehicles. There are different kinds in bidirectional charging like Vehicle-to-Home (V2H), Vehicle-to-Building (V2B), Vehicle-to-Vehicle (V2V), and V2G. While EV batteries can be used as a power source by individual EV owners at home either during outages or on the purpose of reducing household load by V2H [52, 53], V2V [54] facilitates the electricity exchange among a group of EVs in a community. Thus, it helps to keep the power reserve within the community and to reduce the grid load. V2G [55] is the most common bidirectional charging where the exchange of electricity is between grid and EV.

Despite the advantages of Vehicle-to-X (V2X) technology, such as supporting an efficient integration of renewable energy [56] and a seamless operating of power grids in terms of PQ [57, 58], it still requires improvements in the market for commercial use. Furthermore, a suitable incentivizing program for the EV owner is necessary in order to encourage ignoring the rapid battery degradation due to frequent charge and discharge activities [59]. It is worth mentioning that many of the proposed G2V smart charging approaches are structured in such a way that it is enhanced to incorporate V2X charging in the future.

B. Stakeholder Precedence

As described in Section 2.2.1, there are four main stakeholders involved in an ecosystem

of EVs: grid-relevant actors (DSO and ES), CSPs, and EV users. Clearly, all of them have conflicting goals; thus, a smart charging approach shall be a balanced compromise of all requirements and goals. To clear the main objectives of a proposed solution, the designer has to contemplate the precedence of each actor. There are three possible focus points for the precedence factor:

B.1 Grid: Smart charging schemes [24, 60, 61] are built with the focus on mitigating grid-related concerns due to the high EV penetration. The main grid-related challenges are load flattening, PQ concerns, economic costs, resource availability, safety concerns, and supply-demand management. However, grid-oriented strategies can attend to user-satisfaction by adopting incentive schemes as a reward to the users for their contribution towards maintaining stable PQ in the grid.

B.2 EV-related service provider: Any actor in between an EV user(s) and the power grid belongs to a this set of actors, e. g., EV aggregator, residential EV fleet operator, and CSP. Since such an actor is an intermediate actor, it intends to balance both user and grid requirements in order to reduce the installation, operational, and maintenance costs. Furthermore, the service providers aim to maximize their profit by selecting an optimal charging strategy for the connected EVs, wherein the utilization of the charging infrastructure increases the profit increase as well by exploiting the incentives introduced by the grid operator.

B.3 End-user: The developed approaches in this category [62, 63, 64, 65] focus on delivering satisfying charging energy to the user, e.g., meeting the user demand by maximizing the available charging energy taking into consideration the primary grid constraints. However, delivering complete user satisfaction during charging can be a challenging task due to the various financial, infrastructural, and grid constraints. The main issues related to the user are minimizing charging costs, driving range, security, battery properties, higher SoC, and short waiting times. The user satisfaction level can be measured based on how well the strategy tends to the user concerns mentioned above.

The authors of [66] review and discuss thoroughly different charging controlled strategies with respect to the concerns of the grid, service provider, and user. Although finding a balance between the user and the grid is a common goal and intention of all approaches, most of them usually tend to lean towards one more than the other. As a result, the precedence criterion is vital, as it helps to set a clear goal on what aspects of charging will be given more importance and what parameters are considered.

C. Mobility Pattern

By developing a smart charging solution, real scenarios for simulation are required in order to show the usability of the solution in real life. Considering the different mobility aspects

such as dynamic arrival/departure times give an opportunity to researchers for generating such real scenarios on one hand. On the other hand, it increases the complexity of the problem formulation. According to [67], there are two possibilities for modeling the EV mobility for the simulation sake:

C.1 Static: The EV is considered as a fixed load for a certain time. The EV stays plugged in the CS for the whole considered time duration and the temporal factors are ignored completely [24, 60, 68, 69]. The static assumption is not realistic, but it helps in studies to get an idea of how the algorithms work and the main parameters needed to formulate the problem definition.

C.2 Dynamic: The researcher considers any sort of mobility traits by the strategy design and evaluation. There are two possibilities for studying the dynamicity of the mobility patterns: (1) The different information of EVs such as individual arrival/departure time is assumed to be available beforehand through either user's input or forecasting methods [70]. (2) It is assumed that no prior knowledge is at hand, and the arrivals/departures of EVs are unpredictable besides other information such as initial SoC and required energy [71, 72, 73, 74]. Although the first option is unrealistic in many cases; nevertheless, it is used to focus on understanding the core methodology and parameters.

D. Mode of Charging

There are two ways to provide an EV with the required energy, namely, direct charging by connecting the EV to an energy supply equipment and swapping the near-empty EV battery for a full one at a Battery Swapping Station (BSS).

D.1 Direct Charging: As mentioned in Section 2.2.2, the EV can be charged via either AC or DC by using a single phase or three phases. The charging time is in the ranges from 6-24 hours depending on the capacity of EV battery by slow charging (up to 11 kW). The charging with up to 20 kW reduces the charging time to 2-8 hours. The DC charging method is used to charge EVs rapidly (up to 100 kW) in 10-30 minutes [46]. This kind of charging is usually found at commercial places or gas stations.

D.2 Battery Swapping: This is the fastest method for the EV user as it provides an immediate charging solution. It is especially popular among public transport like electric taxis or buses. The research on the challenges of battery swapping is less common when compared to direct charging [75, 76]. While there are obvious advantages of this method for an end user, efficient use of stored batteries at the BSS can act as storage devices, provide V2G facilities, and make renewable source a reliable alternative. However, smart charging strategies are also relevant for the BSS to control charging or discharging of the stored batteries [77, 78, 79].

E. Application Domain

Developing a smart charging architecture needs dimensioning of the segment of reality for which the architecture is designed. The size and technical specifications of the studied system play a significant role in designing and deploying the solution. There are four possible application domains where the smart charging approach can be applied:

E.1 Regional/Sectional: The solution is applied by the utility to the whole low voltage grid (or a bigger section of the grid). The solution maintains simultaneously multiple parking lots, CSs, and wall boxes [60, 80, 81].

E.2 Public: Smart charging schemes applied individually on scenarios of public EV service providers like CSs, parking lots, multiplex, etc. [72, 82].

E.3 Residential: Strategies for controlling the charging of residential community, or building EV management are designed [64, 83, 84].

E.4 Private: The controlling strategy is applied only on the installed system at the households, namely, wall boxes [85, 86].

Hence depending on the objective of a particular smart charging architecture, the control strategies can be implemented at different levels of the distribution grid. Some research work considers multi-level architecture, which involves EV charging control strategies to be present at one or more levels [87, 88, 89, 90].

2.2.4 A Classification of Charging Management Approaches

Charging management includes strategies that focus on the algorithmic way of controlling and scheduling all controllable active EV charging operations in parallel. There are many pilot projects on charging management and numerous research efforts every year for developing efficient and smart approaches. This section focuses on the classification of G2V approaches[9]. Since the classification is built from algorithmic point of view, it does not take into account the infrastructural, communication, or storage costs. Sub-classes in charging management strategies are explained below.

A. Time Scheduling

Time scheduling is a strategy where an algorithm decides a charging plan for either an EV or a set of EVs. However, a simple charging plan in terms of scheduling is a set of binary decisions, whether to charge an EV or not. It can be extended to include information about the charging's start and stop times, charging locations, and charging rate. Apart from that, the main objective of time scheduling is shifting the load to off-peak hours in order to fill the overnight valley of the power grid load curve along with satisfying user

[9]The same classification is valid for V2X, it can be extended in the same way.

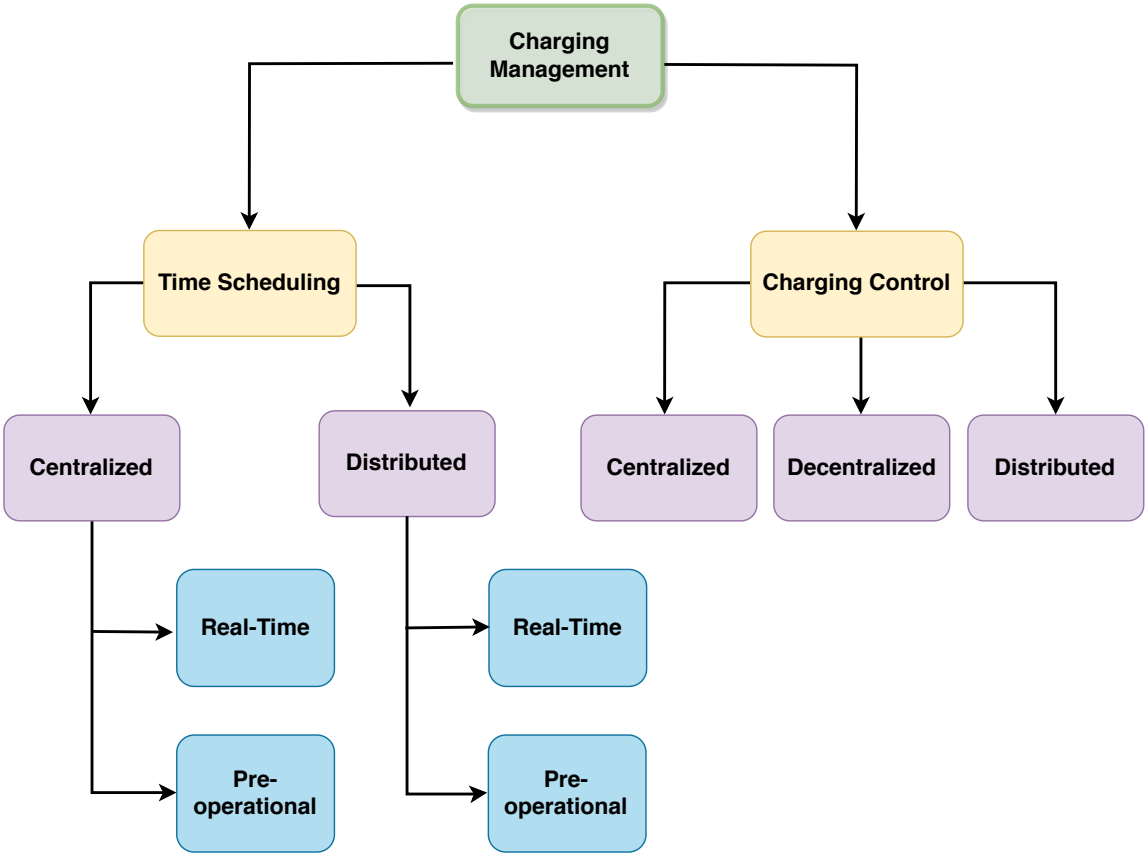

Figure 2.8.: Classification of Charging Management Approaches

requirements. Time scheduling can be implemented in different ways; on one hand, the schedule decision can be made either centrally or distributively. On the other hand, it can be either pre-operational/day-ahead scheduling or real-time/decisive scheduling. The different kinds are explained in the next sections.

A.1 Centralized Time Scheduling: It is a type of scheduling where the charging schedule of EVs is directly determined at the central aggregator. The aggregator function is usually either placed at a CSP or performed by an EV fleet operator to the subscribed EV owners. However, two possibilities of carrying out the scheduling are stated next:

- **Pre-operational Scheduling:** This kind of scheduling [70, 91, 92] usually assumes a static scenario of EVs. The aggregator calculates a day-ahead charging schedule of EVs based on the EV charging demands and historical information. EV information such as driving pattern, arrival/departure, and charging properties of the EV are used by the aggregator to forecast the EV load or the energy consumption of future trips. The information mentioned above can be obtained not only through prediction but also by direct inputs from actively participating or subscribed users. Other information such as conventional load and electricity prices can also be predicted/calculated by

the DSO and ES or the central aggregator itself. There are numerous prediction and energy analysis studies proposed in research work [93, 94, 95].

However, the EVs are assumed/expected to follow this schedule motivated by incentive or reward schemes [96, 97]. Thus, the charging schedule can be seen as a recommended optimal schedule for EVs to minimize the cost of EV charging rather than a hard restriction [62, 83, 98].

- **Real-time Scheduling:** The adaptive scheduling algorithms [74, 82, 99, 100] go under this category in terms of considering the dynamic change of the ecosystem parameters, e.g., the arriving/departing of EVs and the violating of grid constraints. For example, in [83], though the aggregator pre-schedules charging time in advance, the charging priority of plugged-in EVs are calculated by aggregator in real-time. EVs are selected to charge according to the priorities values, and if the target load is reached, EVs with the low priority are scheduled to charge in the next time-step.

A.2 Distributed Time Scheduling: The concept of distributed scheduling is that the schedule decision is the combined effort of higher and lower entities in the system [87, 88]. In this type of time scheduling, though the schedule of charging times is decided by EV users or at CSs - to charge or to be idle for each scheduling interval of a connection period -, the computational presence of higher entity in the system is essential to decide on the final charging schedule. For example, the waiting time at a CS or an energy cost value based on the total load demand is calculated and sent back to the end entities to re-evaluate their decision [101]. A game-theoretical approach is used to obtain a near-optimum charging schedule for the day by each EV charger [102, 103]. This schedule decision, similar to centralized scheduling, can be performed pre-operational/time-ahead or in real-time.

B. Charging Control

By approaches classified under this category, the distribution of power resources among the EVs being charged is regulated in real-time based on a grid or EV-related factors, unlike time-scheduling. There are plenty of charging control strategies in the literature. They are differentiated through the efficiency and the studied use case. To the best of the author's knowledge, the research under this classification usually follows real-time strategies. Nevertheless, the control strategies can be classified into three categories [38] based on the location where the majority (entire) of the charging decision is carried out, namely, centralized, decentralized, and distributed.

B.1 Centralized Charging Control: These approaches involve maintaining a master-slave relationship, where the central unit has control over the end nodes of the network, usually EVs. It is the most common control strategy and has been studied by many research work as a method to incorporate coordinated EV charging [62, 63, 64, 69].

Here, a central aggregator or a central intelligent unit holds the sole responsibility of calculating optimum charging power for all connected EVs. The aggregator can be maintained by

the utility (DSO) or CSP. The centralized structure of the smart charging infrastructure also depends on the size of the problem under consideration, hence positioning of the central unit (discussed in Section 2.2.3) can be in multiple locations in the power distribution grid, e. g., multiple parking lots.

The aggregator, wherever positioned, has to have the highest level of knowledge regarding its child elements to monitor and control the charging process. Bidirectional communication between elements of the power grid and aggregator is necessary. For example, an EV aggregator collects information from the EVs regarding various charging parameters, such as maximum charging rate, charging period, arrival/departure time, expected SoC, battery type, etc. depending upon the parameters used in their algorithm. Most of the research work assumes this knowledge is held at the aggregator with negligible communication delay using communication technology.

While the centralized approaches would be an easy and convenient strategy for the controlled charging of EVs, they are unreliable due to the existence of a single point of failure. Moreover, they have scalability issues because of the high communication requirements as well as computation time, which is not practical for a large fleet. Finally, users are not comfortable to hand over their charging control and trip information to an aggregator [38].

B.2 Decentralized Charging Control: It includes strategies where complete control of the EV charging process is solely at the lowest node, namely, CS/EV. The decentralized charging control is predominantly price-based mechanisms [104]. The charging power and time are decided at EV to minimize the charging price and maximize the SoC at the same time. Hence the charging control is entirely independent. While the electricity price is made known to the EV users via an ES, other information such as user preferences and battery properties are known and available locally at the Database (DB) of the local node. In a strictly decentralized approach, each end node makes its controlling decision despite other end nodes in the ecosystem; however, it can be enhanced by adding price calculation strategies at higher levels to solve grid-related concerns [105, 106, 107, 108]. It is safe to assume that most decentralized charging control is mainly user-oriented; nevertheless, some approaches consider the local voltage as the only indicator of the grid status in order to alter the used power capacity[23].

B.3 Distributed Charging Control: It can also be termed as a hierarchical coordination strategy. There is an EV aggregator or a higher unit, which does part of the computation, and other end nodes. In other words, the work of the charging decision is neither the sole responsibility of a higher unit nor independently decided by the end nodes. That requires multiple entities in the architecture to work together to calculate an adequate charging power. However, the higher unit can do a calculation of either a service-price or an indicator of the situation at the grid, e. g., congestion signal [24, 61] and peak-shaving [109]. The communication among the higher and lower entities can be unidirectional [24,

65, 81], or bidirectional [109, 110]. For example, authors of [109] propose an approach where an EV sends its charging decision back to the higher unit.

In contrast to the centralized control, EVs need not share their information with the aggregator or among themselves preserving their privacy, which in turn means, the upper-level node needs not to reveal its own sensitive information. The distributed control can be perceived as the combination of centralized and decentralized approaches. It is recognized that they are similar to the centralized methods by the presence of an aggregator or higher computational unit, but retaining the control at the end node makes them closer to the distributed ones. Another advantage is that there is no single point of failure, hence distributed control is more reliable and robust, also scalable as the integration of additional agents do not require significant changes to the overall system.

2.3 Summary and Discussion

Heretofore, DSOs have the responsibility to meet the requirements of PQ (see Section 2.1.2) in their low and medium voltage networks. Due to the increasing installation of CSs and RESs, such a task becomes more challenging. Especially, the PQ parameters of a feeder line can change noticeably due to unexpected and unusually high loads. Furthermore, the location of that load plays a significant role; the closer to the transformer, the less relevant PQ impact on other consumers connected to other feeder lines, as will be seen in Chapter 3.

Load adjustment is used by DSOs to counteract some PQ-relevant issues in the distribution grid, specifically, voltage control. It has been mostly performed on relatively big loads such as CSs. Unfortunately, load control cannot affect all different aspects of the PQ since they are too volatile and short-lived. For example, harmonics introduced by the rectifier of one or multiple CSs/EVs, flickers, and short-term voltage drops in the range of 100 ms to 300 ms. Additionally, EN 50160 determines the boundaries to comply with as the average values of ten minutes or two hours. Hence, the short-term flicker does not violate these boundaries since it is a voltage deviation in a time interval of much less than one second. Due to these reasons, load control is determined as a strategy for long-term voltage regulation.

As contrary to the high and medium voltage grids, one phase connections can be found in the low voltage grid, which in turn causes the appearing of voltage imbalance because of the unequal loads on the single phases. In general, public CSs are connected via three phases; nevertheless, the number of used phases depends on the technical specification of either the EV or the CS. For example, a Renault ZOE can be charged with only 10 Ampere by using a domestic single phase socket. Still, it also supports also 3-phasing fast-charging up to 32 Ampere. Hence, an appropriate approach deciding about the used phase and the used power could help to mitigate voltage unbalances as we will see in Chapter 3.

The stabilization of the frequency of the public AC power systems is mainly the job of the Transmission System Operators (TSOs) and balancing groups. While a higher grid frequency indicates a lack of demand (plus losses) in comparison to the feed-in, lower frequency points to the contrary, hence, a load control at a large scale could provide an additional mean in order to stabilize the frequency. Although the regulation of the charging power to react to the current frequency situations is feasible, this large scale orchestration of CSs is out of the scope of this thesis.

Smart techniques of charging management are a necessity to help in a smooth transition of a high EV penetration in the coming years. To that end, charging management should go hand in hand with infrastructural advancements such as AMI and RES integration, which in turn supports the successful adoption of e-mobility as the future form of transport.

Time scheduling strategies focus on shifting the load in time to manage the charging demand of EVs with the objective of the valley-filling of the power grid load curve. Most scheduling strategies rely on predicting strategies based on historical data. Hence, the time scheduling carries a major disadvantage as the user behavior is irregular, and assumptions about the user-related uncertainties can bring down the performance of the strategies. Though some real-time scheduling strategies do not depend on the predicted data [111], time scheduling strategies, in general, do not focus on the charging rate modification. Hence, charging control strategies give potentially more flexibility to the grid operator in order to overcome in real-time the emerging issues such as congestion of the grid elements and PQ issues.

Among charging control strategies, many studies adopt centralized approaches that possess a distinct disadvantage of being a single point of control. Extensive communication overhead, costs, scalability are some of the limitations of centralized strategies. Furthermore, a coordinated control at different levels of a hierarchical distributed system such as the power grid becomes infeasible with centralized control, as discussed in [112]. Decentralized charging control theoretically overcomes the aforementioned problems by making the EVs take complete control of charging, so the problem size is reduced to just one unit. There might be an imbalance in the orientation of the architecture as the pure decentralized strategies do not adequately heed to the grid-related concerns [113]. Assuming the pricing scheme is fixed, it suffers again from prediction errors.

Additionally, decentralized approaches either depend only on local grid data at the CS or assume all the necessary grid data is available locally at the controller. While the former assumption is not enough to reflect the grid status completely, the latter ignores the fact of data lacking from the distribution grids. In contrast, the distributed charging control follows a hierarchical control strategy, where both grid and user-related concerns are accounted as it retains the control at different points in the power system. The computational load is distributed among the active participants, which reduces the stress on the aggregator or upper entities. Data and control are partly localized, addressing the data privacy concern

of users. Furthermore, the EV charging ecosystem contains multiple actors who prefer to share information about their assets as little as possible, specifically the DSO about the low voltage grid. Therefore, distributed approaches are likely the best solutions to keep the communication among the actors as low as possible and to separate the different concerns of ecosystem actors.

Most existing distributed solutions focus on calculating the price signal on the higher nodes, e. g., aggregator. Some of them ignore the complexity of the power grid entirely and assume an indication of a power grid status is given or calculated in a centralized way. That calculation considers either the voltage or the congestion in the grid. A sophisticated indication mechanism is required where more PQ parameters can be integrated easily. Further, an efficient communication scheme for exchanging required data among the software components is a priority to reduce the cost and delay as well. To the best of the author's knowledge, all smart approaches do not take into account the little incentives right now but focus only on the overall economic benefit for society, which unfortunately is not yet reflected in the regulatory regimes. Heretofore, a reward system incentivizing a grid-friendly behavior of a consumer is missing, so a realization of such a scheme is a valuable benefit of any solution, as depicted in Table 2.3, where the second column (R_1) contains only (x). Moreover, Table 2.3 shows the big focus on solving the congestion problem in power grid (columns R_3 and R_4) while voltage issues are little addressed (R_2) since considering them adds more complexity to the studied system. Furthermore, most of the related work sees the management problem of EVs charging only from an algorithmic perspective, therefore, applicability concerns such as interoperability are completely ignored.

Ref.	R_1	R_2	R_3	R_4	R_5	R_6	R_7	R_8	R_9	R_{10}	R_{11}
[80]	x	x	✓	✓	✓	✓	✓	x	x	x	✓
[114]	x	x	✓	✓	✓	✓	✓	x	x	x	✓
[115]	x	x	x	✓	✓	x	✓	✓	x	x	✓
[116]	x	✓	✓	✓	x	✓	✓	x	x	x	✓
[117]	x	x	✓	✓	x	x	✓	x	x	x	✓
[118]	x	x	✓	✓	x	✓	✓	x	x	x	✓
[119]	x	x	✓	✓	x	✓	✓	✓	✓	x	✓
[120]	x	✓	✓	✓	✓	x	✓	✓	✓	x	✓
[121]	x	x	x	✓	✓	✓	✓	✓	x	x	✓
[122]	x	x	x	✓	x	✓	✓	✓	✓	x	✓
[123]	x	✓	✓	✓	✓	x	✓	✓	x	x	✓
[124]	x	✓	✓	✓	✓	✓	✓	✓	✓	x	✓

Table 2.3.: Analysis of Selected Articles According to Design Requirements Mentioned in Section 1.2

Based on the previous discussion, a novel distributed grid-friendly smart charging architecture is proposed in this thesis, which considers the real-time conditions of the grid by using an event-driven architecture to collect data. Additionally, the approach applies a smooth

change of the charging power capacity to avoid drastic grid state changes. Inspired by Internet, the architecture is based on a novel notification mechanism in smart grids. It informs the control units about both the overloading of the grid elements (specifically the transformer and feeder lines) and the voltage magnitude at specific points in the grid, e. g., at a CS or critical points in the grid. Although the architecture supports only the V1G paradigm, it can be extended to V2G one. Last but not least, it takes into account the different condition on each power phase so a kind of phase balancing is enabled.

Next, the means of controlling PQ via CSs are discussed not only theoretically but also via simulation.

3 Means of Controlling Power Quality using EV Charging Stations

In the context of electric circuits, an electrical load is a component in which the current is transformed into other forms like heat, light, work, etc. From the circuit perspective, a load is defined by its impedance, which comprises Resistance (R) and a Reactance (X)[1]. From a physical standpoint, loads are seen as the electrical characteristics of individual devices.

Through considering a load as being defined by its impedance, any low voltage grid can contain three basic types of loads:

- Resistive loads: They consist of any heating element such as lights and toasters. It draws current in the same proportion with the apply voltage.
- Inductive loads: Electrical motors are the main parts of these loads; fans and vacuum cleaners are two examples of many. In a purely inductive load, voltage leads the current in an AC system, so a delay or phase shift of the maximum, minimum, and zero points occurs. Hence, an inductive load consumes reactive power.
- Capacitive Loads: They include energy stored in materials and devices, such as capacitors. No devices are assorted as a stand-alone capacitive load in the way light-bulbs are labeled resistive, and air conditioners are categorized inductive. In contrast to the inductive loads, the current leads the voltage in capacitive loads.

Loads are typically modeled in an aggregated way in the broad context of power systems. So “load” may denote to an entire household, a city block, or all customers within a given area. Consequently, the term load has attributes beyond impedance which relate to aggregate behavior, such as demand timing, from the perspective of electrical utilities.

The focus of this chapter is a public EV charging system as an emerging and non-trivial aggregated load in the distribution grid. It consists of electric elements with different characteristics; hence, it cannot be classified as one of the aforementioned pure types. Therefore, a closer look at the architecture of an EV charging system is taken in Section 3.1. Wherein, the different possible control parameters of a CS are discussed in detail theoretically

[1] According to [33], the electrical resistance is the property of a material or electric device to resist the flow of direct current through it, while the electrical reactance is is the property of a device to influence the relative timing of an alternating voltage and current due to that element’s inductance or capacitance.

and by simulation in Section 3.2. Consequently, a formulation of an optimization problem describing a grid-friendly operation of a CS using the identified parameters is introduced in Section 3.3.

3.1 EV Charging System

Technically, all charging systems withdraw AC current from the grid and convert it to DC current at an appropriate voltage for charging the battery. However, any EV charging system consists of two main components: CS and the EV charger; Figure 3.1 exemplifies how the key functions of an AC charging system are implemented[2]. The CS just supplies the vehicle with the energy, usually in the form of a high voltage AC or DC supply. Thus, CSs don't ***normally*** have the electrical elements that must convert the electrical energy into a form, which can be used directly on the battery, namely, the rectifier[3], power control unit, and converter. While charging functions are entirely contained within the vehicle for the so-called "on-board" AC charger, they are split between the CS and the vehicles for the so-called "off-board" DC charger.

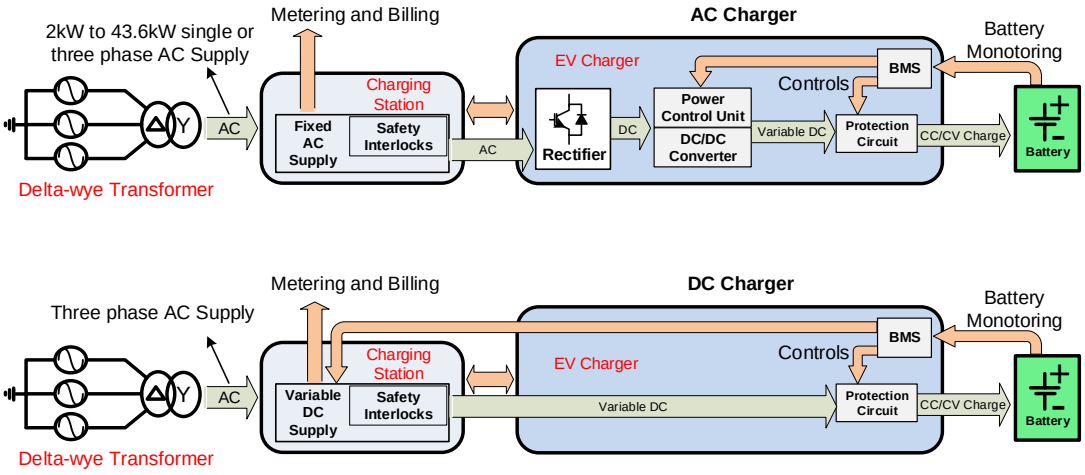

Figure 3.1.: EV charging System: on-board vs. off-board charger
Inspired by https://www.mpoweruk.com/infrastructure.html

By analyzing the components of an EV charging system in Figure 3.1, there are theoretically several different control parameters that can help to maintain the quality of power. Nevertheless, the current hardware and communication protocols, such as OCPP is still limited to active power control only and, in the best case, on different phases by OCPP 2.0. Some of those parameters are listed below:

[2]The illustration is based on the standard SAE J1772, however, it is still suitable for clarifying the main components of any EV charging system.

[3]While rectifiers convert AC to DC, converters can convert also DC to AC or DC from one voltage level to another.

1. **Charging Station Location**: As the authors of [125] state, improper positioning and sizing of CSs can lead to a negative impact on the distribution system, particularly an increase in network power losses, line congestion, and more degradation in voltage profile. The high number of researches in the literature about this problem reflects its importance for not only the grid operators but also CSPs on the purpose of the fast adoption of EVs [126, 127, 128, 129]. However, the actual impact depends not only on the distance to the transformer but also on fixed lines characteristics, surrounding loads, and generators. As a result, the location of a CS can only be considered as a passive way of controlling the power quality during grid connection planning.

2. **Real Power Control (P)**: A public CS with 50 kW ($\approx$ two 22 kW AC charging operations in parallel) can potentially bring the grid to its physical limits, resulting in grid congestion and voltage problems. Hence, a reduction of the charging power for a certain time can help regarding those concerns. Furthermore, a CS with variable demand is an optimal consumer of the installed PV output in the low voltage grids during peak PV supply, specifically, with huge numbers of installed PV peak power.

3. **Power Factor Correction (PFC)**: Similar to the configurable PV inverters [130, 131], a CS can assist the power grid theoretically in regulating the ratio of reactive power (Q) at a particular grid location. Such functionality is related to developing a more advanced rectifier system embedded either in DC CSs or built-in the EVs for AC charging; see Figure 3.1. So to maintain voltage stability, the rectifier can either consume the reactive power from nearby devices to deal with the voltage rise or increases locally injected reactive power to meet the voltage drop. However, PFC will enhance the electrical efficiency and longevity of inductive loads when appropriately sized. But it may also have harmful side effects on sensitive industrial equipment (e. g., harmonics) if not treated by qualified, experienced professionals.

   Although ISO 15118[4] supports adjusting the P and Q at the car rectifier (AC charging) by negotiating respective parameter configurations, existing CSs in the market do not provide an interface for such functionality through well-known communication standards.

4. **Phase Balancing**: The European power transmission and most of its distribution grid are operated as a three-phase system. Unbalanced phases usually occur because of variations in loads on phases. Because of their relatively high power demand, public CSs are commonly supplied by using three phases as well. Via providing different load levels on the three phases, it is assumed that DC CSs can decrease phase imbalance at the grid connection point or in the whole low voltage grid [132]. Additionally, the voltage imbalance can be improved locally with a balancing factor. Still, the same

[4] ISO 15118 is an international standard defining a V2G communication interface for bi-directional charging/discharging of electric vehicles.

balancing factor does not guarantee the reduction of voltage imbalance on other nodes, more details in Section 3.2.4).

After this theoretical discussion of the main potential CS parameters, a simulation analysis is introduced next, in which the impact of changing the values of the different parameters at different points in the grid is shown.

3.2 Simulative Study of the Local Adjustment of CS Parameters in a Low Voltage Grid

The main goal of this section is understanding to what extent the impact of CS propagates through the distribution grid. To that end, not only the different values of P and Q of a CS have been tested but also install locations.

3.2.1 Simulation Setup

The simulation is carried out using the power simulation tool PowerFactory from "DIgSILENT"[5]. PowerFactory provides three main options for simulations:

- Static: The conventional load flow simulation is an example since it presumes that the active and reactive power demand are constant values independent of the actual voltage magnitude at the corresponding bus. Thereby, the load is modeled as a constant impedance.
- Dynamic: In reality, the demand of the various kinds of residential, commercial, and industrial loads is a function of the system voltage and frequency. So in voltage-dependent loads, the current is a polynomial function of the actual voltage on the respective node. The standard load flow simulation in PowerFactory applies a constant power load model, thereby, it varies the impedance on change of input voltage, either the load flow voltage or the rated voltage, to keep the power constant. If the voltage dependency of loads is taken into account, it can seriously influence the results of the load flow and power flow simulations. It also affects the dynamic behavior of the system [133].
- RMS simulation: It is a tool that can be used for analyzing the dynamic behavior of a system in the time domain, particularly in terms of voltage and frequency. By default, the loads are set to be modeled as static in RMS simulation. RMS simulation allows importing the (P, Q) values for each load for a predefined period from a file. However, PowerFactory applies a constant power model., but the rated voltage is used since the voltage dependency is not considered in this case.
  In order to achieve realistic results, both the voltage dependency of busbars and varying

[5] https://www.digsilent.de/en/powerfactory.html

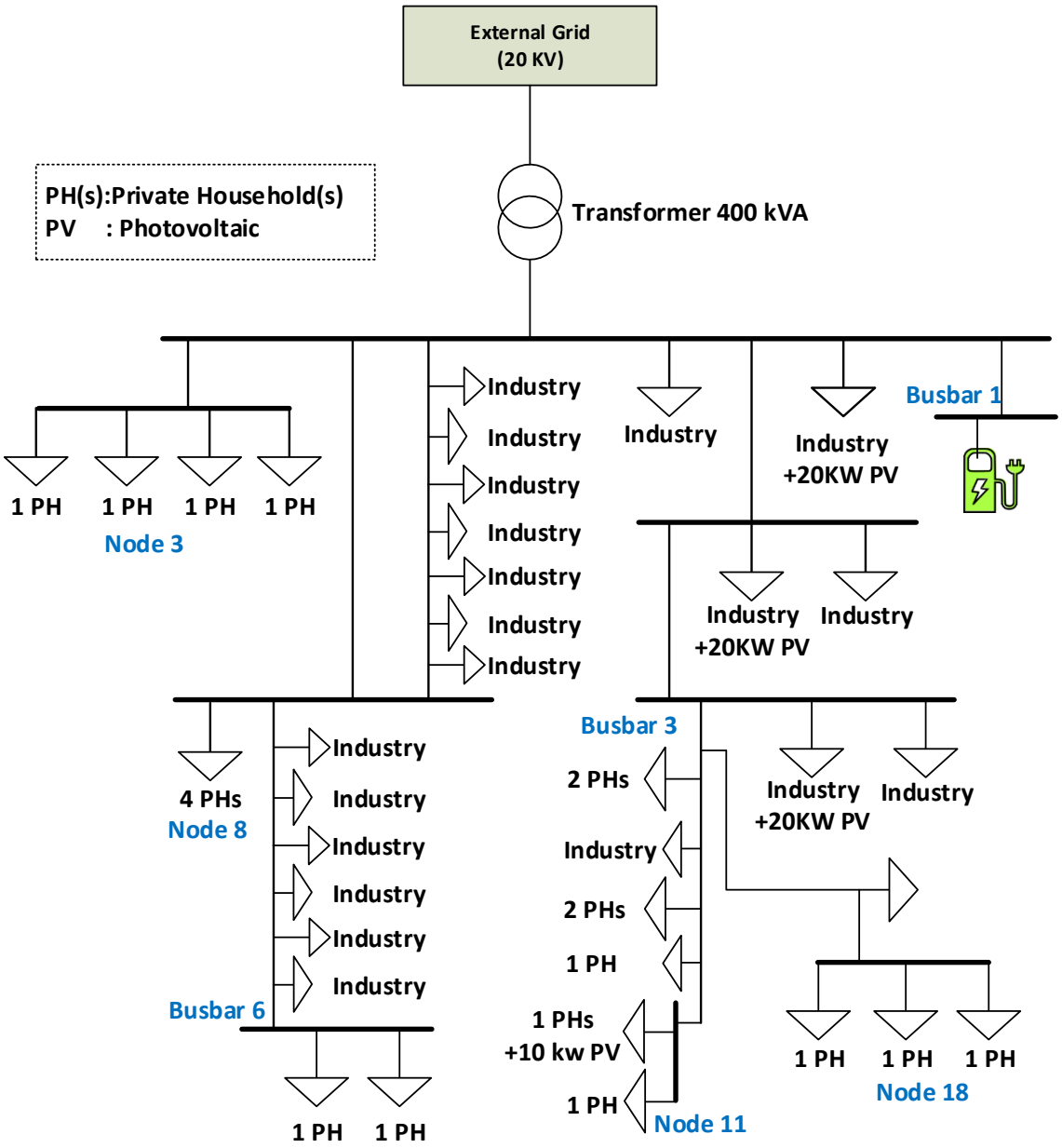

Figure 3.2.: Test Distribution Grid

power demand of the loads have to be taken into account. Thus, instead of using general load elements from the PowerFactory library for each industry, household, and PV generator, a separated composite model is created [134]. Each model consists of three standard single-phase loads connected to one bus; each representing a phase. The connection of the loads is phase-to-neutral. Other components are a neutral bus, data file, measurement devices, and a calculation block. The voltage measurement devices are connected to the buses (including neutral) to obtain the actual voltage magnitude values for each simulation step. The time-series data file contains the input values of P and Q for each phase with a resolution of one second. Thus, the impedance is recalculated using the measured voltage magnitude on each step of the dynamic simulation so that the load voltage dependency is taken into account.

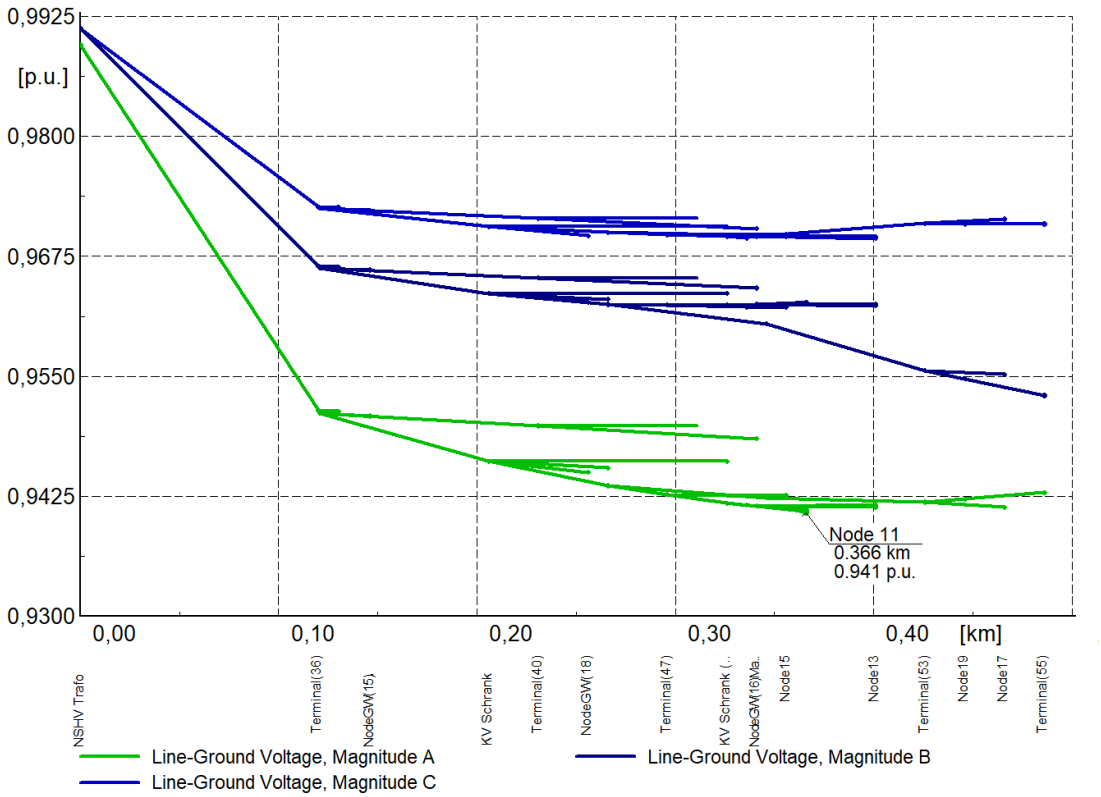

Figure 3.3.: Line voltage drop analysis (starting at the low-voltage side of the transformers terminal

Using the composite models mentioned above, a low-voltage distribution network located in a small city in Germany is implemented. It consists of a single 2-winding transformer with a high voltage side of 20 kV and a low voltage side of 0,4 kV; 54 buses (nodes) including 22 buses representing industries, 19 buses representing households, and three buses for PV systems. The nominal frequency of the system is 50 Hz. The transformer rating is 0,4 MVA. The schematic illustration in Figure 3.2 depicts the distribution of the industrial loads, PVs, and households in the grid. Finally, it is assumed that PV inverters do not perform any kind of PFC.

Three kinds of 24-hour profiles are fed into the simulation: realistic household load profiles, load profiles of "Bundesverband der Energie- und Wasserwirtschaft e.V" (BDEW) for industries [135], and real generation profiles for the PV systems. While the profiles of households provide active and reactive power per phase, BDEW profiles provide only values of active power. Hence, the value of PF and its type (lagging or leading) remained uncertain and assuming it is required. Since industries typically have inductive loads, a PF of 0.95 lagging is used. Moreover, the used three-phase profiles create a load imbalance among the different phases in the simulated grid.

Since the major focus is on the impact of EV charging on the grid, the simulation time is fixed to a two-hours charging operation through the most critical time on a winter working day. It is between 17:00 and 19:00, where the voltage level at the different grid nodes

reaches its lowest value without active EV charging, and the transformer load is at its peak. An analysis of the line voltage drop of the grid (starting at the terminal of the transformer on the low-voltage side) is performed and depicted in Figure 3.3. Since time-variant profiles used for the simulation, line voltage drops of the grid are dynamic and depend on loads of all connected instances. Therefore, it is not possible to define a node that has the highest voltage drop for the whole day. Hence, the line voltage drop analysis has been performed for the point in time where the transformer faces the highest load, which is at 62880 s = 17:28. As can be seen in the result (Figure 3.3), node 11 with a line distance of 366 m from the transformer is facing the highest voltage drop for this point in time. Therefore, it is considered as a critical point in this grid as well as its feeder.

3.2.2 Assessing the Impact of the CS Location and Real Power (P)

In order to assess the role of the CS location on the voltage deviation, three different locations for installing the CS are chosen; (1) close to the transformer, (2) middle of a critical feeder line in terms of voltage drop - highly loaded cable at the beginning of the critical feeder-, and (3) at the end of the non-problematic feeder. Furthermore, the maximum consumed power of a CS is varied among three values 22 kW, 44 kW, and 88 kW, which corresponds to a single charging process with a type 2 plug, two, and four parallel charging processes, respectively. As depicted in Figure 3.4, the voltage deviation is nearly increasing linearly with the amount of attached power with small differences on the three phases because of the different attached loads at the separate feeder. While the CS located close to the transformer has minimum voltage deviation, the one in the middle of the critical feeder suffers much higher than another at the end of a different feeder line due to highly loaded cable at the beginning of the critical feeder. Worth of mentioning, the voltage drop on electrical feeders depends basically on two parameters: the impedance of the feeders and the current flowing through the feeders.

3.2.3 Assessing the Impact of the Power Factor Correction

At the same three locations mentioned above, the previous experiment is repeated with alternating the PF to investigate the impact of PFC at CS. To that end, an equal power factor is used in all three phases, while three different values (1.0, 0.9, and 0.8 leading) are tested. Figure 3.5 shows the voltage deviation at several nodes and busbars only on phase A since the other two phases yield similar results. The effect of PFC is evident in the scenarios where the CS is close to the transformer and at the end of the feeder. Charging with a PFC even reduces the maximum voltage deviation on phase A against to not charging at all. Otherwise, the voltage deviation is improved slightly at the critical location. But it is not reaching the voltage level in the “not charging” scenario. Furthermore, experiments show an improving effect of PFC on the voltage imbalance. The highest effect is visible at the middle of the feeder location since the most significant difference in the voltage deviation on phase A can be observed there.

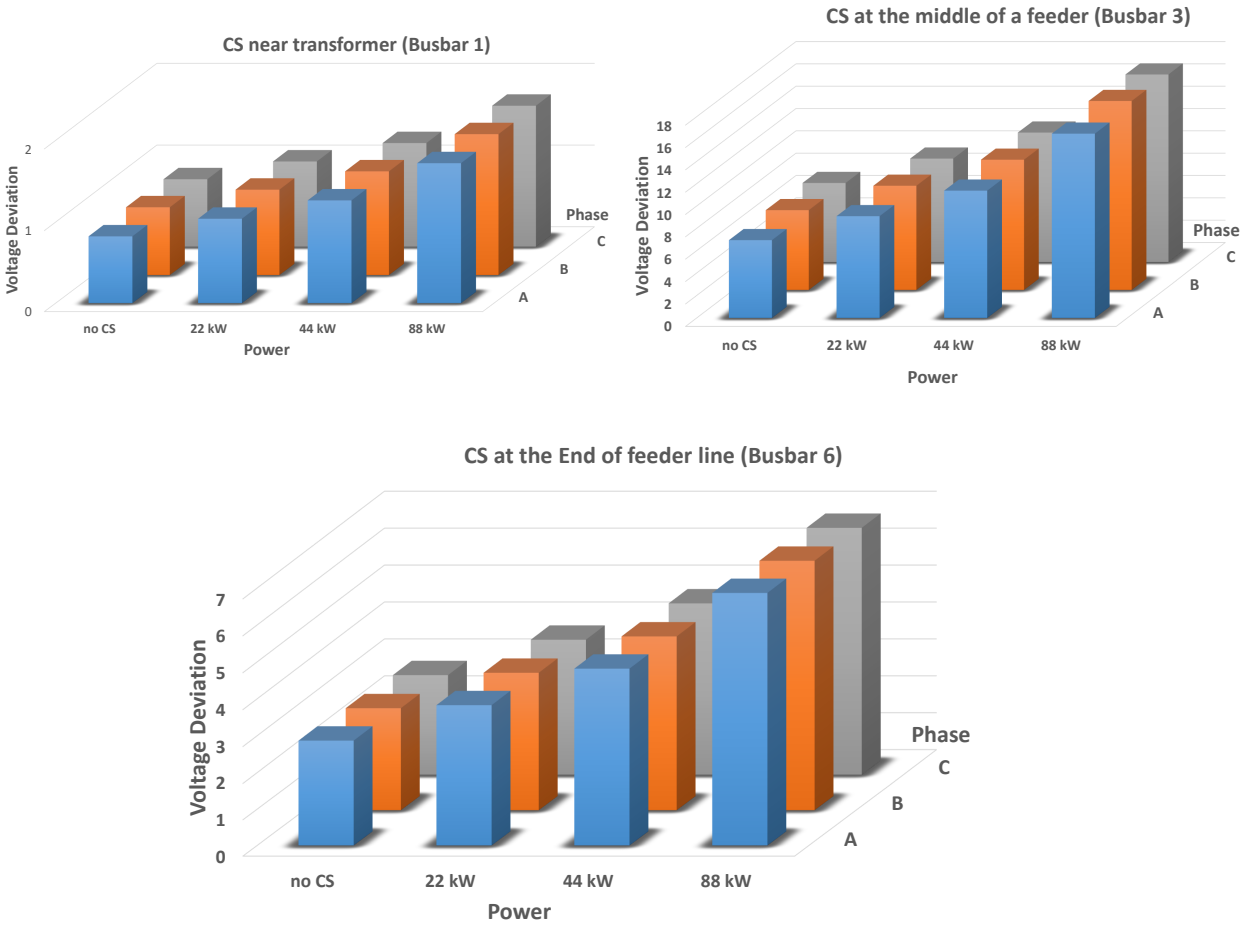

Figure 3.4.: Maximum Voltage Deviation at a CS (under-voltage): Different power and location

3.2.4 Assessing the Impact of Phase Balancing

In contrast to the simple power reduction with an equal power distribution across phases, a carefully adjusted balancing factor might be useful for keeping the CS power output at a higher level, which in turn may contribute to the correct distribution of the overall system load among phases. For example, if one phase is overloaded with three-phase CS, the power can only be reduced on this single phase, and it is not necessary to reduce the power on other phases. Otherwise, the power reduced on this overloaded phase can be shared between the two other phases as long as hardware limitations for each phase allow that.

In reality, the possibility of total power P_{total} distribution across phases is different from $\frac{P_{total}}{3}$. Rather it depends on the capacity of each line, e.g., if a CS's maximum power is 44 kW, each of three phases is commonly limited to transmit $\frac{44}{3}$ kW plus some margin. Within this margin or in the case when the power supplied to the EV is less than maximum CS power, it is possible to vary a balancing factor. Assuming the required charging capacity is 35 kW (or 35 kVA with unity PF) and phase C is overloaded; hence, the power on this

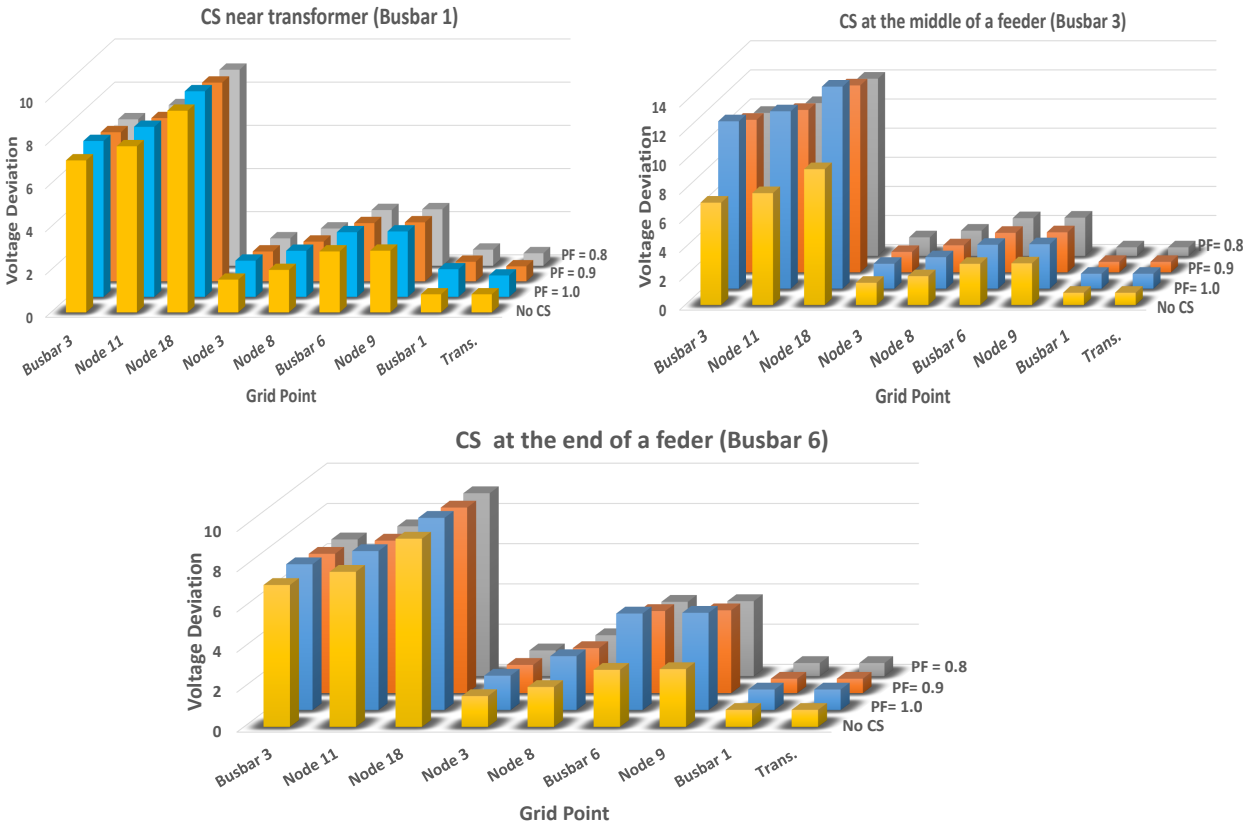

Figure 3.5.: Effect of PFC on the Voltage Deviation at Different Locations

phase must be reduced so equal distribution is no more valid in order to use the required capacity.

However, the "Voltage Symmetry" metric measures the symmetry in a percentage of the three-phase voltages. On one hand, voltage symmetry is defined as the ratio of the negative sequence voltage component to the positive sequence voltage component regarding the IEC 61400-21 standard. On the other hand, it is a hundred times the absolute value of the maximum deviation of the line-neutral voltage from the average voltage on a three-phase system divided by the average voltage regarding IEEE 112 standard. For sake of simplicity, the latter definition is used to calculate the balanced power used on each phase $P^{\phi}_{balanced}$, as depicted in Equations (3.1). This set of equations is applied in each time step (t) to calculate the power for the next time step (t+1).

$$U_{avg}(t) = \frac{\sum_{\phi \in \{a,b,c\}} U_{\phi}(t)}{3}$$
$$P^{\phi}_{balanced}(t) = P^{\phi}_{imbalanced}(t) + P^{\phi}_{imbalanced}(t)\frac{U^{\phi}(t) - U_{avg}(t)}{U_{avg}(t)} \quad where \quad \phi \in \{a,b,c\} \tag{3.1}$$

In order to test the effect of load balancing on voltage imbalance, a 44 kW CS is connected in the middle of the critical feeder line at Busbar 3 in Figure 3.2. The simulation time is only two minutes, where the voltage imbalance and voltage deviation are obvious and high,

as seen in Figure 3.6. Additionally, a unity PF is assumed and a balancing factor at each simulation step based on Equation (3.1) is applied. Hence, the voltage deviation changes differently on each phase, so the maximum voltage imbalance is even smaller than one in a scenario without any installation of a CS, as depicted in Figure 3.7. That is because power is shifted from the initially more loaded phase B (during the considered time) to the less loaded phases A and C.

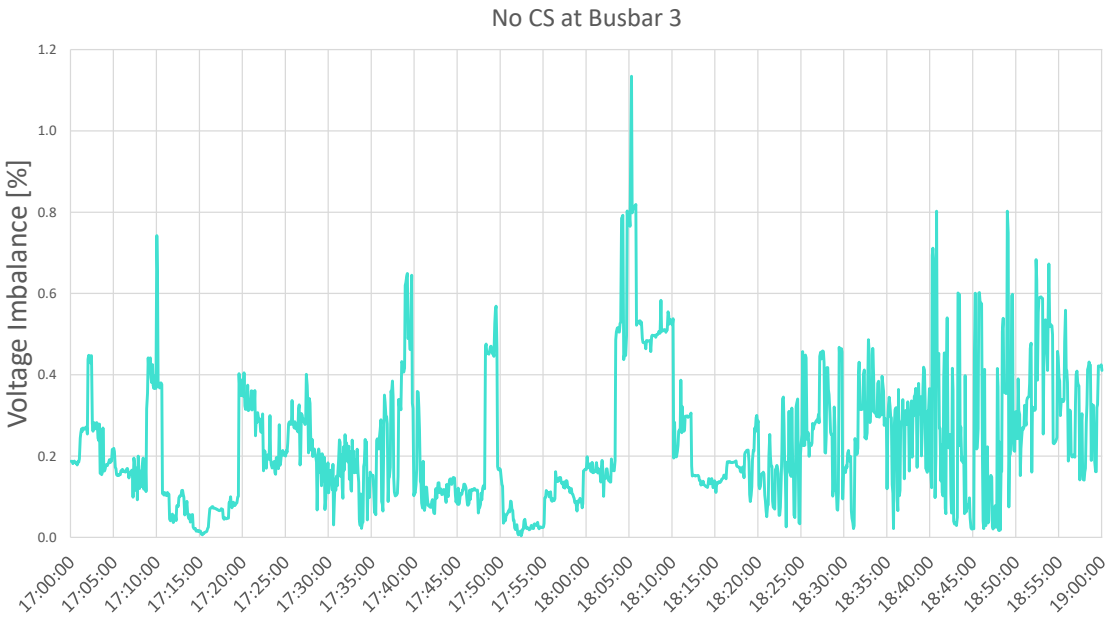

Figure 3.6.: Voltage Imbalance Factor at Busbar 3 (No CS Installed)

The effect of phase balancing on different nodes is easy to see in Figure 3.7; it varies and does not have the same local effect on other critical nodes of a system. That is due to different load properties on each phase other nodes might have, and the applied balancing mechanism at CS connected to Busbar 3 changes the resulting loading on other nodes causing an increased/decreased voltage imbalance.

Based on this simulative study, three main facts about the possible effects of CS parameters are derived and used as a basis for developing a grid-friendly smart charging solution. These are:

1. ***The optimal configuration of CS parameters varies with its location.***

2. ***The impact of a CS is not only local but can propagate to neighboring nodes and even to distant parts of the grid, e. g., PF and real power adjustment.***

3. ***With a load balancing approach, voltage imbalance can be improved locally with a well-chosen balancing factor but the same balancing factor does not guarantee the reduction of voltage imbalance on other nodes.***

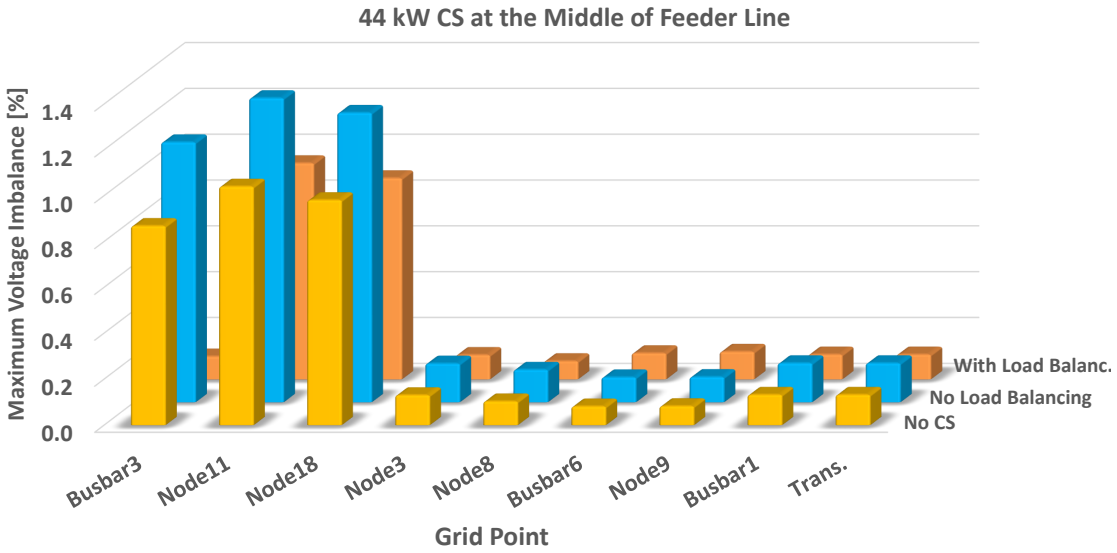

Figure 3.7.: Maximum Voltage imbalance for 2 Minutes Time Interval; Load Balancing only at Busbar 3

3.3 Grid-friendly Operation of a Charging Station

As it has been seen via simulations in previous sections, an optimal configuration of CS parameters depends on a set of naturally dependent factors, e.g., the amount of reactive power (Q) in the system, load on each phase, and the physical limitations of grid lines that determine the actual voltage deviation and voltage imbalance. Furthermore, it is shown that the initial PQ parameters on each phase at each individual grid point may vary. Additionally, the impact of the CS is not only local but propagates to some extent to other parts of the grid. As a result, charging control becomes a challenging task because of the complicated and dynamic nature of the power system. However, researchers used to formulate this kind of problems as an optimization problem where the different constraints of the system are taken into consideration and searching for the optimum mostly be done in a centralized way [136, 137].

In the next sections, an optimization problem for finding the optimal values of a CS's charging parameters is investigated. Thereby, the individual configuration of the active (P) and reactive power (Q) of a CS is assumed to be technically doable on the fly during the charging process via a smart controller. First, a linear approximation of the unbalanced distribution grid is stated to simplify the problem formulation. For that sake, all required variables are described in Table 3.1.

Variable	Definition	Range
U_n	Nominal voltage of the system	$\in \mathbb{R}_+$
N	Number of buses in the grid except CSs buses	$\in \mathbb{N}$
$\{cs_i\}$	Set of CS buses	-

Variable	Definition	Range
ϕ	Phases index	$\in \{a, b, c\}$
π_n	Unique parent bus of bus n	-
$\mathscr{C}_n$	Set of children buses of bus n	-
$\mathscr{P}_n$	Subset of phases of bus n	$\subseteq \{a, b, c\}$
u_n	Vectors of voltage magnitude for all phases of bus n	$\in \mathbb{R}_+^3$
q_n	Vectors of reactive power for all phases of bus n	$\in \mathbb{R}^3$
p_n	Vectors of active power for all phases of bus n	$\in \mathbb{R}^3$
s_0	Vectors of apparent power for all phases of transformer	$\in \mathbb{R}_+^3$
s_0^R	Vectors of rated apparent power for all phases of transformer	$\in \mathbb{R}_+^3$
$\mathscr{L}_{ij}$	Distribution line connecting a pair of buses (i, j)	-
$Z_{\mathscr{L}_{ij}}$	The related phase impedance matrix of line $\mathscr{L}_{ij}$	$\in \mathbb{C}^{3\times3}$
Z_0, Z_+, Z_-	Zero-, positive-, and negative-sequence impedance	$\in \mathbb{C}$
$P_{\mathscr{L}_{ij}}$	Vector of active power flows on all phases of line $\mathscr{L}_{ij}$	$\in \mathbb{R}^3$
$Q_{\mathscr{L}_{ij}}$	Vector of reactive power flows on all phases of line $\mathscr{L}_{ij}$	$\in \mathbb{R}^3$
$S_{\mathscr{L}_{ij}}$	The complex power flows on all phases of line $\mathscr{L}_{ij}$	$\in \mathbb{R}^3$
$\mathscr{S}$	Set of active CSs in the system	-
x_{cs}	Total Active power consumed by a CS	$\in \mathbb{R}_+$
$p_{cs}^a, p_{cs}^b, p_{cs}^c$	Active power consumed by a CS on phases A, B, and C	$\in \mathbb{R}_+$
$q_{cs}^a, q_{cs}^b, q_{cs}^c$	Reactive power by a CS on phases A, B, and C	$\in \mathbb{R}$
$\mathscr{M}_{cs}$	Maximum physical capacity of a CS	$\in \mathbb{R}_+$
$Imbalance_{cs}^U$	Voltage imbalance factor at a CS	$\in \mathbb{R}_+$
$\omega_1, \omega_2^\phi, \omega_3$	Weights of the multi-objective function	$\in \mathbb{R}_+$
$\lambda_{cs}^{min}, \lambda_{cs}^{max}$	Thresholds for voltage constraint at a CS	$\in \mathbb{R}_+$
λ_{imb}	Threshold for voltage imbalance at a CS	$\in \mathbb{R}_+$
λ_T	Threshold for transformer apparent power	$\in \mathbb{R}_+$
$\mathscr{K}$	Set of critical points (buses) defined by the DSO	$\subseteq \{1..N\}$
Ω_k^ϕ	Weights of voltage objective for critical point k	$\in \mathbb{R}_+$
$\lambda_k^{min}, \lambda_k^{max}$	Thresholds for voltage constraint at critical point k	$\in \mathbb{R}_+$

Table 3.1.: Description of Variables in Section 3.3

3.3.1 Modeling Unbalanced Distribution Grids

It is assumed that the CS is connected to a radial distribution grid comprising of $N + 2$ buses indicted by $n \in \mathbb{N}_0 := \{0, 1, 2, .., N\} \cup \{cs\}$ and phases indexed by $\phi \in \{a, b, c\}$. The transformer bus numbered by $n = 0$. Every non-feeder bus $n \in \mathbb{N}$ has a unique parent bus indexed by π_n. The distribution line connecting a pair of buses (i, j) is denoted as $\mathscr{L}_{ij}$. For bus n, let also $\mathscr{C}_n$ denote the set of its children buses, and $\mathscr{P}_n \subseteq \{a, b, c\}$ the subset of its phases. A linearized grid model proposed in [123, 138] is adopted here to simplify the formulation of our problem using a three-phases AC model.

Let u_n, q_n, and p_n be respectively the 3-dimensional vectors of voltage magnitude, reactive power injection, and active power injection for all phases of bus n, e.g., $\{u_n^a, u_n^b, u_n^c\}$. For line $\mathscr{L}_{ij}$, let $Z_{\mathscr{L}_{ij}} \in \mathbb{C}^{3\times3}$ be the related phase impedance matrix. Furthermore, $P_{\mathscr{L}_{ij}}$ and $Q_{\mathscr{L}_{ij}}$ are defined as the vectors of (re)active power that flows on all phases of line $\mathscr{L}_{ij}$. If line losses are relatively small (i.e. $Z_{\mathscr{L}_n}.\mathscr{L}_{ij} << S_{\mathscr{L}_{ij}}$ where $S_{\mathscr{L}_{ij}}$ is the complex power flows on all phases of line $\mathscr{L}_{ij}$) and voltages are roughly balanced in terms of angle, i. e., the voltage of different phases differs in angle by $\approx 120°$ [138], the linearized multi-phases power flow model reads:

$$p_n = \sum_{k\in\mathscr{C}_n} P_{\mathscr{L}_{nk}} - P_{\mathscr{L}_{\pi_n n}} \qquad n \in \{0..N\} \cup \{cs\} \tag{3.2a}$$

$$q_n = \sum_{k\in\mathscr{C}_n} Q_{\mathscr{L}_{nk}} - Q_{\mathscr{L}_{\pi_n n}} \qquad n \in \{0..N\} \cup \{cs\} \tag{3.2b}$$

$$u_{\pi_n}^2 - u_n^2 = Re\{Z^*_{\mathscr{L}_{\pi_n n}}(P_{\mathscr{L}_{\pi_n n}} + jQ_{\mathscr{L}_{\pi_n n}})\} \qquad n \in \{0..N\} \cup \{cs\} \tag{3.2c}$$

where

- $$Z_{\mathscr{L}_{\pi_n n}} = \begin{vmatrix} Z_0 & 0 & 0 \\ 0 & Z_+ & 0 \\ 0 & 0 & Z_- \end{vmatrix}$$

  Where Z_0, Z_+, and Z_- are the zero-sequence, the positive-sequence and the negative-sequence impedance of line $\mathscr{L}_{\pi_n n}$ respectively.
- $Z^*_{\mathscr{L}_{\pi_n n}} = diag(A) \times Z_{\mathscr{L}_{\pi_n n}} \times diag(\overline{A})$
- $A = [1 \quad \alpha \quad \alpha^2]^T$
- $\alpha = e^{-j\frac{2\pi}{3}}$
- $(\overline{x})$ denotes the complex conjugation.
- For most typical operating conditions, the disparity in angles of the voltage phasors at two buses i and j connected by a $\mathscr{L}_{ij}$ is less than 10-15 degrees. It is sporadic ever to see such angular separation exceeding 30 degrees. Thus, it is assumed that the angular separation across any transmission line is “small”. Moreover, one might be tempted to accept the approximation that the sine function goes to zero with small angles. Therefore, only the real part is considered in Constraint (3.2c).
- If not all phases are given, power injection, flow vector, and phase impedance matrices are zero-padded.
- For holding the voltage Constraint (3.2c), the entries of u_n are arbitrarily set to the corresponding entries of u_{π_n} when u_n is linked with non-existing phases.
- In order to linearize the voltage Constraint 3.2c, it is assumed that vector u_n and u_{π_n} contain the ***squared*** voltage magnitudes.

3.3.2 Problem Formulation

Since it is assumed that the smart controller can vary the PF as well as the active power on each phase at the CS, six configuration parameters of a CS are considered as decision variables $\{p^a_{cs}, p^b_{cs}, p^c_{cs}, q^a_{cs}, q^b_{cs}, q^c_{cs}\}$ of a multi-objective problem. Firstly, the total active power used by the CS, $x_{cs} = p^a_{cs} + p^b_{cs} + p^c_{cs}$, has to be maximized by minimizing the difference between the maximum physical capacity of the CS, $\mathscr{M}_{cs}$, and x_{cs}. Since the departure of EVs from homes and public CSs is non-deterministic, it is reasonable to assert that EV owners are greedy and prefer to finish charging their EVs as soon as possible to avoid range anxiety and long waiting time. Secondly, the RMS value of the voltage on each phase $\phi \in \mathscr{P}_{cs}$ at the CS (u^ϕ_{cs}) is as possible close to the nominal voltage of the system $U_n = 230$ V. Worth mentioning that the total reactive power, $q^a_{cs} + q^b_{cs} + q^c_{cs}$, consumed or injected by the CS plays a significant role regarding this objective. Thirdly, an additional objective regarding the voltage imbalance is that $Imbalance^U_{cs} = 100\frac{max|U^\phi_{cs} - U_{avg}|}{U_{avg}}$ (according to IEEE 112 standard) should be minimized. These objectives are normalized and weighted by ω_1, ω^ϕ_2, and $\omega_3 \in \mathbb{R}_+$. The selection of weight values depends on the main concern of the designed controller.

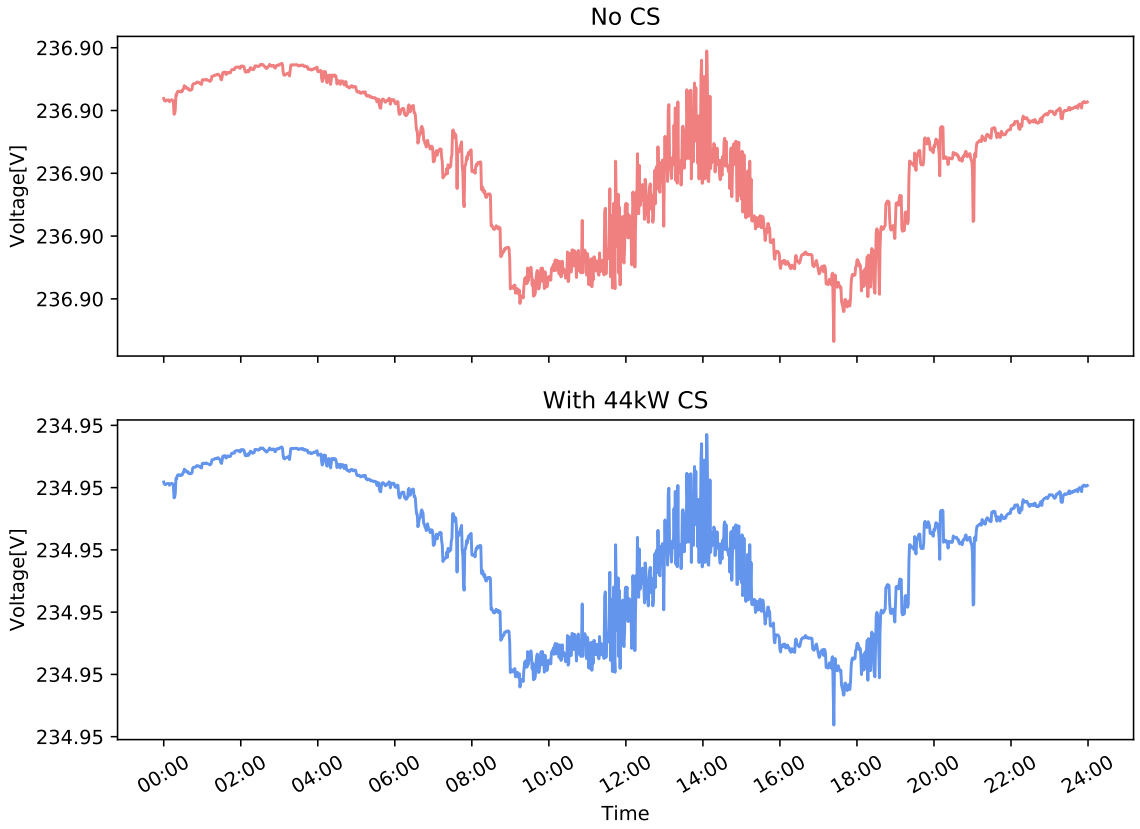

Figure 3.8.: The Voltage at Busbar 1 in Two Cases: no CS installed and 44 KW CS installed

However, this kind of problems are termed as Many-objective Optimization Problems (MaOPs) since the number of objectives grows beyond three. These problems are classified

as intractable with regards to both time and space [139], which means they possess a degree of complexity that is not solvable. In other words, they are generally not possible to be solved precisely, rather solving an approximation to the actual problem or finding a local optimum are applied. Moreover, the use of Pareto dominance, which is the corner-stone of Multi-Objective Problems (MOP) algorithms, becomes ineffective since the solutions in these higher-order spaces no longer dominate one another. Additionally, adding a non-linear AC power flow model[6], which describes the power flow through each distribution line, makes the problem more complicated. As a result, the linearized multi-phases power flow stated in Equations (3.2) is used to simplify the problem. Thus, the stated problem described in Formulae (3.3) becomes a continuous linear problem with negative values of decision variables since it is assumed that the CS can both inject and consume reactive power. However, negative and positive values of active power at the CS is also possible if V2G technology is considered. Since this thesis focuses only on V1G, no negative values of variables $(p^a_{cs}, p^b_{cs}, p^c_{cs})$ are possible. For clarity, it is avoided to mention the constraints regarding the network operating limits (see Section 2.1.2) in Equations (3.2), namely, voltages.

$$
\begin{aligned}
\min_{p^a_{cs},p^b_{cs},p^c_{cs},q^a_{cs},q^b_{cs},q^c_{cs}} \quad & \omega_1 \frac{\mathscr{M}_{cs} - x_{cs}}{\mathscr{M}_{cs}} + \sum_{\phi \in \mathscr{P}_{cs}} \omega_2^{\phi} \frac{|U_n - u^{\phi}_{cs}|}{U_n} + \omega_3 \, Imbalance^{U}_{cs} \\
\text{subject to} \quad & x_{cs} = p^a_{cs} + p^b_{cs} + p^c_{cs} \\
& x_{cs} \leq \mathscr{M}_{cs} \\
& p_n = \sum_{k \in \mathscr{C}_n} P_{\mathscr{L}_{nk}} - P_{\mathscr{L}_{\pi_n n}}; \qquad n \in \{0..N\} \cup \{cs\} \\
& q_n = \sum_{k \in \mathscr{C}_n} Q_{\mathscr{L}_{nk}} - Q_{\mathscr{L}_{\pi_n n}}; \qquad n \in \{0..N\} \cup \{cs\} \\
& u^2_{\pi_n} - u^2_n = Re\{Z^*_{\mathscr{L}_{\pi_n n}} (P_{\mathscr{L}_{\pi_n n}} + jQ_{\mathscr{L}_{\pi_n n}})\}; \quad n \in \{0..N\} \cup \{cs\}
\end{aligned}
\tag{3.3}
$$

Based on the simulation results in Section 3.2, the impact of a certain load is locally concentrated, but it can be distributed to other nodes on the same feeder line or a near feeder. Therefore, the objective function in Formulae (3.3) can be extended to include a new objective(s) regarding the voltage at a critical point(s) $k \in \mathscr{K} \subseteq \{0, .., N\}$ predetermined by the DSO. That objective(s) is weighted by Ω^{ϕ}_k as follows.

$$
\min_{p^a_{cs},p^b_{cs},p^c_{cs},q^a_{cs},q^b_{cs},q^c_{cs}} \omega_1 \frac{\mathscr{M}_{cs} - x_{cs}}{\mathscr{M}_{cs}} + \sum_{\phi \in \mathscr{P}_{cs}} \omega_2^{\phi} \frac{|U_n - u^{\phi}_{cs}|}{U_n} + \sum_{k \in \mathscr{K}} \sum_{\phi \in \mathscr{P}_k} \Omega^{\phi}_k \frac{|U_n - u^{\phi}_k|}{U_n} + \omega_3 Imbalance^{U}_{cs}
$$

In reality, the DSO has no ambition to keep the voltage close to U_n as much as possible since it is not required, according to EN 50160 and other standards. Otherwise, the particularities of each connection point in the distribution grid could reflect the need to keep the voltage

[6]The problem is non-linear because the power flow into load impedance is a function of the square of the applied voltages.

higher than a certain threshold to avoid a big voltage drop at the end of the feeder line. For example, the voltage at busbar 1 in the grid illustrated in Figure 3.2 is always higher than U_n even when installing 44 KW CS, as depicted in Figure 3.8, since it is very close to the transformer. As a result, the objectives of the voltage deviation minimization can be replaced by a set of constraints. Similarly, the voltage Imbalance objective can be replaced by a constraint as well. Hence, the optimization problem described in Formulae (3.3) can be reformulated as follows:

$$
\begin{aligned}
\min_{p^a_{cs},p^b_{cs},p^c_{cs},q^a_{cs},q^b_{cs},q^c_{cs}} \quad & \frac{\mathscr{M}_{cs} - x_{cs}}{\mathscr{M}_{cs}} \\
\text{subject to} \quad & x_{cs} = p^a_{cs} + p^b_{cs} + p^c_{cs} \\
& x_{cs} \leq \mathscr{M}_{cs} \\
& p_n = \sum_{k \in \mathscr{C}_n} P_{\mathscr{L}_{nk}} - P_{\mathscr{L}_{\pi_n n}}; \qquad n \in \{0..N\} \cup \{cs\} \\
& q_n = \sum_{k \in \mathscr{C}_n} Q_{\mathscr{L}_{nk}} - Q_{\mathscr{L}_{\pi_n n}}; \qquad n \in \{0..N\} \cup \{cs\} \\
& u^2_{\pi_n} - u^2_n = Re\{Z^*_{\mathscr{L}_{\pi_n n}}(P_{\mathscr{L}_{\pi_n n}} + jQ_{\mathscr{L}_{\pi_n n}})\}; \quad n \in \{0..N\} \cup \{cs\} \\
& \lambda^{min}_{cs}\, U_n \leq u_{cs} \leq \lambda^{max}_{cs}\, U_n \\
& \lambda^{min}_{k}\, U_n \leq u_{k} \leq \lambda^{max}_{k}\, U_n; \qquad k \in \mathscr{K} \\
& Imbalance^U_{cs} \leq \lambda_{imb}
\end{aligned}
\tag{3.4}
$$

Moreover, the DSO would like to avoid the congestion of distribution branches and transformers since persistent overloading could cause damage to conductors, overheat transformers, and degrade their insulation. Thus, the apparent power flows through a branch or a transformer have to be smaller than a certain percentage of the rated apparent power of it (s^R). For simplicity, we include only one constraint about the most important point of the grid, namely, the transformer:

$$
s_0 < \lambda_T\, s^R_0 \quad ; \qquad \lambda_T, s_0, s^R_0 \in \mathbb{R}^3_+
$$

However, the modified optimization problem described in Formulae (3.4) includes only one objective, which can be replaced by maximizing the charging power x_{cs} instead of minimizing the difference. In other words, a utility of greedy EV owners by their charging rate x_{cs} is defined. That utility function measures the satisfaction of EV owners, which is proportional to the rate at which his/her EV is charged.

By considering multiple active chargers $cs_i \in \mathscr{S}$ installed in the low voltage grid, the main objective of the formulated problem becomes not only grid-friendliness, but also fair allocation of the available capacity of the network among the active CSs. Authors of [140] discussed multiple fairness criteria based on the global objective function of the optimization problem. In this thesis, the notation of proportional fairness is adopted in a similar way to the authors of [24]. According to the authors, this kind of fairness is the only

one that provides a scale-invariant Pareto optimal solution and conforms to the axioms of fairness specified in game theory. Additionally, it is achieved if the value of a global objective function is maximized, which is the sum of the logarithm of the utility functions $log(x_{cs_i})$. This function is infinitely differential, increasing, and strictly concave on its interior domain. As a result, the optimization problem is modified as follows:

$$
\begin{aligned}
\max_{x_{cs_i}, q^a_{cs_i}, q^b_{cs_i}, q^c_{cs_i}} \quad & \sum_{cs_i \in \mathscr{S}} log(x_{cs_i}) \\
\text{subject to} \quad & x_{cs_i} = p^a_{cs_i} + p^b_{cs_i} + p^c_{cs_i}; \qquad cs_i \in \mathscr{S} \\
& x_{cs_i} \leq \mathscr{M}_{cs_i}; \qquad cs_i \in \mathscr{S} \\
& p_n = \sum_{k \in \mathscr{C}_n} P_{\mathscr{L}_{nk}} - P_{\mathscr{L}_{\pi_{nn}}}; \qquad n \in \{0..N\} \cup \mathscr{S} \\
& q_n = \sum_{k \in \mathscr{C}_n} Q_{\mathscr{L}_{nk}} - Q_{\mathscr{L}_{\pi_{nn}}}; \qquad n \in \{0..N\} \cup \mathscr{S} \\
& u^2_{\pi_n} - u^2_n = Re\{Z^*_{\mathscr{L}_{\pi_{nn}}} (P_{\mathscr{L}_{\pi_{nn}}} + jQ_{\mathscr{L}_{\pi_{nn}}})\}; \quad n \in \{0..N\} \cup \mathscr{S} \\
& \lambda^{min}_{cs_i} U_n \leq u_{cs_i} \leq \lambda^{max}_{cs_i} U_n; \qquad cs_i \in \mathscr{S} \\
& \lambda^{min}_{k} U_n \leq u_{k} \leq \lambda^{max}_{k} U_n; \qquad k \in \mathscr{K} \\
& Imbalance^U_{cs_i} \leq \lambda_{imb} \qquad cs_i \in \mathscr{S} \\
& s_0 < \lambda_T \, s^R_0
\end{aligned}
\tag{3.5}
$$

The proposed problem presents an increased computational complexity, which is mainly caused by two factors. The first corresponds to the inherent network non-linearities[7]. The second is the size of low voltage networks. As a consequence, conventional optimization approaches can be inadequate because of the local maximum solutions. In contrast, heuristic or meta-heuristic techniques are considerably time-consuming and cannot be applied in real-world conditions [141]. However, solving such a problem by a centralized entity can provide proof about the con(di)vergence of the proposed system in Chapter 4. Next, a simplified version of the proposed problem is discussed.

3.3.3 Case Study

One typical approximation used by researchers in the domain of power systems is assuming that the system is completely balanced, not only in terms of voltage angle but also of magnitudes. Thus, a single-phase system is considered instead of a three-phase one. Such an approximation simplifies the problem but ignores the role of a CS in minimizing the voltage imbalance in the grid ultimately. Based on the fact that both CS and communication protocol support neither the reactive power control nor the loads balancing among the phases nowadays, the respective objectives (constraints) can be disregarded in this use case. There are, however, strong arguments in favor of active power control (P) [142]:

[7] The linear approximation described in Section 3.3.1 deals with this point partially.

- Contrary to grid reinforcement and On Load Tap Changer (OLTC)-like technologies, it does not involve additional CAPital EXpenditure (CAPEX) cost; In Section 5.1.4.1, a comparison between OLTC-based solutions and SC-based solutions is stated.
- Due to the high R/X ratio of low voltage lines, one kvar of reactive power in a low voltage network has an impact itself much smaller than the one of one kW of active power. Hence, the effect of active power P on voltage is usually many times stronger than the effect of reactive power Q in distribution grids.
- Contrary to reactive power control and OLTC-like technologies, active power curtailment allows current constraints (overloads) to be resolved, not just voltage problems.

Additionally, only one critical point is considered instead of $|\mathscr{K}|$[8]. Thus, the simplified version of the optimization problem can be described as Formulae (3.6).

$$
\begin{aligned}
\max_{x_{cs_i}} \quad & \sum_{cs_i \in \mathscr{S}} log(x_{cs_i}) \\
\text{subject to} \quad & x_{cs_i} \leq \mathscr{M}_{cs_i}; && cs_i \in \mathscr{S} \\
& p_n = \sum_{k \in \mathscr{C}_n} P_{\mathscr{L}_{nk}} - P_{\mathscr{L}_{\pi_n n}}; && n \in \{0..N\} \cup \mathscr{S} \\
& q_n = \sum_{k \in \mathscr{C}_n} Q_{\mathscr{L}_{nk}} - Q_{\mathscr{L}_{\pi_n n}}; && n \in \{0..N\} \cup \mathscr{S} \\
& u_{\pi_n}^2 - u_n^2 = Re\{\hat{Z}_{\mathscr{L}_{\pi_n n}}(P_{\mathscr{L}_{\pi_n n}} + jQ_{\mathscr{L}_{\pi_n n}})\}; && n \in \{0..N\} \cup \mathscr{S} \\
& \lambda_{cs_i}^{min}\, U_n \leq u_{cs_i} \leq \lambda_{cs_i}^{max}\, U_n; && cs_i \in \mathscr{S} \\
& \lambda_0^{min}\, U_n \leq u_0 \leq \lambda_0^{max}\, U_n \\
& s_0 < \lambda_T\, s_0^R
\end{aligned}
\tag{3.6}
$$

Where $Z_{\mathscr{L}_{ij}}$ is the complex impedance of the line $\mathscr{L}_{ij}$, which is a vector sum of the reactance (X) and the resistance (R) in the complex plane.

$\lambda_{cs_i}^{min}$	$\lambda_{cs_i}^{max}$	λ_0^{min}	λ_0^{max}	λ_T	$\mathscr{M}_{cs_i}$
0.97	1.03	0.97	1.03	0.375	22 kW

Table 3.2.: Values of the Main Parameters in Formulae (3.6)

The simplified problem is similar to Optimal Power Flow (OPF) problems introduced by J. Carpentier for the first time in 1962 [143]. It is one of the most challenging optimization problems in power system engineering. The goal of OPF is to find the optimal setting of a given power system that optimizes the objective function of a system, such as a system loss, bus voltage deviation and total generation cost subjected to a set of constraints, particularly

[8] More than one critical points can be considered, but that would increase the computation time without any actual addition in such a small grid.

power flow equations, and operating limits [144]. However, the convergence and the computational time of OPF are questionable when it is applied to large scale systems [145] because of the non-linearity of the power flow equations. In the literature, plenty of approximations of an OPF model are proposed to improve the performance of any OPF solver, e.g., Linearized AC OPF model [146], quadratic AC OPF model [147] and DC OPF model [148].

The complexity and approximation of such a problem are out of the scope of this work since they are thoroughly studied in the literature. Hence, a linear OPF model is just adopted to find a solution for the case study described in the next paragraph.

In the grid illustrated in Figure 3.2, four CSs with capacities of 22 kW installed in four different locations: two close to the transformer at busbar 1, one at Node 8, and one at Node 11 that was defined as a critical point in terms of voltage. It is assumed that the four CSs are active for the whole simulation time with their maximum capacities 22 kW. Three scenarios are adopted to show how a centralized controller can adjust the used charging power to keep the voltage and the transformer load in the predetermined boundaries. (1) Uncontrolled charging operations (UC), (2) no active charging operations (Baseline_Min), and (3) controlled charging operations (SC) via centralized controller solving the problem stated in Formulae (3.6) in each simulation step. The different parameters are defined in Table 3.2. A simulation of a one day runs and the optimal solution is calculated for each step based on the status of the grid in the previous step, i. e., the different values of loads and generation units in the grid. The goal of this case study is to show that the formulated problem is solvable. The computation time of the solution is not a part of this discussion.

The initial analysis of the results shows that roughly the periods between 8:00 - 12:00 and between 16:00 - 20:00 are peak hours in the day, where the load in the grid is high. It is resulting in a voltage drop greater than 3% (voltage thresholds) and overloading at the transformer even during the Baseline_Min scenario. During this time, SC restrains from further adding the CSs loads to the grid by reducing the charging power at each CS to a minimum value (it is assumed to be 1.3 kW in this case). Thus, avoiding further strain on the situation of the grid. As the algorithm supports only V1G, the degraded power quality during the peak hours cannot be compensated by the SC.

As depicted in Figure 3.9, the transformer crosses the threshold for 72.2% of the day during the Baseline_UC scenario. The centralized SC prevents the transformer from overloading completely. The effect of the overloading constraint appears clearly during the afternoon between 12:00 and 15:00, where the SC fills the valley in the transformer load in Baseline_Min without violating the voltage constraints.

Comparing the voltage level at the critical node in the SC scenario to the baseline scenarios is depicted in Figure 3.10. As seen in the graph, the centralized algorithm controls CS demands in such a way that the voltage level is among the thresholds during the off-peak times.

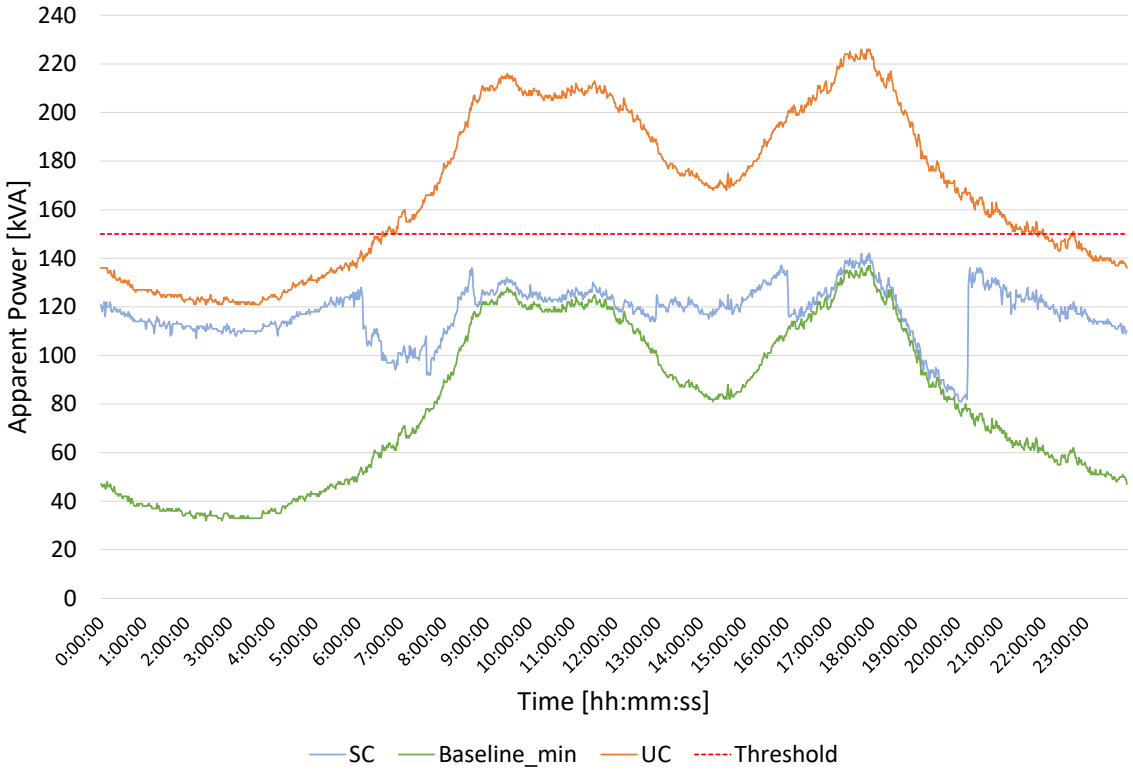

Figure 3.9.: Apparent Power at the Transformer

Unlike the overloading, the voltage sticks to the voltage in the scenario Baseline_Min during the on-peaks times. Otherwise, the voltage tries to be closer to the minimum threshold, $\lambda_{cs_i}^{min} U_n \approx 224\ V$, as much as possible since it means more consumption, i. e., more load causes a higher voltage drop.

As the proportional fairness is a part of the objective function in the stated problem in Formulae (3.6), Figure 3.11 shows the active power of all four CSs and the overall utilization. Within the time range, 00:00 - 07:00, when the low voltage at the critical point results in reducing the used capacity at the CS installed there, the CSs at non-critical locations can charge nearly with their maximum charging power. The first clear collaboration between CSs appears between 06:30 and 08:30. After that, starting at 09:00, all CSs react and reduce their charging power accordingly to the minimum value since no solution can keep the voltage at the critical point within the predefined thresholds. Therefore, the minimum values are used. The consumed energies by CS_1, CS_2, CS_3, and CS_4 are 259.33, 177.66, 264.53, and 238.47 kWh respectively. It is worth mentioning that the installation place of a CS plays a significant role in deciding the amount of allocated power since the realization of voltage constraints depends notably on the surroundings loads and the distance to the transformer.

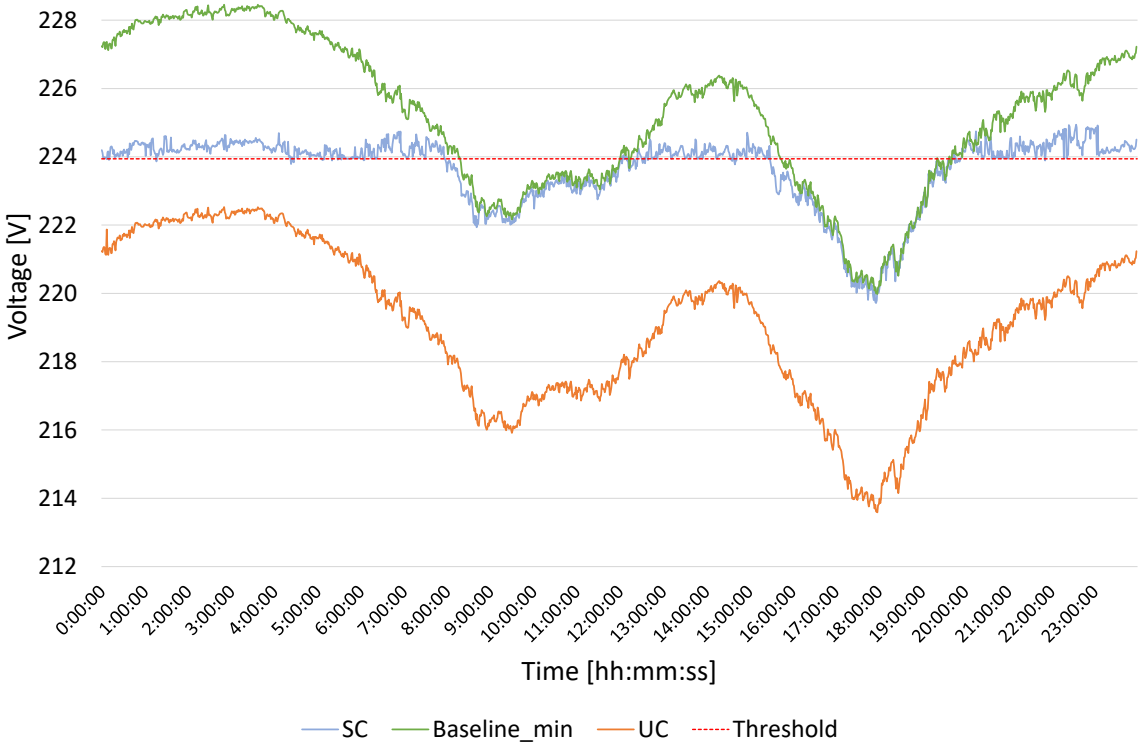

Figure 3.10.: Voltage Level at the Critical Node

3.4 Summary

In this chapter, the influence of a single three-phase CS on PQ in a distribution grid is studied, particularly, voltage deviation and voltage imbalance. Various study cases are analyzed via simulations of charging processes using a realistic grid model; thereby, it is assumed that a CS has a configurable rectifier and charging parameters can be potentially changed "on the fly" (during the charging process) depending on the actual PQ state in the grid. The simulation shows that the impact of a CS is not only on the local bus, but it can propagate to other buses of the system. Furthermore, the load balancing approach can improve voltage imbalance locally (only magnitude) with a certain balancing factor but does not guarantee the reduction of voltage imbalance on other nodes.

Finally, an optimization problem concerning a CS's parameters has been formulated that can be configured during the execution of a charging operation. The optimization problems can find the best possible solution for a CS's configuration parameters taking into account both power quality and the fairness among the active CSs. The drawback of this solution is the time complexity because of the required power flow analysis on each iteration. However, a linear model of the power grid is used to relax the problem.

Nevertheless, the centralized solutions are not very attractive for both the grid operator (namely, DSO) and the CSP, since it needs a total share of knowledge among the actors. Furthermore, they are computationally exhausting in a large scale scenario. Additionally,

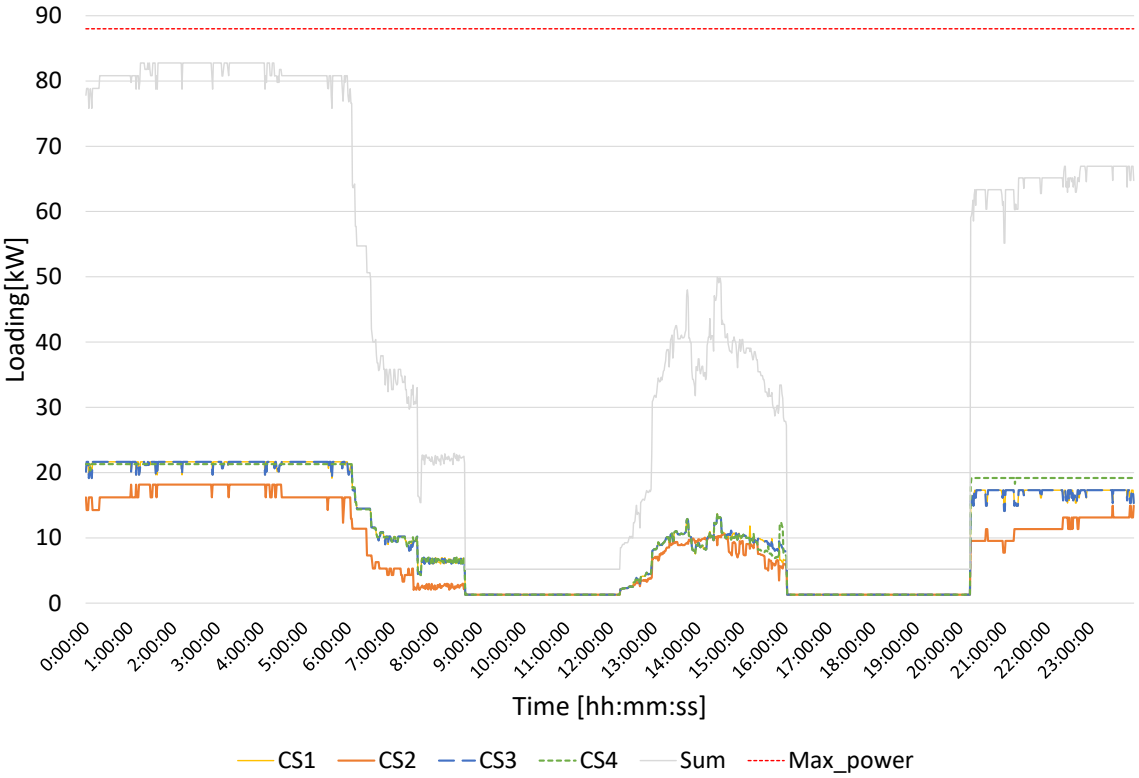

Figure 3.11.: Charging power at four CSs. Each colored line represents a CS. Grey is the sum power of all CSs, and the red line is rated maximum power of all CSs.

the DSO should be able to collect data from every single bus and connection point in the grid, which involves many risks such as privacy, cost, and communication infrastructure. Therefore, a distributed solution considering most of these requirements is required and proposed in the next section.

4 Distributed Grid-Friendly Smart Charging Architecture

Publication References[1]:

- A. Alyousef, D. Danner, F. Kupzog, and H. De Meer. “Design and Validation of a Smart Charging Algorithm for Power Quality Control in Electrical Distribution Systems.” ACM e-Energy ’18
- A. Alyousef, D. Danner, F. Kupzog, and H. De Meer. “Enhancing Power Quality in Electrical Distribution Systems Using a Smart Charging Architecture.” Energy Informatics, 1(1):28 2018
- A. Alyousef and H. de Meer. “Design of a TCP-like Smart Charging Controller for Power Quality in Electrical Distribution Systems.” ACM e-Energy ’19.

Let us consider an abstract system, which generates some output and whose states evolve under the influence of two types of inputs, namely, the control variables and the disturbances (either observed or unobserved). In general, the control goal is commonly to get the system output to follow the desired trajectory. Consequently, two main categories of control systems are identified:

- Open-loop control: Also known as a non-feedback system. Thereby, the value of control variables is set irrespective of the values of both disturbances and system output. Therefore, an open-loop system is supposed to obey its input command or setpoint independent of the final result.
- Closed-loop control: Also known as a feedback control system. Thereby, the value of the control variable is chosen dependent on the output of the system. Whereby, some portion of the output is returned to the input to form part of the system reaction. Those systems allow automation in many of industrial and environmental settings, and regulate processes in Industrial Control Systems (ICSs) such as Supervisory Control And Data Acquisition (SCADA) and Distributed Control Systems (DCSs).

[1]The research work from these papers that is included in the thesis was carried out and documented by the author of this thesis.

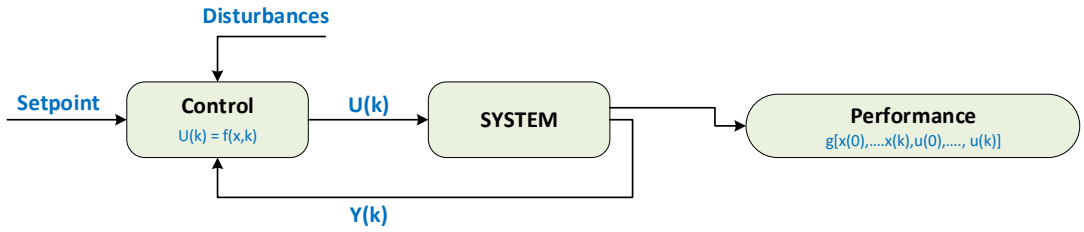

Figure 4.1.: Closed-loop System with Performance Optimization [150]

In system theory [149], it is assumed that a closed-loop system of a discrete-time model with performance evaluation and optimization has the data flow illustrated in Figure 4.1. Here the output of the system is used to evaluate some function $g()$, which defines a performance measure for the system over a time interval. It is also sometimes referred to as performance metric or cost function.

The power grid, as one of those complex systems, is classified in most of the literature as a dynamic and time-varying system. It is used to apply a discrete-time model to analyze and design smart solutions of the power grid by using discrete load and generation profiles, e.g., power flow analysis. In this chapter, a distributed grid-friendly smart charging architecture is introduced using the scheme of the closed-loop system. The performance evaluation of this proposed system measures the grid-friendly behavior of a charging system and the satisfaction of the main stakeholders as well, namely, DSO, CSP, and EV user.

The chapter starts with introducing the traffic light model as the main idea of the proposed system, and then, the system is described in general. Afterward, a detailed description of each part of the proposed architecture is stated,including an event-driven data gathering mechanism, a notification mechanism in distribution grids, and two smart controllers for controlling the charging power at CSs.

4.1 Traffic Light Model

The BDEW proposes a roadmap [151] for a realization of smart grids in Germany to ensure stability and efficiency through the flexibility of both the networks themselves and their users. This roadmap introduces the concept of the traffic light model to the smart grid, which "governs the fundamental interaction between market and network based on system conditions of green, amber(yellow), and red". This concept aims to describe the energy market in which DSOs or TSOs may demand local and temporal flexibility, depending on their network situation (amber phase). The authors of [152] describe the traffic light concept in more detail, and the preliminary design of the amber state is proposed. However, DSOs calculate present and forecast status of their network segment and allocate one of the three traffic light phases as follows:

- Green - Market Phase: No critical network situations exist and no intervention of the DSO in the market.
- Amber - Interaction Phase: Potential or actual network shortage/surplus in the defined network segment exists, so the DSO utilizes the flexibility offered by market participants to mitigate the damage.
- Red - Network Phase: The DSO must intervene directly to remedy the direct risk to the stability of the system.

The authors of [153, 154] propose an implementation of the yellow state based on forecasts. In the case of a predicted power quality problem, the market mechanisms are used to buy flexibility for this time window. An updated version of the traffic light concept is introduced in [154], which may be used by the DSO to control Demand Response (DR) units. The proposed approach depends on information from power flow calculation based on the joint load schedule of DR units and the residual loads.

The proposed approach in this thesis can be seen as an implementation of the amber state of the traffic light model, as mentioned earlier, which depends on real-time conditions and extends the current amber state by adding several new states within it by predefined thresholds. In this way, the flexibility introduced by the e-mobility sector can be used more efficiently, considering the requirements of both the grid and the running charging processes.

4.2 System Proposal

The author proposes a system in which a public CS can react immediately to different events happening in a distribution grid in terms of overloading the assets and the degradation of power quality, more specifically, voltage drops on a feeder line. The reactions of each CS are independent of other CSs and might based (only) on the current state of the grid, regardless of the reactions of the other existing CSs in the system. The proposed mechanism complies with three crucial design criteria. Firstly, it needs to be scalable in terms of the number of involved CSs. Secondly, it is based as much as possible on locally available data at the CS, such that it can even react in case there is a communication problem with the monitoring mechanism of the grid. Third, it separates the concerns of CSPs and DSOs. Hence, the proposed architecture is distributed and located on the actuator side, which is the CS in our case.

In order to monitor the power quality, it is essential to measure voltage, current, frequency, harmonic distortion, and waveform at different points of the grid [155]. In this work, a monitored point is referred to as a MP. In this regard, power quality is indicated by Grid State Indicators (GSIs), e.g. the voltage level or loading of grid elements, such as the transformer or feeder lines. Furthermore, these GSI classes are computed/measured directly at MP in real-time, e. g., calculation of RMS values, or are computed using multiple

measured GSIs values at different MPs, e. g., the minimum voltage on an individual feeder line.

As the proposed architecture enables the response to different power quality issues in nearly real-time, a data stream in high resolution is required (e. g., in a 3 seconds interval). On one hand, real-time handling of big data streams requires a data processing architecture that needs to be generic, scalable, and fault-tolerant [156]. On the other hand, the measured GSIs values are most interesting when they are beyond a certain threshold, e. g., the voltage is higher or lower than $\pm$ 10% of the nominal voltage [21]. In the architecture shown in Figure 4.2, an event-driven streaming service is assumed, like *Apache Kafka* [157], to be existing as real-time data handling for events from the power grid [158, 159, 160]. These events are triggered by MPs due to unusual GSIs values[2] and sent to the Kafka cluster, e. g., using cellular networks or dedicated Internet access.

However, the collected GSIs values are forwarded to controller components, that are located at CSs. The responsibility of these controllers is to indicate the present status of the low voltage grid and to choose appropriate actions in order to mitigate stress on the power grid arising from emerging power quality issues. As depicted in Figure 4.2, power quality estimation is performed by a component called *PQ-Indicator*, which responds to triggered events from Kafka. For example, in case of voltage fluctuations that refer to degradation of the power quality, it estimates the power quality gradually, then, asks the so-called SC to decrease/increase the charging rate in order to counteract the voltage fluctuation and, hence, improve power quality.

The output of *PQ-Indicator* is a power quality indicator, called `PQ-Indic`. It is a fuzzy indicator defined within the range of $[-1, 1]$, and it adopts the traffic light model. Within this normalized range, (-1) corresponds to either a complete shutdown of the charging process or a reduction to the minimum required power in order to be able to control the EV charging later. In contrast, the value $(+1)$ represents the maximum power capacity of the CS. The smart charger applies a smooth or drastic change on the used charging power capacity depending on the value of `PQ-Indic`. However, the reason behind separating power quality indication and control logic is due to the different interests of the involved parties. From the CSP perspective, the PQ-Indicator is a black box, which is configured by the DSO depending on the characteristics of each low voltage grid individually, e. g., applying different thresholds for voltage boundaries. In contrast, the CSP configures the SC according to its business model.

One of the main requirements of this architecture is the continuous limitation of the charging power capacity at a CS during a charging process. That is possible with OCPP in version 1.6 that defines the communication between SC and CS. In version 2.0 [161], CSs and charge points support smart charging profiles. These profiles can set constraints to the maximum amount of power (by defining external profiles at a high stack level) that is delivered during

[2]Time-driven approach can be applied instead of event-driven one

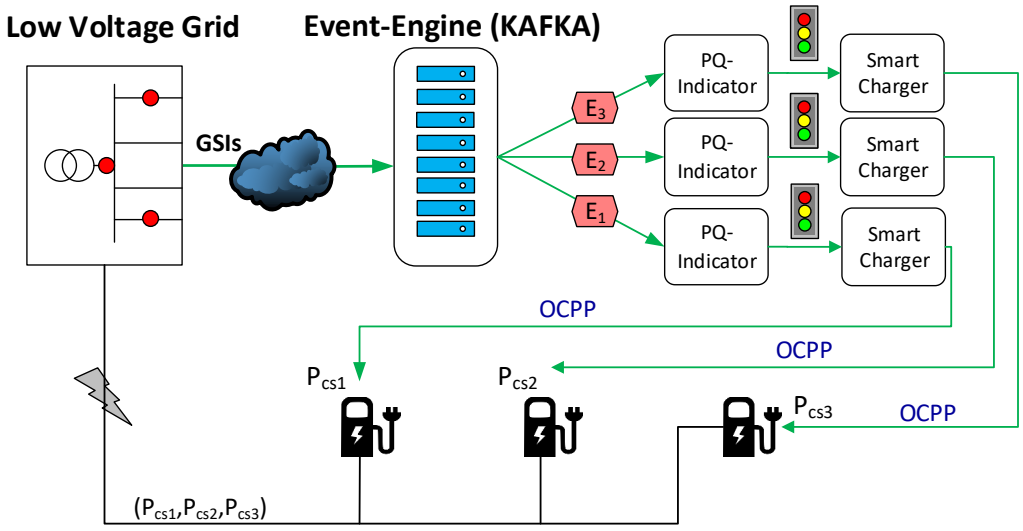

Figure 4.2.: Schematic Smart Charging Architecture

the charging transaction and enable dynamic charging profiles for smart charging purposes. Hence, CSs are able to react to specific behaviors directly without further control signals. According to OCPP 2.0, CSs can handle different types of charging profiles: ChargingStationMaxProfile, TxProfiles, and ChargingStationExternalConstraints. Those different profiles are stacked and used by their prioritized stack level. The Composite Schedule combines the different profile types by calculating the minimum in each time interval. Furthermore, the concept of using such charging profiles is seen as a promising direction for better power planning of charging processes in the future since these profiles are generated based on the power constraints of both the vehicle and the grid.

The proposed system does not require us to predict SoC or EVs mobility. In that regard, the connection point of the CS is considered instead of a single connector. The CS is able to contribute to any events of the grid as long as one charging connector is active. The total demand of the CS (aggregated of all connectors) can be controlled every few minutes. However, a fair or proportional distribution can be used for coordinating the available capacity at the connection point among the active connectors. As a result, quick response to changes in the distribution grid due to fluctuations in uncontrolled loads is possible since neither prediction models of EV arriving rate nor charging behavior of the end-users is required.

4.3 Measurements and Event-driven Architecture

According to [162], there are two distinct data classes in smart grids:

1. Operational data (GSIs) which is the electrical data of the grid that represents real and reactive power flow, voltage, etc.

2. Metering usage data which is associated with energy consumption.

Smart Meters (SMs), sensors, and PMUs are the main sources of that data collected in the form of time-series with various granularity depending on a specific control objective and application [163]. For example, while a SCADA system collects data every 25 s, an AMI system collects data every 1-15 minutes. This data can be either saved in the memory card of the MP[3] for further analysis or transferred in real-time via communication channels for using them as an input for any kind of smart grid solutions. The transmission has to be reliable, privacy protected[164], effective in terms of data size, and well beneficiary-oriented. Thereby, the data flow within a smart grid comprises three steps:

1. Data gathering: The locally collected data can be either fetched or pushed periodically or triggered by certain events.

2. Data processing: Analytic models can be used to extract extended information from the raw gathered data. Enhancing the knowledge about grid behavior and supporting control decisions are the main advantages of such further processing.

3. Data utilizing: The collected data is beneficial in the following both cases: (1) building advanced prediction models [165] and (2) implementing real-time smart grid solutions supporting grid stability.

However, utilities face a great number of challenges from strategy to performance in data management, particularly, management of massive data volume. Thus, new paradigms of metering are required to reduce the cost of storing and processing such a vast quantity of data. For example, the energy metering is typically time-based metering where a regular time interval is defined to measure the energy values. Simonov and *et al.* proposed in [166] an event-based energy metering. Their approach is based on recognizing specific events, occurring in the power consumption pattern, that modify the previous trend of evolution of the consumption, and transmitting the energy resulting between these events. Likewise, operational data is generated by monitoring the grid in a time-driven approach and the transition to an event-driven scheme similar to Generic Object Oriented Substation Event (GOOSE) in standard IEC 61850 [167], particularly in the distribution grid, is rational to address the following challenges for a DSO:

- Unfortunately, the lack of the infrastructure or data analysis skills to deal with all data collected impedes a full use of it by utilities. Furthermore, only the abnormality of grid behavior is essential in terms of controlling and overcoming grid issues of power quality [168].

- The issues arise from big data in terms of processing, transmission, and storing.

[3] In the context of this work, MP is used to represent all possible measuring devices.

- The event-driven scheme can enable the “publish/subscribe” messaging pattern in order to keep the transmitted data over the communication channel as small as possible. The rationale behind that is that the reliability and quality of power supply can be increased by controlling selected flexible assets whose controllable parameters are different, e.g., active power and reactive power. For example, it is unrealistic to expect help from currently installed CSs in the market regarding harmonics issues, since only the active power control is feasible technically, neither harmonics or reactive power control is supported.

Figure 4.3 depicts a possible implementation of the aforementioned event-driven data collector by using two open-source techniques: Apache Kafka and Akka streams [169]. Apache Kafka is a well-known distributed streaming platform that provides a scalable and resilient event store. It is used to build reliable and real-time data pipelines to transfer data between systems or applications. The events are stored in topics for which multiple producers and consumers may exist. However, to enable efficient real-time processing of these data streams, the reactive streams [170] initiative comes into play, e. g., Akka streams. It provides a standard for asynchronous stream processing, with non-blocking back-pressure. That means that the consumer(s) should not be overwhelmed by the producer(s), thus letting the streaming solution implement and control bounded queuing. Moreover, the size of each sent event is relatively small; it equals $104 + 17n$ bytes, where n is the number of measured GSIs. The embedded data in the event includes two Universally Unique IDentifier (UUID) for the MP and its location, timestamp, and Kafka header. Hence, a Long-Term Evolution (LTE) connection for each MP with an approximated data volume of one GB would be enough. A benchmark and performance analysis of Apache Kafka is carried out and stated in Section 5.2.

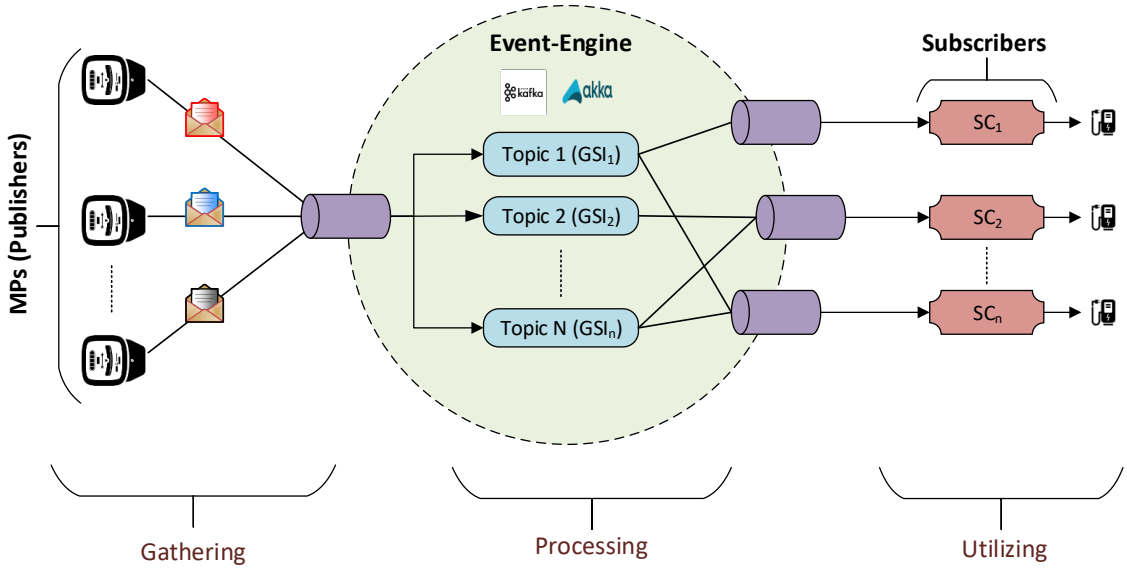

Figure 4.3.: Event-driven Data Collection in Smart Grids

4.4 Real-time Indication of the Status of a Distribution Grid

The authors of [24] introduce a comparison between a packet-switched communication network such as the Internet and the power distribution grid. According to their study, many concepts of the Internet have equivalents or good approximations in the power grid, namely, congestion, topology, sending measurements and controlling signals, self-protection, and uncontrolled loads. The only main difference is the congestion notification. While the Internet has two types of congestion feedback: explicit and implicit, the distribution grid has none of them originally. Precisely, the implicit mechanism is almost impossible[4] according to [24], whereas the explicit one does not exist in most of the distribution grids because of the lack of installed measurement devices. The trade-off between cost and leveraging is the reason behind that lack

The proposed indication mechanism complies with four design criteria. First, excessive intelligence unnecessarily complicates the system. Second, it assigns a higher weight to local conditions than to remote ones. The locally concentrated impact of DG and uncontrolled loads provides further evidence in this respect. Third, it takes into account that the connection points in the grid are not on the same degree of importance, e.g., the transformer is extremely important in the low voltage grid as a single point of failure. Fourth, apart from the location of the raising PQ issue, the grid status cannot be binarily classified into good or bad, rather coarse-grained indication is possible. In other words, the DSO considers some operating conditions in the grid as not optimal but no need for applying contingency measures. Thus, a very subtle change in the behavior of the controllable loads in the grid can move back into the optimal (normal) operating conditions.

Algorithm: PQ-Indicator

The goal of the PQ-Indicator is to estimate the grid status based on different GSI values at different MPs in the grid. Since most low voltage networks are built as 3-phase systems, the PQ-Indicator estimates the status of each phase individually. However, the output of the PQ-Indicator can be used by any controller to decide about suitable actions of the controllable load based on real-time measured GSI values, e.g., CSs or PVs. Apart from the possibility of using PQ-Indicator in many smart solutions, the main focus in this work is the e-mobility smart solutions.

[4] In [171], it has been shown that local sensing of the line voltage or frequency at end nodes can be used to implicitly infer the aggregate demand or the power imbalance at higher levels in the distribution network.

Input: A set of tuples containing the GSI, the MP and the value of the GSI at that MP $(K_k, MP_j, v_{j,k})$.
Output: An indicator for each phase that represents the PQ in the low voltage grid. The indication defined as a tuple of a value within [-1,1], called `PQ-Indic`, and the main influencing GSI, e.g., load, voltage, etc.

The input value of the PQ-Indicator is modeled as $m \times n$ matrix ($M_{m\times n}$ in 4.1), where m is the number of MPs, and n is the number of GSI classes.

$$M_{m\times n} = \begin{bmatrix} v_{1,1} & v_{1,2} & v_{1,3} & \dots \\ v_{2,1} & v_{2,2} & v_{2,3} & \dots \\ \vdots & \vdots & \vdots & \dots \end{bmatrix} \in (\mathbb{R} \cup \{\perp\})^{m\times n} \tag{4.1}$$

where $v_{j,k} \in \mathbb{R}$ is the value of GSI class K_k at MP_j. In case the input data does not include a GSI value at MP_j, the value is set to $v_{j,k} = \perp$.
Using this input matrix, additional GSI classes can be calculated, e.g., the average, min, or max values of a GSI class K_k over several MP_j. The used aggregation function $g : (\mathbb{R} \cup \{\perp\})^m \to \mathbb{R}$ ignores the $\perp$ entries of the matrix. The resulting new GSI class is denoted as

$$\overline{K_k} = g(v_{j,k}), j = 1..m. \tag{4.2}$$

Furthermore, a function $h : (\mathbb{R} \cup \{\perp\})^n \to \mathbb{R}$ can be defined which calculates a new GSI class using the existing GSI values at the same MP_j, e. g., the apparent power S_i at point p_i is calculated based on the real power Pi and PF, i.e., $S_i = P_i/PF_i$. Another good example is calculating the overloading percentage of a transformer based on its temperature and the phase imbalance factor. The resulting new GSI class is denoted as

$$\widehat{K_j} = h(v_{j,k}), k = 1..n. \tag{4.3}$$

In the remainder of this work, the author does not distinguish between composed GSI classes $\overline{K_k}$ in Equation (4.2) or $\widehat{K_j}$ in Equation (4.3), and the original GSI classes K_k, but always refer to them by K_k.

The situation of the power grid is distinguished between good, critical, and not optimal. In the last case, impending problems can be avoided by requesting subtle changes in the behavior of big loads such as CSs. Hence, the design of the PQ-Indicator adapts the traffic light model with three colors that describe the status of the grid. The colors are defined on top of a calculated fuzzy indicator `PQ-Indic`, as depicted in Figure 4.4. In that regard, the six thresholds (setpoints), $ER_k, RY_k, YG_k, GY_k, YR_k, RE_k$, for the red, yellow, and green ranges are defined for each GSI class k separately. As a guideline, power quality standards

Figure 4.4.: Traffic Light Model on Top of `PQ-Indic`.

such as EN 50160 [21] can be used. Additionally, historical data about the low voltage grid is used by the DSO to determine the correct values of those thresholds of each GSI. While the negative value of `PQ-Indic` means that a reduction in CS demand is required, the positive one refers to a required increase. As a result, two kinds of red signals exist (R^+, R^-) and yellow signals as well (Y^+, Y^-).

- **Red**: Represents a critical situation in the grid. A relatively drastic action (e.g., increase/decrease of the CS demand) has to be taken by each active SC in order to mitigate the stress on the grid. The red color is defined for a `PQ-Indic` $\in [ER, RY] \cup [YR, RE]$, where $ER = -1$, $RY = -0.7$, $YR = 0.7$ and $RE = 1$, for example.
- **Yellow**: Represents a warning phase. The situation is not critical but still cannot be considered as optimal. A subtle action of a SC can be enough to move back into a stable status. In the yellow state, the grid still has higher priority over the EV user, therefore, the requirements of the charging process can be taken into account only to a certain degree. `PQ-Indic` $\in (RY, YG] \cup [GY, YR)$, where $YG = -0.3$ and $GY = 0.3$, for example.
- **Green**: Represents a stable phase, thus, no need for any further SC reactions concerning the grid. Hence, the concerns of the EV user are prioritized over the grid's, thereby, increasing or decreasing the charging capacities is possible, but not required. `PQ-Indic` $\in (YG, GY)$.

Plenty of functions can be used to translate the values of a GSI class K_k to a single value `PQ-Indic`$_k$. For simplicity, the piece-wise linear interpolation function t_k in Equations (4.4) (also see Figure 4.5) is used. It does not only preserve the order of the GSI values and maps the range of different GSI classes to the same smaller range of $[-1, 1]$, but also allows

weighting and shifting of the range of individual GSI classes because of its nature. Thus, the $\texttt{PQ-Indic}_k$ for GSI class K_k is equal to $t_k(K_k)$.

$$t_k(x) = \begin{cases} ER & \text{if } x \in (-\infty, ER_k) \\ \frac{RY \cdot (ER_k - x) + ER \cdot (x - RY_k)}{ER_k - RY_k} & \text{if } x \in [ER_k, RY_k] \\ \frac{YG \cdot (RY_k - x) + RY \cdot (x - YG_k)}{RY_k - YG_k} & \text{if } x \in (RY_k, YG_k] \\ \frac{GY \cdot (YG_k - x) + YG \cdot (x - GY_k)}{YG_k - GY_k} & \text{if } x \in (YG_k, GY_k) \\ \frac{YR \cdot (GY_k - x) + GY \cdot (x - YR_k)}{GY_k - YR_k} & \text{if } x \in [GY_k, YR_k) \\ \frac{RE \cdot (YR_k - x) + YR \cdot (x - RE_k)}{YR_k - RE_k} & \text{if } x \in [YR_k, RE_k] \\ RE & \text{if } x \in (RE_k, \infty) \end{cases} \tag{4.4}$$

Afterwards, the different $\texttt{PQ-Indic}_k$ are combined using the following criteria A_1, A_2, and

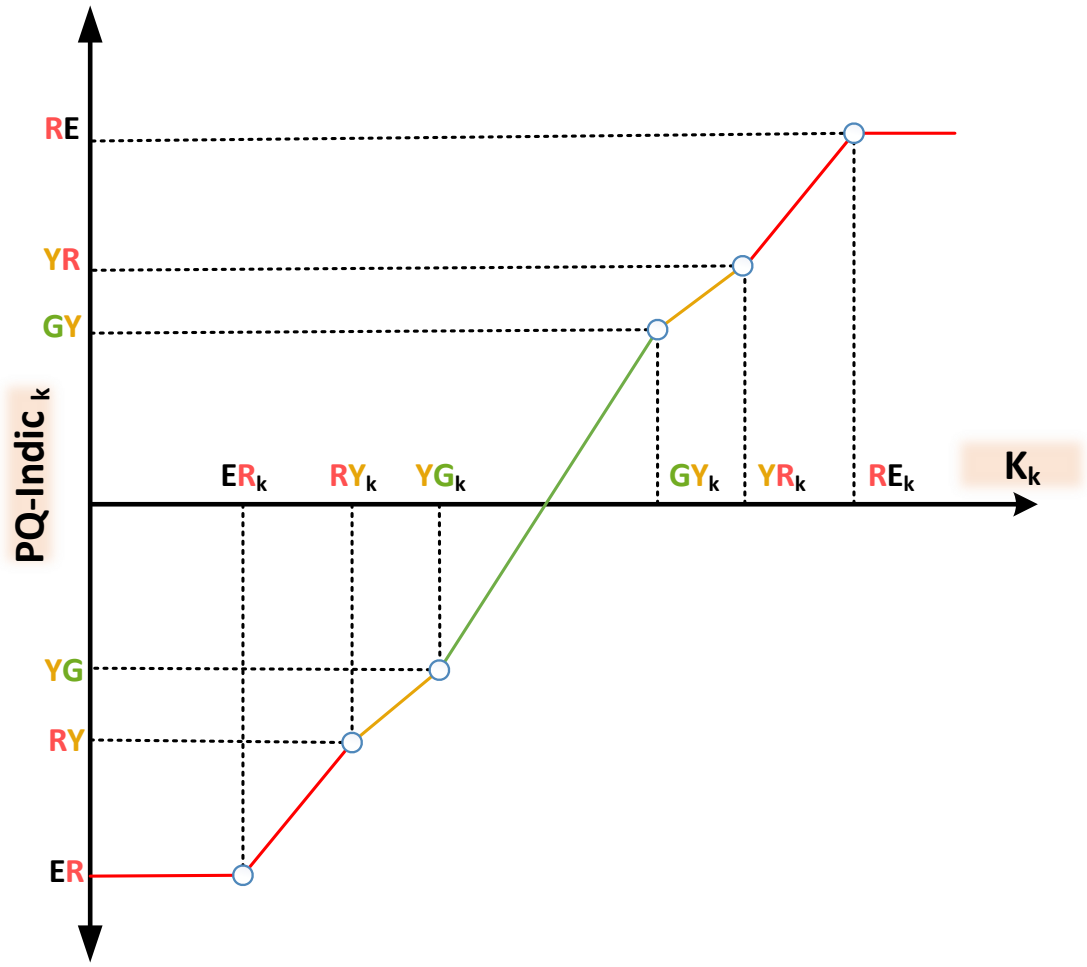

Figure 4.5.: The translation function $t_k(x)$ that translates GSI values to $\texttt{PQ-Indic}_k$.

A_3, which are in descending order according to their importance in terms of grid stability. In this work, only those three criteria have been focused on because existing charging stations

have only the capability to mitigate overloading and voltage level by limiting the charging power (see Section 3.3.3). Nevertheless, this list might be extended to include additional criteria such as harmonics and frequency deviation.

(A_1) Overloading an element of the grid

Power distribution equipment, such as transformers or cables, have an upper thermal limit, which should only be exceeded for a short time. The specific thresholds can vary with the equipment type. An example that depends on the maximum allowed apparent capacity S_{max} is given in Table 4.1. In the case of a transformer, the values are chosen in a way, such that the transformer is operated below its maximum apparent power and optimally with the highest efficiency. However, in an unbalance 3-phase system, there is a relation between the transformer overloading and the phase imbalance. Such an assumption will cause the apparent power to look like a lousy metric to express the overloading thresholds. Nevertheless, that slight difference between balanced and unbalanced systems has no significant impact on the definition of the criteria (A_1).

ER_k	RY_k	YG_k	GY_k	YR_k	RE_k
S_{max}	$y \cdot S_{max}$	$z \cdot S_{max}$	$w \cdot S_{max}$	$x \cdot S_{max}$	0

Table 4.1.: The thresholds of GSI class from criterion A_1 where the constant values $x \leq w \leq z \leq y \in [0, 1]$.

(A_2) Voltage level

As seen in Chapter 3, different load and generation scenarios can cause the voltage level to increase or decrease in some regions of the low voltage distribution system. Additionally, the sine voltage signal has to be stable according to EN 50160 standard (see Section 2.1.2), thereby, its main mathematical variables should stay in certain boundaries, namely, magnitude and frequency. In this criteria, the voltage magnitude is the leading and the only focus since frequency control is usually happening at higher levels, and its a part of the TSO's responsibilities. However, voltage frequency can be discussed and added as a separate criterion.

As the estimation of the grid is carried out phase-by-phase, the voltage level is measured between the phase and the neutral (conductor). Generally, defined thresholds for the voltage GSI class are shown in Table 4.2.

ER_k	RY_k	YG_k	GY_k	YR_k	RE_k
0.9 U_n	0.95 U_n	0.99 U_n	1.01 U_n	1.05 U_n	1.1 U_n

Table 4.2.: Thresholds of the Voltage GSI Class from criterion A_2.

(A_3) Phase imbalance

Phase imbalance of a three-phase system exists when one or more of the line to line voltage in a three-phase system is mismatched in terms of either magnitude or angle.

A three-phase load is usually connected with a shunt compensator. If the load changes unbalanced, the compensator must generate the reactive power required to restore the system to a balanced state [172]. The CS can play a similar role theoretically to the aforementioned compensator, as discussed in Chapter 3. Therefore, the proposed PQ-Indicator is a phase-based estimator which, in its turn, allows different reactions on each phase if it is technically possible.

Based on the fact that present CSs cannot control the charging process per phase and only the overall charging power is considered, the PQ-Indic values can be aggregated as follows:

$$\underset{\phi\in\{A,B,C\}}{agg}(\texttt{PQ-Indic}_\phi) = \begin{cases} \underset{\phi\in\{A,B,C\}}{avg}(\texttt{PQ-Indic}_\phi) & \textbf{if} \quad \forall\, \phi \in \{A,B,C\}: \\ & \texttt{PQ-Indic}_\phi \in G \\ \underset{\phi\in\{A,B,C\}}{max}(\texttt{PQ-Indic}_\phi) & \textbf{else if} \quad \forall\, \phi \in \{A,B,C\}: \\ & \texttt{PQ-Indic}_\phi \in G \cup Y^+ \cup R^+ \\ \underset{\phi\in\{A,B,C\}}{min}(\texttt{PQ-Indic}_\phi) & \textbf{otherwise} \end{cases} \tag{4.5}$$

where $\texttt{PQ-Indic}_\phi$ is the PQ-Indic value of phase $\phi \in \{A, B, C\}$. It is intended to use a conservative aggregation when phases are in different colored states since phase balancing is performed locally by the CS. In contrast, aggressive aggregation is used when the grid is asking for load increase on one or more phases while other states are at least green. In that case, a charging increase is allowed on all phases; hence, the maximum is chosen to mitigate the most prominent problem first. In the case of green states on all phases, the average best reflects the situation.

As the considered criteria have different priorities in terms of grid stability and the primary concern of the SC is the local stability as part of the global one, the PQ-Indicator uses a 3-layer hierarchical logic to decide about the (local) grid state as depicted in Figure 4.6. As the highest priority, criteria A_1 represents the transformer loading. For this purpose, the translation function $t_k(x)$ in Equations (4.4) is applied to the measured load of the transformer to calculate $\texttt{PQ-Indic}_{A_1}$. In case $\texttt{PQ-Indic}_{A_1}$ is colored red, a critical load reduction or increase is required, and then, the PQ-indicator will ignore criteria A_2 returning $\texttt{PQ-Indic}_{A_1}$ as overall PQ-Indic of the grid. Otherwise, the PQ-Indicator will compute three more values regarding the criteria A_2 describing the voltage in three places in the grid: $\texttt{PQ-Indic}_{A_2}^{CS}$ at the CS, $\texttt{PQ-Indic}_{A_2}^{Tran}$ at the transformer and $\texttt{PQ-Indic}_{A_2}^{Critical}$ at a critical point in the low voltage grid. In order to determine the critical point for each CS, several points with low and high voltage magnitude in the low voltage grid are identified, and the one which is most influenced by changes of the CS's charging behavior is chosen.

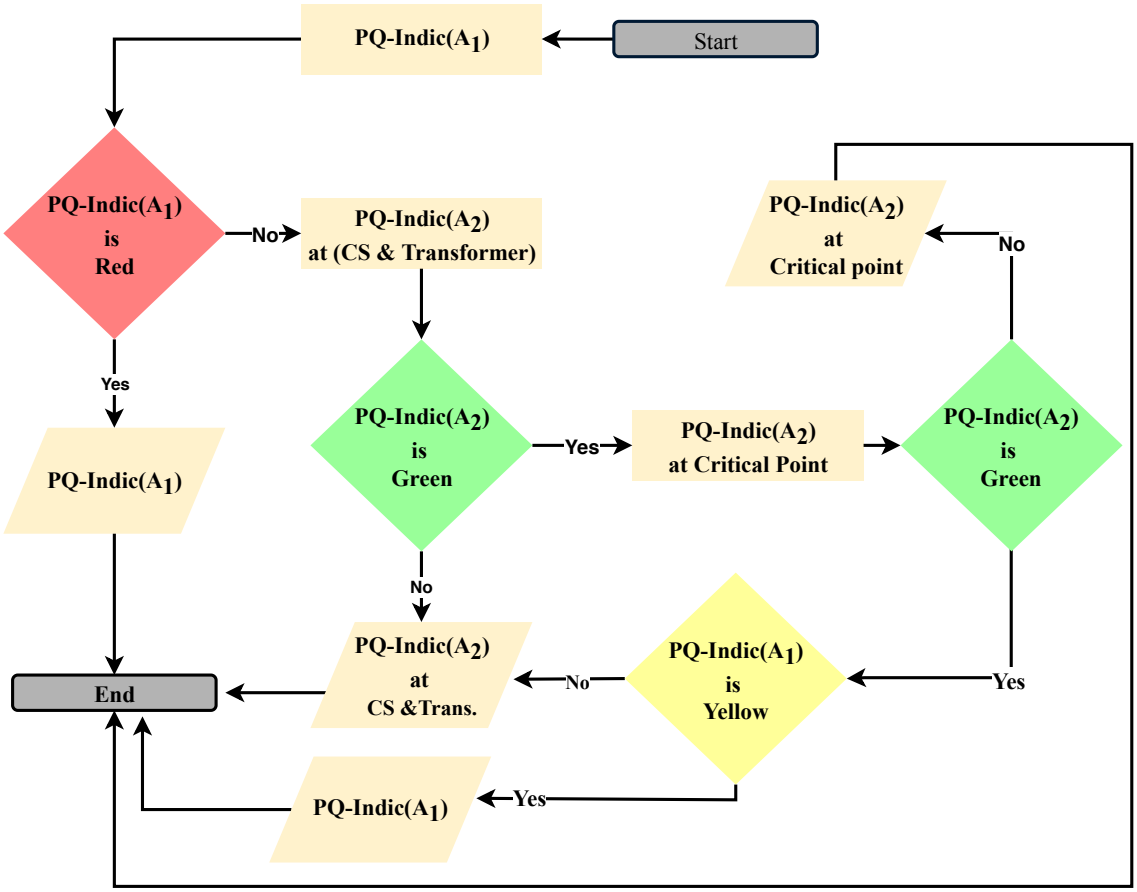

Figure 4.6.: Hierarchical Decision Logic of the PQ-Indicator Based on the Traffic Light Model

On the second level, the PQ-Indicator will use Algorithm 4.1 to indicate the state of the grid regarding A_2. In case $\texttt{PQ-Indic}_{A_2}$ is colored yellow or red, this value is directly returned. Otherwise, the output is calculated by the third level taking the situation at the critical point into account. Hence, if the PQ-Indic at the critical point is colored yellow or red, $\texttt{PQ-Indic}_{A_2}^{Critical}$ is used as an output of the PQ-Indicator. Otherwise, $\texttt{PQ-Indic}_{A_1}$ is reconsidered to avoid the yellow state of the transformer. If the transformer has no overload, the PQ-Indic at the charging station $\texttt{PQ-Indic}_{A_2}^{CS}$ defines the return value.

The PQ-Indicator should use the logic mentioned above for each phase, and a tuple of three values $[\texttt{PQ-Indic}_A, \texttt{PQ-Indic}_B, \texttt{PQ-Indic}_C]$ is calculated at the end. Furthermore, the main influencing GSI is appended. In our case, it is one of the values $\{Load, Voltage\}$. Next, the forwarded values should be adjusted based on the criteria A_3 using Equations (4.5), if the CS performs self-management of phase balancing, i. e., it is not controllable technically.

Data: phase-to-neutral voltage at CS and transformer on a certain phase $\in \mathbb{R}_+$
ER=-1, RY=-0.7, YG=-0.3, GY=0.3, YR=0.7, RE=+1
Result: PQ-Indic$_{A_2} \in [-1, 1]$
if ($PQ\text{-}Indic_{A_2}^{CS}$)$\leq$ ***RY*** **then**
  return ($PQ\text{-}Indic_{A_2}^{CS}$)
else
  if $PQ\text{-}Indic_{A_2}^{Tran} \leq$ ***YG*** **then**
    if ($PQ\text{-}Indic_{A_2}^{CS}$) $\geq$ ***YR*** **then**
      return ($PQ\text{-}Indic_{A_2}^{CS}$. $|PQ\text{-}Indic_{A_2}^{Tran}|/2$)
    else
      if ***GY*** $\leq PQ\text{-}Indic_{A_2}^{CS} <$ ***YR)*** **then**
        Return (GY)
      else
        if ***YG*** $< PQ\text{-}Indic_{A_2}^{CS} <$ ***GY)*** **then**
          return (YG)
        else
          return (min ($PQ\text{-}Indic_{A_2}^{CS}$,$PQ\text{-}Indic_{A_2}^{Tran}$))
        end
      end
    end
  else
    if $PQ\text{-}Indic_{A_2}^{Tran} \geq$ ***GY*** **then**
      if ***RY*** $<$ ($PQ\text{-}Indic_{A_2}^{CS}$) $\leq$ ***YG*** **then**
        return (YG)
      else
        if ***YG*** $< PQ\text{-}Indic_{A_2}^{CS} <$ ***GY)*** **then**
          return (GY)
        else
          return (max ($PQ\text{-}Indic_{A_2}^{Tran}$,$PQ\text{-}Indic_{A_2}^{CS}$))
        end
      end
    else
      return ($PQ\text{-}Indic_{A_2}^{CS}$)
    end
  end
end

Algorithm 4.1: Indication of power quality regarding criteria A_2 at a CS.

4.5 Smart Charger for Electric Vehicles

It is assumed that the smart charging algorithm starts once a vehicle is plugged into a CS connector. It uses real-time indications of the PQ-Indicator as a single input about the grid. Additionally, it considers the energy requirements of the end-user. Furthermore, the SC should avoid drastic changes in charging power. Otherwise, the EV might see these changes as a bad quality power and disconnects from the connector as a result.

Input: A tuple of the `PQ-Indic` and the main influencing GSI per phase $\phi \in \{A, B, C\}$. Additionally, an aggregated charging profile of cs_i denoted as $\mathscr{C}_i(t)$.
Output: The total power capacities of a CS, which can be distributed among the active connectors in different ways, e.g., equally or fairly distributed.

However, a SC has two options to react to the arrival of a new `PQ-Indic` at time t:

1. The SC reacts immediately and changes the charging capacity.

2. The SC maintains a First-In-First-Out (FIFO) queue called LastValuesStore (LVS) with a length of n to store the arriving values of `PQ-Indic` in a time window with length T. The queue is updated with each new arrival of a `PQ-Indic` value. Thus, SC reacts periodically at the end of each time window. A weighted average of the existing values in the queue is calculated. The output refers to a weighted average indicator of grid status at time t ($S^W(t)$). In case no events arrived during this time window, the SC assumes a bad connection service and goes to the conservative mode.

Equation (4.6) depicts how the weighted average indicator is calculated, where ω_k is a list of the same size as LVS and contains weights for each index of LVS_k. ω_k is defined in such a way that the most recent `PQ-Indic` values are given higher weights thus more importance compared to the earlier values.

$$S^W(t) = \frac{\sum_{k=1}^{n} \omega_k \, LVS_k}{\sum_{k=1}^{n} \omega_k} \tag{4.6}$$

The time management of a SC is discussed comprehensively in Section 4.6.

Next, two different kinds of algorithms are described. While the first is based on using a FSM to represent the different states through a charging operation, the second mimics the congestion mechanism of TCP.

4.5.1 Algorithm: FSM-based Smart Charger

A FSM [173] (sometimes called finite-state automaton) is a mathematical model of computation that can be implemented with hardware or software to represent sequential logic and specific computer programs. At any given time, a FSM can be in exactly one of the finite numbers of states. A transition among two of those states is a response either to some external inputs or the satisfaction of a condition. However, any FSM is described by a five-element tuple: $(Q, \Sigma, \delta, q_0, F)$:

- Q = a finite set of states.
- Σ = a finite and nonempty input alphabet.
- δ = a series of transition functions.
- q_0 = a starting state.
- F = a set of accepting states or end states.

4.5.1.1 General Description and States

The algorithm of the SC is modeled as a FSM, which stores the last `PQ-Indic` values, SoC, and a Boolean value (EV is unplugged). The FSM used within a SC is depicted in Figure 4.7. The described FSM consists of seven states $Q = \{red^-, yellow^-, green, yellow^+, red^+, gray, blue\}$ that are grouped into three different types:

- Operational states: low red, low yellow, green, high yellow, and high-red state represent the different `PQ-Indic` color ranges.
- Standby state: The gray state models the charging state after the desired SoC is reached.
- End state $F = blue$: With maximum SoC or unplugged EV, it is no longer possible to control the charging operation[5].

The low-red state is considered as the start state $q_0 = red^-$ since the charging operation will start slowly, and a SC adopts a conservative approach concerning the grid stability.

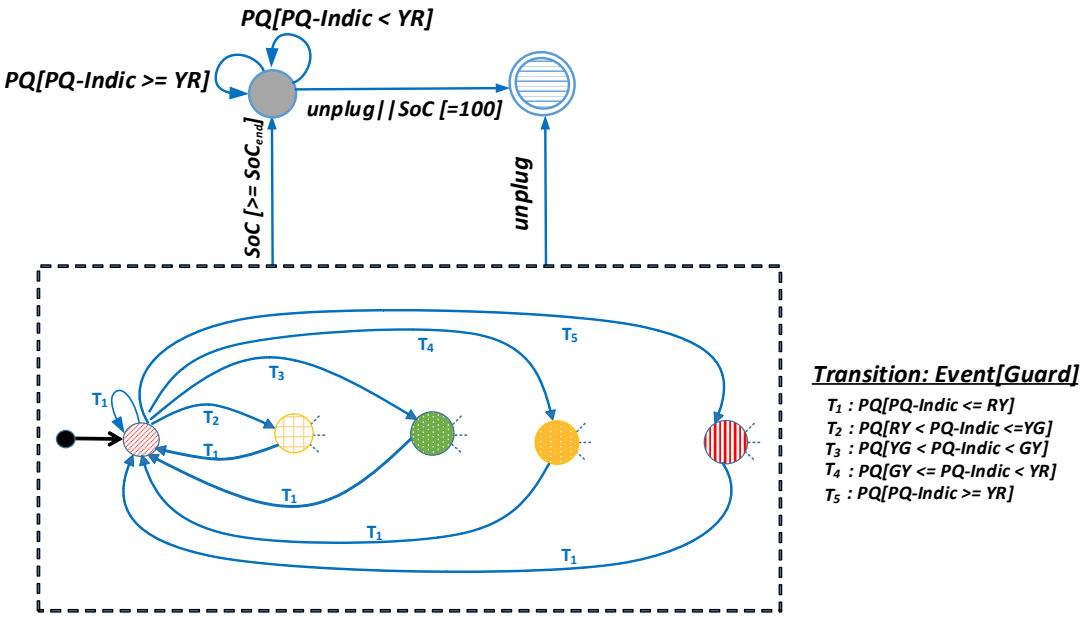

Figure 4.7.: FSM of the Smart Charger based on the Traffic Light Model.

In our case, the transitions (δ) in the FSM are labeled by two parts: *Event* and *Guard*; thus, Σ = {`PQ-Indic`, SoC, unplugged}. In the proposed FSM, there are three kinds of *events* that

[5] In the case of multiple connected EVs, the transition to gray- and blue-states consider the status of all connected EVs, i. e., all EVs reach the desired level of SoC, full battery, or unplugged.

can trigger the state transition: Input of a new PQ-Indic value[6], unplugging of the vehicle, and a change of the SoC of the battery. Each state transition can have a prerequisite, which is modeled by the logical condition of a *guard*. If the condition of a guard does not match, the FSM remains in its current state. Finally, each state transition can have an *action* that specifies the output of the SC. In our case, the action defines the new total charging power of the ongoing charging processes.

The transition to the end state ($blue$) occurs whenever the driver unplugs the vehicle or the battery is fully charged (equals SoC = 100). If the desired SoC_{end} (defined by the end-user) is reached, the FSM transits to the charging standby state ($gray$ state). Within this state, the SC can react on critical grid situations using the still plugged EVs, only in case of the PQ-Indic value $\in R^+$, hence requires an increase of charging power capacity. All other values of PQ-Indic are resolved as charging with the minimum required capacity. The reason behind that is the implementation of the proposed SC supports only G2V. Worth mentioning, supporting V2G is possible and needs only some slight changes. However, this is a part of future work.

In Figure 4.7, for simplification within the box containing the operational states, only the outgoing and incoming transitions of the red^- state are shown. All other states are connected similarly to each other. Furthermore, the state machine can transit from any operational state to the standby and end state.

4.5.1.2 Transitions and Actions

In this section, the total used charging capacity of all active charging processes at charging station cs_i at time t is denoted as $\mathscr{U}_i(t)$. The maximum physical capacity of cs_i is written as $\mathscr{M}_i$, and the aggregated charging profile of the CS is denoted as $\mathscr{C}_i(t)$. In all cases, the *action* of transitions, which reveals the new charging power, should not be bigger than $\mathscr{M}_i$. A safety upper margin is defined by $\mu < 1$ in order to stay aligned with the users charging profile regarding the battery state of health and the charging duration. This safety margin is used as a buffer to compensate grid problems that may lead to a slight reduction of charging power. The other way round, the minimum charging power needs to be set to a value $\mathscr{C}_i^{min}$ higher than zero to avoid the disconnection of the vehicle.

The action of the transitions mainly relies on the destination state, which is equal to the color of the new input PQ-Indic value. In the following, the single transitions are given by *source* $\rightarrow$ *destination*. The source and destination can also be an asterisk, which is a wildcard value.

- $* \rightarrow red^-$
  If the new PQ-Indic value is colored low-red, the SC needs to reduce the charging power. Since this state is considered to be highly critical for the grid, the resulting

[6]Either an aggregated PQ-Indic $S^W(t)$ regarding Equation (4.6) or a single event-based value of PQ-Indic.

action is defined in a polynomial way. Δ is calculated as the percentage of change in the currently used power.

$$\begin{aligned} \Delta &= (\texttt{PQ-Indic} + 1)^{\alpha} \\ \mathscr{U}_i(t+1) &= \max\left(\Delta\ \mathscr{U}_i(t)\ ,\ \mathscr{C}_i^{min}\right) \end{aligned} \tag{4.7}$$

The parameter α in Equations (4.7) needs to be higher than 1 to match a polynomial decrease. Therefore, $\Delta \in [0, 0.3)$ because of $\texttt{PQ-Indic} \in [-1, -0.7]$. As a result, the decrease of the charging power is greater than 70 % of the currently used charging power in any case.

The parameter α can be defined depending on the source of the transition or by comparing it with the last `PQ-Indic` value.

- $* \rightarrow \{yellow^-, yellow^+\}$
  If $\texttt{PQ-Indic} \in Y^+ \cup Y^-$, the gird is not stable, but it is not highly critical like in the red states. Hence, the transitions to this state can partially consider the users' charging profile. The change in the charging power capacity is calculated by a linear function, which depends on the `PQ-Indic` value and can be parameterized by the source state of the transition.

$$\begin{aligned} \Delta_1 &= 1 + \varrho_1\ (\texttt{PQ-Indic} + YG + 0.1) \\ \Delta_2 &= 1 + \varrho_2\ (\texttt{PQ-Indic} + GY - 0.1) \end{aligned} \tag{4.8}$$

$$\mathscr{U}_i(t+1) = \begin{cases} \min\left(\Delta_1\ \mathscr{U}_i(t)\ ,\ (1+2\mu)\ \mathscr{C}_i(t+1)\ ,\ \mathscr{M}_i\right) & \texttt{PQ-Indic} \geq GY \\ \max\left(\Delta_2\ \mathscr{U}_i(t)\ ,\ \mathscr{C}_i^{min}\right) & \texttt{PQ-Indic} \leq YG \end{cases}$$

In Equations (4.8), parameters ϱ_1 and $\varrho_2 \in \mathbb{R}_+$ can be configured by the source of the transition similar to α in the previous transition. However, the new charging power is limited by the minimum of $\mathscr{C}_i^{min}$ and the maximum of $\mathscr{M}_i$ in all cases.

- $* \rightarrow$ green
  If $\texttt{PQ-Indic} \in G$, the gird is stable. In this regard, a linear increase or decrease of the currently used charging power is applied until the charging profile plus the safety margin is reached.

$$\begin{aligned} \xi &= \frac{\texttt{PQ-Indic} + GY + 0.1}{2} \\ \Delta_1 &= \xi\ (1+\mu)\ \mathscr{C}_i(t+1) \\ \Delta_2 &= \frac{\mathscr{U}_i(t) - (1+\mu)\ \mathscr{C}_i(t+1)}{2} \end{aligned} \tag{4.9}$$

$$\mathscr{U}_i(t+1) = \begin{cases} \min\left(\mathscr{U}_i(t) + \Delta_1\ ,\ (1+\mu)\ \mathscr{C}_i(t+1)\right) & \mathscr{U}_i(t) \leq (1+\mu)\ \mathscr{C}_i(t+1) \\ \mathscr{U}_i(t) - \Delta_2 & \mathscr{U}_i(t) > (1+\mu)\ \mathscr{C}_i(t+1). \end{cases}$$

- $* \rightarrow red^{+}$
  If the new `PQ-Indic` value equals the high-red state, the grid is in highly critical status, and the SC must increase the charging power. Hence, a polynomial function is defined for transitions to this state.

$$\begin{aligned} \Delta &= 1 + \omega\ (\texttt{PQ-Indic})^{\chi} \\ \mathscr{U}_i(t+1) &= \min\left(\Delta\ \mathscr{U}_i(t)\ ,\ \mathscr{M}_i\right) \end{aligned} \tag{4.10}$$

  The parameters ω and χ in Equations (4.10) can be defined depending on the source of the transition or by comparing it with the last `PQ-Indic` value. The parameter ω must at least be lower than $\frac{\mathscr{M}_i}{\mathscr{U}_i(t)}$ and bigger than 1, and χ must be lower than 1 in order to match a polynomial increase. Obviously, Δ is bigger than 1, because ω is bigger or equal to 1, and `PQ-Indic` is a positive value.

- $* \rightarrow$ gray
  The gray state represents the standby phase of the charging process. In this phase, the SC only responses to highly critical grid situations by increasing the charging rate. Otherwise, the charging power is continuously reduced until it reaches $\mathscr{C}_i^{min}$ again in a linear way.

$$\begin{aligned} \Delta &= 1 + \omega\ (\texttt{PQ-Indic})^{\chi} \\ \mathscr{U}_i(t+1) &= \begin{cases} \min\left(\Delta\ \mathscr{U}_i(t)\ ,\ \mathscr{M}_i\right) & \texttt{PQ-Indic} \geq YR \\ \max\left(\vartheta\ \mathscr{U}_i(t)\ ,\ \mathscr{C}_i^{min}\right) & \texttt{PQ-Indic} < YR \end{cases} \end{aligned} \tag{4.11}$$

  The parameters χ and ω in Equations (4.11) are similarly defined as in transitions to the high-red state. Additionally, ϑ is a real number $\in (0, 1)$

Finally, an oscillation between two different states (red^{+} and red^{-}) needs to be avoided since this affects the stability of the SC. Hence, the parameters α and χ which are used as exponential factors in the aforementioned definitions of both states, need to be different.

4.5.2 Algorithm: TCP-like Smart Charger

Since the FSM-based SC takes into account only the current status of the grid to determine the correct power allocation at the CS, a different controller considering the previous grid status is designed in order to show the impact of a short-term history of the grid status on

the behavior of the SC. To that end, a SC inspired by the TCP congestion mechanism is designed and discussed in this section.

4.5.2.1 Internet Congestion Avoidance vs. Smart EV Charger

To achieve congestion avoidance on the Internet, TCP uses schemes such as a *slow start* [174]. The mechanism is heavily influenced by the "end-to-end argument" [175], whereby the congestion control is mostly a function of Internet hosts. TCP maintains a *Congestion Window* ($Cwnd$) in order to limit the total number of unacknowledged packets that may be in transit end-to-end. Similarly, grid operators use demand controlling to counteract some issues in the distribution grid, specifically, voltage drops and assets overloading. A demand controlling has been mostly performed on relatively big loads such as public CSs.

However, an essential difference between the Internet and power network should be noted. Congestion in the network causes longer Round Trip Times (RTTs) because of increasing the packet queues at routers. The Internet's TCP/IP uses RTT to detect congestion autonomously. By using the statistics of the measured RTTs, a Re-Transmission Timeout (RTO) is calculated on-the-fly. In contrast, the congestion in power grids is defined by events generated when some predefined thresholds are crossed, e.g., voltage drop.

Two factors determine the response time of any load controller. In essence, the arriving time of an event and the technical specifications of the controllable load, e.g., some EVs see the rapid changes in charging power as a sign of bad power quality; thus it disconnects from the CS. While the latter can be seen as a correspondence of flow control mechanism of TCP, the former depends on the delay coming from data gathering, data processing, and consuming of an event by the controller. As a result, the response time of a smart controller including the time of both notification and actuating is bounded by the technical constraints of both the charging power adaptation by the car and the power grid. By analyzing the process chain for measuring, analysis, and decision making (end-to-end delay), that delay is usually upper bounded by the frequency adaptation of charging power by the car. So the smart charger is designed to react periodically based on all arrived events (notifications) in that time horizon. Nevertheless, a SC can react differently in terms of quickness based on the degree of importance of the arriving event. The response time can be adjusted dynamically in a similar way to the RTO, as discusses in Section 4.6.

By analogy between the problem at hand with the network congestion of the Internet as depicted in Table 4.3, the TCP-Reno[7] slow-start mechanism is adapted in order to implement a smart charging controller. While an implicit notification mechanism based on receiving or losing acknowledgment of the sent data packet is existing on the Internet, a PQ-oriented mechanism described in Section 2.1.2 is used.

[7] RFC 6582.

	Internet	Power Grid
Topology	Mesh Networks Sources, destinations Routers, links	Radial Networks Generators, loads Substations, feeders
Congestion	Buffer of routers	Transformer, feeders
Congestion Notification	Explicit Implicit	Not existing Only local measurements
Congestion Window	Limit the total number of unacknowledged packets	Control of relatively big demands, e. g., a discrete charging rate of EVs
RTO	Based on statistics of the measured RTTs	Event-driven
Flow Control	Receiver window	Technical specifications of the EV bounds the charging power

Table 4.3.: Internet vs. Power Grid

In TCP slow start, there are multiple events: Time out, crossing the thresholds ($THOLD_{ss}$), and duplicate ACK. Each of those events requires accordingly different approaches to deal with in terms of congestion: Initialization (Init.), Slow Start (SS), Congestion Avoidance (CA), and Fast Re-transmit and Recovery (FRR). Table 4.4 depicts a comparison between the TCP slow start and EV SC as follows:

How is the network status perceived?

- **In TCP:** TCP perceives congestion on an end-to-end feedback basis between the sender and the receiver, by looking out for acknowledgments received after the packets are sent. Both the number and content of the acknowledgments are an indication of the status of the network.
- **In SC:** The status of the distribution grid is indicated based on certain predetermined GSI thresholds by the PQ-Indicator. Here, the indication mechanism is explicit and based on measurement data.

How to control the sending rate/charging power?

- **In TCP:** By scaling of $Cwnd$. The basic idea is that when the sender learns about the status of the network, it triggers an action to slow down/speed up the sending rate of packets.
- **In SC:** With changing the charging power allocated to the CS. When the SC learns about a critical/warning status in the distribution system, it reduces/increases the currently used charging power of the corresponding CS.

What are the events that trigger actions?

- **In TCP:** While receiving ACKs in time means no congestion in the network, timeout indicates the loss of packet or ACK, mostly due to congestion in the network. Otherwise, receiving duplicate ACKs indicates a situation where the packets are being delivered out of order that implies the loss of one or more packets in transit.
- **In SC:** For detecting events, the SC looks out for `PQ-Indic`; the output of PQ-Indicator. In the case of `PQ-Indic` $\in G$, it is considered as no issues in the grid. Otherwise, if `PQ-Indic` $\in R^-$, it is similar to the timeout event of TCP. Finally, `PQ-Indic` $\in Y^-$ indicates a warning, similar to duplicate acknowledgments in the slow start. However, `PQ-Indic` $\in R^+ \cup Y^+$ is considered as changing the maximum limit of possible charging capacity. More details are presented in Section 4.5.2.2.

How are the SS and CA phases distinguished?

- **In TCP:** There is a threshold $THOLD_{ss}$; Until this threshold, an exponential increase of $Cwnd$ is taking place (SS phase), while above this limit a linear increase is applied (CA phase).
- **In SC:** Similar to TCP, a threshold value is defined up to which the power increase is quick. An additional exponential increase is considered so that the allocated power at CS increases exponentially using a predefined constant (ϵ) called a change-rate. Above the threshold, the power increase turns linear w.r.t. the same constant ϵ.

Aspect	Slow Start	EV Charging
Events	Timeout, ACKs, $THOLD_{ss}$	Color signal, $THOLD_{ss}$
Status perceived	Based on ACKs received	GSI Thresholds
Participants	Sender, Internet (Receiver)	CS, Distribution grid
Control parameter	Sending rate	Charging Power
State	FRR, CA, SS	Critical, Warning, Good

Table 4.4.: TCP Slow-Start *vs.* Smart EV Charging

4.5.2.2 Methodology

Similar to Section 4.5.1, the used capacity of an active charging process at charging station cs_i at time t is denoted as $\mathscr{U}_i(t)$. The maximum physical capacity of cs_i is written as $\mathscr{M}_i$, and the user's charging profile is denoted as $\mathscr{C}_i(t)$. Furthermore, the minimum charging power needs to be set to a value $\mathscr{C}_i^{min}$ higher than zero to avoid disconnection of the vehicle. A safety upper margin is defined by $\mu < 1$. Additionally, a limit β is defined where $\mu < \beta < 1$ to distinguish between the warning and critical increase required in the power grid, i.e., the case of `PQ-Indic` $\in R^+ \cup Y^+$. Hence, three limits max_G, max_{Y^+}, and max_{R^+} are defined respectively for each increasing signal G, Y^+, and R^+ as given in Equations (4.12):

$$\begin{aligned} max_G &= (1+\mu)\mathscr{C}_i(t) \\ max_{Y^+} &= (1+\beta)\mathscr{C}_i(t) \\ max_{R^+} &= \mathscr{M}_i \end{aligned} \tag{4.12}$$

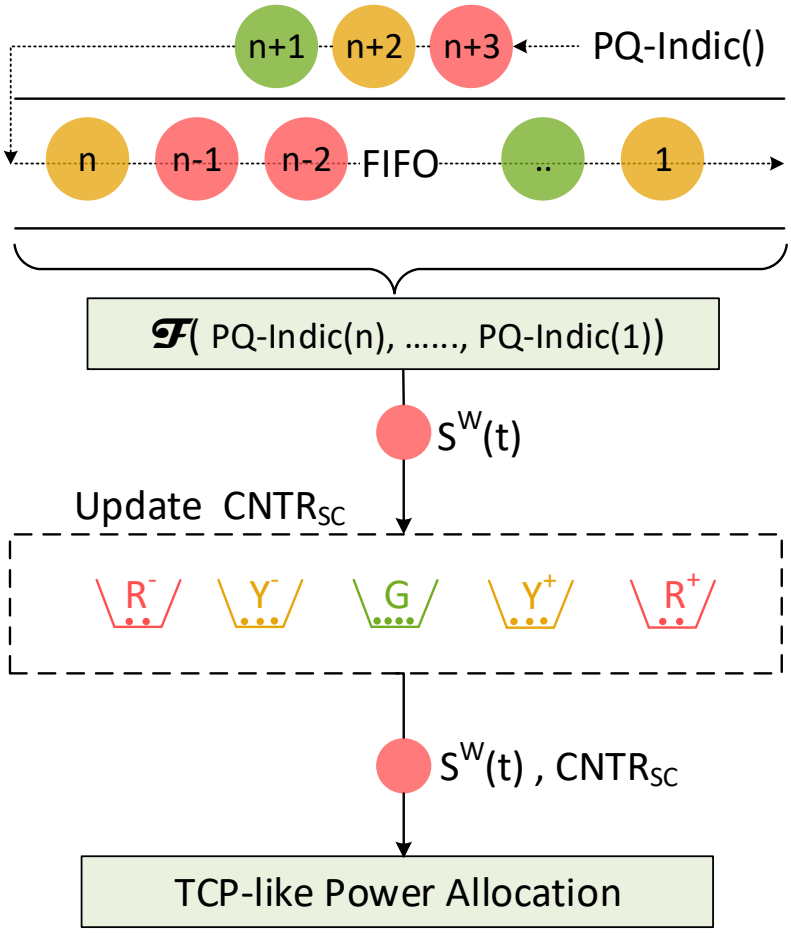

Figure 4.8.: TCP-like Smart Charger

Similar to TCP, a threshold $THOLD_{ss}$ is maintained that defines the point where SS phase stops and the CA phase begins.

The logic of SC contains three steps, as depicted in Figure 4.8. In the first step, the SC estimates the most dominating states of the grid $S^W(t)$ in the last seconds. That estimation is based on a predefined-size set of previous indications of grid states, namely, `PQ-Indic(t)`. The importance of this step rises in the case of performing the state indication and reactions of SC in a different frequency. Usually, the grid indication is done more frequently than the SC reaction for the purpose of accuracy. For example, the indication is done every 15 seconds, but SC reacts every minute. Next, the SC distinguishes among the different events in a similar way to the TCP slow start as described in Table 4.4 by setting a set of counters $CNTR_{SC}$ for each color signal. Finally, the SC allocates a suitable amount of power based on the correct reaction for each considered state like the slow start algorithm. The steps mentioned above are described in detail below.

1. **Calculating a weighted average indicator of the grid status** $S^W(t)$

   To that end, Equation (4.6) is used.

2. **Updating the SC counters** $CNTR_{SC}$

The SC maintains a counters array $CNTR_{SC}$, which holds counters for each of the operational states based on the traffic light model. The counters $CNTR_{R^-}$, $CNTR_{Y^-}$, $CNTR_G$, $CNTR_{Y^+}$, and $CNTR_{R^+}$ keep in track the number of consecutive occurrences of the states red^-, $yellow^-$, $green$, $yellow^+$, and red^+ respectively. The values saved in $CNTR_{SC}$ are essential to determine the action that needs to be taken in the next step. Initially, each counter is initialized as zero. For simplification purposes, the symbol $S(t)$ is used instead of $S^W(t)$ in order to refer to the current grid operational phases calculated in step 1.

During each SC step and based on the value of $S(t)$, the corresponding counter $CNTR_{S(t)}$ is incremented by one. Additionally, a change in $CNTR_G$ is performed depending on the updated value of $CNTR_{S(t)}$. The reason for this additional change is an added importance for the green status, as it plays a role in the exponential growth of the charging power during the SS phase in Algorithm 4.2. Whereas the number of correctly received acknowledgments in each step determines the exponential growth of $Cwnd$ implicitly in TCP slow start, an accumulator is required in the author's approach since the indication of the grid status is done in each step by a single value $S(t)$. Hence, $CNTR_G$ is incremented or kept unmodified for the phases that indicate an increase in charging power, namely, $green, yellow^+$, and red^+. Equations (4.13) depicts how $CNTR_G$ is used to calculate the exponential value on change-rate (ϵ) during the SS phase of Algorithm 4.2.

$$\begin{aligned} \mathscr{U}_i(t+1) &= \mathscr{U}_i(t) + \epsilon^{CNTR_G} \qquad \mathscr{U}_i(t) < THOLD_{ss} \\ \mathscr{U}_i(t+1) &= \mathscr{U}_i(t) + \epsilon \qquad \mathscr{U}_i(t) >= THOLD_{ss} \end{aligned} \tag{4.13}$$

Thus, for every $S(t) \notin G$, all counters $CNTR_{SC}$ except $CNTR_{S(t)}$ are set to zero since the consecutive occurrence of an event is more significant than each event (similar to the TCP slow start). Eventually, $CNTR_G$ and $CNTR_{S(t)}$ are updated as follows:

- $S(t) \in R^+$: Both $CNTR_{R^+}$ and $CNTR_G$ are incremented by one.
- $S(t) \in Y^+$: $CNTR_{Y^+}$ is increased by one. If updated $CNTR_{Y^+}$ is one, $CNTR_G$ does not change. Otherwise, $CNTR_G$ is incremented by one.
- $S(t) \in R^-$: $CNTR_{R^-}$ is incremented by 1. If updated $CNTR_{R^-}$ is one and the previous phase is green, then $CNTR_G$ is decremented by one. In all other cases, $CNTR_G$ will be set to zero.
- $S(t) \in Y^-$: $CNTR_{Y^-}$ is incremented by one. If updated $CNTR_{Y^-}$ is one, $CNTR_G$ does not change since it can be a transit status. If $CNTR_{Y^-} = 2$, $CNTR_G$ is decremented by 1; otherwise, $CNTR_G$ is set to zero.
- $S(t) \in G$: $CNTR_G$ is incremented by one. However, the first green signal causes a decrement by one in any other counter if its value is not already zero. That is a precautionary measure assuming the first green might be a transient phase,

so that the situation might return to unstable phases. Otherwise, the other four counters are set to zero.

3. **TCP-like allocating of the charging power**

   Based on the output of the previous two steps: $CNTR_{sc}$ and $S(t)$, appropriate action is taken to determine the charging power $\mathscr{U}_i(t+1)$ in the next time step. The algorithm should start slowly by setting $\mathscr{U}_i(0)$ equal to $\mathscr{C}_i^{min}$ since a conservative approach concerning the grid stability is adopted. The initial value of $THOLD_{ss}$ is set to a portion ψ of the predefined user's charging profile in each time slot t; $THOLD_{ss} = \psi\ \mathscr{C}_i(t)$.

   Algorithm 4.2 depicts how SC adjusts the active power and the threshold based on the value of $S(t)$. However, the algorithm does not conform entirely with the TCP slow start algorithm since there is no perfect match between the Internet and the studied system, namely, the power grid. In addition to the changing of max limits clarified at the beginning of this section using Equations (4.12), making drastic changes similarly to the slow start by setting the values of $THOLD_{ss}$ and $\mathscr{U}_i(t)$ is avoided. Such a change can either lead to ping-pong effect or a negative impact in terms of voltage drop. Precisely, neither $THOLD_{ss}$ nor $\mathscr{U}_i(t)$ is set to zero through timeout event, for example. Otherwise, this action is configured based on the nature of each charging process. For that, three additional parameters are defined: λ_1, λ_2, and λ_3; where $0 \leq \lambda_3 \leq \lambda_2 \leq \lambda_1 \leq 1$.

   Finally, the case of $S(t) \in Y^+ \cup R^+$ is not described in detail in Algorithm 4.2 and merged with the case of the green status. However, similar to the first $yellow^-$, the first $yellow^+$ is ignored and the maximum limit regarding Equations (4.12) from the second consecutive $yellow^+$ is changed. While the first red^+ equals to two consecutive $yellow^+$, two or more consecutive red^+ adjust the maximum limit to be max_{R^+}. Furthermore, Algorithm 4.2 distinguishes between standby state and unplug state similar to the FSM-SC.

4.6 Management of Time Reactions of Smart Chargers

In the previous section, two possibilities for managing SC time reactions are discussed and proposed, namely, event-driven reactions and periodical reactions. The former can cause high oscillation in the changing of used charging power at the CS since the arrival rate of the events can be high - specifically, the arrival of `PQ-Indic` values - which can be seen as bad power quality from the perspective of the EV. In contrast, the latter avoids the oscillation problem, but it leads to simultaneous reactions of a set of SCs to the same signal (when a time window with the same length is considered by all SCs), which could cause a ping-pong effect. Notably, the signals when the transformer is overloaded or the voltage at the critical point is in red status. Further issues regarding the periodic reaction are: (i) too

Data: $S(t) \in [-1, +1]$
$red^-, yellow^-, green, yellow^+, red^+$
$updated\ CNTR_{sc}, \mathscr{M}, \mathscr{C}_i^{min}$
$\lambda_1, \lambda_2, \lambda_3, THOLD_{ss}, \epsilon$
Result: $\mathscr{C}_i^{min} \leq \mathscr{U}_i(t) \leq \mathscr{M}_i$
if $SoC < SoC_{end}$ **then**
  /* Operational State */
  switch $S(t)$ **do**
    case red^- **do**
      if $CNTR_{R-} = 1$ **then**
        /* Duplicate acknowledgments */
        $THOLD_{ss} = \lambda_1\ \mathscr{U}_i(t)$
        $\mathscr{U}_i(t+1) = THOLD_{ss}$
      else
        /* Time Out */
        $THOLD_{ss} = \lambda_2\ \mathscr{U}_i(t)$
        $\mathscr{U}_i(t+1) = \lambda_3\ \mathscr{U}_i(t)$
      end
      $\mathscr{U}_i(t+1) = max(\mathscr{U}_i(t+1), \mathscr{C}_i^{min})$
      break
    end
    case $yellow^-$ **do**
      if $CNTR_{Y-} = 1$ **then**
        /* Warning: no change */
        $\mathscr{U}_i(t+1) = \mathscr{U}_i(t)$
      else
        /* Duplicate acknowledgments */
        $THOLD_{ss} = \lambda_1\ \mathscr{U}_i(t)$
        $\mathscr{U}_i(t+1) = THOLD_{ss}$
      end
      $\mathscr{U}_i(t+1) = max(\mathscr{U}_i(t+1), \mathscr{C}_i^{min})$
      break
    end
    otherwise do
      Calculating MAX based on Equation (4.12)
      if $\mathscr{U}_i(t) < THOLD_{ss}$ **then**
        /* Slow start stage */
        $\mathscr{U}_i(t+1) = \mathscr{U}_i(t) + \epsilon^{CNTR_G}$
      else
        /* Congestion avoidance stage */
        $\mathscr{U}_i(t+1) = \mathscr{U}_i(t) + \epsilon$
      end
      $\mathscr{U}_i(t+1) = min(\mathscr{U}_i(t+1), MAX)$
    end
  end
else
  if $SoC < 100$ **then**
    /* Standby State, $gray$ */
    switch $S(t)$ **do**
      case $yellow^+, red^+$ **do**
        Calculating MAX based on Equation (4.12)
        if $\mathscr{U}_i(t) < THOLD_{ss}$ **then**
          /* Slow start stage */
          $\mathscr{U}_i(t+1) = \mathscr{U}_i(t) + \epsilon^{CNTR_G}$
        else
          /* Congestion avoidance stage */
          $\mathscr{U}_i(t+1) = \mathscr{U}_i(t) + \epsilon$
        end
        $\mathscr{U}_i(t+1) = min(\mathscr{U}_i(t+1), MAX)$
      end
      otherwise do
        $THOLD_{ss} = \lambda_1\ \mathscr{U}_i(t)$
        $\mathscr{U}_i(t+1) = THOLD_{ss}$
        $\mathscr{U}_i(t+1) = max(\mathscr{U}_i(t+1), \mathscr{C}_i^{min})$
      end
    end
  else
    /* Unplugg */
    $\mathscr{U}_i(t+1) = 0$
  end
end

Algorithm 4.2: TCP-like Charging Power Allocation

slow startup time, which is needed by the SC to reach the targeting charging profile $\mathscr{C}_i(t)$, (ii) late appropriate actions in the case of a critical situation arises in between two periodic steps. The startup times issue can be tackled by applying a quick update through the startup phase of the charging operation (e.g., the first five to ten minutes) after that an appropriate Time Management Mechanism (TMM) is applied.

However, both mechanisms can not entirely solve the typical synchronization(concurrency) issue raised in any distributed system. Therefore, more time for analyzing and managing the reaction times of an active SC is allocated. Thereby, SCs adjusts the time of the next reactions - by adjusting the waiting time between two consecutive reactions - more dynamically depending on various internal and external parameters. Thus, more efficient usage of the available resources is possible. In this section, three further TMMs are proposed. The goal of this section is not finding the optimal TMM to be applied later, but rather, showing different possibilities that can be analyzed in detail in Chapter 5.

4.6.1 Simple Mechanism

By this TMM, the only factor that influences the waiting time is the current state of the grid. Depending on the grid's state, different limits for the target waiting time are used:

- If `PQ-Indic` $\in G$, the SC can wait for a longer time than in any other state but smaller than MAX_TIME.
- If `PQ-Indic` $\in Y^- \cup Y^+$, the waiting time should not exceed Y_LIMIT; where $Y\_LIMIT = (MAX\_TIME + MIN\_TIME)/2$.
- If `PQ-Indic` $\in R^- \cup R^+$, the SC should react as fast as possible, but the waiting time should be longer than MIN_TIME.

However, the waiting time does not leap to the phase limit suddenly but takes steps to reach that limit. In this regard, the last waiting time is retained and is referred to as $NextStep(t)$. In this context, t stands for the decision time when the waiting period starts. Besides, a constant value γ is used as a parameter to determine the shift in waiting time (step-size). Initially, $NextStep(t)$ is set to MIN_TIME to allow SC to reach the charging profile faster. Nevertheless, the SCs react differently depending on the state of the grid as follows.

If `PQ-Indic` $\in R^- \cup R^+$, the SC has to reach MIN_TIME by lowering its waiting time as fast as possible using Equation (4.14). The reduction in the waiting time depends on two parameters: the value of $\gamma \leq MIN\_Time$ and the number of consecutive red signals $|R|$. The second parameter is used to adapt the waiting time faster for each subsequent detection of a red phase and, therefore, to approach the minimum time faster. In Equation (4.14), the

multiplication by two is just to accelerate the reduction in the red phase in comparison to the yellow phase.

$$NextStep(t+1) = NextStep(t) - 2\,|R|\,\gamma \tag{4.14}$$

In the case of `PQ-Indic` $\in G$, the SC raises the waiting time as no drastic action is currently required. A conservative approach is adopted by adding only γ to $NextStep(t)$, as depicted in Equation (4.15).

$$NextStep(t+1) = NextStep(t) + \gamma \tag{4.15}$$

In the case of `PQ-Indic` $\in Y^- \cup Y^+$, the SC tries to reach Y_LIMIT. Since this limit is the average of MIN_TIME and MAX_TIME, the SC has to check if the waiting time has to be reduced or increased to reach Y_LIMIT. As seen in Equation (4.16) and similar to the red phase, subsequent occurrences of yellow cause a faster adjustment of the waiting time. However, multiplying by two is eliminated. While constantly switching between red and yellow signals results in a slight decrease in the waiting time, the constant changes between a green and a yellow signal maintain the waiting time.

$$NextStep(t+1) = NextStep(t) \pm\ |Y|\,\gamma \tag{4.16}$$

4.6.2 ALOHA-like Mechanism

The main drawback of the simple TMM is that it does not address the oscillatory problem directly since SCs often react at the same time. In order to avoid the ping-pong effect, the number of simultaneous adaptions of the charging power $\mathscr{U}_i(t)$ needs to be limited if no critical situation is present in the grid. However, the SCs should still be able to react simultaneously in critical phases since this will help to quickly dissolve the problem in the grid. Such a problem is similar to the multiple access problem in computer networking [176], where multiple sending and receiving nodes are all connected to the same, single, and shared broadcast channel, e.g., avoid a collision in the wireless communication channels. Computer networks have protocols of so-called *multiple access protocols*. By them, nodes regulate their transmission into the shared broadcast channel, e.g., by adopting Time-Division Multiplexing (TDM), Frequency-Division Multiplexing (FDM), or Slotted ALOHA [177]. The aim is to derive the throughput-delay tradeoff and stability issue. By analogy, TMM inspired by slotted ALOHA is proposed and described in this section. Slotted ALOHA is selected since it is very simple and highly decentralized.

To that end and similarly to the simple TMM, MIN_TIME and MAX_TIME are defined as the lower and upper limits for the waiting time, respectively. Also, γ is defined the same way as in the simple TMM, but it is initialized with the value MIN_TIME. Since the collision (i.e., simultaneous reactions) can't be detected automatically in this context like

computer networking[8], a minor change in the distributed architecture has to be adopted. So each SC keeps tracking other SCs in the grid to be able to recognize if one of them has already reacted within the current time slot. The tracking information does not contain any information about the step-size but a coordination flag managed by a coordinator[9]. The flag is released at the beginning of each slot. It is noted, the goal of this TMM is not to avoid the collision among SCs altogether, but to mitigate its impact slightly. Hence, the idea of using a flag for preventing simultaneous reactions can be ignored completely when the number of involved CSs is big.

However, as long as the SC doesn't detect a reaction from other SCs, i.e., the flag is not taken, the charging power will be allocated as usual. But if another SC already decided to react within the current slot, the backoff mechanism will be used to determine when the SC will try again to change its charging power $\mathscr{U}_i(t)$. Thereby, an algorithm inspired by the Binary Exponential Backoff Mechanism (BEBM) [179] implemented by ALOHA is used to determine randomly the $backoffTime$, which will be waited before the subsequent reaction try. By slotted ALOHA, a node re-transmits its frame in each subsequent slot after the detection of a collision with a certain probability ρ until the frame is transmitted without a collision. While SC can adopt a probability-based approach likewise for deciding about making a reaction in a time slot, another approach based on the number of consecutively performed reactions can be carried out. Accordingly, it is referred to as $\#reaction \in \mathbb{N}_0$. Additionally, a random number $x \in \mathbb{N}_0$ is generated, where $0 \leq x \leq 2^{\#reaction}$. As depicted in Equation (4.17), random number x is multiplied with γ to determine the $backoffTime$.

$$backoffTime = Min(x * \gamma, MAX\_TIME) \tag{4.17}$$

It is also made sure that the calculated $backoffTime$ cannot go over MAX_TIME. In case the selected $backoffTime$ is higher, MAX_TIME is set as the $backoffTime$.

To avoid exhausting the flexibility of a single SC, a cap of $\#reaction$ is introduced by the number of consecutive reactions. Furthermore, $\#reaction$ is reduced at each backoff by x. Thus, the waiting time reaches a ceiling, and thereafter, it does not increase any further. Hence, the SC has to react regardless of the other SCs actions.

4.6.3 Sophisticated Mechanism

The previous two approaches ignore entirely the ability of the CS to react to a particular event. For example, if `PQ-Indic` $\in R^+$ and SC charges at minimum capacity, the waiting time between the currently taken step and the next one should be the minimum possible

[8] In computer networking, collision detection is carried out by a transmission station through sensing transmissions from other stations while it is transmitting a frame. Otherwise, it is very crucial and difficult to detect the cause-root of changes in GSIs of a power grid to react appropriately.

[9] With this modification, the architecture is still distributed [178].

time. Otherwise, the time waited before the next step is taken should be the maximum allowed time as the SC is not able to take any action to help the grid status if PQ-Indic $\in R^-$. Therefore, the difference between the current used capacity $\mathscr{U}_i(t)$ and the maximum physical capacity $\mathscr{M}_i$ has to be considered. That is categorized by a value Δ in Equation (4.18).

$$\Delta = \frac{\mathscr{M}_i - \mathscr{U}_i(t)}{\mathscr{M}_i} \tag{4.18}$$

Similar to the simple and ALOHA-like TMMs, the waiting time is also adjusted regarding the grid status, i.e., the considered PQ-Indic values. That means, two CSs with the same Δ should not wait the same time if the grid status is different. For example, a CS with $\Delta = 0$ should wait the maximum possible time when the value of PQ-Indic $\in R^+$ because the CS is not able to take any action that is beneficial for the grid at that moment. However, the same CS with the same Δ should only wait a fraction of the maximum time possible if the value of PQ-Indic $\in G$, which means the capacity can be increased. But the waiting time has to be reduced to the MIN_TIME only when PQ-Indic $\in R^-$. Thus, the waiting time can be written as a function of Δ and PQ-Indic: $f(\Delta, \texttt{PQ-Indic}) : \Big([0,1],[-1,+1]\Big) \rightarrow [0,1]$. An additional help function $g(\texttt{PQ-Indic}) : [-1,+1] \rightarrow [0,1]$ is used to represent the relation between the waiting time and PQ-Indic individually. Thus, the function $f(\Delta, \texttt{PQ-Indic})$ is defined according to Equations (4.19). It is also illustrated in Figure 4.9 as well, which shows that function $f(\Delta, \texttt{PQ-Indic})$ has two maximums in terms of waiting time at points (1,-1) and (0,1), while points (0,-1) and (1,1) represent the minimum points.

$$\begin{aligned} g(\texttt{PQ-Indic}) &= 0.5 + \frac{\arctan(\texttt{PQ-Indic})}{\frac{\pi}{2}} \\ f(\Delta, \texttt{PQ-Indic}) &= (1-\Delta) * g(\texttt{PQ-Indic}) + \Delta * g(-\texttt{PQ-Indic}) \end{aligned} \tag{4.19}$$

By using Δ as a weight in function $f()$, the curve generated by function $g()$ is adjusted for each individual SC, and the time that a SC will wait for is dependent of both the current grid situation as well as the CS ability to act in a way that benefits the grid. Finally, a projection of the output of function $f()$ in the range $[MIN\_TIME, MAX\_TIME]$ is required. So while $f(\Delta, \texttt{PQ-Indic}) = 0.0$ means $NextStep(t+1) = NextStep(t) + MIN\_TIME$, $f(\Delta, \texttt{PQ-Indic}) = 1.0$ sets $NextStep(t+1) = NextStep(t) + MAX\_TIME$.

4.6.4 The Behavior of SC during the Waiting Time

In order to respond quickly to any emerging critical situation in the grid, the SC checks all the arrived PQ-Indic during the waiting time. If PQ-Indic $\in R^- \cup R^+$, the SC has to carry out, depending on the TMM, a new calculation of the waiting time. That allows the SC to lower the waiting time if it is possible, furthermore, the SC can directly react if the situation in the grid is detected as very critical. In all cases, the adjustment should not increase the waiting time from the previous step to avoid long waiting times.

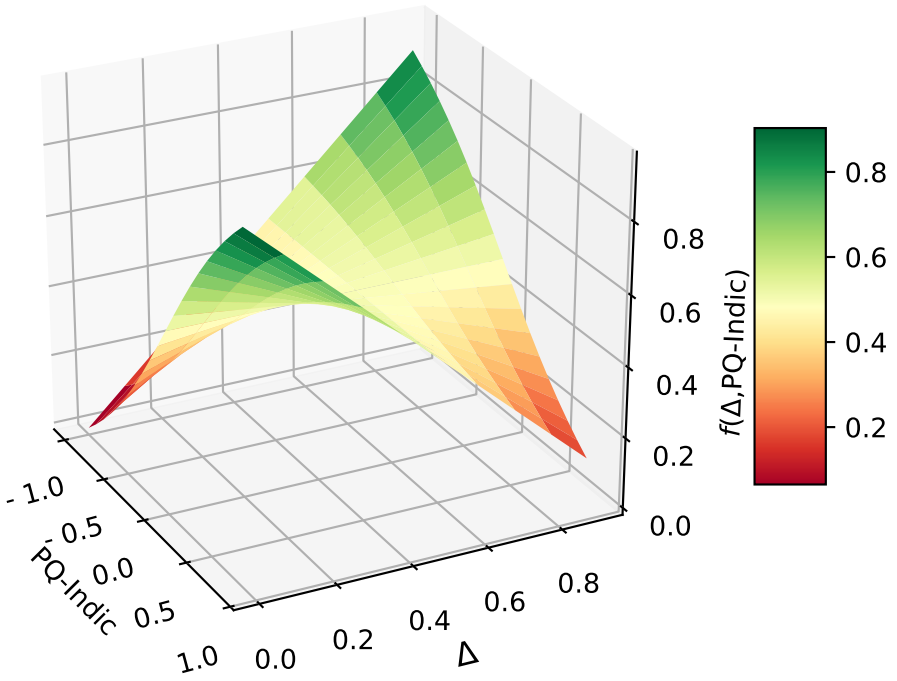

Figure 4.9.: Illustration of Function $f(\Delta, \texttt{PQ-Indic})$ in 3D Space

4.7 Summary

In this chapter, a distributed smart charging architecture as a closed-loop system is presented. It is based on a real-time data stream for triggering events in the distribution grid. So the event-driven system enables an efficient communication scheme in terms of cost and performance. It is intended to be a grid-friendly, stakeholder concerns-aware, and scalable architecture. The system also targets a proportional fairness through distributing available grid resources among the different running charging processes.

The traffic light model is applied to use the introduced flexibility of the e-mobility sector to the grid in a convenient way. Hence, a distributed notification mechanism about the grid status is introduced. It considers not only the voltage level at different points of the grid, but also load at the transformer and phase imbalance. The design of such a mechanism adopts a hierarchical approach, so considering more grid concerns beyond the ones mentioned above is possible.

Moreover, two smart controllers are introduced. While the first considers only the current grid status, the second takes into account a set of previous grid statuses in order to decide about the most suitable value of the charging capacity in the next time step. To the end of solving the synchronization problem among the active SCs, different TMMs are presented and discussed; one mechanism is inspired by slotted ALOHA used in computer networking for solving a similar problem.

Finally, Table 4.5 shows the main variables used or defined in the context of Chapter 4. Those variables will be used next in Chapter 5 to perform an in-depth analysis of the different concepts of the proposed architecture using simulation.

Variable	Definition	Range
`PQ-Indic`	Output of PQ-Indicator	$\in [-1, +1]$
`PQ-indic`$_\phi$	`PQ-indic` at phase $\phi \in \{A, B, C\}$	$\in [-1, +1]$
ER_k, RY_k, YG_k GY_k, YR_k, RE_k	Thresholds of GSI class k	$\in \mathbb{R}$
ER, RY, YG GY, YR, RE	Thresholds of the traffic light model	$\in [-1, +1]$
R^-	Low red range of `PQ-Indic`	$\in [ER, RY]$
Y^-	Low yellow range of `PQ-Indic`	$\in (RY, YG]$
G	Green Range of `PQ-Indic`	$\in (YG, GY)$
Y^+	High yellow range of `PQ-Indic`	$\in [GY, YR)$
R^+	High red of `PQ-Indic`	$\in [YR, RE]$
$S^W(t)$ or $S(t)$	Weighted average indicator over time window T	$\in [-1, +1]$
$\mathscr{M}_i$	Maximum physical capacity of a cs_i	$\in \mathbb{R}_+$
$\mathscr{U}_i(t)$	Total charging capacity of cs_i at time t	$\in \mathbb{R}_+$
$\mathscr{C}_i(t)$	Time-slotted charging profile of cs_i	-
$\mathscr{C}_i^{min}$	Minimum charging power of cs_i	> 0
μ	Saftey upper margin of the charging profile	$\in [0, 1]$
SoC_{end}	The desired SoC set by the end-user	$\in [0, 100]$
$red^+, yellow^+, green$ $red^-, yellow^-, gray$ $blue$	States of FSM	-
α	Exponentiation factor of transition to red^-	≥ 1
ϱ_2	Linear factor of transition to $yellow^-$	≥ 1
ϱ_1	Linear factor of transition to $yellow^+$	≥ 1
χ	Exponentiation factor of transition to red^+	≤ 1
ω	Linear factor of transition to red^+	$\in [1, \frac{\mathscr{M}_i}{\mathscr{U}_i(t)}]$
max_{R^+}	Maximum increase in red^+ phase at cs_i	$= \mathscr{M}_i$
max_G	Maximum increase in $gree$ phase at cs_i	$= (1 + \mu)\mathscr{C}_i(t)$
max_{Y^+}	Maximum increase in $yellow^+$ phase at cs_i	$\in [max_G, max_{R^+}]$
β	Parameter for calculating max_{Y^+}	$\mu < \beta < 1$
$THOLD_{ss}$	Threshold distinguishes SS and CA phases	$\in (0, \psi\ \mathscr{C}_i(t))$
ψ	Parameter for determining $THOLD_{ss}$	$\in (\mu, 1)$
$CNTR_{SC}$	Vector of counters	$\in \mathbb{R}_+$
ϵ	Change-rate of TCP-like SC	≥ 2
$\lambda_1, \lambda_2, \lambda_3$	Parameters of changing $THOLD_{ss}$ and $\mathscr{U}_i(t)$ through SS and CA phases	$\in [0, 1]$

Variable	Definition	Range
MIN_TIME	Minimum Waiting time of a SC	$\in \mathbb{R}_+$
MAX_TIME	Maximum Waiting time of a SC	$\in \mathbb{R}_+$
γ	Step-size for TMM	$\in (0, MIN\_TIME]$

Table 4.5.: Description of Main Variables Defined in Chapter 4

5 Analysis

This chapter is split into two parts: The first introduces a comprehensive evaluation of the proposed architecture in Chapter 4 using simulation. That includes (1) analyzing and evaluating the impact of the overall system regarding the main concerns of grid operators and end-users, and (2) a benchmark of Kafka as an example of an event-engine. The analysis includes a description of the simulation setup, scenarios, metrics, assumptions, and results.

The second part deals with practical considerations regarding the realization of the proposed smart charging solution. Thereby, the possible challenges that a real-life implementation of SC might face are introduced. That includes the application scope of the proposed architecture, technical, and regulatory challenges.

5.1 Overall Evaluation of the System

5.1.1 Simulation Setup

For all the following evaluation scenarios in this section, the co-simulation framework *AIT Lablink* is used [180]. However, the required components (described in Chapter 4) for testing the proposed architecture are implemented as LabLink clients, as depicted in Figure 5.1. Lablink supports communication among those clients using the publish/subscribe concept facilitated by Message Queuing Telemetry Transport (MQTT)) message bus. As a result, Kafka as an event-engine is not shown in this setup, and its performance is assessed separately using a different setup in Section 5.2. However, the PQ-Indicator subscribes for the GSI values from different MPs in the grid and publishes the calculated grid indications that are subscribed by the SC. The CS subscribes for the charging signals of the SC for further changes in its charging process. The CS client allocates the charging power on three phases either equally or in such a way supporting the phase imbalance since the architecture is phase-based designed. Lablink supports central simulation manager *Synchost* that provides sync service to initialize, synchronize, and control of the simulation flow configuration centrally among the Lablink clients [181]. As the satisfaction of EV drivers is one of the system's primary goals besides the grid-friendliness, a model of an EV is implemented in the simulation framework. This model, however, is held as simple as possible by containing only necessary information from the data source, which are the arrival time, the requested departure time, and the requested energy. Additionally, a simple model of the EV battery is included, which is simplified to a single stage linear charging. Of course, this is not

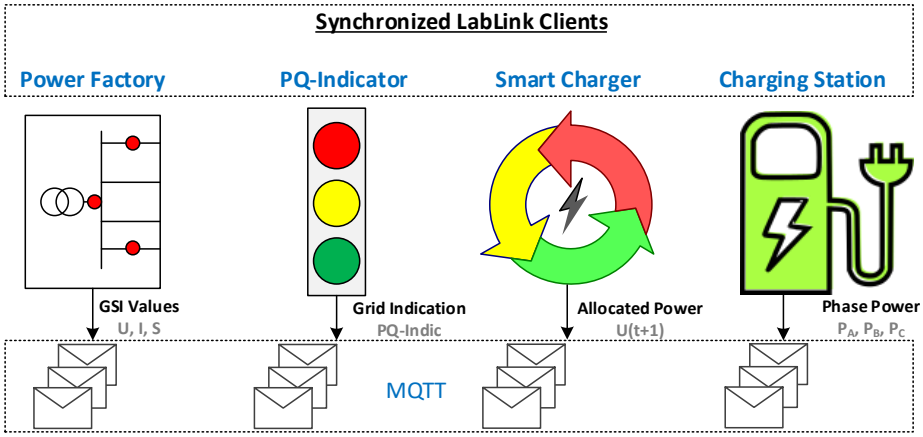

Figure 5.1.: Client-based Evaluation Setup Using Lablink

particularly reflecting reality, but it should not have an impact on the general aim of this work. The goal is not to examine to what exact levels of SoC the SC algorithm is able to charge EVs, but rather to provide a comparison and relationship between the SC and UC scenarios.

5.1.1.1 Grid Model

The used grid is similar to the used one in Chapter 3, with 64 cables connecting 22 households, 21 industrial loads, 3 PV systems, and four connected charging stations. The maximum distance to the transformer is given by a cable with a length of 485 meters. DIgSILENT PowerFactory [182] is the grid simulation tool used with composite models and it is one of the LabLink clients. Four charging stations cs_i are placed at different points in the grid. One charging station (cs_2) is located as far as possible from the transformer at the critical point of the grid in terms of voltage drop at node 11. cs_4 is located at the second main feeder line that is supplied by the transformer. The remaining two stations (cs_1 and cs_3) are located near to the transformer at Busbar 1, as it is the case in the real grid. As mentioned previously, three kinds of 24-hour profiles are fed into the simulation: realistic household load profiles, BDEW load profiles for industries, and real generation profiles for the PV systems.

5.1.1.2 EV Mobility Data

Although there are many data sources to choose from, the selection of data for an "as realistic as possible" simulation should not be treated lightly. Not all data are well fit for all testing scenarios. Therefore, to make the simulation and the results as realistic as possible, one needs to see the advantages and disadvantages of using different data sources for his application. For example, it would hardly make sense to use real data acquired from home CSs, which mainly charge at evening or night, when the goal of the work is to evaluate an algorithm, which is intended to be used in public CSs at noon most of the time.

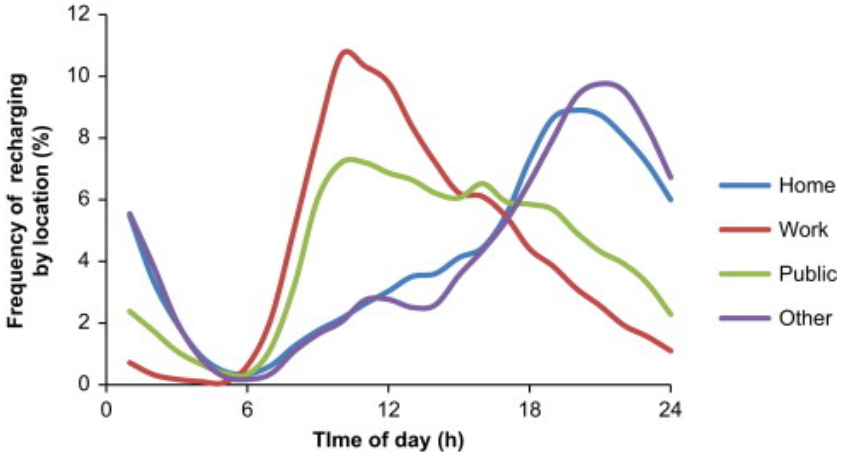

Figure 5.2.: Recharging profiles extracted from recharging events at home (1610), work (3278), public (2110), and other (706) [189]

Therefore, even though real data would be used, the results may not be applicable on the actual intended test case, as the basic conditions of both scenarios differ. First of all, the methodology and criteria of determining such a suitable data source for the test case of this work are presented before showing how and why that data of that source can be further split into meaningful scenarios.

When trying to conclude which kind of data source is the best fit for the own case, there are two main types of data sources for EV mobility and charging patterns. The first possibility is to generate an own EV model of patterns based on real data of even conventional internal combustion engine vehicles. This method has its origin in the fact that there has been excessively more data gathered from conventional engine cars than from EVs, which can be used to derive charging behavior and decisions of the EV users, e.g., German Mobility Panel (MoP). The use of this method can be seen in the work of [183, 184, 185, 186]. The other possibility is to use existing data sets gathered from CS directly, as done in [187, 188, 189, 190]. This method has the advantage of not being prone to conventional engine based influences, which would have to be considered in the first method. Using real EV charging data rather gives a quick data source, which already has every aspect of EV included, such as charging behavior, demand, and mobility patterns of EV users.

There are many criteria to be noticed for selecting a suitable EV data source for the evaluation of SC algorithms, two of which are interesting from the perspective of this work, in particular:

- **Informative, representative, and easy to access data**: The data source needs to not only provide an enormous amount of charging sessions, but they rather also have to describe different scenarios. Moreover, the data needs to be easy to access. In the scope of this work, it is crucial to have the chosen data set represent an extensive amount of test cases and scenarios of different dates and time spans. That is important to show that the SC algorithm is reliably working at any time throughout the year.

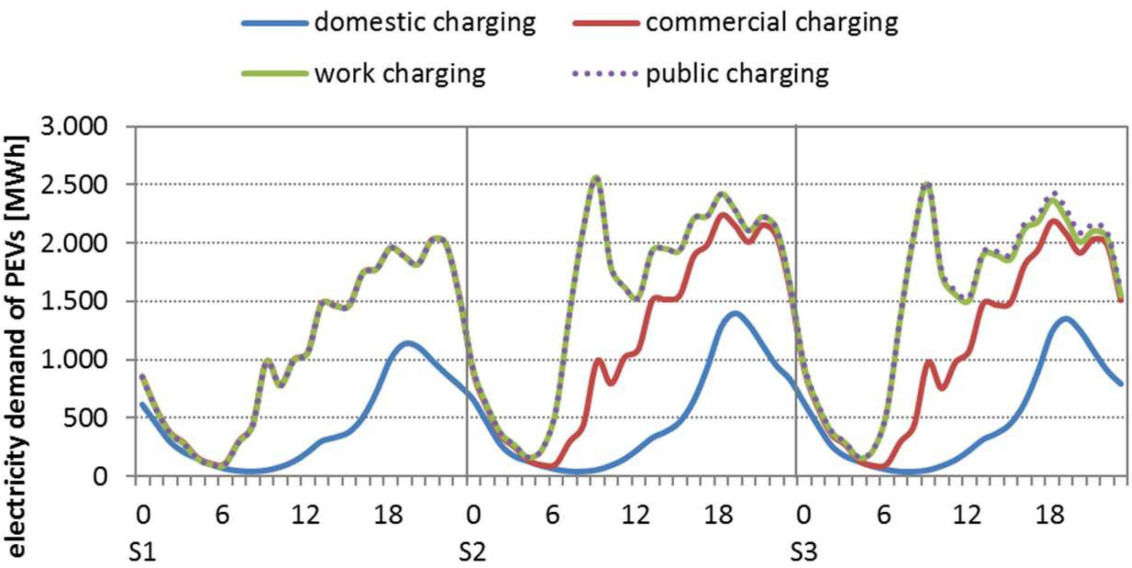

Figure 5.3.: Electricity demand of PEVs without DR based on ALADIN and eLOAD models in combination with MoP and Entso-E [191]

Using a massive amount of charging sessions gathered within a short period is not a good idea since it can heavily bias the results. For example, the seasonal behavior of users can differ from summer to winter. Further, the data should be recent and representative of the current or future time, as the given algorithm will be used in technologies developed in the future. All this data has to be accessible for the scope of this work, which means it has to be free to use to all (or most) of its extents.

- **Fitting the patterns of the tested system**: The goal of this work is to test the algorithm for the test case of public access CSs. There can be huge differences between charging data of public, work, or home CSs. While public and work stations experience a peak demand at around morning and noon to afternoon, home stations mostly peak their demand in the evening and at night. That can also be seen in the work of [189], where the authors show in Figure 5.2 that the frequency of recharging is very similar for work and public locations, whereas home locations are clearly different. That was concluded by examining data from the SwitchEV trial[1], which consisted of trials to analyze 44 EVs in total over one year. Also, the authors of [191] show that work and public CSs have a very similar pattern, as can be seen in Figure 5.3. The used data models are a realistic representation of public or work CSs since it is built using a combination of multiple realistic sources, namely MoP, ALADIN, eLOAD, and Entso-E.

Adaptive Charging Network (ACN) is an open data set of mobility patterns introduced in [192]. It is updated daily and therefore contains a growing number of charging sessions. Based on the aforementioned criteria, the ACN is used in this work as the data source. So

[1] http://wiki.fot-net.eu/index.php/Switch_EV

the charging profiles for the simulations of the evaluation are generated out of it. While the data derived from surveys or end reports of individual projects becomes basically outdated very soon, ACN, in contrast, has the advantage of being flexible in choosing data from any day dating back to April 2018 up to the recent day. That results in over 30000 charging sessions, as constituted in summer 2019, which cover all time spans throughout the year. Also, the acquisition of the data is effortless and free to use. Furthermore, the ACN data fits the needed pattern for testing SC algorithms, since there is theoretically only a need for data from public access CSs. Even though the CSs of the ACN are mainly located at working places, the stations at Caltech are also open for public use. Even purely, workplace-based data seems to be fit for public access scenarios, as they show a very similar pattern.

5.1.2 Metrics

$<M_1>$ **Transformer loading (S)**: Since it is one of two criteria considered in the design of PQ-Indicator, evaluating the impact of SC here is required, particularly, in terms of the total time of the transformer overloading.

$<M_2>$ **Voltage at the critical point (U)**: The hierarchical logic of PQ-Indicator regarding criteria (A_2) prioritizes the local condition over the remote ones in terms of voltage. Consequently, fixing the local voltage is guaranteed if the voltage at the critical point is fixed. Therefore, considering the voltage at the connection point of each CS is required but not more significant than focusing on the voltage drop at critical points in terms of voltage. Therefore, only the voltage magnitude at the critical point is analyzed in-depth.

$<M_3>$ **Consumed energy (E)**: In any distributed system where multi processes share the same resources, a lot of attention should be paid to the starvation problem and the way of distributing the resource among the processes (i.e., fairness). However, this problem is more critical and hard to be addressed in the power grid since the position of the CS plays a significant role by deciding how much power can be used. For example, the closer to the transformer, the fewer local power quality issues and more power can be used. As a result, the way of allocating the charging power among the CSs needs to be evaluated by taking into consideration the significant role of the local operating conditions of each CS by determining the used charging power.

To that end, the energy distribution at each CS is computed using the trapezoidal rule[2] for calculating the area under the power curve. Furthermore, the percentage of energy portion allocated to a cs_i is calculated by dividing its energy portion by the sum of all other CSs.

[2]https://en.wikipedia.org/wiki/Trapezoidal_rule

Finally, this metric is used not only on the level of CS but also on the level of an individual EV in order to express the energy amount stored in the battery, and thereby, a simple battery model is used.

<M_4> **Average Service Coverage (ASC)**: For evaluating the impact of the SC to the users of the CSs, the number of vehicles charged to a certain extent, as used by [193], will be shown. In this work, this metric $ASC \in [0, 1]$ shows the percentage of requests covered, and it is given as ASC_ζ of EVs charged to at least a certain limit ζ. There are limits considered here to examine if the SC algorithm has different coverage results to different acceptance limits. Whereas many acceptance limits may lie at 100% of the requested energy, other users may already be satisfied with only a certain percentage of their requested energy delivered. Equations (5.1) depicts the definition of this metric,

$$\begin{aligned} ASC_\zeta &= \frac{1}{N}\sum_{j=0}^{N} x_j \\ x_j &= \begin{cases} 1 & \frac{E_{deliv}(j)}{E_{req}(j)} \geq \zeta \\ 0 & \text{Otherwise} \end{cases} \end{aligned} \tag{5.1}$$

where N is the total number of EVs charged to any extent in a chosen scenario. Moreover, $E_{deliv}(j)$ and $E_{req}(j)$ are delivered and initially requested energy by EV_j, respectively.

For example, let $\zeta = 0.8$ which means the request of an EV user is considered covered and therefore considered fully charged if the EV is charged to at least 80% of the requested energy. Thus, if there is a set of six EVs charged to a certain percentage of their requested energy, given as $[40\%, 50\%, 60\%, 81\%, 80\%, 90\%]$, the metric $ASC_{\%80}$ will give the following result:

$$ASC_{\%80} = \frac{1}{6}(0 + 0 + 0 + 1 + 1 + 1) = \frac{3}{6} = 0.50$$

which means, in turn, that a half of EVs got charged to an extent which is considered to cover the request of the respective user.

This metric roughly shows if the SC is capable of charging enough a similar number of EVs compared to the UC scenario. In this work, two limits can be chosen. On one hand, ζ is set to 100% to show how far the SC can charge EVs to the full extent of their requests. On the other hand, ζ is set to 80% to show if the SC is at least able to charge the EVs to a "somewhat acceptable" range. These limits will be particularly interesting when comparing them to the respective results of the UC scenario.

<M_5> **Quality of Experience (QoE)**: According to [194], QoE is "the degree of delight or annoyance of the user of an application or a service.". Generally, it is accepted that the quality experienced by a network service user is dependent on the Quality of Service (QoS) of the network, in a non-trivial and often non-linear way[195]. From

the point of view of an operator, QoE is an essential aspect in keeping the customer satisfied and thus diminishing churn. Hence, numerous mechanisms are introduced for QoE driven networks resource management with the purpose of maintaining quality above a certain threshold for every user; a challenge arises in terms of a fair allocation of available resources among users.

T. Hoßfeld et al. show in [195] the difference between the QoS and the QoE fairness, which is widely represented with the Jain's fairness index [196]. Whereas QoS considers fairness from a perspective of the system, QoE takes into consideration the perspective of the users. As an example, the issue of distributing downloading capacities is used. Therefore, the QoS would consider the download rate distributed equally between the users as fair, whereas the QoE would, for example, consider the heterogeneity of the users' devices. Jain's fairness index is the metric most frequently used for the QoS, which is described in detail in the work mentioned above. The authors proposed a generic QoE fairness index (F), which may be used to compare QoE fairness across the system and applications. That proposed index F assumes that the standard deviation σ of the QoE values quantifies the dispersion of the user's QoE in the system.

In this work, the proposed index F is adopted to determine the overall QoE in one simulation run. The standard deviation of the delivered energy E_{dilev} to the requested one E_{req} ratios of EVs will be used. Hence, the QoE metric $F \in [0, 1]$ is computed as depicted in Equation (5.2),

$$F = 1 - 2 * \sigma(\Delta\text{E}) \tag{5.2}$$

where σ is the standard deviation of ΔE, which is the set of the percentages of all performed charging requests of EV_j at the considered CSs in the simulation run. That set is defined as follows:

$$\Delta\text{E} = \left\{ \frac{E_{deliv}(j)}{E_{req}(j)}; j = 1, ..., N \right\}$$

It is worth mentioning that the maximum fairness is reached when $F_{max} = 1$. In contrast, the minimum fairness $F_{min} = 0$ is found when the standard deviation is at its maximum.

$<M_6>$ **Quality of Grid (QoG)**: This metric is defined with an inspiration of QoS in order to show how happy the grid operator is with our service, namely DSO. One approach to define this metric is to see it as the percentage of time in which a value of any considered GSI_k is out of green range $(YG, GY)_k$ for a particular scenario. Notably, the

transformer is overloaded, or the considered voltage magnitude is above or below the respective thresholds. Thus, the QoG metric G is given as defined in Equations (5.3),

$$G = \frac{1}{|T|}\sum_{t=0}^{T} G(t)$$
$$G(t) = \begin{cases} 1 & \exists\, K_k(t) \notin (YG, GY)_k \qquad k \in \mathbb{N} \\ 0 & \text{otherwise} \end{cases} \tag{5.3}$$

where $K_k(t)$ is the value of GSI class k at time t, and T is the time steps of the simulation during off-peak times. $G \in [0, 1]$ represents a better QoG when it reaches smaller values. It is crucial to exclude the on-peak times from calculation since the thresholds can be set to a value where the baseline itself crosses the thresholds during those times. Therefore, to prevent the baseline influencing the measurement of the performance of SC, K_k has to cross the baseline as a "second threshold" as well to count as, for example, a voltage drop or overloading. In other words, a charging operation takes place during this time slot and has an impact on the grid.

However, this is a simple approach, as it does not show to what extent the overloading of the transformer or voltage drop is happening, i. e., overloading of 150 kVA is accounted for as same as overloading of 200 kVA in a given 100 kVA threshold scenario. More complex metrics and formulas can be introduced in the future. However, this shall not be in the scope of this work, as the proposed metric is enough to see a general relationship between the QoG and QoE.

<M_7> QoG vs. QoE ($Norm$): Another metric showing the relation between QoG and QoE is needed since QoE probably has overall better results in the UC scenario in comparison to the SC one and vice versa. That is to be expected, as UC is ignoring the status of the grid completely.

To that end, the difference $\Delta^G = G^{UC} - G^{SC} \in [-1, 1]$ of QoG and the difference $\Delta^F = F^{UC} - F^{SC} \in [-1, 1]$ of the QoE between SC and UC scenarios are calculated. The former (Δ^G) shows the impact of the smart charger on the grid. Additionally, it shows a positive impact when reaching high, positive values, while showing a negative impact when reaching low or negative values. The latter (Δ^F) indicates the QoE, which needs to be sacrificed to achieve that increase in QoG. Also, it shows the negative impact of the smart charger on the QoE when reaching high, positive values while showing a positive impact when reaching low or negative values. However, Δ^G and Δ^F are expected to be positive most of the time in our study cases[3].

[3] As a workaround to avoid getting negative values in Equation (5.4), the negative values of both Δ^G_d and Δ^F_d can be replaced by zero since they means SC is not beneficial to DSO or it costs nothing to CSP.

In order to see a general tendency over multiple data sets $D = \{\text{Set of selected simulation days}\}$, Δ^G and Δ^F are averaged over all days used for the simulation as depicted in Equations (5.4).

$$\begin{aligned} \Delta^G_{avg} &= \frac{1}{|D|} \sum_{d \in D} (\Delta^G_d) \\ \Delta^F_{avg} &= \frac{1}{|D|} \sum_{d \in D} (\Delta^F_d) \end{aligned} \tag{5.4}$$

Finally, to calculate how many percentage points of the QoE need to be sacrificed for each percentage point of QoG the smart charger achieves, the averaged overall QoE is normalized by the averaged overall QoG metric, given by

$$Norm = \Delta^F_{avg} / \Delta^G_{avg} \tag{5.5}$$

$Norm \in \mathbb{R}$[4] shows the number of percentage points of QoE that have to be sacrificed for achieving one point of QoG. Negative results are theoretically possible and would show that the smart charger is either better in terms of QoE or worse in terms of QoG than the UC scenario. Since SC is usually better in terms of QoG and worse in terms of QoE, additionally, averaging over many days scenarios reduces the impact of exotic results, this special case is not probable. Hence, it is not considered further in this work.

$<M_8>$ **Grid Friendliness (GF):** The main goal of the SC is to react to emerging events in the grid in terms of PQ and assets overloading. These reactions cause some deviations between the supposed used power capacity, which is represented by the related charging profile, and the used one via measuring through the charging operation. Such a grid-friendly behavior of CS has to be awarded. Inspired by a point-based system of incentives, where the desired behavior is rewarded with collectible points or symbols, a translation of the CS behavior to points that can be awarded by the utility is proposed. The collected points by CS are distributed among influenced EV users based on certain criteria, e. g., a partial fulfillment of user charging requirements. Payback[5] is exemplary for a point-based reward system, where customers collect points by buying certain products that can later be turned into discounts. This approach falls under the terminus of gamification and has been applied in a variety of contexts, most commonly learning, education, health, and fitness behavior [197].

To that end, a certain amount of points is assigned to each SC reaction to an event generated by PQ-Indicator. Based on the definition of grid friendliness in Section 1.1, there are three different estimations of CS behavior: positive, negative, and neutral.

[4] Fieller's theorem is used for calculating the confidence interval of the ratio.

[5] https://www.payback.de/

In a similar way, the number of awarded points can be positive, negative, or zero. In further detail, when the status of the power grid is indicated as green, the SC follows the profile and neutral charging operation can be seen as long as the grid is in the green status. In the case of yellow and red indications, an appropriate reaction results in adding/subtracting a certain number of points to/from the CS current balance.

Consequently, GF is defined based on (1) the size of the SC response, i. e., the difference between actual (measured) power P^m at time t and $t-1$, (2) the distance to the charging profile, i. e., the difference between $\mathscr{C}_i(t)$ and $P^m(t)$, and (3) the importance of the event required a SC response, i. e., the value of `PQ-indic`. The total number of points is weighted by the duration (T_e) of an event $e(t)$ in minutes (until the next event $e(t+1)$ is triggered). Otherwise, ignoring the indication or inappropriate reaction is penalized by cutting off a certain number of points from the current balance. Similar to any other points-system, DSO can agree with interested CSOs on a pricing scheme, e.g., every 100 GF points equal 1€.

Hence, GF $\in \mathbb{Z}$ is defined for several events $e(t)$ arrived at cs_i as depicted in Equations (5.6). Thereby, the first three cases represent the awarding mechanism, i. e., positive reactions from SC. The fourth case is the green state, and the reaction of SC is seen as neutral to DSO. Finally, SC is penalized in the last two cases since it ignores the received event completely.

$$GF_{cs_i} = \left\lfloor 10 \sum_{e=0}^{N} T_e \; GF_e \right\rceil$$

$$GF_e = \begin{cases} \Omega_1(e) & (P^m(t) \geq 2\; P^m(t-1) \bigvee P^m(t) = \mathscr{M}_i) \\ & \bigwedge e(t) \in \{red^+, yellow^+\} \\ (\frac{P^m(t)}{P^m(t-1)} - 1)\; \Omega_1(e) & (P^m(t-1) < P^m(t) < 2\; P^m(t)) \\ & \bigwedge e(t) \in \{red^+, yellow^+\} \\ (1 - \frac{P^m(t)}{P^m(t-1)})\; \Omega_1(e) & (P^m(t) < P^m(t-1) \bigvee P^m(t) = \mathscr{C}_i^{min}) \\ & \bigwedge e(t) \in \{red^-, yellow^-\} \\ 0 & \mathscr{C}_i(t) = 0 \bigvee e_k \in \{green\} \\ -\; \Omega_2(\texttt{PQ-Indic}(e))\; P^m(t) & (P^m(t) \geq P^m(t-1)) \\ & \bigwedge e(t) \in \{red^-, yellow^\} \\ -\; \Omega_2(\texttt{PQ-Indic}(e))\; |\mathscr{M}_i - P^m(t)| & (P^m(t) \leq P^m(t-1)) \\ & \bigwedge e(t) \in \{red^+, yellow^+\} \end{cases}$$

$$\text{where,} \quad \Omega_1(e) = \Omega_2(\texttt{PQ-Indic}(e))\; (|\mathscr{C}_i(t) - P^m(t)| + |P^m(t-1) - P^m(t)| + 1)$$
$$\Omega_2(\texttt{PQ-Indic}(e)) = \lfloor |\texttt{PQ-Indic}(e)| + YR + 0.1 \rceil \tag{5.6}$$

Where N is the number of triggered events during the considered time interval, $\{t-1, t\}$ are the arrival times of two consecutive events, and `PQ-Indic`(e) is the value of `PQ-Indic` accompanying with event e(t).

5.1.3 General Assumption

While working on this thesis, some issues occurred when there was a need to adjust the simulation to the new test case. In the following list, all assumptions made in this work have been laid and categorized into three main groups. The interconnected nature of the charging ecosystem enforces many assumptions considering the requirements of the main three actors of the system: grid operators, CSPs, and end-users.

1. Low Voltage Grid:

   - DSO knows its distribution grid very well, particularly the impact of transient EV loads in its grid. Based on this knowledge, it sets the thresholds of the different GSI and defines the critical points. Additionally, all grid-relevant configurations of a PQ-Indicators are determined after an in-depth analysis of historical data of the grid.

   - Overload or voltage issues can be detected within a few cycles of its occurrence before the invocation of voltage/congestion control mechanism. Hence, it gives the controlling mechanism the chance to reduce/increase the transient EV loads.

   - Transformer overloading can be attributed entirely to its downstream loads. Consequently, if a measurement at a node indicates congestion, it can be enhanced by sending a congestion event to the subscribed nodes through the event-engine.

   - In this work, an imbalanced three-phase system means only an imbalance in terms of voltage magnitude. The voltage angle is assumed to be balanced all the time and left out of consideration.

   - It is not possible to infer congestion and voltage issues implicitly at the end nodes. Therefore, they must be explicitly signaled.

2. Communication Networks:

   - The distribution grid is equipped with communication infrastructure and measurement devices. The network is broadband, reliable, and has low latency. It is assumed that all CSs experience roughly the same delay when they receive signaling packets (this is never exactly true but simplifies the analysis).

   - MPs are able to generate events, and an event-engine such as Kafka is set up in order to enable the publish/subscribe messaging pattern.

- The speed-of-light propagation delay between the MP and charger through the event engine is small and typically is smaller than 1 ms. Furthermore, the total delay in the controlling loop is minimal to allow the smart charger to react in time to the considered issues in the grid.

3. CS and EV:

   - CS is owned by CSP, which agreed by a contract with DSO on operating the CS regarding the indications signal received from the PQ-indicator. Such a grid-friendly behavior is awarded by the DSO. For example, it grants a reduced grid access fee to the CSP.
   - The configuration parameters of SC are set by the CSP based on its business model and sensitivity analysis of the different parameters for each test case.
   - Every connected CS has a charging profile, which is available at its disposal. Such a profile is calculated based on the reservation or the historical demand data of the CS. It is an aggregation of all (possible) plugged in EVs at CS.
   - The charging rate can vary without any constraints within the maximum charging power value at the CS.
   - The maximum and minimum power constraints will be known at the beginning of the algorithm. The charging rates comply with technical specifications of EVs been charging.
   - An EV battery can be charged at any rate less than the maximum Amperage rating of its charger, independent of its state of charge, i. e., saturation phase is ignored. Similarly, the automatic disconnection of EV from CS is disabled.
   - Battery degradation due to regular charging rate modification is negligible.
   - In the simulation, single connector CSs are used. To handle this, EVs are queued, and plug(in)/out happens immediately to free up the connector. Furthermore, EV disconnects, when done charging or reaching the requested departure time.

4. Mobility Data:

   - Preprocessing the ACN data: According to ACN, users can adjust their requested energy and requested departure time via an app on their smartphones. It is assumed that the latest user input is chosen if there are multiple user inputs. If there is no user input about required energy for a charging operation happened voluntarily, a mean battery capacity of 37.2 kWh is used [198].
   - Requested power calculated from requested energy: Most of the parameters needed to charge an EV are provided by ACN: the arrival time, the departure time, and the requested energy. However, the requested charging power is missing in the ACN data set. As the power is needed for the simulation, it will

be calculated as $P = \frac{E_{req}}{T_{dep} - T_{conn}}$, where T_{dep} is the requested departure time, and T_{conn} is the requested connection time. However, most charging service providers only provide discrete values for charging power to choose from. These values can differ from region to region, see Table 2.2.3. The values used in this work are based on the CSs and connector standards in Bavaria[6]: 3.7/7.4/11/22/43/50 kW. When choosing 50 kW, it is assumed to be a DC charging.

Further, it is assumed that CSs in the simulation have a connector compatible with any standard available to serve any of those requests. Also, it is assumed that any EV in the charging profiles fulfills given standards to be able to receive the requested power. The requested charging power is always rounded up to the next upper limit. That will reflect more realistic charging requests, as they are done in those limits in reality.

- The maximum physical capacity of CS ($\mathscr{M}$): In principle, it is a known constant at the beginning of the simulation run. To shrink the impact of SC and avoid a drastic increase, $\mathscr{M}$ is set dynamically to be the maximum between the double of requested charging power in the charging profile $\mathscr{C}_i(t)$ and 50 kW.

5.1.4 Results, Test Cases, and Scenarios

After setting up the simulation, defining the metrics, and stating the assumptions, meaningful test cases have to be defined in order to show the added value of the proposed solution using metrics. For each test case, three scenarios are considered. First, the best-case scenario, where no CS is connected to the grid during the simulation period. Thus, no significant power quality issues in the grid are implied. Second, the worst-case scenario, where all four CSs are connected to the grid and they are charging without any control. The third scenario is SC scenario having controlled charging at all CSs. The first two scenarios form the Baseline_Min and UC respectively.

5.1.4.1 Test Case 1: Continuous charging with a fixed rate

It is assumed that all four CSs are connected to the grid and charging continuously with a constant charging profile $\mathscr{C}_i(t)$ through the whole simulation period. The goal of such a test case is to show the impact of the SC on the considered parameters of a distribution grid, particularly metrics M_1, M_2, and M_3. Worth mentioning, this test case is grid-oriented, and all performed tests can be done using data from ACN DB. But using a fixed charging rate enables us to cover more cases in terms of raising PQ issues in the grid and simplifies choosing the suitable values of thresholds. Furthermore, it allows a clear comparison among the proposed algorithms - namely TCP-SC and FSM-SC -, centralized solution stated in section 3.3 and a decentralized solution based only on the local voltage measurements. If not stated otherwise or differently, it is assumed that CSs support only controls over

[6]https://ladeatlas.bayern/

the total consumed power. Precisely, the power is distributed on all three phases equally, so $\texttt{PQ-Indic}_{\phi}$ values are aggregated using Equations (4.5), as discussed in Section 4.4. Finally, SCs responds periodically every five minutes to smooth the voltage curve and avoid unnecessarily changes every minute, as will be seen in the discussion of TMMs in the question $<Q_4>$.

	ER	***RY***	***YG***	***GY***	***YR***	***ER***
Load (kVA)	400	300	150	0	0	0
Voltage (V)	220.94	222.94	223.94	237.94	238.94	240.94

Table 5.1.: Thresholds of the GSI Classes: Overloading and Voltage Level

The GSI thresholds for voltage and loading of the transformer are configured in the PQ-Indicator, as shown in Table 5.1. From EN 50160, it is known that the voltage level must be within $\pm 10\%$ of the nominal voltage during 95% of the week measured by 10 minutes mean RMS values [21] in low and medium voltage networks. As the maximum allowed voltage deviation including the medium voltage network is constantly transmitted to the low voltage grid in case no OLTC is installed, a smaller range of $\pm 3\%$ and a simulation step of one minute are used. Due to the setup of the test grid, overloading of the transformer starts at 37.5% of the rated apparent power of the transformer, which is given by 400 kVA.

	TCP-Like SC						FSM-based SC				
μ	ψ	β	ϵ	λ_1	λ_2	λ_3	α	ϱ_1	ϱ_2	χ	ω
0.1	0.6	0.25	2.0	0.75	0.5	0.25	1.2	1.5	1.2	0.7	$\frac{1}{4} \cdot \left(1 + \frac{\mathscr{M}_i}{\mathscr{U}_i(t)}\right)$

Table 5.2.: Main Parameters Configurations of SCs in Simulation

The different parameters used in the smart charging algorithms are shown in Table 5.2. $\mathscr{C}_i^{min}$ is 1.3 kW, the minimum charging power provided by the SC to a CS to stay connected. For this test case, a constant user charging profile of 22 kW for each cs_i is used. Furthermore, the maximum power that can be provided by the SC is set to 30 kW, which is also assumed to be the maximum physical limit of all CSs ($\mathscr{M}_i$). Regarding TCP-like SC, the change-rate constant (ϵ) value taken for the test is 2. Note that this value should not be less than 2, since doing so would beat the basic idea of control actions in Algorithm 4.2, which is having power increase higher during SS phase than CA one. The remaining parameters are chosen in a way that is best suited for the smooth transition of the charging control signal and its effect on the grid. To that end, a sensitivity analysis is carried out but not included in the thesis since it depends on the properties of the grid and the considered charging operations.

The initial analysis of the results shows that periods between roughly 8:00 - 12:00 and 16:00 - 20.00 are peak hours in a day where the load in the grid is high. It is resulting in a voltage drop greater than 3% and overloading at the transformer even during the Baseline_Min scenario. During this time, SC restrains from further adding the CS load to the grid by reducing the charging power at CS to a minimum value ($\mathscr{C}_i^{min}$). Thus, avoiding further strain on the situation of the grid. As the algorithm assumes only one direction charging, i.e., G2V, the degraded power quality during the peak hours cannot be compensated by the SC. Thus, the focus is only on explaining the results from SC during off-peak hours in detail in the rest of this chapter.

This section aims to answer the following questions regarding the results obtained by simulation in the tested grid:

<Q_1> ***How do the proposed SC algorithms improve the considered grid GSIs classes?***
First, metric M_1 is considered for evaluating the loading of the transformer in terms of the total apparent power (S). As depicted in Figure 5.4, the transformer crosses the threshold for 72.2% of the day during the UC scenario. While FSM-based SC reduces this value to around 5%, TCP-like SC reduces the value to 1.3% of the day. Furthermore, the total energy crossing the threshold is 27% higher in the scenario of the FSM-based SC in comparison to the scenario with the TCP-like SC. As a result, the TCP-like SC prevents overloading at the transformer efficiently and contributes to a stable power quality of the grid in terms of assets overloading better than FSM-based SC.

Second, metric M_2 is used whereby the voltage level at the critical node in SC scenario to the baseline scenarios is compared, as depicted in Figure 5.5. Thus, the algorithms control CSs such that voltage level is mostly above the threshold line and falls mostly within 1 V below the threshold limit by crossing. In the worst case, the voltage drops to 222.4 V for the whole day. The SC rectifies the voltage drop below the threshold value by reducing the power allocation at the CS in the next step. In the Baseline_Min scenario, the voltage level during off-peak hours is well above the threshold and drops to a critical level during the UC, precisely, 213.5 V. Furthermore, the magnitudes of the voltage drop spikes are higher by TCP-like SC in comparison to the ones of FSM-based SC. The fast increasing actions taken by the TCP-like SC in the slow-start stage are the reason behind those high spikes. For example, the PQ-Indicator indicates a stable situation at the grid in the period between 00:00 and 6.30, so the algorithm performs a standard SS exponential increases, which can cause sudden voltage drop during fast increasing of the load at specific points of time. Finally, the number of times when the voltage level crosses the threshold with TCP-like SC is 11% more than that of FSM-based SC. In the worst case, the voltage drops to 223.2 V by FSM-based SC in comparison to 222.4 V by the TCP-like SC. The voltage control achieved when using FSM-based SC is comparatively better than that of TCP-like SC.

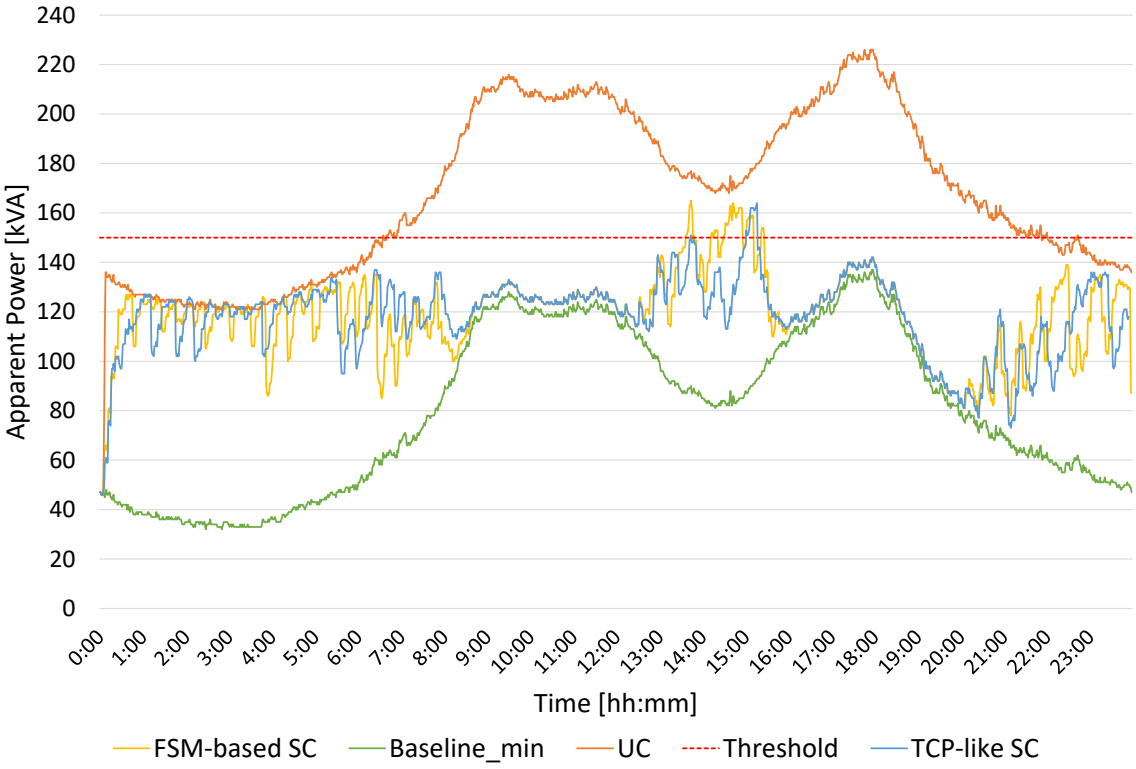

Figure 5.4.: Distributed Controllers: Apparent Power at the Transformer

Third, metric M_3 is discussed whereby the charging power allocated by SCs and the total power utilized for smart EV charging is depicted in Figure 5.6. During peak hours of the day, the used power by each CS is at the minimum value. During off-peak hours, the typical saw-tooth pattern of $Cwnd$ in the algorithm of TCP slow start is being reflected by TCP-like SC in terms of charging power at each CS as depicted in Figure 5.6b.

The CS connected at the critical node (cs_2) is allocated limited power when compared to the other three CSs due to the voltage fluctuations at that point of the grid. During the first six hours of the day, the charging power is at maximum for cs_1, cs_3, and cs_4 since fixing the voltage at the critical node needs only the reaction of cs_2; the increase at cs_2 happens with small steps in comparison to other CSs. The charging power is reduced at all stations either when the situation hits warning or critical phases locally at any CS or when reactions of the SC_2 are not enough to keep the voltage of the critical point in the green range. For example, it can be seen in Figure 5.6 for the time between 06:00 AM and 08:00 AM.

For more precise analysis, the energy distribution at each CS is calculated by performing area under the curve calculation using Figure 5.6. The total energy provided for CSs using FSM-based SC is around 3% more than the case of using TCP-like SC. The reduced energy distribution value when using TCP-like SC is due to the higher level of reduction action taken by the controller during critical phases. The surpassing

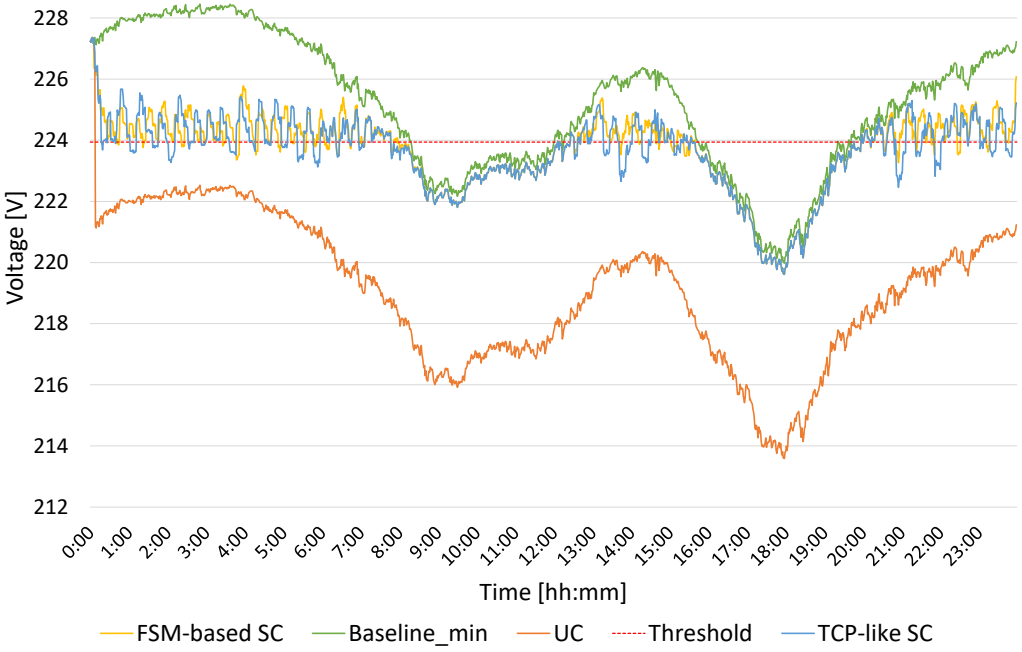

Figure 5.5.: Distributed Controllers: Voltage Level at the Critical Node

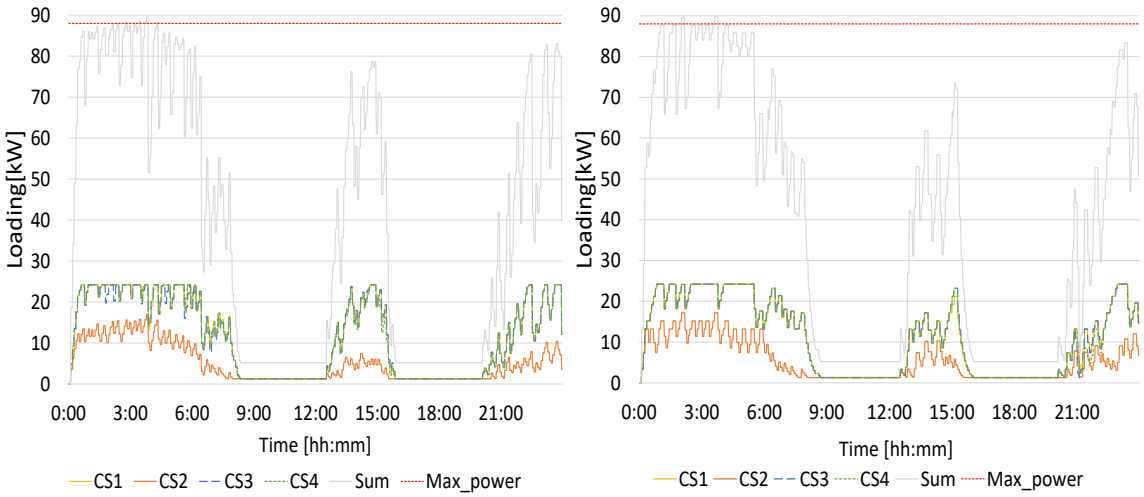

(a) FSM-based SC **(b)** TCP-like SC

Figure 5.6.: Charging power at four CSs. Each colored line represents a CS. Grey is the sum power of all CSs. The red line is the aggregated power from all charging profiles of all CSs.

of TCP-like SC - in terms of avoiding the transformer overloading - provides further evidence in this respect.

As seen in Table 5.3, while the energy portion of cs_2 during FSM-based SC is 26.5% of the average energy distribution to other CSs, it is around 40% using TCP-like SC. That could lead us to conclude that TCP-like SC is fairer, but usually one run is not enough. This property is studied thoroughly in Section 5.1.4.2 using metric M_5.

Finally, it can be concluded by observing the results that using TCP-like SC makes

	FSM-based SC	TCP-like SC
CS_1	51.20	39.91
CS_2	13.39	16.24
CS_3	51.48	41.00
CS_4	48.46	40.92

Table 5.3.: Energy Distribution in KWh among CSs between 12:30 and 16:00

allocating more power to cs_2 possible by limiting the used power by other CSs, namely, cs_1, cs_3, and cs_4. The matching of power curves of cs_1, cs_3, and cs_4 most of the time, which leads in its turn to the same amounts of consumed energy (see Figure 5.6 and Table 5.3), emphasizes the fairness of the proposed controller in the case no special local operating conditions take place. For example, the voltage criterion limits the used charging power at cs_2. Otherwise, all CSs will be able to use the same power all the time.

<Q_2> ***How good is the proposed solution in comparison to both centralized and decentralized solutions?***

Throughout this question, the proposed algorithms are compared with a centralized controller described in Section 3.3 and a decentralized approach based on Additive Increase Multiplicative Decrease (AIMD) algorithm [176]. AIMD is a feedback control algorithm best known for its use in TCP congestion control. The basic idea behind this approach is to increase the charging power at CS additively (using change-rate $\epsilon = 2$ similar to TCP-like SC) as long as the locally measured voltage at the CS is not crossing a certain lower threshold, namely, YG_U. If the local voltage at CS falls below that boundary, SC reacts by altering the charging power multiplicatively to decrease the charging power at once. E.g., a factor of $\Gamma = 0.50$ will be responsible for cutting the used power to half of its previous value and portrays a rapid change. AIMD-based SC is depicted in Algorithm 5.1. Worthy of mentioning, the main intention is the comparison among the different SCs to show the shortage of local conditions for building a smart controller. Developing a new sophisticated controller is not a goal of this section at all. The comparison depends on the different metrics defined in Section 5.1.2. Next, metrics M_1, M_2, and M_3 are discussed in detail. Looking at metric M_1 in Figure 5.7 shows that AIMD-based SC ignores the threshold of the transformer completely in particularly from the afternoon to the evening. That is expected since it is a local voltage-based approach. In general, the curve sticks to the UC scenario since cs_1, cs_3, and cs_4 charge most of the time with maximum capacity (see Figure 5.9) and ignore the voltage fluctuations at cs_2 entirely. Furthermore, both FSM-based SC and TCP-like SC follows the curve of the centralized controller in general. Remarkably, deep/high spikes disappear in the centralized scenario. The main difference is between 12:30 and 16:00, where the centralized controller shows more strict behavior and allocates less total power for all CSs. Worth to mention, the centralized controller looks for the

Data: average local voltage at cs_i ($u(t)$), $\mathscr{M}_i$, $\mathscr{C}_i^{min}$, YG_U, GY_U
Result: Charging power at time t: $\mathscr{C}_i^{min} \leq \mathscr{U}_i(t) \leq \mathscr{M}_i$
if $\Big(u(t) > YG_U \;\; \& \;\; \mathscr{U}_i(t) \leq (1+\mu)\; \mathscr{C}_i(t)\Big) \| \Big(u(t) > GY_U \;\; \& \;\; \mathscr{U}_i(t) \leq \mathscr{M}_i\Big)$ **then**
    /* Increase power */
    $\mathscr{U}_i(t+1) = min(\mathscr{U}_i(t) + \epsilon, \mathscr{M}_i)$
else
    if $u(t) \leq YG_U$ **then**
        /* Decrease power */
        $\mathscr{U}_i(t+1)) = max(\Gamma\; \mathscr{U}_i(t)\;, \mathscr{C}_i^{min})$
    else
        /* Do not change */
        $\mathscr{U}_i(t+1) = \mathscr{U}_i(t)$
    end
end

Algorithm 5.1: AIMD-based SC

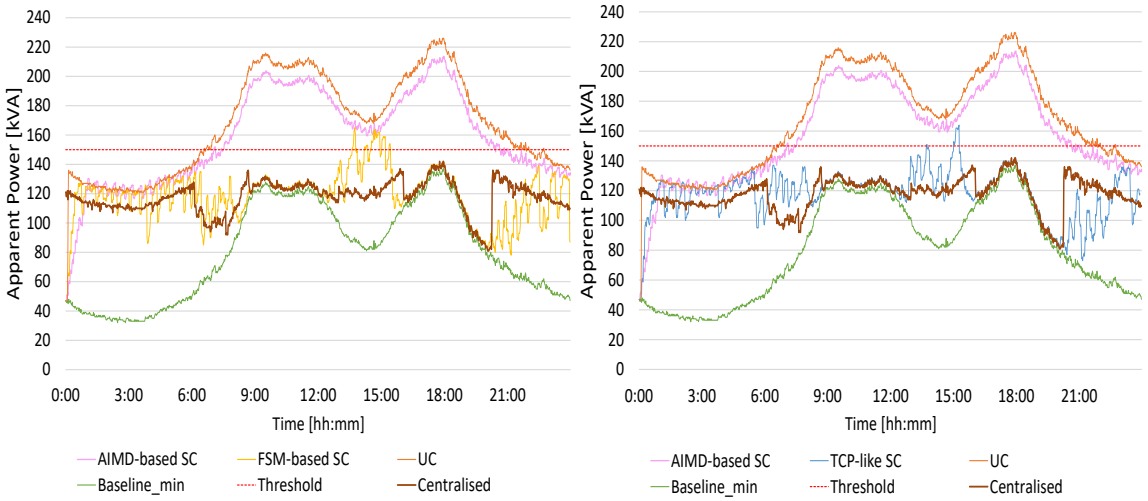

Figure 5.7.: Distributed vs. Decentralized and Centralized SCs: Loading at Transformer

solution, which meets the safe operational limits and reaches a fair distribution of available resources among active CSs.

Analyzing the voltage curves in Figure 5.8 shows that all SCs keep the voltage at the critical point around the threshold through off-peak times. While the centralized controller is very strict, so it allows no drops below the threshold during off-peak times and stick to the Baseline_Min during on-peak times, other controllers have many spikes. AIMD-based SC can not stick to the curve of Baseline_Min scenario in on-peak times since the bad voltage at the critical point is handled only by cs_2, which restrains its capacity to the minimum, but that is not enough. Meanwhile, other CSs continue charging with their maximum since they suffer no PQ issues because of their locations

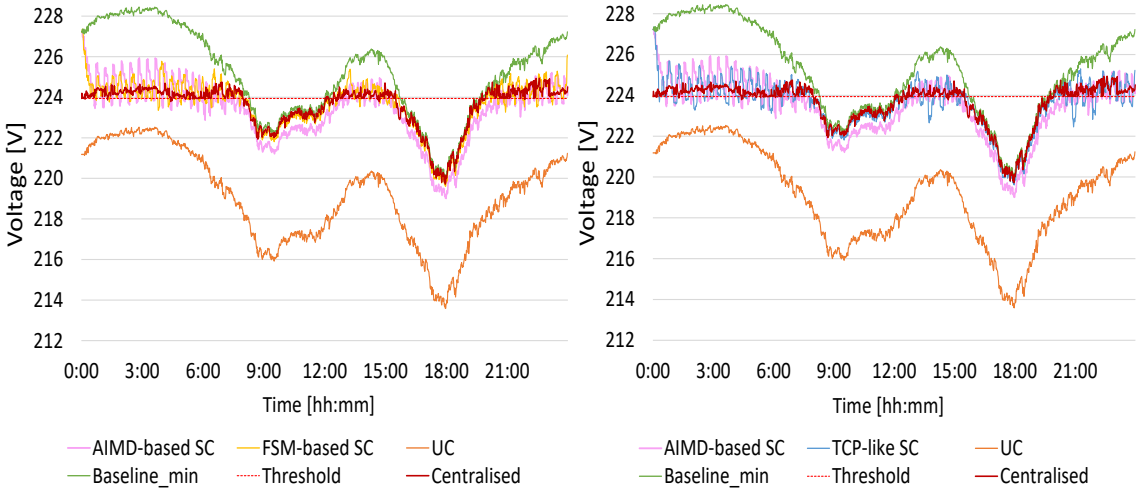

Figure 5.8.: Distributed vs. Decentralized and Centralized SCs: Voltage at the Critical Point

close to the transformer(cs_1 and cs_3) or in a different feeder line with no high load (cs_4).

Even AIMD-based SC allows allocating more power to the different CSs; this allocation is not fair, as depicted in Figure 5.9. Thereby, only cs_2 reduces its power to deal with voltage issues at the critical point. The comparison with the power curves of the centralized controller in Figure 3.11[7] shows no convergence between decentralized and centralized solutions. In contrast, FSM-based SC and TCP-like SC converge at almost to the solution of the centralized controller. The main difference is in the power allocated to cs_2, where the power magnitudes are lower in comparison to the centralized approach.

We can conclude that the two distributed controllers can respond in better shape to the transformer loading when the local voltage is not enough to infer about the congestion in a grid not running to its limits. Furthermore, depending on local conditions causes unfairness among CSs in terms of available resources distribution, which, in turn, leads to a different level of satisfaction of end-users.

<Q_3> ***Does the control of the individual phase improve the algorithm in terms of consumed energy and phase imbalance?***
To that end, the experiment mentioned above is repeated with an assumption of the possibility to control the consumption on every single phase, i.e., PQ-Indicator sends an individual $\texttt{PQ-Indic}_\phi$ for each phase, so no aggregation function is used. For simplicity and because of very similar results, only results of FSM-SC are depicted and discussed. Thus, a separate FSM for each phase is set instead of one for the whole CS.

[7]Regarding the centralized controller, the curves of power at CSs with $\mathscr{M}_i = 30$ kW are almost very similar to the ones in Figure 3.11, where $\mathscr{M}_i = 22$ kW. Therefore, it is not drawn again.

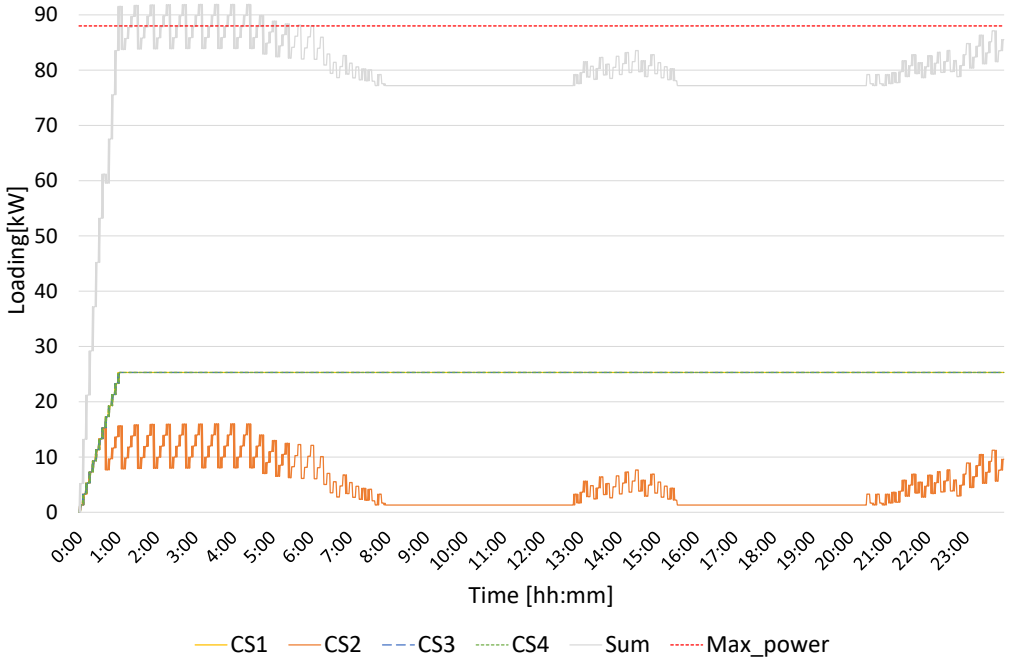

Figure 5.9.: AIMD-based SC: Charging Power at Four CSs

Only M_2 and M_3 are considered particularly at cs_2 since it is installed at the critical point and suffers from less power allocation in comparison to other CSs.

Figure 5.10 shows the voltage magnitude on each phase compared to the values of two other scenarios: Baseline_Min and aggregation-based SC, where FSM-based SC uses the aggregation function in Equations (4.5). Clearly, the voltage on the initially overloaded phase B is improved; its magnitudes are even better than the ones in the Baseline_Min scenario. In contrast, the voltage on phases A and C are similar or sometimes worse than the values of aggregation-based SC; more load is put on them. That can be justified depending on the type of three-phase wiring. It is assumed to be (Wye) or "star" in this simulation where each phase is connected to a neutral wire. Thereby, the neutral line carries the total neutral current from the three phases. That current is substantially the unbalanced current from the three phases[8].

However, this kind of control allows increasing the portion of energy allocated to cs_2 with keeping the voltage in the green range as much as the aggregation-based SC does. This approach increases the total energy consumption of cs_2 up to 35 kWh in comparison to only 13.39 kWh in the original scenario between 12:30 and 16:00, which equals to 69% of the average energy distribution to other CSs. Figure 5.11 states the power allocation at cs_2 using aggregation-based SC (red line) and the sum of power allocation on each phase besides the total sum using the phase-based SC (blue lines).

[8]By applying Kirchhoff's current law to the neutral node, the currents of three phases sum to the total current in the neutral line. In the balanced case the vector sum $I_A + I_B + I_C = I_N = 0$

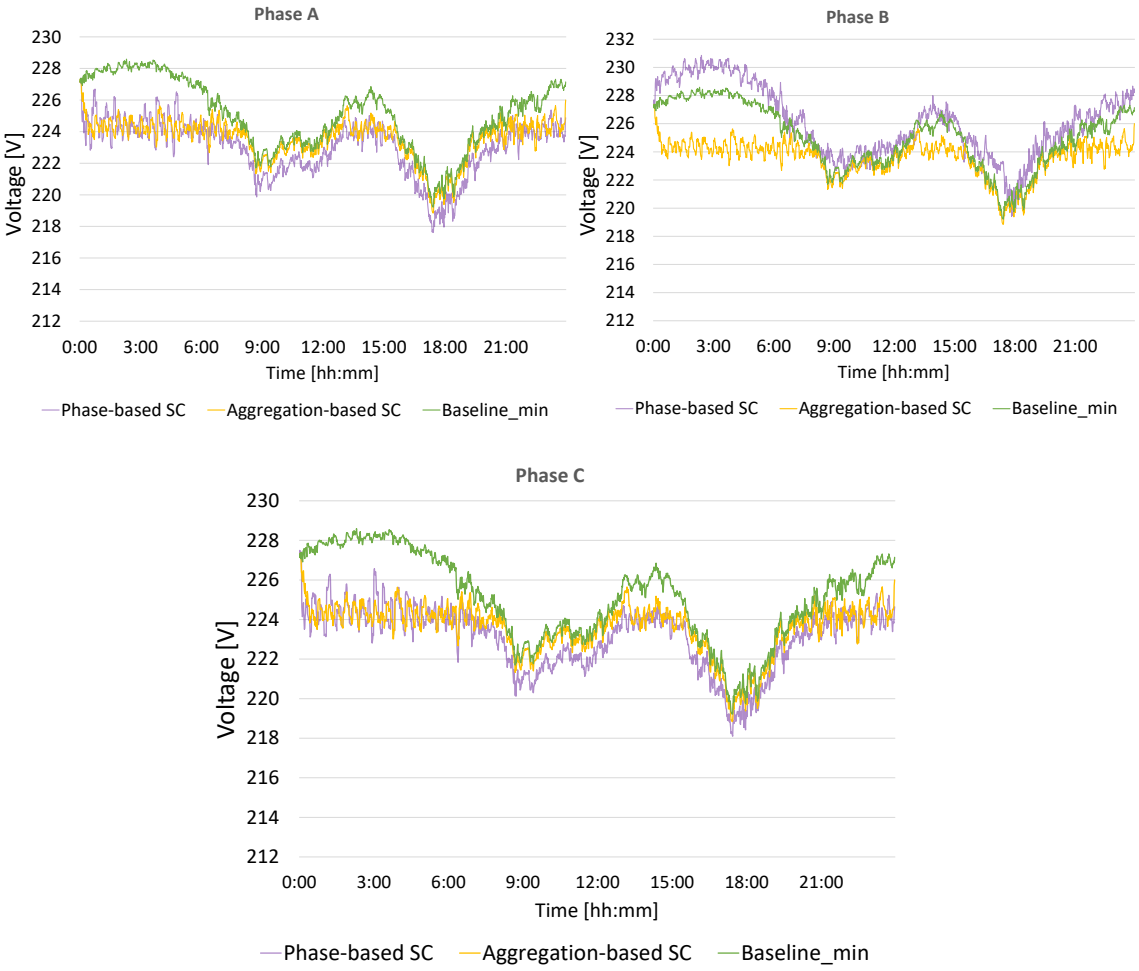

Figure 5.10.: Voltage Level at the Critical Point Using Phase aware FSM-based SC

To conclude, the phase-based controller increases the maximum voltage imbalance factor at cs_2 from 1.03% using the aggregation function to 1.9%. The imbalance factor still in the allowed range of EN50160, i. e., smaller than 2%. While the aggregation-based SC keeps the maximum imbalance factor close to the value in Baseline_Min (1.02%), the phase-based SC increases it in the allowed range but enabling more energy consumption.

$<Q_4>$ ***What impact do the proposed TMMs in Section 4.6 have on the proposed solution?*** One important reason for the development of a TMM is to improve further the usage of the available resources of the grid. In that regard, the mechanisms will be compared by looking at the amount of energy the four CSs received during the simulated 24 hours, i.e., metric M_3 on the level of CS. The results of different mechanisms are compared with those from two scenarios where the SC reacts periodically every one minute or five minutes. In the latter scenario, the weighted average of received values of `PQ-Inidc` over the last five minutes is calculated similarly to step (1) in TCP-like SC.

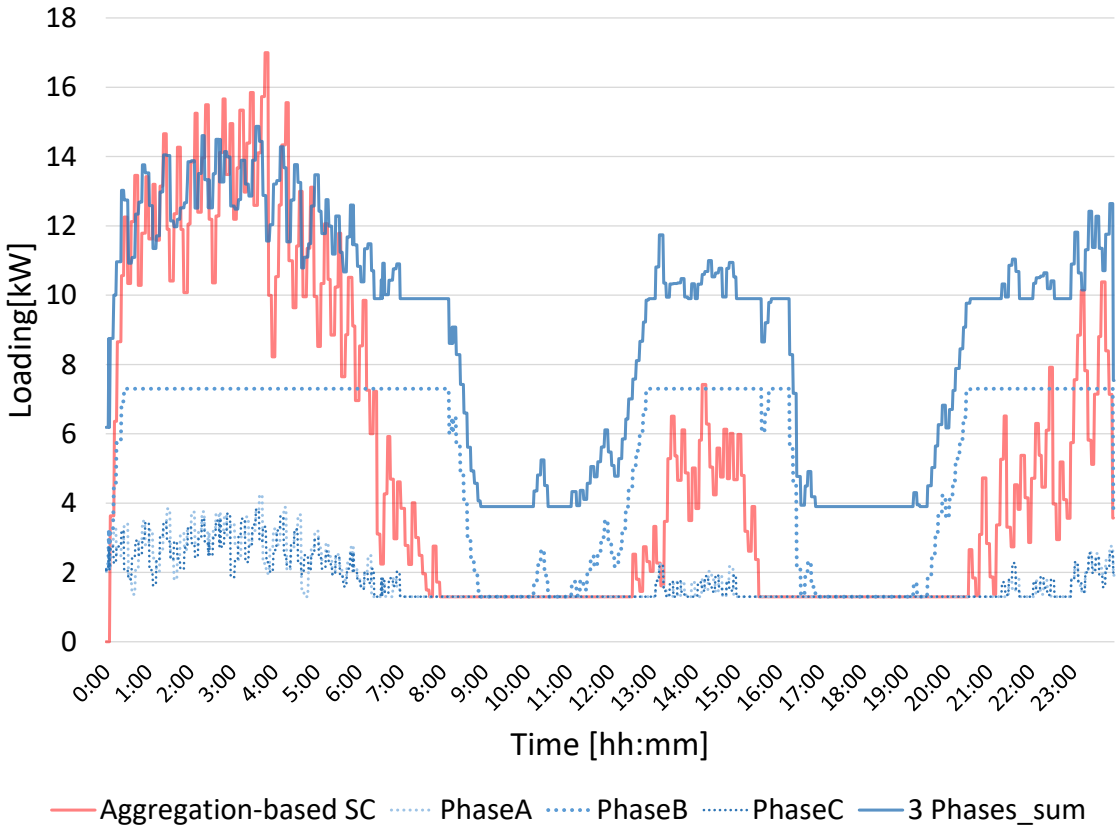

Figure 5.11.: Power Allocation at cs_2 Using FSM-based SC with(out) Aggregation Function

For answering this question, only the results of TCP-like SC are presented since it shows better results over FSM-based SC in terms of power allocation, as depicted in $<Q_1>$. For the simulation, the maximum time MAX_TIME that SC can wait before reacting to a new value of `PQ-Indic` is set to five minutes. The minimum time MIN_TIME is set to 60 seconds, and therefore, it is equal to the constant step size of the smart charging approach without any timing mechanism. The step size γ, by which the waiting time can be adjusted, is set to 30 seconds. As an effect of γ being chosen as a smaller value as the simulations step size, the adaptation of the waiting time is slowed down, which helps to prevent the ping-pong effect.

	1 min.	5 min.	Simple	ALOHA-like	Soph.
cs_1	203.39	267.69	275.33	224.34	248.20
cs_2	129.20	129.51	130.21	123.75	132.84
cs_3	203.39	267.84	275.36	241.90	248.14
cs_4	203.66	266.21	275.33	227.00	246.74
$Total$	739.63	931.25	956.22	819.00	874.92

Table 5.4.: Energy Distribution in KWh among CSs for the Whole Simulation Day

Analyzing the consumed energy by each CS shows that the total amount of energy consumed by all CSs differentiates among the different TMMs, as depicted in Table 5.4.

Although periodical (5 min.) and simple TMMs enable a high energy consumption in comparison to other TMMs, they show a lower percentage of cs_2 portion to the total sum (fairness); it is ≈13.5%. Otherwise, the ALOHA-like and sophisticated TMMs allocate less energy, but show fairer sharing behavior among CSs; the cs_2 portion is ≈ 15% of the total sum. Moreover, rapid reaction using TMM with periodical response every one minute does not result in consuming more energy by CSs, rather the total amount is the lowest among all other TMMs.

In general, having a long response time is better from the perspective of the EV since it means a less frequent change of the charging power, which is more healthy to the battery. Regarding this point, the sophisticated TMM has a longest average response time by ≈202 seconds, the ALOHA-like and simple TMMs have an average time of ≈ 102 and 185, respectively. Worth of mentioning, the standard deviations and confidence intervals are not stated since they are tiny.

However, all the proposed TMMs keep the transformer not overloaded most of the time (below the defined threshold), but the sophisticated mechanism guarantees that by 100%, i. e., no values of transformer load is higher than the defined threshold. In terms of voltage; the ALOHA-like and periodical (1 min.) TMMs cause high oscillation, while the remaining TMMs show almost the same behavior.

Figure 5.12 shows the load of all CSs using the different TMMs. It is clear that the ALOHA-like (Figure 5.12b) and the periodical (1 min.) TMMs (Figure 5.12d) oscillate clearly more than other TMMs.

To conclude, different strategies for timing management might be necessary depending on system priorities. Through the evaluation, it is found that the simple and periodical (5 min.) TMMs performed best when it came to getting as much as possible power to active CSs while keeping the grid operating within the safe limits; The simple TMM is favored above the periodical mechanism. In a system where the fairness between CSs is of importance, however, a more sophisticated approach might perform better. In the evaluation, the sophisticated TMM shows the best performance out of all developed approaches in this regard.

$<Q_5>$ ***Which is better, OLTC-based solution or SC-based solution?***
For answering this question, it is assumed that a transformer supporting OLTC technology is used in the grid instead of the typical transformer. Using the OLTC, the adjustment of the voltage in the connected low-voltage grid can be made without performing further changes in the grid, particularly, no control on the CS demand. The experiment is repeated with the UC scenario and active OLTC. The tap changes based on the voltage level at the critical point in order to keep it in the green range all the time, however, by increasing or decreasing the tap position. It is significant to mention that OLTC is not designed to react directly to the overloading of the transformer. Nevertheless, the voltage of the high/low side of the transformer is the primary factor

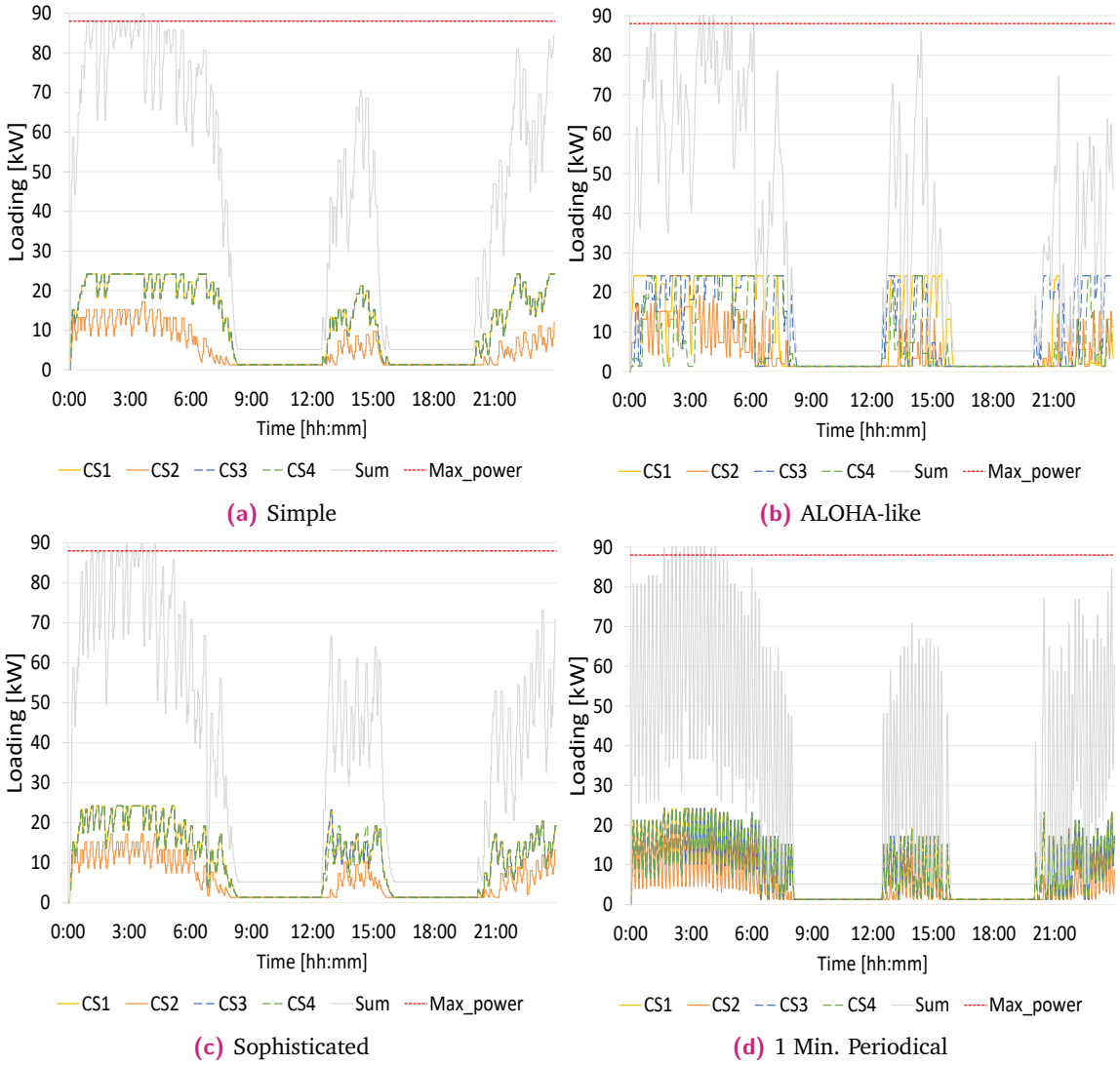

(a) Simple **(b)** ALOHA-like

(c) Sophisticated **(d)** 1 Min. Periodical

Figure 5.12.: Charging power at four charging stations using different TMM. Each colored line represents CS. Grey is the sum power of all CSs

in increasing or decreasing the tap position. In some cases, the impedance of the grid is considered as well. Finally, an additional voltage per tap is set to 2,8%.

As depicted in Figure 5.13, seven tap changes are required to keep the voltage of the critical point in the green range throughout the whole day; the highest tap position is zero, and the lowest one is -2. The tap change from -1 to -2 is required only during on-peak times, e.g., between 08:00 and 12:00. The voltage curve at the critical point using the OLTC transformer is even better than the one in the Baseline_Min scenario. The described scenario, where only one central OLTC transformer is used for connecting the low-voltage grid with an external medium-voltage grid, faces a downside that the OLTC only allows the regulation of the whole low-voltage grid. In case of high voltage discrepancies at different locations in the low-voltage grid exist, these discrepancies cannot be solved using only one central OLTC. For example, the voltage curve of cs_1 (it is connected close to the transformer) gets into yellow and

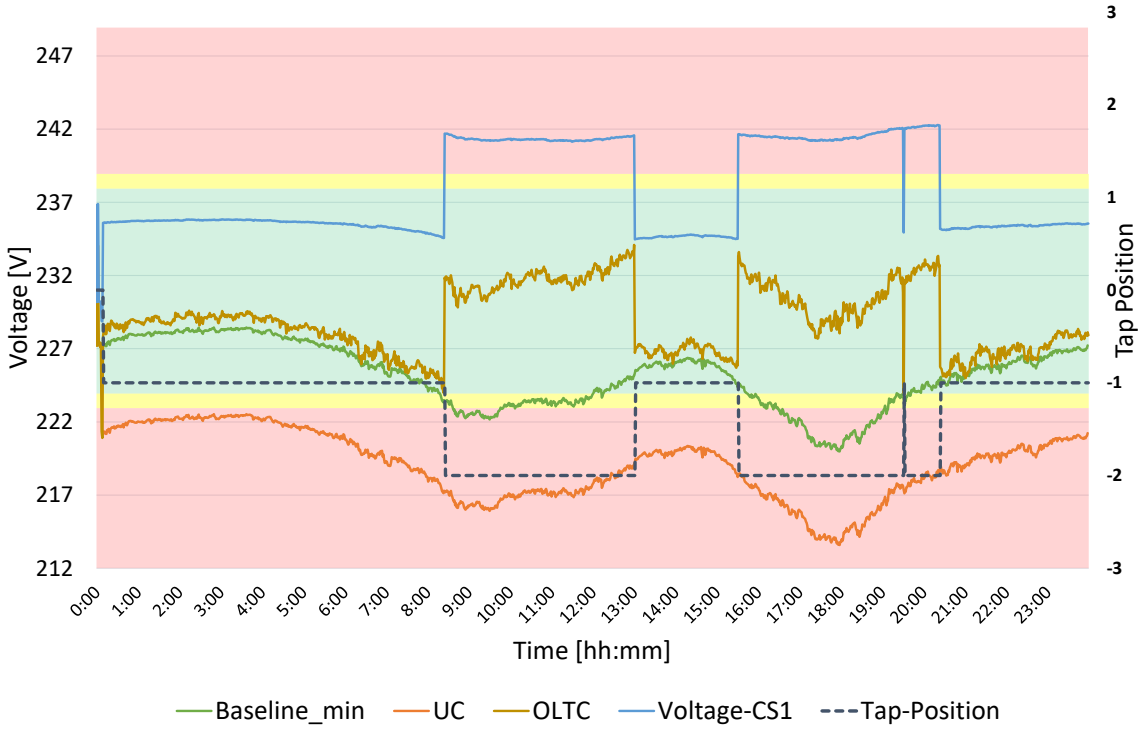

Figure 5.13.: Voltage at cs_1 and the Critical Point using OLTC

red ranges during on-peak times in contrast to the voltage of the critical point. That contradicts the design goals of the proposed system in Section 1.2. To solve such cases, the installation of additional OLTCs or other Demand Side Management (DSM) and Supply Side Management (SSM) mechanisms might be necessary.

Although OLTCs are great instruments for fast voltage regulation, grid operators may try to reduce the number of tap-changes to a minimum. The reason for that, as explained in [199], lies in the most common operational problem connected with OLTC. Each tap-change causes physical stress to the transformer and therefore lowers its remaining expected lifetime.

5.1.4.2 Test Case 2: Test with different days-scenarios

The main focus of this test case is to compare the proposed algorithms in terms of stakeholders' concerns, namely, EV drivers, CSPs, and DSOs. The assessment focuses on the formerly defined metrics M_4, M_5, M_6, M_7, and M_8. To that end, ACN data is used. It is evident that randomly selecting charging sessions will not reflect reality quite well. Naturally, drivers have individual motivations for trips and charging stops; therefore, these specific behaviors generally have to be taken into account. In particular, universally observable patterns appearing over the entirety of the data set are fundamental.

However, there are significant differences in power demand between weekdays and weekends. It is obvious that the general traffic is much less at the weekend than at workdays. Therefore, the power demand at public and work stations goes down as well. Authors of

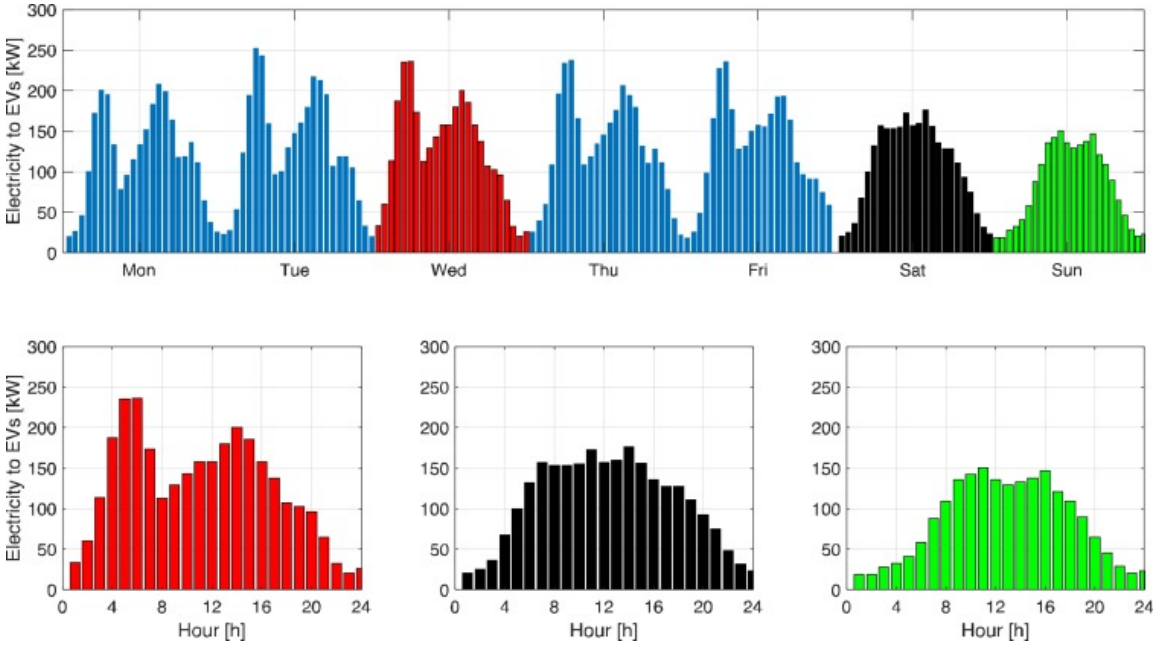

Figure 5.14.: Average EVs demand per week: weekly evolution (upper graph) and zoom for Wednesday, Saturday, and Sunday (lower graph)[187]

[187] show in Figure 5.14 that there are differences in peak demands between weekend and weekday. They further show that the pattern of demand profiles does not differ significantly between workdays and likewise does not differ between Saturday and Sunday. This data is gathered from ElaadNL from the Netherlands but shows a similar pattern to the data gathered from the MoP in Germany [183]. Therefore, lower and different demands on weekends can indeed be assumed to be inherent in the driving behavior of EV users.

	Jan	Feb	Mar	Apr	May	Jun	Jul	Aug	Sep	Oct	Nov	Dec
Deviation of # of events from average.	0.94	0.84	0.63	0.85	0.89	0.99	1.28	1.04	1.04	1.30	1.19	1.02
Charging time [min]	25.3	23.4	22.2	20.8	20.0	19.6	20.1	19.4	19.1	20.2	21.6	22.8

Table 5.5.: Yearly variations on charging times and number of charging events for the Norwegian charging data[184]

Furthermore, some research work shows that there are quite a few differences in EV charging patterns as well between summer and winter times. As depicted in Table 5.5 [184], there are deviations of the amount of charging events and the charging times throughout the year. They conclude that the deviations of the amounts of charging requests are based on vacation times. Although their used data set is from Norway and therefore depends on that nation's vacation periods, it can be assumed, based on the conclusion of the authors, that every country has its own deviations, as they have their own vacation periods. The exact numbers are not crucial for this work, as they will already be integrated into the used data source. More relevant here is to see that most definitely there are differences, which could make testing different seasons a relevant aspect of this work.

The differences of power/energy demands and requested connection/departure times of those scenarios could have an impact on the behavior and effectiveness of a SC algorithm, which definitely needs to be examined. Nevertheless, using different charging profiles will be at least beneficial for showing the impact of the smart charger on the grid and the user satisfaction for a variety of test scenarios.

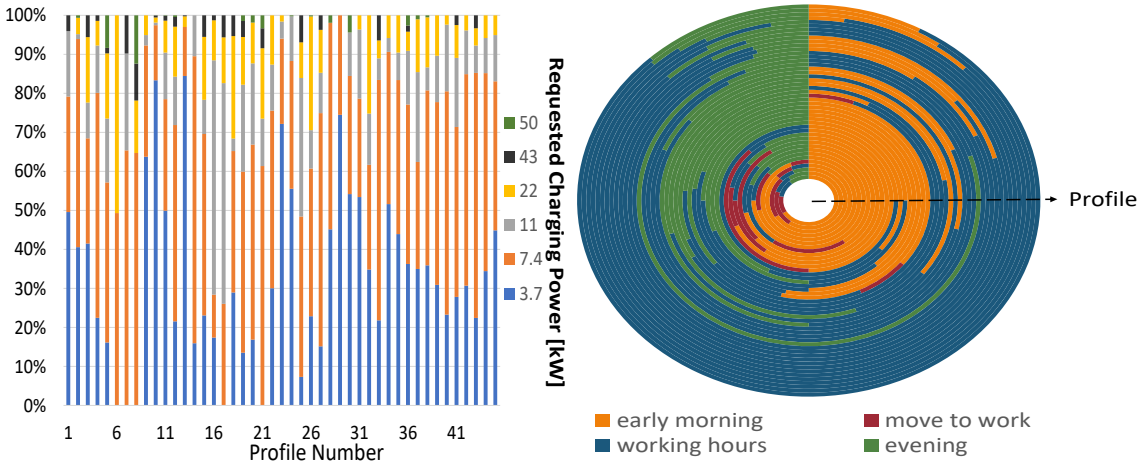

(a) Percentage of Different Charging Level in Each Profile

(b) Percentage of Arrival Times Distribution over Four Periods

Figure 5.15.: Forty-five-day-profiles

To that end and based on the discussion mentioned earlier, the ACN database is used, and a profile-generator is developed in order to extract CS profiles for different scenarios. The generator creates 24-hour charging profiles for CSs, and it uses predefined-configurations such as location, season, and day to extract pertinent and representative data for each scenario. Since our grid is built using load profiles of a workday in winter, that information is passed to the profile-generator. So 45 profiles from the winter of 2019, excluding holidays and weekends, are created. While Figure 5.15a depicts the diversity in the requested charging power by showing the accumulated percentages of each charging level in each profile, Figure 5.15b shows the accumulated percentage of arrival periods of EVs in each profile. The day is divided into four arriving periods: early morning (00:00-06:00), move to work (06:00-09:00), working hours (09:00-17:00), and evening (17:00-00:00). Clearly, charging during the working hours is dominating in many profiles.

The simulation runs 100 times for each scenario using those 45 profiles with ensuring not to use the same profile twice in each run. The different combination that can be obtained exceeds one million. Each run takes about 10 minutes, and parallelism is not possible since it requires many expensive license keys of PowerFactory. That makes each 100 runs need about 16 hours. With testing five scenarios, it is about five days. Therefore, the simulation ran for only 100 times.

For the sake of defining the thresholds of voltage and load, the UC scenario is considered. Data about Mean, Max, and Min of both voltage and transformer loading from 100 runs are

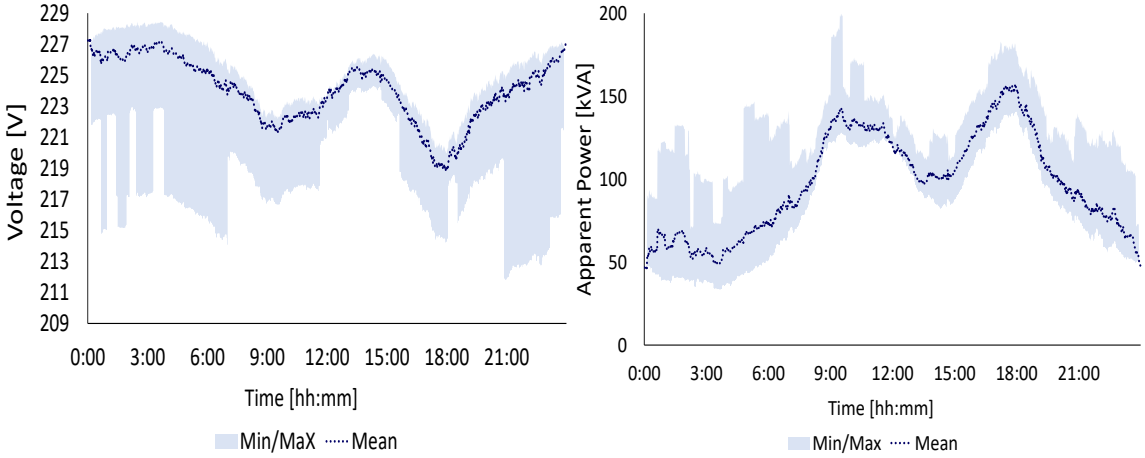

Figure 5.16.: Min, Max, and Mean of Main GSIs in different days-scenarios: Voltage and Transformer Loading

collected and depicted in Figure 5.16. Analyzing this data results in setting the thresholds in Table 5.6. Further, all other simulation parameters are similar to ones in test case 1 except μ; it is set to 0.2 to give more freedom to SCs to compensate for the degradation in service outside grid stressing times.

	ER	*RY*	*YG*	*GY*	*YR*	*RE*
Load (kVA)	400	300	150	0	0	0
Voltage (V)	216.94	218.94	219.94	233.94	234.94	236.94

Table 5.6.: Thresholds of the GSI Classes in Test Case 2: Overloading and Voltage Level

After fixing the different thresholds, 100 runs of the simulation are carried out for each of the following five scenarios: UC, AIMD-based SC, FSM-based SC, TCP-like SC, and the centralized controller described in Section 3.3. Next, an in-depth analysis of metrics: ASC, QoE, QoG, NORM, and GF is introduced.

The metric ASC has no meaning without the total number of charged EVs in each scenario since the early finishing of a charging operation allows starting a new one immediately from the EV waiting queue. Therefore, the total number of charged EVs alongside with the ratios of ASC is shown in Figure 5.17. One EV more is charged in the AIMD scenario in comparison to the UC scenario. That is expected since AIMD depends only on the local voltage conditions and ignores transformer overloading completely, so it can finish charging tasks much faster than other controllers except the centralized one. Although the centralized SC is more strict and prioritizes the grid concerns over the user ones, it can charge the same number of EVs as in AIMD scenario. The parameter μ is not considered in the optimization problem described in Formulae (3.6), but the controller can choose the best charging powers in the range $[\mathscr{C}_i^{min}, \mathscr{M}_i]$, which gives it more freedom to use more power when it is possible beyond the

charging profile[9]. Hence, the centralized scenario is granted the full flexibility to serve the grid and to satisfy users' requirements in a fair way. However, the distributed controllers charge the same number of EVs in the UC scenario with a higher value of the ASC ratio. The UC scenario has only an ASC value of (80%) since CSs follow a dedicated charging schedule, so many cars have to charge for less time since the connector is occupied by another EV. With TCP-like SC, the lowest rate is accomplished because of all the considerations it does and the way it reacts to warning signals. Even though FSM-based SC also consider the threshold of the transformer, it manages to achieve a good overall service. It achieves a rate even above the UC scenario and very close to the AIMD scenario.

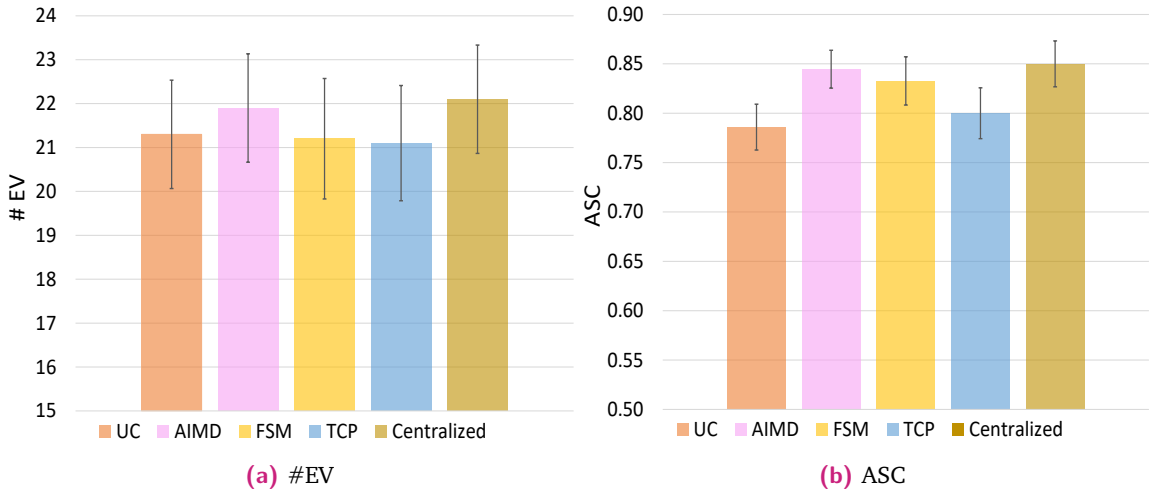

(a) #EV **(b)** ASC

Figure 5.17.: ASC (ζ=100%) and the Total Number of Charged EVs in Each Scenario

In terms of metric M_5 (QoE), the UC scenario is performing well. It manages to keep the differences between the delivered rates among the dispatched customers at all CSs smaller than an active SC does. No decrease in charging power during charging operations at the CS increases obviously the chance for the customer to receive its expected share of energy. The values of QoE does not reach one in Figure 5.18a since some EVs will leave without getting enough energy because of time restriction relevant to the occupancy of the single CS connector. The AIMD scenario has the lowest QoE value for creating a discrepancy of emitted energy among the users more often in comparison to the distributed SCs. The reason behind that is the local perspective of each SC, specially cs_2, which has to deal with the local voltage issues alone without any help from other CSs in the system. FSM-based SC has the best performance among the smart charging solutions for serving the customers more equally; its QoE value is even approximately equal to the one of the centralized approach. Worth to mention, it is supposed that the centralized controller guarantees a fair power allocation among the active users as the objective function of the optimization problem is formulated to serve this goal. TCP-like SC also does a good job, but only a little better than

[9]It is noteworthy, this approach is not battery-friendly, and it might lead to more battery life degradation in comparison to other approaches. However, it is applied for the sake of comparison in terms of both the grid-friendliness and the fairness.

the decentralized approach. However, all SCs have to sacrifice QoE points to help the grid.

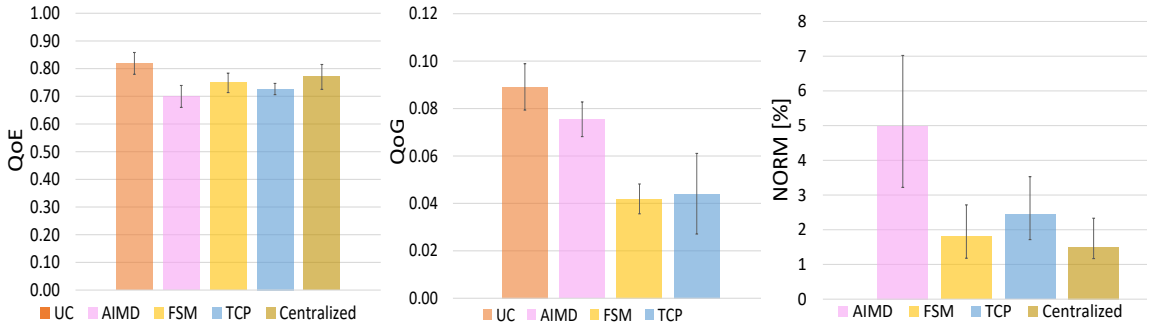

(a) QoE **(b)** QoG **(c)** NORM

Figure 5.18.: Means of QoE, QoG, and NORM for Each Scenario (100 Runs)

By examining the metric QoG, it is clear to see that the UC scenario achieves the biggest score[10] in terms of being a burden to the grid in Figure 5.18b. The frequent and protracting violations of the transformer threshold or the voltage threshold through charging without any kind of grid supporting results in a high QoG value of UC scenario compared to the scores achieved by the distributed SCs. Further, the QoG rate of AIMD-based SC is also high since it ignores any crossings of the transformers threshold in the simulation; thus, the count of violations in total increases. The more sensitive SCs - namely, FSM-based and TCP-like SCs - do their job very well when it comes to minimizing the violations. In only approximately 4% of the time, the grid is negatively affected by crossing through thresholds of green range. FSM scenario achieves a marginally better rate after 100 runs, but both distributed mechanisms help a lot to keep the QoG value low and therefore support the grid. The strict control of the centralized algorithm allows no violation either in voltage or transformer load during off-peak times; hence, its QoG value is zero. Worth to mention, on-peak times are excluded from the calculation of QoG.

To see how many points of the fairness metric, namely QoE, have to be sacrificed in order to improve the metric QoG, metric M_7 (Norm) is calculated and depicted in Figure 5.18c. It shows that AIMD-based SC has the worst performance, as expected. Thus, for decreasing and therefore improving the QoG metric by one point, it would be necessary to lower the quality of experience for the customers by almost 5 points. While FSM-based SC has to give away only $\approx$1.8 points to enhance QoG, the sacrifice of TCP-like SC is about 2.25 points. FSM-based SC shows the best result and even very close to the centralized controller, which is supposed to be the fairest and the strictest approach.

Throughout the evaluation of metric M_8 (GF), PQ-Indicator is assumed to be active but not considered in the reactions of UC, AIMD, and centralized scenarios, i. e., `PQ-Indic` at a time

[10] Positive score means negative impact, i. e., the considered GSIs are out of the green range for more time, see Equation 5.3.

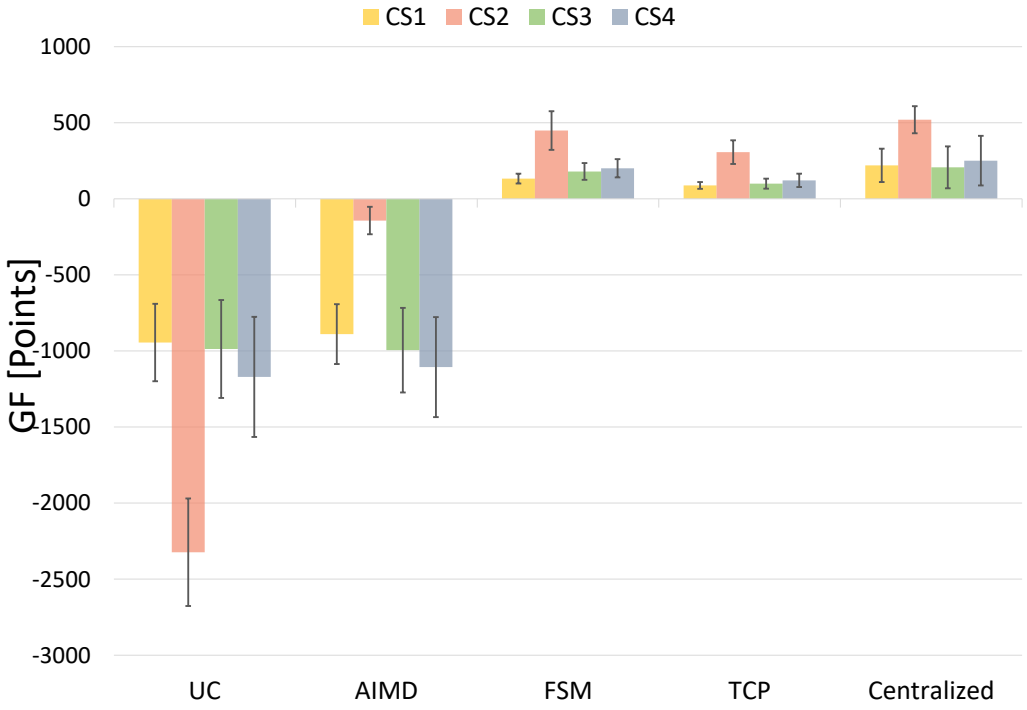

Figure 5.19.: Average Total Number of GF Points Obtained by Each CS in an Individual Scenario

point (t) is used only to assess the reaction of SC. However, it can be observed that only the distributed SCs besides the centralized controller achieve a positive total number of points at each CS in Figure 5.19. These results reflect the smart reactions of the individual SCs. In the UC scenario, there is no control at the CS, so it never reacts to any kind of warning signals raised by the grid operator. Hence, it gets penalized while CS continues serving EVs. Especially at cs_2, which is located at the critical point, the GF score is the worst since the local voltage falls below the threshold more often at this CS than it happens at other CSs.

Taking a look at the score of AIMD-based SC shows that ignoring the transformer state results in a negative GF value for all four CSs. The only achievement of AIMD-based SC is to get a much better score at cs_2 in comparison to the other CSs. The frequently crossing of the voltage thresholds at the critical point leads SC at cs_2 to react appropriately, whereas these events are ignored by other CSs or react improperly. Precisely, they are not aware of them since only the local voltage is considered; thus, cs_1, cs_3, and cs_4 get high penalties.

Regarding the distributed SC, they get a positive score at all four CSs. They earn to stand out with their smart reactions and collect more beneficial points than penalties in the mean of the 100 different simulation runs. Again, the scores achieved by FSM-based SC are relatively better than the ones of TCP-like SC. Both have results close to the centralized controller, which has a higher number of points since drastic changes at all CSs are possible in each step, unlike distributed SCs. Moreover, all CSs obtain a fair share of the total

number of awarding points. Worth to mention, a slight modification by calculating the GF metric of TCP-like SC is made, whereas no points either as a penalty or as an award are assigned in the warning phase. Otherwise, the total number of points would be negative since ignoring one signal needs many consecutive good reactions to compensate for the damage.

5.2 Benchmark of Apache Kafka

As proposed in Section 4.3, Kafka Apache can be used as one of many mechanisms of event-driven real-time data collections in smart grids. The goal is the realization of the publish/subscribe messaging pattern. Kafka is a distributed messaging system written in the programming language Scala. It was originally developed by LinkedIn and introduced to the Apache Software Foundation as an open-source project in 2011. Besides this open-source solution, there are also other software projects similar to Kafka on the market like RabbitMQ [200], NATS messaging system [201], or Amazon Kinesis [202]. Kafka's clear strength is its performance and its ability to scale further than all mentioned software projects, so these alternatives are not discussed further in this thesis.

The deployment of the proposed architecture in this thesis requires a Kafka cluster serving one or two medium voltage networks, at least. Hence, the high event density at the Kafka cluster causes probably increasing processing time which in turns leads to undesirable delay by delivering events to the consumer. While such an increasing delay is not critical in other application domains such as social media, it is very crucial when we talk about real time control systems in smart grids. As a result, a benchmark of the open-source stream-processing software platform Apache Kafka for some scenarios in the smart grid is important. To that end, the following two scenarios are considered where the main difference is the intensity of generated events:

1. Energy metering data from households: it is similar to the scenario proposed in [166]. This scenario could be found in the near future with AMI. In this work, it is assumed that the households sent the most current electricity meter reading as soon as 4 Wh have been consumed.

2. Grid monitoring by DSOs: It is based on the needs of a DSO. It is assumed that a DSO monitors its distribution grid by installing a limited number of high quality measuring devices at a certain location in the grid, namely, MPs. Each MP collects data about 114 GSIs. The measured voltage, one of the 114 measured values, is the trigger for transmitted events. If the voltage level exceeds a fixed defined range, an event is triggered. From this point on, events with a resolution of one second are triggered until the voltage level returns to the defined range. Each sent event consists of all 114 GSIs

5.2.1 Apache Kafka

To better understand the benchmark, it is essential to have an overview of the architecture of Apache Kafka and how it works. This overview is given in Figure 5.20.

Kafka, which runs as a cluster on one or multiple servers, stores all published records until the configurable retention period has expired, regardless of whether they have been consumed. In categories called topics, Kafka cluster stores streams of records. The topic is the core abstraction Kafka provides for a stream of records, to which records are published. Topics in Kafka are always multi-subscriber, i. e., a topic can have zero, one, or many consumers that subscribe to the data written to it. A producer publishes a stream of records to one or more Kafka topics. The producers determine to which topic the records should be sent. They also determine which record is to be sent to which partition. Each sent record consists of a key, a value, and a time stamp. A consumer subscribes to one or more topics and processes the stream of records produced to them. Every consumer assigns himself to a consumer group. Each record published on a topic is assigned to exactly one consumer instance per consumer group. In Kafka, the communication between clients and the servers uses a binary protocol over TCP. Kafka needs forcibly a central service that maintains distributed synchronization, naming, and configuration information, which is called ZooKeeper.

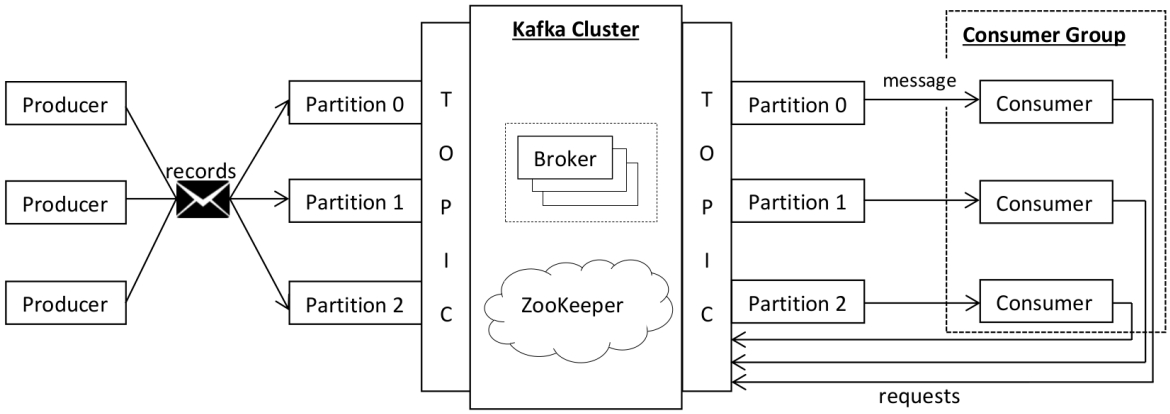

Figure 5.20.: Overview of the Kafka Architecture[11]

5.2.2 Simulation Setup

A simulation framework is built using two simulators, as depicted in Figure 5.21, namely, PowerFactory and OMNET++. With the simulation software PowerFactory, a whole day from a low voltage network with synthetic profiles from [135] is simulated. The simulated day was a working day. In order to realistically map the communication network, many MPs

[11]The figure is drawn by Florian Blaha.

are represented as nodes in OMNET++. They generate events and send them out through an Ethernet network to a Kafka server. Finally, a Kafka producer instance is created for each MP to schedule and send the events. The size of each sent event is equal to $104 + 17\ n$ bytes, where n is the number of GSIs. The embedded data in the event includes two UUIDs for the MP and its location, timestamp, and Kafka header. In parallel, a consumer for each partition is created on the server. It receives the data and measures the Kafka processing time. Studying the communication delay between the server and the consumer is ignored since it can be approximated to the delay between the producer and the server. Appendix A.1 contains more information about the used configuration of the Kafka server, consumers, and producers, the .NED file of the Omnet scenario is included as well.

A simulation of 900 seconds runs on a server with the following specification. The operating system is Ubuntu 16.04.05 LTS, and the available Random Access Memory (RAM) is 128 GB. The server has 20 Central Processing Unit (CPU) with a clock speed of 2.2 GHz each, which leads to 40 due to hyper-threading. As a hard drive, there are two Solid-State-Drives (SSDs) in a Redundant Array of Independent Disks (RAID) configuration mounted. The server is used exclusively for this task, so no other tasks were running in parallel.

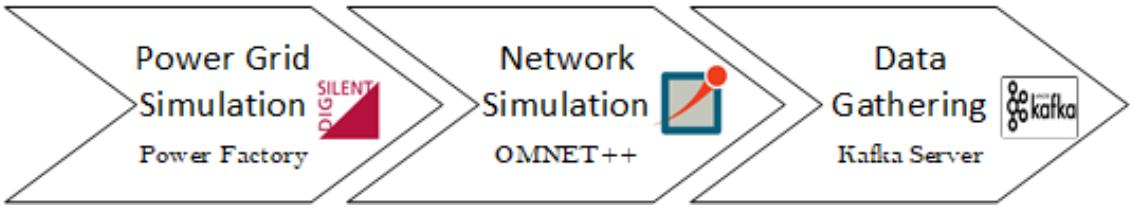

Figure 5.21.: Simulation Setup

Since the idea is to see the ability of Kafka to deal with a big number of synchronized events and process them in a correct way, the number of nodes in the simulation is changed linearly: 6k, 12k, and 18k nodes. Further, three metrics are considered:

- Event density: The number of events per time segment of exactly 3.9 seconds, which is calculated according to the Rice's formula for histograms with the maximum event quantity of 18k smart meters.

- Processing time: The time between the arrival at the Kafka broker and the arrival at the corresponding consumer.

- Transmission delay: The delay artificially generated by OMNET between the Kafka producer and the Kafka server.

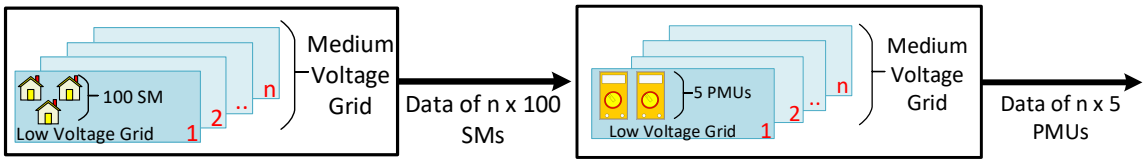

(a) Energy Metering Scenario (b) Grid Monitoring Scenario

Figure 5.22.: Scenarios of Kafka Applications in Smart Grids

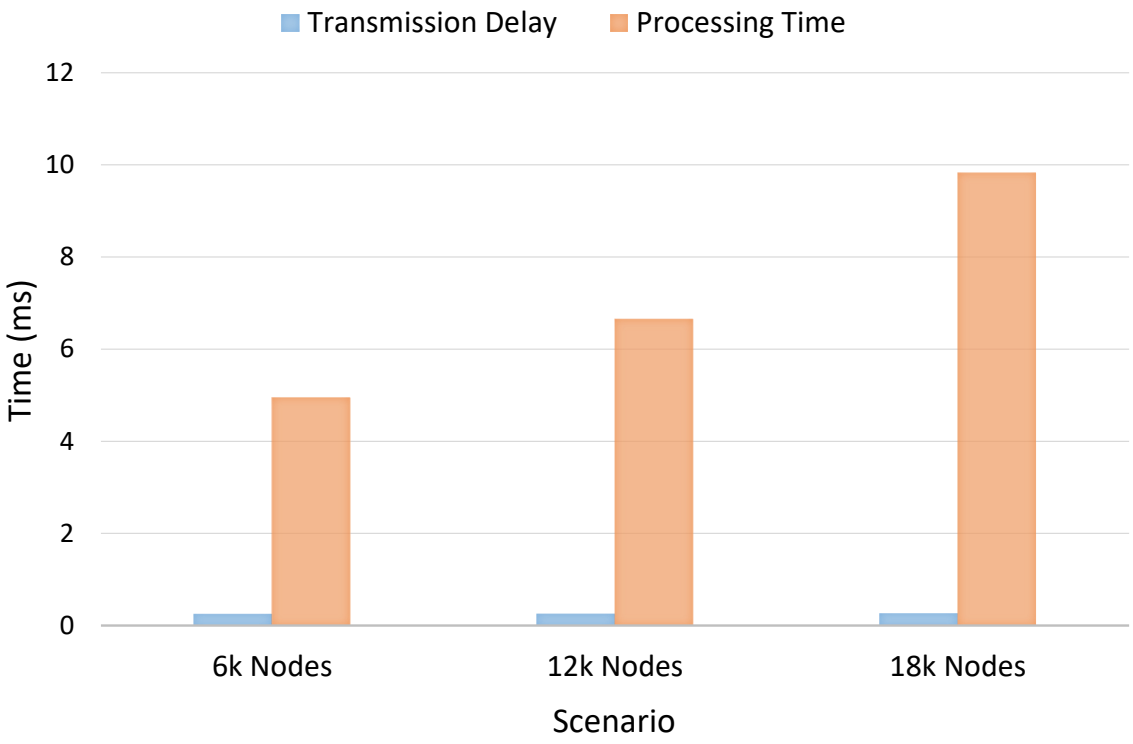

Scenario	Event density		Processing time (ms)		Transmission time (ms)	
	Max	Mean	Mean	CI (95%)	Mean	CI (95%)
6k nodes	1436	550	4.95	0.014	0.25	0.003
12k nodes	2867	1100	6.65	0.018	0.25	0.002
18k nodes	4289	1652	9.82	0.041	0.26	0.002

Table 5.7.: Benchmark of Energy Metering Scenario

5.2.3 Results

5.2.3.1 Energy metering data from households

In this scenario and as depicted in Figure 5.22a, it is assumed that 100 smart meters per low-voltage network are installed, which leads to 6k, 12k and 18k smart meter for 60, 120, and 180 low voltage grids respectively. As depicted in Table 5.7, an almost linear behavior of the Kafka can be observed with a linear increase in smart meters. All average processing times are in a low range of milliseconds and are still far below one second even with the

maximum peak times of individual messages. Further, the average transmission delay is very small in comparison to the processing time.

5.2.3.2 Grid monitoring by the DSO

In this scenario, and as depicted in Figure 5.22b, it is assumed that 5 five high-quality measuring devices are placed in each low-voltage network, and the voltage value is the only event trigger. The event density in this scenario is smaller than the density in the previous scenario. Hence, the processing time at the Kafka is shorter as well. Most of the delay in this scenario is caused by Kafka, where the transmission delay is minimal, see Table 5.8. Similar to the previous scenario, Kafka shows a linear behavior in terms of processing time by increasing the number of nodes linearly.

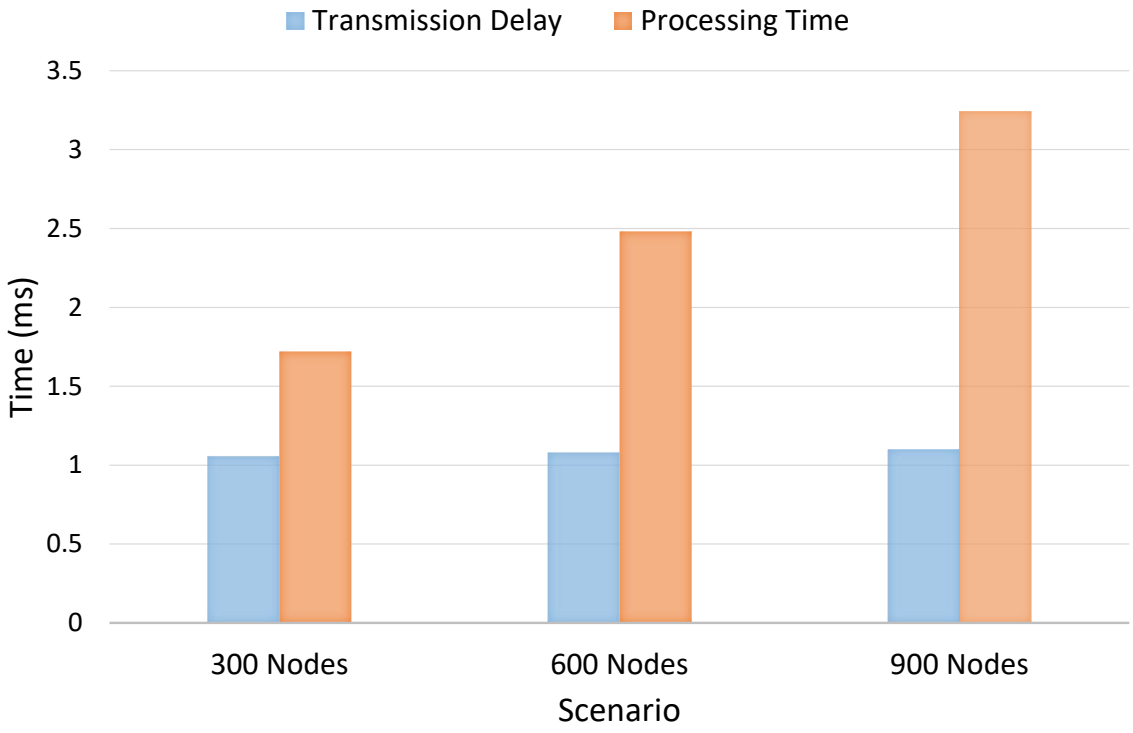

Scenario	Event density		Processing time (ms)		Transmission time (ms)	
	Max	Mean	Mean	CI (95%)	Mean	CI (95%)
300 nodes	26	6.5	1.72	0.091	1.05	0.029
600 nodes	50	12.3	2.48	0.078	1.07	0.022
900 nodes	70	18.3	3.24	0.076	1.09	0.021

Table 5.8.: Benchmark of Grid Monitoring Scenario

5.2.3.3 Discussion

All processing times obtained from the iterations of the two scenarios are in the lower millisecond range, as can be seen in Table 5.7 and Table 5.8. Even outlier times of single

events are far below one second; only 9 ms in the worst case[12]. Such low processing times allow Kafka real-time data collection from the smart grid. Furthermore, the cluster did not show significant changes or any abnormalities of the processing time on the times, when the density of events was increased. However, the processing time is longer than the transmission delay in all test scenarios, which makes the Kafka platform the bottleneck of the proposed architecture in terms of delay.

The tests also showed that the linear increase in the total amount of events resulted in a linear increase in the average processing time of the cluster. Therefore Apache Kafka is sufficiently scalable for this test case. Even an extreme increase in the data size of the individual events has not led to any conspicuities, which shows that Kafka can handle a large number of small events as well as a moderate number of significant events very well.

Based on these factors, it can be concluded that Apache Kafka is very well suited as an ICT platform for gathering event-driven real-time data from the smart grid. The research question is whether the ICT platform Apache Kafka can scale. The answer is yes, and Kafka provides a possible implementation.

5.3 Practical Applicability

The section deals with practical considerations regarding the realization of the proposed smart charging solution in Chapter 4. Thereby, the possible challenges that a real-life implementation of SC might face are introduced. That includes the application scope of the proposed architecture, technical, and regulatory challenges.

5.3.1 Scope of Application

The deployment of a smart charging solution offers the potential for an alternative to regular grid enhancement. Such an alternative can not be only more economical but also more applicable in some cases where the capacity expansion of the distribution grid cannot be realized or can only be realized by incurring high costs. Since the cost of any smart charging solution depends directly on the number of users (CSs connected to the system), such a solution offers a benefit of flexibility over the typical grid upgrades where the overall (high) cost is a fixed initial investment regardless of the number of users involved. This flexibility could be economically beneficial if the proportion of EVs is not increasing as expected/planned. Apart from using the installed ICT infrastructure for charging control, it also could give added value in cases of PQ monitoring, energy theft identification, or additional grid-friendly ancillary services on system-level, like frequency control with local congestion management. Furthermore, such a solution could help to temporize maximum e-mobility in the grid expansion because of the limitation of construction works, i. e., the

[12]IEC 61850 standards obligate 4 ms application layer to application layer delay for the substation automation.

spread of EVs increases too rapidly, so that grid expansion is not feasible in all grids at the same time.

The authors of [203] introduce a detailed analysis of the impact and the cost of deploying the proposed solution. The authors analyze different scenarios and stated that economic grid modernization measures such as a smart charging solution could be preferred by DSOs over a conventional grid expansion in three scenarios:

1. The grids from the 1980s or earlier when the emerging new technologies such as renewable systems and e-mobility are not considered through the planning process: The enhancement of those grids is usually very costly because of the need for excavation and other external services in case of replacing underground cables.

2. The grids with a high density of residential and commercial buildings coupled (probably) to a connection point in urban areas: In this scenario, an extension of the transformer capacity can be problematic and even impossible due to space limitations[13].

3. Unplanned/required grid changes because of unplanned urbanization: For example, a new transformer would have to be installed at a suitable grid point due to the above-average length of the cable. That results in high costs because of the accompanying work, e. g., transformer cabin, a new busbar, and separate access to the medium-voltage network. Worth to mention, smart charging provides more flexibility also in planning urbanization.

In the context of the EU project "ELECTRIFIC"[14], the proposed solution is tested in the field [204] for an old grid (see above). The results show a reduction of 13% in transformer peak loading using FSM-based SC while increasing the power consumption in the valleys, such that the standard deviation of the transformer loading reduces by 44%.

5.3.2 Technical Challenges

The mass deployment of smart charging requires adequate control loops, protocols, technologies, and standards to be adopted concerning:

5.3.2.1 Measurement Infrastructure

Measurement infrastructure is of high value to prove the practical usability of research concepts. However, planning, installing, and operating the measurement infrastructure with the requirement of suitable measurement channels is not trivial and thus consumes quite a lot of time. As a part of the digitalization of the energy transition, Smart Meter Gateway (SMGW) is proposed and examined by the Federal Office for Information Security

[13] https://www.das-doernberg.de/wohnen/e-mobilitaet.html

[14] https://electrific.eu/

in Germany as a secure and privacy-preserved solution for integrating SMs into a communication network [205]. The rollout of SMGW is planned to start soon [206]. Depending on the individual authorization and requirements, that makes it possible to obtain grid data (e. g., current, voltage, frequency) in real-time of the corresponding grid connection point.

Moreover, establishing a suitable data connection (technically and economically) between MPs and a centralized server (e. g., Event engine) has to be considered through setting up a measuring infrastructure. Generally, a mobile data connection is an option, but it is connected to different challenges. Firstly, a suitable network coverage must be available. Secondly, mobile data contracts are costly mainly for end-consumers, whereby the transmission of many measurement data is limited or bound to high costs. In contrast, the benefit of using a Digital Subscriber Line (DSL) solution is that the data volume plays almost no role. Still, a connection to a router with Internet access has to be established not only technically (concerning security, privacy, etc.) but also physically. That is probably associated with excavation work in case of using cables, which results in high costs.

In reality, no MP supports event-driven behavior proposed in Section 4.3[15]. A workaround is developed and tested throughout the EU project "ELECTRIFIC" [5]. The proposed mechanism for data collection can be described as event-based, which means GSI data is processed by "ELECTRIFIC" components as soon as it arrives on a central database. To that end, a Microsoft Windows-based software "WinPQ" fetches GSI values from the measuring devices and stores them in a MySQL database. A Kafka producer monitors all tables and fetches all new records in semi-real-time. Then it writes them on a specific topic in Kafka. A streaming processor is developed that consumes the "raw" GSI data in a time-windowed way and aggregates the data in 30-second averages. The outcome of this process is written to the "metrics" topic in Kafka. Kafka clients (consumers) read the processed data.

During the trial, the proposed workaround guarantees a control loop with an average delay of 30 seconds starting from MP and ending by the reaction of the car.

5.3.2.2 Availability of the Relevant Data

Although the proposed solution in this thesis focuses on the aggregated CS load regardless of the to be charged EVs, distributing the available capacity at the CS among these EVs needs more and more peculiarities to be identified over time. Under certain circumstances, these peculiarities can have a significant influence on the control mechanisms, e. g., the aggregated minimum capacity $\mathscr{C}_i^{min}$. In this regard, the necessary parameters are determined and stored in the DB of the CSP management system. This DB can then be included in the reactions of the SC. Next, the possible categories are explained:

[15] Some well used communication protocols in the domain of IoT assume and support on-event transmission of the data, namely, LoRaWAN and GOOSE.

1. CS Information: It includes the number of installed connectors and their types, as well as the breaking capacity or interrupting rate. Additionally, information about the load management among the active connectors (parallel charging) has to be available, e. g., equal/proportional distribution of the available charging power among all connected vehicles or enabling only one connector at once. Last but not least, the kind of grid connection has to be known either single- or three-phase connection to enable the phase-balancing feature or not.

2. EV Information: Such information is required in order to control each charging operation individually and efficiently, e. g., model, year of manufacture, rectifier type, supported connectors, current SoC, required kilometers, and departure time. The availability of such information allows prioritizing and adjusting the available charging capacity according to both technical EV specifications and requirements of the driver. Moreover, the minimum charging capacity in kW or Ampere per phase must be provided and considered to avoid the interruption or stop of the charging operation by the EV itself.

3. Characteristics of the Battery Management System (BMS): Since the main task of any BMS is the protection of the battery from operating outside the safe operation area, it intervenes through a charging operation in a programmed way to increase/decrease the charging power[16]. Some examples are: the warm-up process of the battery at freezy temperatures, regulation(reduction) of the charging power at too high temperature through charging operation, and a significant change in charging speed, e.g., change from fast to slow charging or slow start mechanisms. As a result, that individual behavior of BMS at specific circumstances should be known to any smart charging algorithm and included in its logic. Furthermore, the degree of battery saturation has to be known as well, where the change from the Constant Current (CC) phase to the Constant Voltage (CV) phase happens. Unfortunately, most of this information is not revealed by manufacturers and needs in-depth analysis of the different BMS integrated with EVs. However, not considering such information will cause inaccuracy or deviation in the behavior of the smart charger from the expected results.

5.3.2.3 Controllability of CSs

Establishing a smart charging solution requires enabling several functions at CS remotely, particularly, meter reading values, CS reservation, and remote power system management actions. The latter includes unlocking the charge plug, managing the CS load, and exchanging the energy contract related data specified in ISO/IEC 15118. Such functions can be

[16] Some BMSs contain integrated PQ-aware system, so it stops/controls the charging operation when harmonics threshold values are exceeded, voltage changes rapidly or phase asymmetry is higher than a predefined threshold. For example, Tesla Model S reduces automatically the charging current by 25% if it detects unexpected fluctuations in input power.

realized either by proprietary or open and interoperable communication protocols. The last-mentioned option allows data to be easily accessed, shared, and collected to improve charging services and plan for infrastructure development, which in turn enables additional energy-related services.

OCPP is one of the most adopted standards by CS manufactures in order to allow CSs and a central management system from different vendors to communicate with each other[17]. Starting from version 1.6, OCPP supports the functions mentioned above besides many others. Further, a new version 2.0 of OCPP was released with new features like a CS load management and phase balancing. Moreover, OCPP can be used with other DR protocols such as OpenADR[208] in order to transform CSs stations into flexible grid resources[209]. Unfortunately, there are currently no CSs in the field, that are providing a native implementation of the OCPP 2.0 protocol, although the standard was released in April 2018. It is difficult to foresee if manufacturers will adopt OCPP 2.0 soon, as most manufacturers waited for a long time (or are still waiting) to implement OCPP 1.6. While OCPP 1.6 is relatively similar to OCPP 1.5 and only introduces the concept of charging profiles, the step to move to OCPP 2.0 is quite a big one.

In the context of the EU project "ELECTRIFC", the author, in collaboration with consortium partners[18] and via direct communication with the manufacturers by 24th of April 2019, obtained a list of CS manufacturers with information about supporting the capacity management and OCPP by their CSs. The list in Table 5.9 shows clearly a significant adoption of the OCPP 1.6 implementing in contemporary and future CSs.

Manufacturer	1.5	1.6	2.0	Note
IES Synergy	✓	✓	In 2020	-
ABL	✓	✓	Ongoing	-
ABB Ltd	✓	✓	In 2020	-
Ensto GmbH	x	x	x	Proprietary load management
Schneider Austria	x	Ongoing	x	Proprietary load management
MENNEKES Elektrotechnik	✓	✓	Ongoing	-
Delta Electronics	x	x	x	Proprietary load management
Swarco AG	x	Ongoing	x	Proprietary load management
EBG compleo	x	Ongoing	x	Proprietary load management
ebee	✓	✓	x	-
Ecotap BV	x	Ongoing	x	Proprietary load management
EVTEC AG	✓	✓	x	-
Tritium Pty Ltd	x	Ongoing	x	-

Table 5.9.: Overview of OCPP Implementation by Main CS Manufacturers in Germany and Austria[5]

[17]OCPP is the de facto network protocol throughout Europe and is used in 78 countries [207].

[18]Particularly has.to.be: https://has-to-be.com

5.3.2.4 Controllability of EVs

Any smart controlling algorithm - either proposed in this thesis or literature- is founded on the ability to make the EV charging use the suggested value by the smart algorithm. Such functionality needs communication between the CSs and EVs. In January 2013, the IEC 62196 Type 2 connector (commonly referred to as MENNEKES) was selected by the European Commission as the official charging plug within the European Union[210]. This connector type enables the required communication via two pins, namely, Proximity Pilot (PP) and Control Pilot (CP), according to standards IEC 61851 and SAE J1772. Thereby, no sophisticated digital signal processors are needed to realize the communication, and it is based on Pulse Width Modulation (PWM).

When the plug is connected, CS stimulates a voltage difference of 12 V on CP as well as on PP. The EV requests a charging state by setting a resistor between the PP and CP wires, according to Table 5.10. With the PWM signal, the CS can define the maximum charging current the EV can drain from the CS. For example, 16% PWM corresponds to 10 A, 25% to 16 A, and 50% to 32 A.

Charging State	Pilot High	Pilot Low	Frequency	Resistance
Not connected	+12 V	-	DC	-
EV connected	+9 V	-12 V	1 kHz	2700 Ω
EV charge	+6 V	-12 V	1 kHz	8800 Ω
Ventilation required	+3 V	-12 V	1 kHz	240 Ω
Error	0 V	0 V	-	-
Unknown/Error	-	-12 V	-	-

Table 5.10.: EV Charging State Requests Using PWM[211]

In [60]*, D. Danner, with a collaboration with the author, carries out PHIL of FSM-SC using a type 2 connector and real EV. As seen in Figure 5.23, the tested real EV follows nearly the simulated power, except during the starting phase which takes some time. Furthermore, D. Danner and et al. state the deviation between the simulation and PHIL happens just when the car reaches its saturation phase and reduces its charging power gradually. That test proves not only the possibility of controlling the charging power at EV but also the need for knowledge about the behavior of BMS, as depicted in Section 5.3.2.2.

5.3.3 Regulatory challenges

According to the German energy legislation[212], EV can be classified in a similar way to heat pumps as a controllable end-use. Hence, it allows DSOs and suppliers to impose reduced network charges for EV charging. In exchange, DSOs are given the right to change consumer demand from controllable loads during fixed on-peak hours, if stress is imposed on the distribution network. Practically, in order to ensure sufficient supply, these tariffs

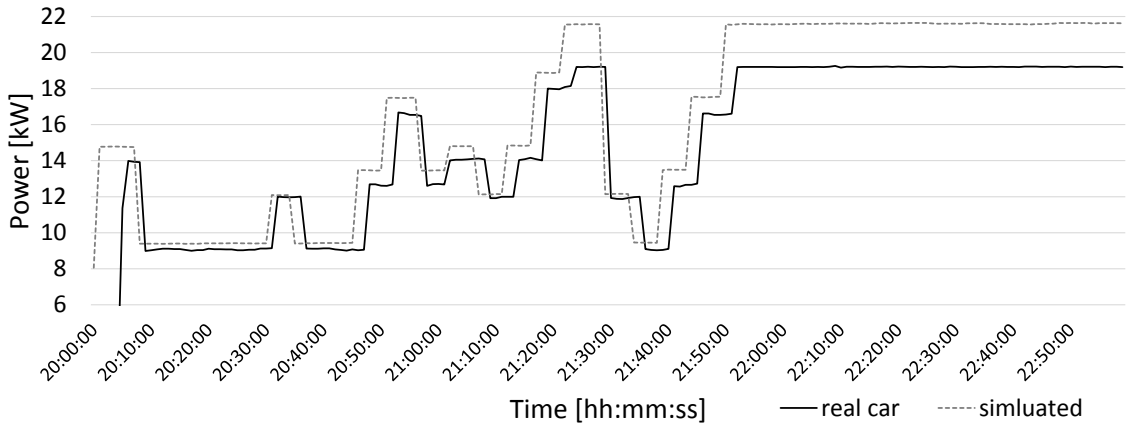

Figure 5.23.: Comparison of the Simulated Charging Signal with the Reaction of a Real Car [60]

allow DSOs to interrupt EV charging during peak hours where appropriate and to return it during off-peak hours. However, a possession of a meter (or smart controller) that can communicate with the DSO and has a function allowing interruption/resuming of charging is a precondition for enabling such a mechanism. In this regard, the proposed architecture in this thesis can play the role of this smart meter, and it can go one step further by determining the times of the required actions automatically through the component "PQ-indicator". In this way, there is no need for a complete switching off (stop) of the charging operation rather a smart power adjustment on the fly.

In Germany, a typical network tariff constitutes 25% of the average consumer's electricity bill, and it consists of three parts: a fixed annual fee ("Grundpreis"), a volumetric fee ("Arbeitspreis"), and a metering charge. The structure of the controllable load tariffs varies in two respects from a standard tariff: the EV owner is not billed any annual fixed charge; additionally, (s)he is set to benefit from a highly discounted volumetric rate throughout the day[50].

Such a solution is inferior, as it does not incentivize the type of flexible consumer behavior that is essential for a low-cost, low-emissions power system. For that sake, a point-based system of incentives can be established (see metric M_8 in Section 5.1.2); thereby, the grid-friendly behavior of an EV user or a CSP can be awarded.

5.4 Summary

In the analysis chapter, first, the simulation setup for the evaluation, including the required data, is described. Then, the assumptions and metrics for the evaluation and comparison of the different smart charging approaches are given, and two cases are described in detail: (1) grid-oriented (2) stakeholder-oriented. After that, the system developed in Chapter 4 is analyzed and results are drawn and compared with centralized and decentralized solutions.

Briefly speaking, the proposed distributed architecture shows the ability to keep the voltage and the transformer loading within the defined thresholds most of the time. It is superior to a decentralized approach and converges to a very rigorous centralized one (in terms of grid friendliness and fairness). Moreover, FSM-based and TCP-like SCs enable - more or less - a fair energy distribution among the active CSs considering the local operating conditions; their results in that terms are very close to the centralized approach, which is supposed to be the fairest.

In terms of QoE and QoG, the results of the distributed controller are very close with a relative advantage of FSM-based SC. Overall, the distributed controllers have a preponderance over the decentralized one. Likewise, the sacrifice introduced by distributed controller to achieve a grid-friendly service in terms of QoE is also small, thereby, about two points have to be given away to increase QoG by one.

Generally, Phase based SC allocates more total power to CS in comparison to an equal demand distribution on three phases. But a cost has to be paid where the local voltage imbalance factor becomes higher but stays in the allowed range.

Moreover, a separate analysis of Apache Kafka's performance proves its suitability as an ICT platform for gathering event-driven real-time data from the smart grid. It is scalable, and the total delay of an event, including generation, processing and consuming times, is less than 10 ms.

Finally, an in-depth analysis of the applicability of the proposed system shows the main requirements, challenges, and opportunities for a wide deployment of such a system, including the availability of required data, the controllability of CSs, the controllability of EVs, and the opportunity for incentivizing the user according to the currently applied regulations. However, PHIL shows the ability of the proposed system to control a real EV using type 2 connector in order to respond to control signals appropriately. Moreover, results from deploying the system, in reality, appears the benefit of the system on responding to unforeseen PQ issues in the grid.

6 Conclusion and Future Work

The expected high penetration of EVs in the future causes a painstaking search of grid operators for applicable, cost-effective, user-friendly, and grid-friendly smart solutions as well. This thesis introduces a novel distributed grid-friendly smart charging architecture and its evaluation in different uses cases. In this chapter, the results of this thesis are discussed, and possible future work is provided.

6.1 Outcomes and Main Results

In this thesis, a new definition of the concept "grid-friendly" charging is introduced as the sum of measurable reactions of a CS on critical levels of PQ parameters. Thereby, the demands of a set of installed CSs in a low voltage grid serve as additional flexibility sources to DSOs. While the grid concerns are prioritized over the user's one, the grid-friendly behavior of EV users is awarded using a point-based system of incentives. Thereby, the grid-friendly points can be exchanged to money based on a previously agreed contract(scheme) among DSOs, CSPs, and EV users. The author argues that the existing smart charging solutions ignore implementing such a concept in combination with other design requirements, such as enhancing the PQ, the solution interoperability, and the separation of concerns of the main stakeholders. This conclusion is a direct result of both a classification of the existing EV smart approaches and an analysis of the main factors for developing an EV smart charging approach, that are carried out throughout this thesis.

First, the four different means of controlling an EV charging system are identified, namely, location, real power control, power factor correction, and phase balancing. The analysis via simulation shows that the impact of a CS is not only local but can propagate to neighboring nodes and even to distant parts of the grid in different ways and values. Subsequently, the problem of providing a fair and grid-friendly charging service is formulated as a linear optimization problem.

Afterward, a scalable distributed smart charging architecture is proposed for the sake of meeting different design requirements, specifically, grid-friendliness. It enables a smart adjustment of the used charging capacity based on unpredictable events in the grid to enhance the grid stability and avoid the activation of contingency measures. Thus, the grid status is indicated as critical, not optimal, and optimal. For sending control signals to CSs, an open standard OCPP is used, which enables increasing the interoperability of the solution. The modular design of the proposed architecture is adopted to support the separation of

concerns of the main stakeholders in the EV ecosystem, so the notification mechanism about grid status is separated from the actuating mechanism. Moreover, the publish/subscribe messaging pattern, used as a part of the architecture, enables an efficient and well-performing communication scheme among the different components.

A developed black box so-called "PQ-Indicator" configured by DSOs notifies events using real-time data. Precisely, such collected data focus on the parameters of the power quality in the low voltage grid, particularly the voltage, phase imbalance, as well as the loading of the transformer. The hierarchical design of the "PQ-Indicator" supports extensibility to include more further grid concerns such as harmonics. Furthermore, the PQ-Indicator estimates the status of each phase individually.

In order to respond to the aforementioned generated indications, two smart controllers are developed in this work. The first, FSM-based SC, is based on fuzzy logic. The second, TCP-like SC, is inspired by the slow-start mechanism used in TCP to control congestion in computer networks. The smart controller avoids rapid changes in the charging power, and rather, subtle adjustments are carried out. On one hand, that keeps off the automatic disconnection by the car because of protection measures integrated into the BMS of the car. On the other hand, it reduces the number and the amount of unnecessary changes.

Additionally, different TMMs among active SCs are proposed and discussed. The goal is to reduce the ping-pong effect and to take into account the available flexibility at the CS by each made reaction. Through the evaluation, different strategies for timing management might be necessary depending on system priorities. While periodical reactions of the SC every 5 minutes allocate more power to CSs, the fairness is worse in comparison to a sophisticated TMM, which takes into account the ability of the CS to react to a particular event.

In addition to a small scale trial in reality to show the applicability of the proposed solution, an in-depth evaluation of the introduced architecture is carried out via simulation. Thereby, a real topology of a low voltage grid is used with suitable load and generation profiles. Moreover, eight metrics are defined to analyze the different sides of the proposed system. Further, two test cases are considered: (1) A static test case using a fixed charging rate for the whole day. (2) A dynamic test case using real mobility data from public charging stations. The former is used to show clearly the impact of the proposed solution on the considered grid parameters apart from the users ' satisfaction. The latter test case focuses more on the satisfaction of the different stakeholders of the system.

The proposed system shows excellent results in terms of voltage control and avoiding transformer loading. It is even better than a decentralized mechanism considering only the local voltage and OLTC-based solution. Additionally, it converges to the solution of a centralized controller. Moreover, the evaluation shows the ability of the proposed solution to increase obviously the consumed energy by a CS installed at a critical point - by about

two times in comparison to a scenario without phase-based controlling - with keeping the voltage phase imbalance within the limits determined by EN 50160 standard. In terms of fairness, FSM-based and TCP-like SCs enable - more or less - a fair energy distribution among the active CSs considering the local operating conditions; Their results in that terms are very close to the centralized approach, which is supposed to be the fairest. Furthermore, the analysis shows that the sacrificing of a part of user satisfaction is required to make the grid operator satisfied as well. As a result, an EV user has to be awarded by DSO indirectly through its CSP for its grid-friendly behavior. To that end, a point-based reward system is proposed in this thesis, precisely, GF points. In that regard, FSM-based SC, which is superior to all other controllers in terms of QoE, QoG, has to lose the fewer percents of QoE to achieve one percent of QoG less (only 1.5 points). The advantage of FSM-based SC is relatively small in comparison to TCP-like SC. The total gathered GF points are positive only by the distributed controllers, and it is very close to the total number collected by the centralized approach.

Finally, a benchmark of Kafka architecture is performed using the simulation to show the suitability of the proposed data collection solution in terms of event delay (transmission + processing) measured between a MP and a smart controller. The simulation shows that a Kafka-based solution ensures a delay of less than one 10 ms through different smart grid scenarios, i. e., Kafka can be used, in addition to many other similar solutions, without big concerns regarding both the events management and the scalability of the solution.

6.2 Future Work

Regarding concrete future work, there are several further possible improvements with the proposed architecture given in this thesis, that are listed in the following:

1. **Considering more PQ issues:** The current design of the introduced indication mechanism (precisely, the design of "PQ-Indicator") considers only the voltage and the transformer load. On one hand, they are the main concerns of any grid operator in low voltage grids because of their critical impact on the total grid stability. On the other hand, the existing CSs in the market support only active power control, which allows both issues above to be resolved more efficiently in comparison to other grid issues.

   New PQ issues like harmonics and load-frequency control (secondary) can be easily considered by adding new criteria to the hierarchical logic of "PQ-Indicator". While dealing with harmonics is ignored in this work since the co-simulation environment

does not support such functionality[1], frequency control is carried out through a demand-side frequency response where an elastic demand can be controlled to provide frequency response. That is exactly similar to what is done by the proposed architecture.

Moreover, the implementation of customized SC reactions based on the forwarded information by "PQ-Indicator" about the most influencing PQ parameters would be interesting as well. In such a way, CSs could choose the most appropriate parameters for responding to the received signal[2]. That will allow considering the technical differences among CSs. For example, the voltage control can also be carried out using reactive power control, but the power loss will be higher.

2. **Dynamic configuration of "PQ-Indicator" instead of a static approach:** It is assumed that the thresholds of the different GSIs are set by DSO based on standards, e. g., EN 50160, and knowledge about the grid extracted through analyzing historical data. However, this assumption is valid and has no significant impact on the performance of the proposed architecture. Still, a dynamic configuration will add a different level of smartness to the solution and save a lot of time and effort. A statistical analysis of the measured data can help by building a model to summarize understanding of what impact controlling has the charging behavior on the different grid points, as done in Chapter 3, e. g., the relationship between the voltage and the distance from the transformer. Further, predictive analytics can be employed to run scenarios that will guide future actions.

3. **Bidirectional power flow**: Apart from the degradation of battery life and the overall efficiency of sending energy to and from the grid, V2G offers technical benefits to the power grid through storage. V2G has a comparatively low cost and a high potential power capacity, it can react fast, and thereby it allows different types of power market to be served[213].

   Although the power flow in this thesis is restricted to only G2V direction, the proposed solution can be extended by a new set of the possible reactions of SC, enabling V2G technology. Those new reactions are beyond decreasing/increasing the used active power. For example, a hierarchical decision mechanism can be implemented in SC logic. Indeed, SC decides on the first level based on the current SoC and the departure time of EV if it continues charging or starts discharging the battery. In the second level, a decision about the amount of used power can be made. In such a way, some connected EVs can inject energy back to the grid to be used by another EV, which has an earlier leaving deadline.

[1] PowerFactory offers the function of harmonics analysis, but the interface to Lablink is missing. To the best of the author, this functionality is not supported by other co-simulators as well.

[2] The six different control parameters of CS ($p^a, p^b, p^c, q^a, q^b, q^c$) are discussed thoroughly in Chapter 3.

4. **Define an appropriate business model including price scheme:** In contrast to cars with a combustion engine, EVs have a bilateral relationship with their charging infrastructure. Additionally, the electricity plug, “The pump”, is shared with other types of demand, such as the demands of households, buildings, and industries. As a result, business case and pricing/revenue models of traditional cars are, in a way, straightforward. Contrariwise, the new and dynamic interconnection across a different ecosystem of EVs requires new models of business, and thereby, many barriers can affect EVs, smart charging pricing, and revenue models.

   Complexities of such models arise, however, if and when smart charging diffuses across society and enters the private consumer market. Therefore, testing the proposed solution with different incentive schemes - precisely, price and grid-friendliness - would be interesting. That might need enhancing and improving the metrics defined in Section 5.1.2 regarding the satisfaction of the different stakeholders.

A Appendix

A.1 Benchmark Kafka

In order to use Apache Kafka as the architecture for event-based real time data necessary for our assumed scenarios, some precautions and settings need to be taken. For example, Kafka offers the possibility that producers can accumulate individual messages and combine them into larger batches and then sending them as a single message. Batching is also used by default, as it represents a massive performance gain. To ensure Kafka as event-driven architecture, batching must be completely deactivated. Also the consumers work with batching, which must also be deactivated. Moreover, producers send without waiting for acknowledgment, since it results by far in the best performance and therefore the events arrive at the broker very soon after the trigger. In addition to the configurations for the Kafka producer and Kafka consumer, the configurations for the Kafka broker also play a central role. Since the benchmark is conducted on a single server, a single broker is also used. The configuration file of Kafka server with the used values is stated as follows:

```
broker.id=0
auto.create.topics.enable=true
num.network.threads=6
num.io.threads=16
socket.send.buffer.bytes=102400
socket.receive.buffer.bytes=102400
socket.request.max.bytes=104857600
log.dirs=tmp/kafka-logs
num.partitions=10
num.recovery.threads.per.data.dir=1
offsets.topic.replication.factor=1
transaction.state.log.replication.factor=1
transaction.state.log.min.isr=1
log.retention.hours=168
log.segment.bytes=1073741824
log.retention.check.interval.ms=300000
zookeeper.connect=localhost:2181
zookeeper.connection.timeout.ms=6000
group.initial.rebalance.delay.ms=0
```

Also, the .NED file describing Omnet scenario is shown below:

```
network Scenario
parameters:
      int numAMI;
      int numKafka;
      int numSubnet = (numAMI/500)+1;
      @display("bgb=925,510");
types:
      channel DSL extends DatarateChannel
       delay = 0ms;
       datarate = 5Mbps;
submodules:
      configurator: IPv4NetworkConfigurator
       parameters:
        @display("p=38,31");
     ami[numAMI]: StandardHost
       @display("p=55,251");
      kafkarouter: Router;
      kafka[numKafka]: StandardHost;
      subNet[numSubnet]: InternetCloud;
      internet: InternetCloud;
connections:
      // Connection Kafka server
      kafkarouter.pppg++ <–> Eth1G <–> internet.pppg++;
      for i=0..numKafka-1
       kafka[i].ethg++ <–> Eth1G <–> kafkarouter.ethg++;
      for i=0..numAMI-1
        ami[i].pppg++ <–> DSL <–> subNet[i/500].pppg++;
      for i=0..numSubnet-1
       subNet[i].pppg++ <–> Eth1G <–> internet.pppg++;
```

Bibliography

[1] J. Delgado, R. Faria, P. Moura, and de A. Almeida. “Impacts of plug-in electric vehicles in the portuguese electrical grid.” In: ***Transportation Research Part D: Transport and Environment*** 62 (2018), pp. 372–385. issn: 1361-9209. doi: https://doi.org/10.1016/j.trd.2018.03.005.

[2] M. Manbachi, A. Sadu, H. Farhangi, et al. “Impact of EV penetration on Volt–VAR Optimization of distribution networks using real-time co-simulation monitoring platform.” In: ***Applied Energy*** 169 (2016), pp. 28–39. doi: https://doi.org/10.1016/j.apenergy.2016.01.084.

[3] N. Leemput, F. Geth, J. Van Roy, et al. “MV and LV residential grid impact of combined slow and fast charging of electric vehicles.” In: ***Energies*** 8.3 (2015), pp. 1760–1783. doi: https://doi.org/10.3390/en8031760.

[4] J. Shen, C. Jiang, and B. Li. “Controllable load management approaches in smart grids.” In: ***Energies*** 8.10 (2015), pp. 11187–11202. doi: https://doi.org/10.3390/en81011187.

[5] ELECTRIFIC. ***D4.3 - Release of the Final Local Grid Management and Data Aggregation and its Description***. Tech. rep. Accessed on 2nd of March 2020. 2019. url: https://cordis.europa.eu/project/id/713864/results.

[6] M. Sterner, F. Eckert, M. Thema, and F. Bauer. “Der positive Beitrag dezentraler Batteriespeicher für eine stabile Stromversorgung.” In: ***Forschungsstelle Energienetze und Energiespeicher (FENES) OTH Regensburg, Kurzstudie im Auftrag von BEE eV und Hannover Messe, Regensburg/Berlin/Hannover*** (2015). Accessed on 20th of March 2020. url: https://www.bee-ev.de/fileadmin/Publikationen/BEE_HM_FENES_Kurzstudie_Der_positive_Beitrag_von_Batteriespeichern_2015.pdf.

[7] P. Danner, W. Duschl, D. Danner, A. Alyousef, and H. de Meer. “Flexibility Reward Scheme for Grid-Friendly Electric Vehicle Charging in the Distribution Power Grid.” In: ***Proceedings of the 3th Workshop on Electric Vehicle Systems, Data, and Applications***. EV-Sys ’18. New York, NY, USA: ACM, 2018. doi: https://doi.org/10.1145/3208903.3213893.

[8] D. Danner, A. Alyousef, P. Danner, W. Duschl, and H. de Meer. “Towards Grid-Friendly Electric Vehicle Charging: Architectural Concept and Field Trials.” In: ***3rd e-mobility power System integration Symposium***. Dublin, Republic of Ireland, 2019. url: https://mobilityintegrationsymposium.org/wp-content/uploads/sites/16/2019/10/3A_1_EMOB19_220_Presentation_Dominik_Danner_WEB.pdf.

[9] IEA Global EV Outlook. “to Electric Mobility.” In: ***IEA: Paris, France*** (2019). Accessed on 20th of March 2020. url: https://webstore.iea.org/global-ev-outlook-2019.

[10] IEA Global EV Outlook. “to Electric Mobility.” In: ***IEA: Paris, France*** (2018). Accessed on 20th of March 2020. url: https://webstore.iea.org/global-ev-outlook-2018.

[11] A. Adepetu, A. Alyousef, S. Keshav, and H. de Meer. “Comparing Solar Photovoltaic and Battery Adoption in Ontario and Germany: An Agent-Based Approach.” In: ***Energy Informatics*** 1.1 (2018), p. 6. issn: 2520-8942. doi: https://doi.org/10.1186/s42162-018-0012-8.

[12] A. Alyousef, A. Adepetu, and H. de Meer. “Analysis and Model-Based Predictions of Solar PV and Battery Adoption in Germany: An Agent-Based Approach.” In: ***Computer Science - Research and Development (CSRD)*** 32.1 (2017), pp. 211–223. issn: 1865-2042. doi: https://doi.org/10.1007/s00450-016-0304-9.

[13] KIT: Karlsruher Instituts für Technologie. ***Strompreise steigen bis 2025 um 70 Prozent***. Acccessed on 26th of April 2020. 2012. url: https://www.welt.de/newsticker/dpa_nt/infoline_nt/wirtschaft_nt/article106310056/Strompreise-steigen-bis-2025-um-70-Prozent.html.

[14] AECOM. ***Energy Storage Study***. Acccessed on 26th of April 2020. 2015. url: https://arena.gov.au/assets/2015/07/AECOM-Energy-Storage-Study.pdf.

[15] Fraunhofer. ***Current and Future Cost of Photovoltaics***. Acccessed on 26th of April 2020. 2015. url: https://www.ise.fraunhofer.de/content/dam/ise/de/documents/publications/studies/AgoraEnergiewende_Current_and_Future_Cost_of_PV_Feb2015_web.pdf.

[16] L. Held, H. Krämer, M. Zimmerlin, et al. “Dimensioning of battery storage as temporary equipment during grid reinforcement caused by electric vehicles.” In: ***2018 53rd International Universities Power Engineering Conference (UPEC)***. 2018, pp. 1–6. doi: 10.1109/UPEC.2018.8542035.

[17] A. Stray, O. Clarke, D. Harvey, and O. Clarke. ***Electric vehicles and the digital revolution: an evolving legal landscape***. Accessed on 20th of March 2020. 2018. url: https://www.intelligenttransport.com/transport-articles/69187/evs-digital-revolution-legal/.

[18] M. Longo, D. Zaninelli, F. Viola, et al. “Recharge stations: A review.” In: ***2016 Eleventh International Conference on Ecological Vehicles and Renewable Energies (EVER)***. 2016, pp. 1–8. doi: 10.1109/EVER.2016.7476390.

[19] ***E.ON grids will be upgraded for 100 percent e-mobility***. Accessed on 20th of March 2020. 2019. url: https://www.eon.com/en/about-us/media/press-release/2019/eon-board-member-thomas-koenig-presents-new-study.html.

[20] Netzbetrieb im VDE (FNN) Forum Netztechnik. ***Versorgungszuverläessigkeit und Spannungsqualität in Deutschland***. Acccessed on 10th of March 2020. 2013. url: https://www.vde.com/resource/blob/824912/2a9a511f3dd6da0e5c00dab2d4db4398/fnn-fakten-versorgungsqualitaet-2013-03-11-1-data.pdf.

[21] EN Standard. “50160.” In: ***Voltage characteristics of public distribution systems*** (2010), p. 18.

[22] K. Kumar and G. B. Kumbhar. “A review on impact of distributed generation and electrical vehicles on aging of distribution transformer.” In: ***2017 3rd International Conference on Condition Assessment Techniques in Electrical Systems (CATCON)***. 2017, pp. 283–288. doi: https://doi.org/10.1109/CATCON.2017.8280229.

[23] E. Ucer, M. C. Kisacikoglu, M. Yuksel, and A. C. Gurbuz. “An Internet-Inspired Proportional Fair EV Charging Control Method.” In: ***IEEE Systems Journal*** (2019), pp. 1–11. issn: 1932-8184. doi: https://doi.org/10.1109/JSYST.2019.2903835.

[24] O. Ardakanian, C. Rosenberg, and S. Keshav. “Distributed control of electric vehicle charging.” In: ***Proceedings of the fourth international conference on Future energy systems***. ACM. 2013, pp. 101–112. doi: https://doi.org/10.1145/2487166.2487178.

[25] L. Mingming and M. Seán. “Enhanced AIMD-based decentralized residential charging of EVs.” In: ***Transactions of the Institute of Measurement and Control*** 37.7 (2015), pp. 853–867. doi: https://doi.org/10.1177/0142331213494100.

[26] P. Dowell. “Effects of eddy currents in transformer windings.” In: ***Proceedings of the Institution of Electrical Engineers***. Vol. 113. 8. IET. 1966, pp. 1387–1394.

[27] M. El-Hawary. ***Introduction to electrical power systems***. Vol. 50. John Wiley & Sons, 2008. isbn: 9780470411377. doi: https://doi.org/10.1002/9780470411377.

[28] IEC Standard Voltages. “IEC Standard IEC 60038.” In: ***Ed*** (2009).

[29] C. Dugan, F. McGranaghan, H. Beaty, and S. Santoso. ***Electrical power systems quality***. Vol. 2. Accessed on 2nd of March 2020. mcgraw-Hill New York, 1996. url: https://www.academia.edu/4111736/Electrical_Power_Systems_Quality_Second_Edition_Roger_C_Dugan.

[30] H. Markiewicz and A. Klajn. ***Power Quality Application Guide, Voltage Characteristic of Public Distribution System***. Accessed on 2nd of March 2020. 2004. url: http://copperalliance.org.uk/uploads/2018/03/542-standard-en-50160-voltage-characteristics-in.pdf.

[31] M. Wanik. “Harmonic Measurement and Analysis during Electric Vehicle Charging.” In: ***Engineering*** 05 (Jan. 2013), pp. 215–220. doi: https://doi.org/10.4236/eng.2013.51B039.

[32] Nicole Woodman, Robert B Bass, and Mike Donnelly. “Modeling Harmonic Impacts of Electric Vehicle Chargers on Distribution Networks.” In: ***2018 IEEE Energy Conversion Congress and Exposition (ECCE)***. IEEE. 2018, pp. 2774–2781. doi: https://doi.org/10.1109/ECCE.2018.8558207.

[33] A. Von Meier. ***Electric power systems: a conceptual introduction***. John Wiley & Sons, 2006. isbn: 978-0-471-17859-0.

[34] “Electromagnetic compatibility (EMC) - Part 3-2: Limits - Limits for harmonic current emissions.” In: ***IEC 61000-3-2:2018*** (2018).

[35] D. Chapman. ***Power Quality Application Guide, The cost of Poor Power Quality***. Accessed on 2nd of March 2020. 2001. url: http://copperalliance.org.uk/uploads/2018/03/21-the-cost-of-poor-power-quality.pdf.

[36] M. Lee, O. Aslam, B. Foster, et al. “Assessment of demand response and advanced metering.” In: ***Federal Energy Regulatory Commission, Tech. Rep*** (2013). Acccessed on 10th of March 2020. url: https://www.ferc.gov/legal/staff-reports/12-08-demand-response.pdf.

[37] M. Sánchez-Jiménez. ***European technology platform SmartGrids–Vision and strategy for Europes electricity networks of the future***. Accessed on 2nd of March 2020. 2010. url: https://ec.europa.eu/research/energy/pdf/smartgrids_en.pdf.

[38] Alexander Schuller. “Electric vehicle charging coordination-economics of renewable energy integration.” In: ***Ph.D. dissertation, Institute of Information Systems and Marketing (IISM)*** (2013).

[39] S. Ramchurn, P. Vytelingum, A. Rogers, and R. N. Jennings. “Putting the" smarts" into the smart grid: A grand challenge for artificial intelligence.” In: ***Communications of the ACM*** 55.4 (2012), pp. 86–97. doi: https://doi.org/10.1145/2133806.2133825.

[40] S. E. de Lucena. “A Survey on Electric and Hybrid Electric Vehicle Technology.” In: ***Electric Vehicles***. Ed. by Seref Soylu. Rijeka: IntechOpen, 2011. Chap. 1. doi: https://doi.org/10.5772/18046.

[41] J. Larminie and J. Lowry. ***Electric vehicle technology explained***. John Wiley & Sons, 2012. isbn: 9781118361146. doi: https://doi.org/10.1002/9781118361146.

[42] D. Naunin. ***Hybrid-, Batterie-und Brennstoffzellen-Elektrofahrzeuge: Technik, Strukturen und Entwicklungen; mit 8 Tabellen***. Kontakt & Studium. expert-Verlag, 2004. isbn: 9783816924333. url: https://books.google.de/books?id=FkK8AQAACAAJ.

[43] batteryuniversity. ***BU-1003a: Battery Aging in an Electric Vehicle (EV)***. Acccessed on 10th of March 2020. 2019. url: https://batteryuniversity.com/learn/article/bu_1003a_battery_aging_in_an_electric_vehicle_ev.

[44] R. Mackiewicz. “Overview of IEC 61850 and Benefits.” In: ***2006 IEEE Power Engineering Society General Meeting***. IEEE. 2006, 8–pp. doi: https://doi.org/10.1109/PSCE.2006.296392.

[45] P. Richardson, D. Flynn, and A. Keane. “Impact assessment of varying penetrations of electric vehicles on low voltage distribution systems.” In: ***Power and Energy Society General Meeting, 2010 IEEE***. IEEE. 2010, pp. 1–6. doi: https://doi.org/10.1109/PES.2010.5589940.

[46] G. Mauri and A. Valsecchi. “Fast charging stations for electric vehicle: The impact on the MV distribution grids of the Milan metropolitan area.” In: ***Energy Conference and Exhibition (ENERGYCON), 2012 IEEE International***. IEEE. 2012, pp. 1055–1059. doi: https://doi.org/10.1109/EnergyCon.2012.6347725.

[47] M. Alonso, H. Amaris, J. Germain G., and J. M. Galan. “Optimal charging scheduling of electric vehicles in smart grids by heuristic algorithms.” In: ***Energies*** 7.4 (2014), pp. 2449–2475. doi: https://doi.org/10.3390/en7042449.

[48] L. Zhaoxi, W. Qiuwei, L. Christensen, A. Rautiainen, and X. Yusheng. “Driving pattern analysis of Nordic region based on National Travel Surveys for electric vehicle integration.” In: ***Journal of Modern Power Systems and Clean Energy*** 3.2 (2015), pp. 180–189. doi: https://doi.org/10.1007/s40565-015-0127-x.

[49] L. Hui-ling, B. Xiao-min, and T. Wen. “Impacts of plug-in hybrid electric vehicles charging on distribution grid and smart charging.” In: ***Power System Technology (POWERCON), 2012 IEEE International Conference on***. IEEE. 2012, pp. 1–5. doi: https://doi.org/10.1109/PowerCon.2012.6401265.

[50] ***Innovation landscape brief: Electric-vehicle smart charging***. Accessed on 12th of March 2020. url: https://www.raponline.org/wp-content/uploads/2019/03/rap-start-with-smart-ev-integration-policies-2019-april-final.pdf.

[51] EU Regulation. “setting emission performance standards for new passenger cars as part of the Communitys integrated approach to reduce CO2 emissions from light-duty vehicles.” In: ***J. Eur. Union*** 140 (2009). Accessed on 2nd of March 2020, pp. 5–6. url: https://eur-lex.europa.eu/legal-content/EN/TXT/PDF/?uri=CELEX:32009R0443&from=EN.

[52] D. P. Tuttle, R. L. Fares, R. Baldick, and M. Webber. “Plug-in vehicle to home (V2H) duration and power output capability.” In: ***Transportation Electrification Conference and Expo (ITEC), 2013 IEEE***. IEEE. 2013, pp. 1–7. doi: https://doi.org/10.1109/ITEC.2013.6574527.

[53] G. Haines, A. McGordon, P. Jennings, and N. Butcher. “The Simulation of Vehicle-to-Home SystemsUsing Electric Vehicle Battery Storage to Smooth Domestic Electricity Demand.” In: ***Proc. Ecologic Vehicles/Renewable Energies - EVRE*** (Jan. 2009).

[54] C. Liu, K. Chau, D. Wu, and S. Gao. “Opportunities and Challenges of Vehicle-to-Home, Vehicle-to-Vehicle, and Vehicle-to-Grid Technologies.” In: ***Proceedings of the IEEE*** 101.11 (2013), pp. 2409–2427. doi: https://doi.org/10.1109/JPROC.2013.2271951.

[55] K. M. Tan, k. V. Ramachandaramurthy, and J. Y. Yong. “Integration of electric vehicles in smart grid: A review on vehicle to grid technologies and optimization techniques.” In: ***Renewable and Sustainable Energy Reviews*** 53 (2016), pp. 720–732. doi: https://doi.org/10.1016/j.rser.2015.09.012.

[56] U. B. Baloglu and Y. Demir. “Economic analysis of hybrid renewable energy systems with V2G integration considering battery life.” In: ***Energy Procedia*** 107 (2017), pp. 242–247. doi: https://doi.org/10.1016/j.egypro.2016.12.140.

[57] P. Pani, A. Athreya, A. Panday, H. Bansal, and H. Agrawal. “Integration of the vehicle-to-grid technology.” In: ***Energy Economics and Environment (ICEEE), 2015 International Conference on***. IEEE. 2015, pp. 1–5. doi: https://doi.org/10.1109/EnergyEconomics.2015.7235108.

[58] C. Battistelli, L. Baringo, and A. Conejo. “Optimal energy management of small electric energy systems including V2G facilities and renewable energy sources.” In: ***Electric Power Systems Research*** 92 (2012), pp. 50–59. doi: https://doi.org/10.1016/j.epsr.2012.06.002.

[59] J. D. Bishop, C. Axon, D. Bonilla, et al. “Evaluating the impact of V2G services on the degradation of batteries in PHEV and EV.” In: ***Applied energy*** 111 (2013), pp. 206–218. doi: https://doi.org/10.1016/j.apenergy.2013.04.094.

[60] A. Alyousef, D. Danner, F. Kupzog, and H. de Meer. “Enhancing Power Quality in Electrical Distribution Systems Using a Smart Charging Architecture.” In: ***Proceedings of the 7th DACH+ Conference on Energy Informatics***. Vol. 1. Best Paper Award. 2018, p. 28. doi: https://doi.org/10.1186/s42162-018-0027-1.

[61] S. Abishek and B. Narayanaswamy. “Congestion control of smart distribution grids using state estimation.” In: ***2013 Fifth International Conference on Communication Systems and Networks (COMSNETS)*** (2013), pp. 1–6. doi: https://doi.org/10.1109/COMSNETS.2013.6465596.

[62] F. Kong, X. Liu, Z. Sun, and Q. Wang. “Smart rate control and demand balancing for electric vehicle charging.” In: ***Proceedings of the 7th International Conference on Cyber-Physical Systems***. IEEE Press. 2016, p. 4. doi: https://doi.org/10.1109/ICCPS.2016.7479118.

[63] P. Bahrevar and M. Esmaili. “Optimal Charging Strategy of Electric Vehicles in Unbalanced Three-Phase Distribution Network.” In: ***Indian Journal of Science and Technology*** 9.S1 (2016). doi: https://doi.org/10.1109/TPWRS.2014.2318293.

[64] P. Richardson, D. Flynn, and A. Keane. “Optimal charging of electric vehicles in low-voltage distribution systems.” In: ***IEEE Transactions on Power Systems*** 27.1 (2012), pp. 268–279. doi: https://doi.org/10.1109/TPWRS.2011.2158247.

[65] K. Zhang, L. Xu, M. Ouyang, et al. “Optimal decentralized valley-filling charging strategy for electric vehicles.” In: ***Energy conversion and management*** 78 (2014), pp. 537–550. doi: https://doi.org/10.1016/j.enconman.2013.11.011.

[66] Q. Wang, X. Liu, J. Du, and F. Kong. “Smart charging for electric vehicles: A survey from the algorithmic perspective.” In: ***IEEE Communications Surveys & Tutorials*** 18.2 (2016), pp. 1500–1517. doi: https://doi.org/10.1109/COMST.2016.2518628.

[67] J. C. Mukherjee and A. Gupta. “A Review of Charge Scheduling of Electric Vehicles in Smart Grid.” In: ***IEEE Systems Journal*** 9.4 (2015), pp. 1541–1553. doi: https://doi.org/10.1109/JSYST.2014.2356559.

[68] N. Chen, T. Quek, and C. W. Tan. “Optimal charging of electric vehicles in smart grid: Characterization and valley-filling algorithms.” In: ***Smart Grid Communications (SmartGridComm), 2012 IEEE Third International Conference on***. IEEE. 2012, pp. 13–18. doi: https://doi.org/10.1109/SmartGridComm.2012.6485952.

[69] S. Marwitz, M. Klobasa, and D. Dallinger. “Comparison of control strategies for electric vehicles on a low voltage level electrical distribution grid.” In: ***Advances in Energy System Optimization***. Springer, 2017, pp. 17–28. isbn: 978-3-319-51795-7.

[70] O. Sundstrom and C. Binding. “Flexible charging optimization for electric vehicles considering distribution grid constraints.” In: ***IEEE Transactions on Smart Grid*** 3.1 (2012), pp. 26–37. doi: https://doi.org/10.1109/TSG.2011.2168431.

[71] Q. Li, T. Cui, R. Negi, F. Franchetti, and M. Ilic. “On-line decentralized charging of plug-in electric vehicles in power systems.” In: ***arXiv preprint arXiv:1106.5063*** (2011). url: https://arxiv.org/pdf/1106.5063.pdf.

[72] L. Yao, Z. Damiran, and W. H. Lim. “Optimal charging and discharging scheduling for electric vehicles in a parking station with photovoltaic system and energy storage system.” In: ***Energies*** 10.4 (2017), p. 550. doi: https://doi.org/10.3390/en10040550.

[73] A. Hernández Arauzo, J. Puente Peinador, M. González, J. Varela Arias, and J. Sedano Franco. “Dynamic scheduling of electric vehicle charging under limited power and phase balance constraints.” In: ***Proceedings of SPARK 2013-Scheduling and Planning Applications woRKshop***. Association for the Advancement of Artificial Intelligence. 2013.

[74] J. García-Álvarez, M. González, C. Vela, and R. Varela. “Electric Vehicle Charging Scheduling Using an Artificial Bee Colony Algorithm.” In: ***International Work-Conference on the Interplay Between Natural and Artificial Computation***. Springer. 2017, pp. 115–124.

[75] R. Rao, X. Zhang, J. Xie, and L. Ju. “Optimizing electric vehicle users’ charging behavior in battery swapping mode.” In: ***Applied Energy*** 155 (2015), pp. 547–559. doi: https://doi.org/10.1016/j.apenergy.2015.05.125.

[76] Y. Zheng, Z. Dong, Y. Xu, et al. “Electric vehicle battery charging/swap stations in distribution systems: comparison study and optimal planning.” In: ***IEEE Transactions on Power Systems*** 29.1 (2014), pp. 221–229. doi: https://doi.org/10.1109/TPWRS.2013.2278852.

[77] Y. Li, Z. Yang, G. Li, et al. “Optimal scheduling of isolated microgrid with an electric vehicle battery swapping station in multi-stakeholder scenarios: A bi-level programming approach via real-time pricing.” In: ***Applied Energy*** 232 (2018), pp. 54–68. doi: https://doi.org/10.1016/j.apenergy.2018.09.211.

[78] Q. Dong, D. Niyato, P. Wang, and Z. Han. “The PHEV charging scheduling and power supply optimization for charging stations.” In: ***IEEE Transactions on Vehicular Technology*** 65.2 (2016), pp. 566–580. doi: https://doi.org/10.1109/TVT.2015.2399411.

[79] B. Sun, X. Tan, and D. Tsang. “Optimal charging operation of battery swapping and charging stations with QoS guarantee.” In: ***IEEE Transactions on Smart Grid*** 9.5 (2018), pp. 4689–4701. doi: https://doi.org/10.1109/SmartGridComm.2014.7007615.

[80] O. Ardakanian, C. Rosenberg, and S. Keshav. “Realtime distributed congestion control for electrical vehicle charging.” In: ***ACM SIGMETRICS Performance Evaluation Review*** 40.3 (2012), pp. 38–42. doi: https://doi.org/10.1145/2425248.2425257.

[81] A. Alyousef, D. Danner, F. Kupzog, and H. de Meer. “Design and Validation of a Smart Charging Algorithm for Power Quality Control in Electrical Distribution Systems.” In: ***Proceedings of the ninth International Conference on Future Energy Systems***. e-Energy ’18. New York, NY, USA: ACM, 2018. isbn: 978-1-4503-5767-8/18/06. doi: https://doi.org/10.1145/3208903.3212031.

[82] C. Chung, J. Chynoweth, C. Qiu, C. Chu, and R. Gadh. “Design of fair charging algorithm for smart electrical vehicle charging infrastructure.” In: ***ICT Convergence (ICTC), 2013 International Conference on***. IEEE. 2013, pp. 527–532. doi: https://doi.org/10.1109/ICTC.2013.6675413.

[83] H. Yano, K. Kudo, T. Ikegami, et al. “A novel charging-time control method for numerous EVs based on a period weighted prescheduling for power supply and demand balancing.” In: ***Innovative Smart Grid Technologies (ISGT), 2012 IEEE PES***. IEEE. 2012, pp. 1–6. doi: https://doi.org/10.1109/ISGT.2012.6175612.

[84] J. E. Contreras-Ocaña, M. Sarker, and M. Ortega-Vazquez. “Decentralized coordination of a building manager and an electric vehicle aggregator.” In: ***IEEE Transactions on Smart Grid*** 9.4 (2018), pp. 2625–2637. doi: https://doi.org/10.1109/PESGM.2017.8273847.

[85] A. Davydova, R. Chakirov, Y. Vagapov, T. Komenda, and S. Lupin. “Coordinated in-home charging of plug-in electric vehicles from a household smart microgrid.” In: ***2013 Africon***. IEEE. 2013, pp. 1–4. doi: https://doi.org/10.1109/AFRCON.2013.6757667.

[86] Y. Shang, Y. Zheng, and L. Jian. “A user independent choice charging strategy for electric vehicle in household smart micro-grid.” In: ***2017 IEEE International Conference on Information and Automation (ICIA)***. IEEE. 2017, pp. 925–930. doi: https://doi.org/10.1109/ICInfA.2017.8079035.

[87] P. Papadopoulos. “Integration of electric vehicles into distribution networks.” Acccessed on 12th of March 2020. PhD thesis. Cardiff University, 2012. url: https://orca.cf.ac.uk/19539/1/2012PapadopoulosPPhD.pdf.

[88] I. G. Unda, P. Papadopoulos, S. Skarvelis-Kazakos, et al. “Management of electric vehicle battery charging in distribution networks with multi-agent systems.” In: ***Electric Power Systems Research*** 110 (2014), pp. 172–179. doi: https://doi.org/10.1002/etep.1840.

[89] E. Karfopoulos and N. Hatziargyriou. “A multi-agent system for controlled charging of a large population of electric vehicles.” In: ***IEEE Transactions on Power Systems*** 28.2 (2013), pp. 1196–1204. doi: https://doi.org/10.1109/TPWRS.2012.2211624.

[90] S. Vandael, N. Boucké, T. Holvoet, and G. Deconinck. “Decentralized demand side management of plug-in hybrid vehicles in a smart grid.” In: ***Proceedings of the first international workshop on agent technologies for energy systems (ATES 2010)***. 2010, pp. 67–74. doi: https://doi.org/10.1109/TSG.2014.2363096.

[91] J. Hu, S. You, J. Østergaard, M. Lind, and Q. Wu. “Optimal charging schedule of an electric vehicle fleet.” In: ***Universities' Power Engineering Conference (UPEC), Proceedings of 2011 46th International***. VDE. 2011, pp. 1–6. doi: https://doi.org/10.1080/00207543.2016.1192695.

[92] A. Eajal, M. Shaaban, K. Ponnambalam, and E. El-Saadany. “Stochastic centralized dispatch scheme for AC/DC hybrid smart distribution systems.” In: ***IEEE Transactions on Sustainable Energy*** 7.3 (2016), pp. 1046–1059. doi: https://doi.org/10.1109/TSTE.2016.2516530.

[93] Z. Liu, Q. Wu, A. H. Nielsen, and Y. Wang. “Day-ahead energy planning with 100% electric vehicle penetration in the Nordic region by 2050.” In: ***Energies*** 7.3 (2014), pp. 1733–1749. doi: https://doi.org/10.3390/en7031733.

[94] S. Aggarwal, L. Saini, and A. Kumar. “Electricity price forecasting in deregulated markets: A review and evaluation.” In: ***International Journal of Electrical Power & Energy Systems*** 31.1 (2009), pp. 13–22. doi: https://doi.org/10.1016/j.ijepes.2008.09.003.

[95] D. Wu, D. Aliprantis, and K. Gkritza. “Electric energy and power consumption by light-duty plug-in electric vehicles.” In: ***IEEE transactions on power systems*** 26.2 (2011), pp. 738–746. doi: https://doi.org/10.1109/TPWRS.2010.2052375.

[96] P. Danner, W. Duschl, D. Danner, A. Alyousef, and H. de Meer. “Flexibility Reward Scheme for Grid-Friendly Electric Vehicle Charging in the Distribution Power Grid.” In: ***e-Energy***. 2018, pp. 564–569. doi: https://doi.org/10.1145/3208903.3213893.

[97] S. Huang, Q. Wu, A. Nielsen, H. Zhao, and Z. Liu. “Long term incentives for residential customers using dynamic tariff.” In: ***Power and Energy Engineering Conference (APPEEC), 2015 IEEE PES Asia-Pacific***. IEEE. 2015, pp. 1–5. doi: https://doi.org/10.1109/APPEEC.2015.7380991.

[98] Z. Zhu, S. Lambotharan, W. Chin, and Z. Fan. “A mean field game theoretic approach to electric vehicles charging.” In: ***IEEE Access*** 4 (2016), pp. 3501–3510. doi: https://doi.org/1109/ACCESS.2016.2581989989.

[99] M. Al Essa and L. Cipcigan. “Reallocating Charging Loads of Electric Vehicles in Distribution Networks.” In: ***Applied Sciences*** 6.2 (2016), p. 53. doi: https://doi.org/10.3390/app6020053.

[100] L. Hua, J. Wang, and C. Zhou. “Adaptive electric vehicle charging coordination on distribution network.” In: ***IEEE Transactions on Smart Grid*** 5.6 (2014), pp. 2666–2675. doi: https://doi.org/10.1109/TSG.2014.2336623.

[101] V. del Razo and H. Jacobsen. “Smart charging schedules for highway travel with electric vehicles.” In: ***IEEE Transactions on Transportation Electrification*** 2.2 (2016), pp. 160–173. doi: https://doi.org/10.1109/TTE.2016.2560524.

[102] S. Bahrami and M. Parniani. “Game theoretic based charging strategy for plug-in hybrid electric vehicles.” In: ***IEEE Transactions on Smart Grid*** 5.5 (2014), pp. 2368–2375. doi: https://doi.org/10.1109/TSG.2014.2317523.

[103] Z. Liu, Q. Wu, S. Huang, et al. “Optimal day-ahead charging scheduling of electric vehicles through an aggregative game model.” In: ***IEEE Transactions on Smart Grid*** 9.5 (2018), pp. 5173–5184. doi: https://doi.org/10.1109/TSG.2017.2682340.

[104] Y. Cao, S. Tang, C. Li, et al. “An optimized EV charging model considering TOU price and SOC curve.” In: ***IEEE Transactions on Smart Grid*** 3.1 (2012), pp. 388–393. doi: https://doi.org/10.1109/TSG.2011.2159630.

[105] F. Neumann. “Optimal Scheduling of Electric Vehicle Charging in Distribution Networks.” PhD thesis. Karlsruhe Institute of Technology, Aug. 2017, p. 2. doi: https://doi.org/10.13140/RG.2.2.13347.96805.

[106] B. Wang, Y. Hu, Y. Xiao, and Y. Li. “An EV Charging Scheduling Mechanism Based on Price Negotiation.” In: ***Future Internet*** 10.5 (2018), p. 40. doi: https://doi.org/10.3390/fi10050040.

[107] K. Qian, C. Zhou, M. Allan, and Y. Yuan. “Modeling of load demand due to EV battery charging in distribution systems.” In: ***IEEE Transactions on Power Systems*** 26.2 (2011), pp. 802–810. doi: https://doi.org/10.1109/TPWRS.2010.2057456.

[108] S. Xu, L. Zhang, Z. Yan, et al. “Optimal Scheduling of Electric Vehicles Charging in low-Voltage Distribution Systems.” In: ***arXiv preprint arXiv:1410.3899*** (2014). doi: https://arxiv.org/abs/1410.3899v3.

[109] H. Xing, M. Fu, Z. Lin, and Y. Mou. “Decentralized optimal scheduling for charging and discharging of plug-in electric vehicles in smart grids.” In: ***IEEE Transactions on Power Systems*** 31.5 (2016), pp. 4118–4127. doi: https://doi.org/10.1109/TPWRS.2015.2507179.

[110] Y. Mou, H. Xing, Z. Lin, and M. Fu. “A new approach to distributed charging control for plug-in hybrid electric vehicles.” In: ***Control Conference (CCC), 2014 33rd Chinese***. IEEE. 2014, pp. 8118–8123. doi: https://doi.org/10.1109/ChiCC.2014.6896359.

[111] J. Kang, S. Duncan, and D. Mavris. “Real-time scheduling techniques for electric vehicle charging in support of frequency regulation.” In: ***Procedia Computer Science*** 16 (2013), pp. 767–775. doi: https://doi.org/10.1016/j.procs.2013.01.080.

[112] J. Taft and P. De Martini. “Ultra-large scale control architecture.” In: ***2013 IEEE PES Innovative Smart Grid Technologies Conference (ISGT)***. 2013, pp. 1–6. doi: https://doi.org/10.1109/ISGT.2013.6497906.

[113] P. Bansal. “Charging of electric vehicles: technology and policy implications.” In: ***Journal of Science Policy & Governance*** 6.1 (2015). Accessed on 12th of March. 2020, p. 38. url: Chargingofelectricvehicles:technologyandpolicyimplications.

[114] J. Rivera, C. Goebel, and H. Jacobsen. “A Distributed Anytime Algorithm for Real-Time EV Charging Congestion Control.” In: ***Proceedings of the 2015 ACM Sixth International Conference on Future Energy Systems***. e-Energy 15. Bangalore, India: Association for Computing Machinery, 2015, pp. 6776. isbn: 9781450336093. doi: https://doi.org/10.1145/2768510.2768544. url: https://doi.org/10.1145/2768510.2768544.

[115] Q. Xiang, L. Kong, X. Chen, et al. “GreenBroker: Optimal Electric Vehicle Park-and-Charge Control via Vehicle-to-Infrastructure Communication.” In: ***2019 IEEE International Black Sea Conference on Communications and Networking (BlackSeaCom)***. 2019, pp. 1–5. doi: https://doi.org/10.1109/BlackSeaCom.2019.8812817.

[116] K. Zhou and L. Cai. “Randomized PHEV Charging Under Distribution Grid Constraints.” In: ***IEEE Transactions on Smart Grid*** 5.2 (2014), pp. 879–887. doi: https://doi.org/10.1109/TSG.2013.2293733.

[117] A. Ghavami, K. Kar, and A. Gupta. “Decentralized charging of plug-in electric vehicles with distribution feeder overload control.” In: ***IEEE Transactions on Automatic Control*** 61.11 (2016), pp. 3527–3532. doi: https://doi.org/10.1109/TAC.2016.2516240.

[118] W. Ma, V. Gupta, and U. Topcu. “On distributed charging control of electric vehicles with power network capacity constraints.” In: ***2014 American Control Conference***. IEEE. 2014, pp. 4306–4311. doi: https://doi.org/10.1109/ACC.2014.6859139.

[119] S. Xu, D. Feng, Z. Yan, et al. “Ant-based swarm algorithm for charging coordination of electric vehicles.” In: ***International Journal of Distributed Sensor Networks*** 9.5 (2013), p. 268942. doi: https://doi.org/10.1155%2F2013%2F268942.

[120] M. Liu, P. K. Phanivong, Y. Shi, and D. S. Callaway. “Decentralized charging control of electric vehicles in residential distribution networks.” In: ***IEEE Transactions on Control Systems Technology*** 27.1 (2017), pp. 266–281. doi: https://doi.org/10.1109/TCST.2017.2771307.

[121] S. R. Sarangi, P. Dutta, and K. Jalan. “IT infrastructure for providing energy-as-a-service to electric vehicles.” In: ***IEEE Transactions on Smart Grid*** 3.2 (2012), pp. 594–604. doi: https://doi.org/10.1109/TSG.2011.2175953.

[122] S. Stüdli, E. Crisostomi, R. Middleton, and R. Shorten. “A flexible distributed framework for realising electric and plug-in hybrid vehicle charging policies.” In: ***International Journal of Control*** 85.8 (2012), pp. 1130–1145. doi: https://doi.org/10.1080/00207179.2012.679970.

[123] L. Zhang, V. Kekatos, and G. Giannakis. “Scalable electric vehicle charging protocols.” In: ***IEEE Transactions on Power Systems*** 32.2 (2016), pp. 1451–1462. doi: https://arxiv.org/abs/1510.00403v2.

[124] P. Rezaei, J. Frolik, and P. D. H. Hines. “Packetized Plug-In Electric Vehicle Charge Management.” In: ***IEEE Transactions on Smart Grid*** 5.2 (2014), pp. 642–650. doi: https://doi.org/10.1109/TSG.2013.2291384.

[125] G. BATTAPOTHULA, C. YAMMANI, and S. MAHESWARAPU. “Multi-objective simultaneous optimal planning of electrical vehicle fast charging stations and DGs in distribution system.” In: ***Journal of Modern Power Systems and Clean Energy*** 7.4 (2019), pp. 923–934. issn: 2196-5420. doi: https://doi.org/10.1007/s40565-018-0493-2.

[126] M. Miralinaghi, B. Keskin, Y. Lou, and A. Roshandeh. “Capacitated refueling station location problem with traffic deviations over multiple time periods.” In: ***Networks and Spatial Economics*** 17.1 (2017), pp. 129–151. doi: https://doi.org/10.1007/s11067-016-9320-3.

[127] P. Sadeghi-Barzani, A. Rajabi-Ghahnavieh, and H. Kazemi-Karegar. “Optimal fast charging station placing and sizing.” In: ***Applied Energy*** 125 (2014), pp. 289–299. doi: https://doi.org/10.1016/j.apenergy.2014.03.077.

[128] F. Marra, C. Træholt, and E. Larsen. “Planning future electric vehicle central charging stations connected to low-voltage distribution networks.” In: ***2012 3rd IEEE International Symposium on Power Electronics for Distributed Generation Systems (PEDG)***. IEEE. 2012, pp. 636–641. doi: https://doi.org/10.1109/PEDG.2012.6254069.

[129] M. Islam, H. Shareef, and A. Mohamed. “Improved approach for electric vehicle rapid charging station placement and sizing using Google maps and binary lightning search algorithm.” In: ***PloS one*** 12.12 (2017), e0189170. doi: https://doi.org/10.1371/journal.pone.0189170.

[130] A. Maknouninejad, N. Kutkut, I. Batarseh, and Z. Qu. “Analysis and control of PV inverters operating in VAR mode at night.” In: ***ISGT 2011***. IEEE. 2011, pp. 1–5. doi: https://doi.org/10.1109/ISGT.2011.5759186.

[131] M. Meraj, S. Rahman, A. Iqbal, et al. “A hybrid active and reactive power control with Quasi Z-source inverter in single-phase grid-connected PV systems.” In: ***IECON 2016-42nd Annual Conference of the IEEE Industrial Electronics Society***. IEEE. 2016, pp. 2994–2999. doi: https://doi.org/10.1109/IECON.2016.7793906.

[132] A. Ul-Haq, C. Cecati, K. Strunz, and E. Abbasi. “Impact of electric vehicle charging on voltage unbalance in an urban distribution network.” In: ***Intelligent Industrial Systems*** 1.1 (2015), pp. 51–60. doi: https://doi.org/10.1007/s40903-015-0005-x.

[133] N. Lal and S. E. Mubeen. “Voltage dependent load in power flow analysis.” In: ***Electrical and Electronics Engineering: An International Journal (ELELIJ)*** 4.2 (2015). Accessed on 12th of March 2020, pp. 65–77. url: https://wireilla.com/engg/eeeij/papers/4215elelij06.pdf.

[134] DIgSILENT GmbH. ***Dynamic Modelling Tutorial***. Acccessed on 12th of March 2020. url: https://www.academia.edu/33570936/DIgSILENT_PowerFactory_Application_Guide_Dynamic_Modelling_Tutorial_DIgSILENT_Technical_Documentation.

[135] T. Tjaden, B. Joseph, and V. uaschning. “Repräsentative elektrische Lastprofile für Wohngebäude in Deutschland auf 1-sekündiger Datenbasis.” In: ***HTW Berlin*** November (2015), p. 8. doi: https://doi.org/10.13140/RG.2.1.5112.0080.

[136] M. Zweistra, S. Janssen, and F. Geerts. “Large Scale Smart Charging of Electric Vehicles in Practice.” In: ***Energies*** 13.2 (2020), p. 298. doi: https://doi.org/10.3390/en13020298.

[137] K. R. Reddy and S. Meikandasivam. “Load Flattening and Voltage Regulation Using Plug-In Electric Vehicle’s Storage Capacity With Vehicle Prioritization Using ANFIS.” In: ***IEEE Transactions on Sustainable Energy*** 11.1 (2020), pp. 260–270. doi: https://doi.org/10.1109/TSTE.2018.2890145.

[138] L. Gan and S. Low. “Convex relaxations and linear approximation for optimal power flow in multiphase radial networks.” In: ***2014 Power Systems Computation Conference***. IEEE. 2014, pp. 1–9. doi: https://doi.org/10.1109/PSCC.2014.7038399.

[139] D. Curry and C. Dagli. “Computational complexity measures for many-objective optimization problems.” In: ***Procedia Computer Science*** 36 (2014), pp. 185–191. doi: https://doi.org/10.1016/j.procs.2014.09.077.

[140] F. Kelly. “Charging and rate control for elastic traffic.” In: ***European transactions on Telecommunications*** 8.1 (1997). Accessed on 12th of March 2020, pp. 33–37. url: https://onlinelibrary.wiley.com/doi/pdf/10.1002/ett.4460080106.

[141] S. Paudyal, C. A. Cañizares, and K. Bhattacharya. “Three-phase distribution OPF in smart grids: Optimality versus computational burden.” In: ***2011 2nd IEEE PES International Conference and Exhibition on Innovative Smart Grid Technologies***. 2011, pp. 1–7. doi: https://doi.org/10.1109/ISGTEurope.2011.6162628.

[142] B. Vinot, F. Cadoux, N. Gast, R. Heliot, and V. Gouin. ***Congestion Avoidance in Low-Voltage Networks by using the Advanced Metering Infrastructure***. Accessed on 12th of March 2020. 2018. url: https://hal.inria.fr/hal-01784386/file/Article.pdf.

[143] J. Carpentier. "Contribution a letude du dispatching economique." In: ***Bulletin de la Societe Francaise des Electriciens*** 3.1 (1962), pp. 431–447.

[144] J. Zhu. ***Optimization of power system operation***. Vol. 47. John Wiley & Sons, 2015. doi: http://dx.doi.org/10.1002%2F9781118887004.

[145] A. Schecterand R. ONeill. "Exploration of the acopf feasible region for the standard ieee test set." In: ***rap. tech., Federal Energy Regulatory Commission*** (2013). Accessed on 12th of March 2020. url: https://pdfs.semanticscholar.org/4c6c/5b875c74e917fac8e101d3a9322ab78a8a6e.pdf.

[146] Z. Yang, H. Zhong, A. Bose, et al. "A linearized OPF model with reactive power and voltage magnitude: A pathway to improve the MW-only DC OPF." In: ***IEEE Transactions on Power Systems*** 33.2 (2017), pp. 1734–1745. doi: https://doi.org/10.1109/TPWRS.2017.2718551.

[147] J. Franco, L. Ochoa, and R. Romero. "AC OPF for smart distribution networks: An efficient and robust quadratic approach." In: ***IEEE Transactions on Smart Grid*** 9.5 (2017), pp. 4613–4623. doi: https://doi.org/10.1109/TSG.2017.2665559.

[148] A. Bakirtzis and P. Biskas. "A decentralized solution to the DC-OPF of interconnected power systems." In: ***IEEE Transactions on Power Systems*** 18.3 (2003), pp. 1007–1013. doi: https://doi.org/10.1109/TPWRS.2003.814853.

[149] L. Von Bertalanffy. "General system theory." In: ***General systems*** 1.1 (1956), pp. 11–17.

[150] C. Cassandras and Stephane S. Lafortune. ***Introduction to discrete event systems***. Springer Science & Business Media, 2009. isbn: 978-0-387-33332-8.

[151] BDEW Bundesverband der Energie- und Wasserwirtschaft e.V. ***BDEW Roadmap, Realistic Steps for the Implementation of Smart Grids in Germany***. Accessed on 12th of March 2020. 2013. url: https://www.bdew.de/energie/bdew-roadmap-smart-grids/.

[152] BDEW Bundesverband der Energie- und Wasserwirtschaft e.V. ***Smart Grid Traffic Light Concept***. Accessed on 12th of March 2020. 2015. url: https://www.bdew.de/media/documents/Stn_20150310_Smart-Grids-Traffic-Light-Concept_english.pdf.

[153] T. Deutsch, F. Kupzog, A. Einfalt, and S. Ghaemi. "Avoiding grid congestions with traffic light approach and the flexibility operator." In: ***Challenges of implementing Active Distribution System Management, CIRED*** 1 (2014). Accessed on 12th of March 2020, pp. 1–4. url: http://www.cired.net/publications/workshop2014.

[154] T. Medved, B. Prislan, J. Zupani, and A. Gubina. "A traffic light system for enhancing the utilization of demand response in LV distribution networks." In: ***2016 IEEE PES Innovative Smart Grid Technologies Conference Europe (ISGT-Europe)***. 2016, pp. 1–5. doi: https://doi.org/10.1109/ISGTEurope.2016.7856303.

[155] C. Sankaran. ***Power quality***. The electric power engineering series. Boca Raton: CRC Press, 2002. isbn: 9780849310409.

[156] M. Stonebraker, U. Çetintemel, and S. Zdonik. "The 8 requirements of real-time stream processing." In: ***ACM Sigmod Record*** 34.4 (2005), pp. 42–47. doi: https://doi.org/10.1145/1107499.1107504.

[157] Apache Software Foundation. ***Apache Kafka: A Distributed Streaming Platform***. Accessed on 12th of March 2020. url: https://kafka.apache.org/.

[158] R. Shyam, H.B. Bharathi Ganesh, S. Sachin Kumar, P. Prabaharan, and K.P. Soman. "Apache spark a big data analytics platform for smart grid." In: ***Procedia Technology*** 21 (2015), pp. 171–178. issn: 2212-0173. doi: https://doi.org/10.1016/j.protcy.2015.10.085.

[159] M. Simonov. "Event-driven communication in smart grid." In: ***IEEE Communications Letters*** 17.6 (2013), pp. 1061–1064. issn: 10897798. doi: 10.1109/LCOMM.2013.043013.122798.

[160] R. C. Fernandez, M. Weidlich, P. Pietzuch, and A. Gal. "Scalable stateful stream processing for smart grids." In: ***Proceedings of the 8th ACM International Conference on Distributed Event-Based Systems - DEBS '14***. New York, New York, USA: ACM Press, 2014, pp. 276–281. isbn: 9781450327374. doi: https://doi.org/10.1145/2611286.2611326.

[161] Open Charge Alliance. "OCPP 2.0." In: ***OCPP Specification*** (2017).

[162] H. Daki, A. El Hannani, A. Aqqal, A. Haidine, and A. Dahbi. "Big Data management in smart grid: concepts, requirements and implementation." In: ***Journal of Big Data*** 4.1 (2017), p. 13. issn: 2196-1115. doi: https://doi.org/10.1186/s40537-017-0070-y.

[163] C. Lo and N. Ansari. "Decentralized Controls and Communications for Autonomous Distribution Networks in Smart Grid." In: ***IEEE Transactions on Smart Grid*** 4.1 (2013), pp. 66–77. issn: 1949-3053. doi: https://doi.org/10.1109/TSG.2012.2228282.

[164] Zhiyuan Sui, Ammar Alyousef, and Hermann de Meer. "IAA: incentive-based anonymous authentication scheme in smart grids." In: ***International Conference on Internet Science***. Springer. 2015, pp. 133–144.

[165] D. Danner and H. de Meer. "State Estimation in the Power Distribution System." In: ***ACM SIGMETRICS Performance Evaluation Review*** 46.3 (2019), pp. 86–88. doi: https://doi.org/10.1145/3308897.3308937.

[166] M. Simonov, G. Chicco, and G. Zanetto. "Event-driven energy metering: Principles and applications." In: ***IEEE Transactions on Industry Applications*** 53.4 (2017), pp. 3217–3227. doi: https://doi.org/10.1109/TIA.2017.2679680.

[167] IEC Smart Grid Standardization Roadmap. "IEC." In: ***Prepared by SMB Smart Grid Strategic Group (SG3), Edition*** 1 (2010). Accessed on 12th of March 2020. url: https://www.iec.ch/smartgrid/downloads/sg3_roadmap.pdf.

[168] M. McGranaghan and S. Santoso. "Challenges and trends in analyses of electric power quality measurement data." In: ***EURASIP Journal on Advances in Signal Processing*** 2007.1 (2007), p. 057985. doi: https://doi.org/10.1155/2007%2F57985.

[169] ***AKKA Streams***. Accessed on 12th of March 2020. url: http://doc.akka.io/docs/akka/current/java/stream/index.html.

[170] ***Reactive Streams***. Accessed on 12th of March 2020. url: http://www.reactive-streams.org/.

[171] T. Ganu, D. Seetharam, V. Arya, et al. "nPlug: a smart plug for alleviating peak loads." In: ***Proceedings of the 3rd International Conference on Future Energy Systems: Where Energy, Computing and Communication Meet***. e-Energy '12. ACM. Madrid, Spain: Association for Computing Machinery, 2012, p. 30. isbn: 9781450310550. doi: https://doi.org/10.1145/2208828.2208858.

[172] J. Chen, W. Lee, and M. Chen. “Using a static var compensator to balance a distribution system.” In: ***IAS’96. Conference Record of the 1996 IEEE Industry Applications Conference Thirty-First IAS Annual Meeting***. Vol. 4. IEEE. 1996, pp. 2321–2326. doi: https://doi.org/10.1109/28.753620.

[173] D. Lee and M. Yannakakis. “Principles and methods of testing finite state machines-a survey.” In: ***Proceedings of the IEEE*** 84.8 (1996), pp. 1090–1123. issn: 1558-2256. doi: https://doi.org/10.1109/5.533956.

[174] V. Jacobson. “Congestion avoidance and control.” In: ***ACM SIGCOMM computer communication review***. Vol. 18. 4. ACM. 1988, pp. 314–329. doi: https://doi.org/10.1145/52324.52356.

[175] D. Clark. “The design philosophy of the DARPA internet protocols.” In: ***ACM SIGCOMM Computer Communication Review*** 25.1 (1995), pp. 102–111. doi: https://doi.org/10.1145/52325.52336.

[176] J. Kurose and K. Ross. ***Computer networking: a Top-Down Approach***. 7th. Addison Wesley, 2013. isbn: 9780133594140.

[177] J. G. Dong and J. S. Wha. “Performance of an exponential backoff scheme for slotted-ALOHA protocol in local wireless environment.” In: ***IEEE Transactions on Vehicular Technology*** 44.3 (1995), pp. 470–479. doi: https://doi.org/10.1109/25.406614.

[178] A. Tanenbaum and M. Van Steen. ***Distributed systems: principles and paradigms***. Prentice-Hall, 2007. isbn: 0-13-239227-5.

[179] N. Song, B. Kwak, J. Song, and M. Miller. “Enhancement of IEEE 802.11 distributed coordination function with exponential increase exponential decrease backoff algorithm.” In: ***The 57th IEEE Semiannual Vehicular Technology Conference, 2003. VTC 2003-Spring.*** Vol. 4. IEEE. 2003, pp. 2775–2778. doi: https://doi.org/10.1109/VETECS.2003.1208898.

[180] M. Faschang, F. Kupzog, R. Mosshammer, and A. Einfalt. “Rapid control prototyping platform for networked smart grid systems.” In: ***IECON 2013 - 39th Annual Conference of the IEEE Industrial Electronics Society***. 2013, pp. 8172–8176. doi: https://doi.org/10.1109/IECON.2013.6700500.

[181] D. Stahleder, D. Reihs, M. Nöhrer, and F. Lehfuss. “Lablink - a novel cosimulation tool for the evaluation of large scale ev penetration focusing on local energy communities.” In: ***CIRED 2018 Ljubljana Workshop on Microgrids and Local Energy Communities***. Accessed on 12th of March. 2020. AIM, 2018. url: https://www.cired-repository.org/handle/20.500.12455/1136.

[182] DIgSILENT. ***Digital Simulation and Network Calculation***. Accessed on 12th of March. 2020. 2018. url: www.digsilent.de/en/powerfactory.html.

[183] M. Michael and D. Christian. “Electric vehicles as flexible loads A simulation approach using empirical mobility data.” In: ***6th Dubrovnik Conference on Sustainable Development of Energy Water and Environmental Systems, SDEWES 2011***. Vol. 48. 1. 2012, pp. 369 –374. doi: https://doi.org/10.1016/j.energy.2012.04.014.

[184] G. Till, F. Simon, J. Niklas, et al. “Fast charging infrastructure for electric vehicles: Todays situation and future needs.” In: ***Transportation Research Part D: Transport and Environment*** 62 (2018), pp. 314 –329. issn: 1361-9209. doi: https://doi.org/10.1016/j.trd.2018.03.004.

[185] D. Nicolò, S. Aruna, and W. John. “Electric vehicle charging choices: Modelling and implications for smart charging services.” In: ***Transportation Research Part C: Emerging Technologies*** 81 (2017), pp. 36 –56. issn: 0968-090X. doi: https://doi.org/10.1016/j.trc.2017.05.006.

[186] L. Haiyang, F. Kun, L. Yiling, S. Qie, and W. Ronald. “Modeling charging demand of electric vehicles in multi-locations using agent-based method.” In: ***Energy Procedia*** 152 (2018). Cleaner Energy for Cleaner Cities, pp. 599 –605. issn: 1876-6102. doi: https://doi.org/10.1016/j.egypro.2018.09.217.

[187] G. Marco, P. Giuseppe, J. Andreea, et al. “Statistical characterisation of the real transaction data gathered from electric vehicle charging stations.” In: ***Electric Power Systems Research*** 166 (2019), pp. 136 –150. issn: 0378-7796. doi: https://doi.org/10.1016/j.epsr.2018.09.022.

[188] X. Erotokritos, M. Charalampos, C. Liana, et al. “A data-driven approach for characterising the charging demand of electric vehicles: A UK case study.” In: ***Applied Energy*** 162 (2016), pp. 763 –771. issn: 0306-2619. doi: https://doi.org/10.1016/j.apenergy.2015.10.151.

[189] A.P. Robinson, P.T. Blythe, M.C. Bell, Y. Hübner, and G.A. Hill. “Analysis of electric vehicle driver recharging demand profiles and subsequent impacts on the carbon content of electric vehicle trips.” In: ***Energy Policy*** 61 (2013), pp. 337 –348. issn: 0301-4215. doi: https://doi.org/10.1016/j.enpol.2013.05.074.

[190] M. Neaimeh, S. D. Salisbury, G. A. Hill, et al. “Analysing the usage and evidencing the importance of fast chargers for the adoption of battery electric vehicles.” In: ***Energy Policy*** 108 (2017), pp. 474 –486. issn: 0301-4215. doi: https://doi.org/10.1016/j.enpol.2017.06.033.

[191] J. Michaelis, T. Gnann, and A. Klingler. “Load Shifting Potentials of Plug-In Electric VehiclesA Case Study for Germany.” In: ***World Electric Vehicle Journal*** 9.2 (2018). issn: 2032-6653. doi: 10.3390/wevj9020021.

[192] Z. J. Lee, T. Li, and S. H. Low. “ACN-Data: Analysis and Applications of an Open EV Charging Dataset.” In: ***Proceedings of the Tenth ACM International Conference on Future Energy Systems***. e-Energy ’19. Phoenix, AZ, USA: ACM, 2019, pp. 139–149. isbn: 978-1-4503-6671-7. doi: http://doi.acm.org/10.1145/3307772.3328313.

[193] C. Luo, Y. Huang, and V. Gupta. “Placement of EV Charging Stations — Balancing Benefits among Multiple Entities.” In: ***arXiv e-prints*** 8.2 (2017). issn: 1949-3061. doi: https://doi.org/10.1109/TSG.2015.2508740.

[194] K. Brunnström, S. Beker, K. De Moor, et al. “Qualinet white paper on definitions of quality of experience.” In: (2013). Accessed on 12th of March. 2020. url: https://hal.archives-ouvertes.fr/hal-00977812/.

[195] T. HoSSfeld, L. Skorin-Kapov, P. E. Heegaard, and M. Varela. “Definition of QoE Fairness in Shared Systems.” In: ***IEEE Communications Letters*** 21.1 (2017), pp. 184–187. issn: 1089-7798. doi: https://doi.org/10.1109/LCOMM.2016.2616342.

[196] R. Jain, D. Chiu, and W. Hawe. “A quantitative measure of fairness and discrimination.” In: ***Eastern Research Laboratory, Digital Equipment Corporation, Hudson, MA*** (1984). Accessed on 12th of March 2020. url: https://arxiv.org/abs/cs/9809099.

[197] J. Hamari, J. Koivisto, and H. Sarsa. “Does gamification work?–a literature review of empirical studies on gamification.” In: ***2014 47th Hawaii international conference on system sciences***. Ieee. 2014, pp. 3025–3034. doi: https://doi.org/10.1109/HICSS.2014.377.

[198] batteryuniversity.com. ***BU-1003: Electric Vehicle (EV)***. Accessed on 12th of March. 2020. url: https://batteryuniversity.com/learn/article/electric_vehicle_ev.

[199] A. Cichon, P. Fracz, and D. Zmarzly. “Characteristic of acoustic signals generated by operation of on load tap changers.” In: ***Acta Physica Polonica A*** 120.4 (2011). Accessed on 12th of March 2020, pp. 585–588. url: http://przyrbwn.icm.edu.pl/APP/PDF/120/a120z4p05.pdf.

[200] ***RabbitMQ***. Accessed on 12th of March. 2020. url: https://www.rabbitmq.com/.

[201] ***NATS Open Source. Simple. Secure. Scalable.*** Accessed on 12th of March 2020. url: https://nats.io/.

[202] ***Amazon Kinesis***. Accessed on 12th of March. 2020. url: https://aws.amazon.com/kinesis/.

[203] ELECTRIFIC. ***D9.6 - Final exploitation framework: Market analysis, project impact and sustainability plan***. Tech. rep. Accessed on 12th of March 2020. 2019. url: https://electrific.eu/project-deliverables/.

[204] ELECTRIFIC. ***D8.4 - Report on the final results of experiments and demonstrations***. Tech. rep. Accessed on 12th of March 2020. 2019. url: https://electrific.eu/project-deliverables/.

[205] ***Technische Richtlinie: BSI TR-03109***. Accessed on 12th of March 2020. url: https://www.bsi.bund.de/SharedDocs/Downloads/DE/BSI/Publikationen/TechnischeRichtlinien/TR03109/TR03109.pdf?__blob=publicationFile&v=3.

[206] ***Rollout rückt näher: Drittes Zertifikat für Smart-Meter Gateway übergeben***. Accessed on 12th of March 2020. url: https://www.bmwi.de/Redaktion/DE/Pressemitteilungen/2019/20191219-rollout-rueckt-naeher-drittes-zertifikat-fuer-smart-meter-gateway-uebergeben.html.

[207] ***Open vs. Closed Charging Stations: Advantages and Disadvantages***. Accessed on 12th of March 2020. url: https://greenlots.com/wp-content/uploads/2018/09/Open-Standards-White-Paper.pdf.

[208] ***OpenADR 2.0 Profile Specification B Profile***. Tech. rep. Accessed on 12th of March 2020. OpenADR Alliance, 2013. url: https://cimug.ucaiug.org/Projects/CIM-OpenADR/Shared%20Documents/Source%20Documents/OpenADR%20Alliance/OpenADR_2_0b_Profile_Specification_v1.0.pdf.

[209] A. Hoekstar and A. Wargers. “Using OpenADR with OCPP.” In: (2015). Accessed on 12th of March 2020. url: https://openadr.memberclicks.net/assets/using%20openadr%20with%20ocpp.pdf.

[210] ***Type 2 charging plug proposed as the common standard for Europe***. Accessed on 12th of March 2020. url: http://www.mennek.es/uploads/media/MENNEKES_Media_information_-Type_2_charging_plug_proposed_as_the_common_standard_for_Europe.pdf.

[211] V. Schwarzer and R. Ghorbani. “Current state-of-the-art of EV chargers.” In: ***EVTC Electric vehicle transportation centre*** (2015). Accessed on 12th of March 2020. url: https://www.hnei.hawaii.edu/sites/www.hnei.hawaii.edu/files/Current%20State%20of%20the%20Art%20EV%20Chargers.pdf.

[212] G. Britz, J. Hellermann, G. Hermes, et al. ***EnWG Energiewirtschaftsgesetz***. Accessed on 12th of March 2020. Beck, CH, 2014. url: https://www.gesetze-im-internet.de/enwg_2005/EnWG.pdf.

[213] L. Noel, G. de Rubens, J. Kester, and B. Sovacool. ***Vehicle-to-Grid: A Sociotechnical Transition Beyond Electric Mobility***. Springer, 2019. isbn: ISBN 978-3-030-04864-8.